2016

The role of the dopamine D4 receptor in modulating state-dependent gamma oscillations

BOSTON UNIVERSITY

SCHOOL OF MEDICINE

Dissertation

THE ROLE OF THE DOPAMINE D4 RECEPTOR IN MODULATING STATE-DEPENDENT GAMMA OSCILLATIONS

by

KATRINA EILEEN FURTH

B.S., University of Rochester, 2010

Submitted in partial fulfillment of the

requirements for the degree of

Doctor of Philosophy

2016

Approved by

First Reader _____

Shelley Russek, Ph.D.
Professor of Pharmacology and Experimental Therapeutics

Second Reader _____

Andres Buonanno, Ph.D.
Senior Investigator, Section on Molecular Neurobiology
National Institute of Child Health & Development, NIH

Third Reader _____

Judith Walters, Ph.D.
Senior Investigator, Neurophysiological Pharmacology Section
National Institute of Neurological Disorders & Stroke, NIH

DEDICATION

I would like to dedicate this work to my loving husband, Salim, my wonderful daughter, Jireh, my parents, and parents-in-law who encouraged me along the way.

Most importantly, I would like to dedicate this work to God. He has blessed me with intellect, ambition, a loving family and the support network that I needed to finish. May this dissertation bring glory to His name.

ACKNOWLEDGMENTS

First, I would like to thank Dr. Shelley Russek, who creatively found a way for me to remain a Boston University graduate student while living in Washington, DC with my family. I am extremely grateful for her dedication to seeing me succeed, and her ingenious ways to secure funding for me during all of my antics. Secondly, I am extremely indebted to Dr. Andres Buonanno, who responded positively when I reached out to him about joining his lab, and encouraged me to seek out the collaboration with Dr. Judie Walters. He has really pushed me to become a better scientist, and provided me with fantastic opportunities to attend conferences and courses and meet the leaders in our field. Thirdly, I would like to thank Dr. Judith Walters for providing me with an exciting, collaborative work environment for performing in vitro electrophysiology and really reawakening my scientific curiosity at a time when I was facing prolonged failure. It has been a great pleasure working in her lab with fantastic group of people who share a strong team mentality.

Elias Leiva-Salcedo provided exceptional mentorship for me by consistently displaying integrity, challenging my scientific thinking, and inspiring me to achieve my full potential. Elias committed countless hours to train me as an electrophysiologist, and consistently showed patience and generosity with his time.

Claire Delaville deserves special recognition and thanks for her role in this work. Claire was my scientific mentor in Dr. Walter's lab for almost three years, during which time she has trained me to perform in vivo electrophysiology, advised me on this work

and on all aspects of my time in graduate school. She has been a great role model and friend.

In addition I must thank everyone who has worked with me on this project. Megan Janssen trained me as an in vitro electrophysiologist; Swagata Basu helped me collect data; Detlef Vullhorst wrote the D4 and gamma oscillations review with me; Caroline Dodge ran a few rats for me and did all of my behavioral scoring; Alex McCoy sorted thalamic cells for me and wrote many of the analysis scripts that I used; Ana Cruz collaborated with me on the phase-amplitude coupling script. Their hard work and enthusiasm has driven this research and made the process highly enjoyable and stimulating.

The members of Andres and Judie's lab create an encouraging and positive environment and deserve thanks for their contributions and friendship, in particular Dr. Claire Delaville, Dr. Kristin Dupre, Dr. Detlef Vullhorst, Dr. Miguel Skizerewski-Prieto, Dr. Swagata Basu, Lolitha, Alex Weiss, Heysol Bermudez, and Collin Lobb.

Thanks also to all the members on my advising committee, Dr. Jen-Wei Lin, Dr. Nancy Kopell, and Dr. Bernat Kocsis. They are a fantastic group of scientists and have been a pleasure to work with and learn from. I appreciate all the time they have given to support me during this work and all the advice and comments they have made.

The Boston University graduate program in neuroscience has provided an excellent place to learn and develop as a researcher and I must thank Dr. Shelley Russek and Dr. Sandi Grasso for their hard work in running the program and making it such a success. I am also so grateful for the highly collaborative environment among our cohort,

and the lasting friendships that I formed in the program. I can imagine a much more competitive environment among my fellow graduate students, and I am grateful for the ways in which they have all supported me.

Lastly I must say a special thanks to my family and friends. They have always been there for me through the numerous highs and lows, steeling my resolve and enabling me to bounce back from the considerable failures involved in performing this work. They have also been immensely helpful in watching Jireh so that I could get work done. You know who you are, thank you.

THE ROLE OF THE DOPAMINE D4 RECEPTOR IN

MODULATING STATE-DEPENDENT GAMMA OSCILLATIONS

KATRINA EILEEN FURTH

Boston University School of Medicine, 2016

Major Professor: Dr. Shelley Russek, Ph. D., Professor of Pharmacology and Experimental Therapeutics

ABSTRACT

Rhythmic oscillations in neuronal activity display variations in amplitude (power) over a range of frequencies. Attention and cognitive performance correlate with increases in cortical gamma oscillations (40-70Hz) that are generated by the coordinated firing of glutamatergic pyramidal neurons and GABAergic interneurons, and are modulated by dopamine. In the medial prefrontal cortex (mPFC) of rats, gamma power increases during treadmill walking, or after administration of an acute subanesthetic dose of the NMDA receptor antagonist ketamine. Ketamine is also used to mimic symptoms of schizophrenia, including cognitive deficits, in healthy humans and rodents. Additionally, the ability of a drug to modify ketamine-induced gamma power has been proposed to predict its pro-cognitive therapeutic efficacy. However, the mechanism underlying ketamine-induced gamma oscillations is poorly understood. We hypothesized that gamma oscillations induced by walking and ketamine would be generated by a shared mechanism in the mPFC and one of its major sources of innervation, the mediodorsal thalamus (MD). Recordings from chronically implanted electrodes in rats showed that both treadmill walking and ketamine increased gamma power, firing rates, and spike-gamma LFP correlations in the mPFC. By contrast, in the MD, treadmill walking increased all three

measures, but ketamine decreased firing rates and spike-gamma LFP correlations while increasing gamma power. Therefore, walking- and ketamine-induced gamma oscillations may arise from a shared circuit in the mPFC, but different circuits in the MD.

Recent work in normal animals suggests that dopamine D4 receptors (D4Rs) synergize with the neuregulin/ErbB4 signaling pathway to modulate gamma oscillations and cognitive performance. Consequently, we hypothesized that drugs targeting the D4Rs and ErbB receptors would show pro-cognitive potential by reducing ketamine-induced gamma oscillations in mPFC. However, when injected before ketamine, neither the D4R agonist nor antagonist altered ketamine's effects on gamma power or firing rates in the mPFC, but the pan-ErbB antagonist potentiated ketamine's increase in gamma power, and prevented ketamine from increasing firing rates. This indicates that D4Rs and ErbB receptors influence gamma power via distinct mechanisms that interact with NMDA receptor antagonism differently. Our results highlight the value of using ketamine-induced changes in gamma power as a means of testing novel pharmaceutical agents.

TABLE OF CONTENTS

LIST OF TABLES

LIST OF FIGURES

LIST OF ABBREVIATIONS

6-OHDA 6-hydroxydopamine

ADHD ..... attention deficit/hyperactivity disorder

AMPA ..... α-amino-3-hydroxy-5-methyl-4-isoxazolepropionic acid

AMPAR ..... AMPA receptor

ANOVA ..... analysis of variance test

CA1 ..... *cornu ammonis* 1

Ca^{2+} ..... calcium

CA3 ..... *cornu ammonis* 3

cAMP ..... cyclic AMP

CNQX ..... 6-cyano-7-nitroquinoxaline-2,3-dione, AMPAR antagonist

COMT ..... catechol-O-methyltransferase

D4R ..... dopamine D4 receptor

dhCA1 ..... dorsal hippocampus *cornu ammonis* 1

DL-AP5 ..... (2*R*)-amino-5-phosphonovaleric acid, NMDAR antagonist

E-cell ..... excitatory neuron

eEPSC ..... evoked excitatory postsynaptic current

EPSP ..... excitatory postsynaptic potential

ErbB4R ..... ErbB4 receptor

FFT ..... fast Fourier transform

FSI ..... fast-spiking interneuron

GABA ..... Gamma-Aminobutyric acid

GABAR..... Gamma-Aminobutyric acid receptor

GAD67.....glutamate decarboxylase-67

GPCR..... G-protein coupled receptor

GWAS..... genome-wide association study

HNK..... hydroxynorketamine

i.p. ..... intraperitoneal

I-cell .....inhibitory neuron

ING ..... interneuron-generated gamma

IPSP.....inhibitory postsynaptic potential

K+ ..... potassium

Kv..... voltage-gated potassium channel

LFP..... local field potential

LTP .....long-term potentiation

MD ..... mediodorsal thalamus

mEPSC.....miniature excitatory postsynaptic current

mIPSC..... miniature inhibitory postsynaptic current

MK-801..... dizocilpine, NMDAR antagonist

mPFC .....medial prefrontal cortex

Na+.....sodium

NMDA ..... N-methyl-D-aspartate

NMDAR..... N-methyl-D-aspartate receptor

NRG ..... neuregulin

PAC..... phase-amplitude coupling

PCA.....principal component analysis

PCP .....phencyclidine, NMDAR antagonist

PFC .....prefrontal cortex

PING ..... pyramidal-interneuron generated gamma

PPI..... paired-pulse inhibition

PSD95 .....postsynaptic density-95, glutamatergic

PV ..... parvalbumin

PV+ interneuron..... parvalbumin-expressing interneuron

RTK..... receptor tyrosine kinase

s.c. .....subcutaneous

sEPSC ..... spontaneous excitatory postsynaptic current

sIPSC.....spontaneous inhibitory postsynaptic current

SNP .....single nucleotide polymorphism

STWA .....spike-triggered waveform average

TH .....tyrosine hydroxylase

t-LTP .....spike-timing dependent LTP

TTX.....tetrodotoxin

VGCC .....voltage-gated calcium channel

VTA .....ventral tegmental area

CHAPTER ONE: Neuregulin, dopamine, cognitive function and gamma oscillations: role of D4 receptors

1.1 Introduction

Schizophrenia is characterized by three distinct symptom clusters– positive, negative and cognitive. Historically, positive symptoms such as hallucinations and delusions have received the most attention, and are often improved by typical and atypical antipsychotics. In contrast, negative symptoms such as social withdrawal, lack of motivation and impaired social interactions, and cognitive impairments including deficits in attention, working memory and executive function are refractory to antipsychotics. The intractability of cognitive symptoms has been a major obstacle in the development of more effective therapies for schizophrenia, especially in light of epidemiological findings indicating that the severity of cognitive symptoms is more predictive of long-term course of the disease than positive symptoms (Green, 1996), and that cognitive impairments are present before the onset of the illness (Reichenberg et al., 2002).

In the medial prefrontal cortex (mPFC), neural synchrony in the gamma frequency range (30-80Hz) is thought to play an important role in cognitive flexibility, working memory, and attention (Cannon et al., 2014; Gregoriou et al., 2015). Indeed, optogenetic inhibition of mPFC interneurons inhibits both gamma power and cognitive flexibility while activation of mPFC interneurons at gamma frequencies restores cognitive flexibility in cognitively impaired mice (Cho et al., 2015). Additionally, it has been proposed that impairments in gamma oscillations play a key role in producing the cognitive deficits observed in psychiatric disorders such as schizophrenia and ADHD

(Pittman-Polletta et al., 2015; Sakurai et al., 2015). Subanesthetic doses of the NMDAR antagonist ketamine elicit psychotomimetic effects with concomitant increases in gamma power in healthy humans similar to those observed in patients with schizophrenia (Anticevic et al., 2015; Kocsis et al., 2013; Krystal et al., 1994). The gamma power increase induced by an acute subanesthetic dose of ketamine has been used as a possible biomarker for investigating the pro-cognitive therapeutic efficacy of novel pharmacological agents (Anderson et al., 2014; Hudson et al., 2016; Ma and Leung, 2014). However, the mechanism underlying ketamine-induced gamma oscillations is poorly understood.

While the importance of dopaminergic modulation of the PFC for proper cognitive functions is well supported by experimental evidence from nonhuman primates and rodents (Goldman-Rakic, 1995; Robbins and Arnsten, 2009), the ways in which altered dopamine (DA) activity contributes to gamma band activity in the PFC is poorly understood. During a treadmill-walking task, which requires attention, gamma power increases in the medial prefrontal cortex (mPFC) in rats with intact dopamine signaling, but not in rats with a lesion of the dopaminergic cells from the ventral tegmental area (VTA) and substantia nigra (Delaville et al., 2015). Additionally, the dopamine D4 receptor (D4R), considered a major D2-type receptor, is prominently expressed in parvalbumin-expressing (PV+) interneurons (Andersson et al., 2012b), has the highest affinity for dopamine of any dopamine receptor (Rondou et al., 2010), and modulates gamma power and cognition *in vivo* (Nakazawa et al., 2015). Therefore, we hypothesized that signaling through the D4R would be fundamental to the walking-induced increase in

gamma oscillations. We further hypothesized that gamma oscillations induced by walking and ketamine would be generated by a shared mechanism in the mPFC, and one of its major sources of innervation, the mediodorsal thalamus (MD).

Here I review the current state of research into the connection between gamma oscillations and cognition, the mechanisms of gamma oscillation generation, and the influence of NMDAR (NMDAR) antagonists on these oscillations. I further examine the role of dopamine in the modulation of network rhythms in the cortex, particularly the PFC and hippocampus, as evidence that dopamine signaling is potently involved in regulating theta and gamma oscillations has emerged. I finish by focusing specifically on the D4R, a receptor strongly implicated in ADHD, and Neuregulin (NRG) signaling through ErbB4 receptors (ErbB4Rs), a pathway genetically implicated in schizophrenia. Recent studies have shown that dopamine signaling via D4R, in a close and synergistic relationship with the NRG/ErbB4R signaling pathway modulates gamma rhythms in the hippocampus and prefrontal cortex (Andersson et al., 2012b; Kocsis et al., 2014; Nakazawa et al., 2015). Taken together with the genetic association of the 7-repeat variant of the human *DRD4* gene with increased risk for ADHD and altered gamma band responses (Demiralp et al., 2007; Gizer et al., 2009), we hypothesized that drugs targeting the D4Rs and ErbB receptors would show pro-cognitive potential by reducing ketamine-induced gamma oscillations. Our results highlight the importance of testing the effects of novel pharmaceutical agents on gamma oscillations induced by ketamine as opposed to gamma oscillations observed in normal animals in the attempt to find pro-cognitive therapeutic agents.

1.2 Overview of gamma oscillations

1.2.1 Mechanisms of gamma oscillation generation

Oscillations in neuronal activity display variations in amplitude (power) over a range of frequencies (Fig 1.1D). Gamma oscillations (30-80Hz) are generated in one of three ways: 1) through recurrent networks of interneurons which inhibit one another for a specific period (ING gamma); 2) through synchronous excitatory activity from pyramidal cells onto interneurons (PING gamma), or 3) through synchronized excitation projected into the region from the thalamus or another cortical region (Tiesinga and Sejnowski, 2009). In interneuron generated (ING) gamma, when a small number of fast-spiking PV+ interneurons start spiking in synchrony, the inhibition on other excitatory pyramidal neurons and interneurons in the network prevents these neurons from spiking until the inhibition from the PV+ interneurons has 'worn off' (Fig 1.2C). This adjusts the timing of other neurons in the network to fire during the small time window without inhibition, thus increasing the number of neurons participating in the synchronized firing (Bartos et al., 2007; Tiesinga and Sejnowski, 2009). The decay time of the inhibition sets the maximum frequency of the oscillation (Buzsaki and Wang, 2012). Importantly, in ING, the interneurons themselves have sufficient excitation to spike in synchrony without a synchronized volley from neighboring pyramidal neurons, although ING gamma typically leads to synchronized spiking of pyramidal neurons as well (Whittington et al., 2011). Experimentally, gamma activity can propogate *in vitro* in the absence of ionotropic glutamatergic signaling (Whittington et al., 1995), further supporting the ING models of gamma oscillations. By contrast, in pyramidal-interneuron generated (PING)

gamma, the inhibitory cells need synchronized inputs from the pyramidal neurons to increase the gamma power (Fig 1.2B&C). One prediction from the PING gamma model is that the firing rates of pyramidal neurons and gamma power should be closely correlated. It is hard to distinguish PING and ING gamma experimentally because either mechanism leads to the synchronized spiking of pyramidal neurons (Tiesinga and Sejnowski, 2009).

Recordings from chronically implanted electrodes can be separated into local field potentials (LFPs) and spiking activity by low pass and high pass filtering respectively (Fig 1.1A&B). Consequently, researchers can examine the relationships between spikes and the phase of oscillations in different frequency ranges, which can be used to probe how certain oscillations are generated and how they influence neuronal activity (Ray, 2015). These recordings are then used to inform computational models. Small modifications in NMDAR-mediated neurotransmission between pyramidal neurons and interneurons can produce prominent changes in frequency and power (Jadi et al., 2015; Neymotin et al., 2011). In fact, models predict that simply reducing NMDA receptor neurotransmission onto interneurons in the oriens layer of the hippocampus increases the gamma power in this region (Neymotin et al., 2011), which suggests that the blockade of NMDA receptors on some neurons may have greater influence on gamma power than blockade of NMDA receptors on other types of neurons.

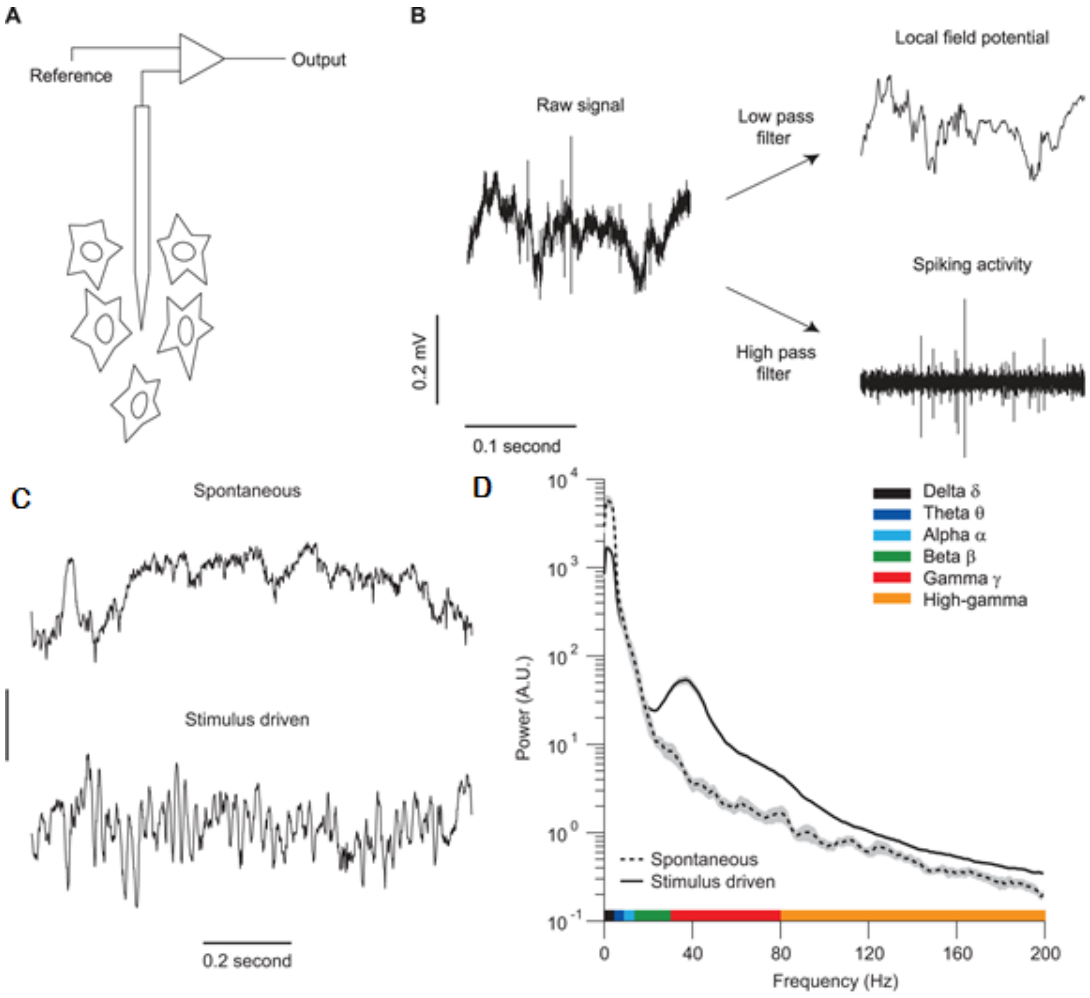

Figure 1.1: Basics of gamma oscillations, adapted from Jia & Kohn (2011). (**A**) Local field potentials (LFPs) and single neuron activity comes from recordings of high impedance electrodes chronically implanted in brain tissue. This raw signal (**B**) is low-pass filtered (<150Hz) to provide the LFP (pictured in **C** and **D**), and it is also high pass filtered (40kHz) to isolate spiking activity. A major focus of this thesis will be the timing of spikes in relationship to local field potentials. **C,D**, Example traces of LFPs from normal animals during spontaneous (ongoing) activity, and task-related recording conditions shown as raw traces (**C**), or as power spectra (**D**). Note that in normal animals, gamma power increases as stimulus salience or task-difficulty increases.

Finally, PV+ interneurons are both essential for the maintenance of gamma oscillations, and may be important in the etiology of schizophrenia (Bartos et al., 2007; Lewis et al., 2011). These PV+ interneurons form inhibitory connections with cell bodies

and axon initial segments of their pyramidal neuron targets. Moreover, they are extensively interconnected through electrical and chemical synapses (for excellent reviews, see: Bartos et al., 2007; Buzsaki and Wang, 2012; Whittington et al., 2011). The central role of PV+ interneurons in the generation of gamma rhythms has been demonstrated using optogenetic techniques *in vivo* and *in vitro* (Cardin et al., 2009; Sohal et al., 2009). Numerous postmortem studies in persons with schizophrenia have also shown changes in PV+ interneurons, in particular decreases in mRNA and protein expression of GAD67 and PV (Lewis et al., 2011), consistent with perturbed maturation of inhibitory PFC circuits during adolescence responsible for abnormal oscillation patterns in adulthood (Benes and Berretta, 2001; Beneyto and Lewis, 2011; Sullivan and O'Donnell, 2012).

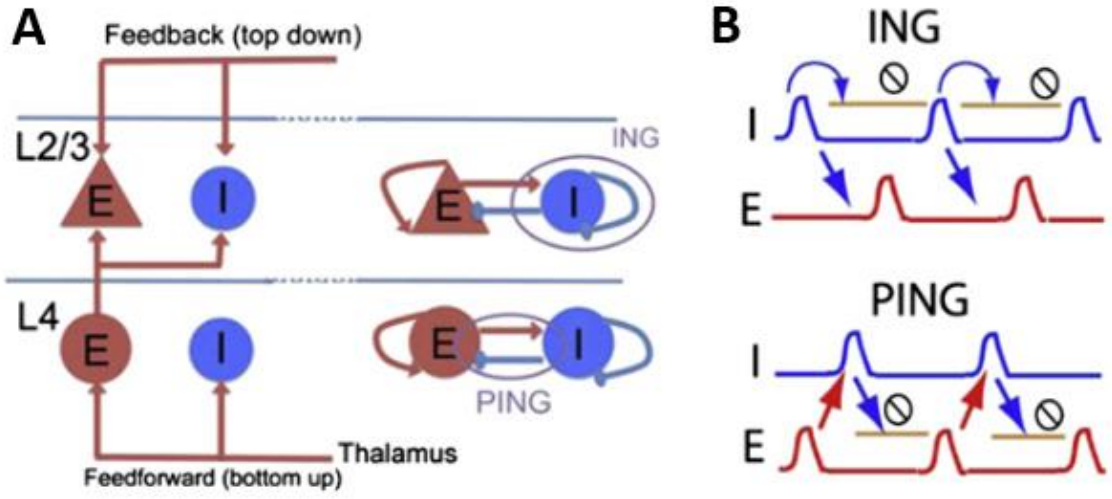

Figure 1.2: Schematic diagrams of ING and PING mechanisms. Adapted from Tiesinga & Sejnowski (2009). (**A**) A simplified representation of the laminar structure of the cortex. Inputs come in to layer 2/3 from other cortical regions (feedback), and other inputs come in to layer 4 from the thalamus (feedforward). In both layers, reciprocally interconnected interneurons form ING networks and reciprocally connected networks of excitatory and inhibitory cells form PING networks. (**B**) Synchronous network activity can be generated via ING networks, in which interneurons synchrony arises because they and neighboring neurons can only spike during a time outside of the time of recovery

from the inhibition. The PING mechanism requires synchronous excitatory volleys to elicit a synchronous inhibitory volley from the interneurons. Thus the decay of inhibition sets the maximum frequency in both the ING and PING gamma.

1.2.1 Cognition correlates with gamma band activity in humans and rodents

Cognitive impairments arise from altered activity in the PFC. In normal humans, spontaneous gamma oscillation power, also referred to as ongoing gamma oscillation power, is low (Fig 1.1C). This gamma power increases in response to salient stimuli or cognitive task demands (Fig 1.1D). The difference between the task related gamma power and the spontaneous ongoing gamma power is called signal-to-noise. Patients with psychiatric disorders that influence cognition, such as ADHD and schizophrenia have reduced signal-to-noise gamma ratios in the PFC (Tost et al., 2005; Winterer and Weinberger, 2004). Local oscillatory network activity in cortical areas, in particular gamma-band rhythms (30-80 Hz), also correlates with working memory and selective attention (Benchenane et al., 2011; Cannon et al., 2014; Womelsdorf and Fries, 2007), and higher cognitive demands correlate with increased gamma power and coherence across different cortical areas (Barr et al., 2010; Cho et al., 2006). Children with ADHD appear to have enhanced ongoing gamma power that only increases slightly in response to a cognitive task (Lenz et al., 2008), suggesting that a reduced signal-to-noise ratio in gamma power may contribute to the cognitive impairments related to ADHD. Similarly, numerous studies have shown that basal, evoked and induced gamma oscillations are altered in schizophrenic patients (for reviews, see Herrmann and Demiralp, 2005; Uhlhaas and Singer, 2010). Most of these studies focused on evoked oscillations in sensory cortices, in particular the auditory cortex for its prominent role in auditory

hallucinations. Patients with schizophrenia have elevated ongoing cortical gamma power (Minzenberg et al., 2010; Spencer et al., 2008; Williams et al., 2009), and have deficits upregulating gamma oscillations in response to cognitively demanding tasks (Barr et al., 2010; Basar-Eroglu et al., 2007; Cho et al., 2006; Haenschel et al., 2009; Kissler et al., 2000; Minzenberg et al., 2010). Taken together, these observations suggest that cognitive deficits are associated with reduced signal-to-noise relationships in regulation of gamma oscillations (Cho et al., 2006).

Cognition also correlates with gamma band activity in rodents. A recent study in rodents provided the first causal link between gamma oscillations and cognition. Optogenetic inhibition of mPFC interneurons inhibits both gamma power and cognitive flexibility while activation of mPFC interneurons at gamma frequencies restores cognitive flexibility in cognitively impaired mice (Cho et al., 2015). Nevertheless, increases in gamma power are not restricted to cognitive demand. In rats, gamma power correlates with arousal as well as cognition (McGinley et al., 2015a; Reimer et al., 2014). Both locomotion and arousal induce a clear spectral peak ~50Hz that is not observed during quiet wakefulness in the mPFC (Delaville et al., 2015) and the visual cortex (Vinck et al., 2015). This gamma range peak is not observed in the first few weeks after a lesion of dopaminergic innervation to the cortex (Delaville et al., 2015), suggesting that gamma range activity related to attention depends on dopaminergic neurotransmission.

Subcortical brain structures may also play an important role in cognition (Kellendonk et al., 2006). For example, a subtle decrease in MD thalamus activity generated selective impairments in cognitive tasks typically ascribed to the activity of the

PFC by reducing beta range synchrony between the MD thalamus and mPFC (Parnaudeau et al., 2013). Therefore, it is important to examine entire neural circuits, and not simply examine the PFC in isolation.

1.3 Effects of ketamine

1.3.1 Translation of ketamine effects from rodents to humans

An acute, subanesthetic dose of the NMDAR antagonist ketamine produces psychomimetic effects in healthy human subjects (Krystal et al., 1994), which can be used as a face valid model of the positive, negative, and cognitive symptoms of schizophrenia (Krystal et al., 1999; Stone et al., 2008, 2012). Ketamine also exacerbates the symptoms of patients with schizophrenia (Lahti et al., 1995). It has also been used as an antidepressant in treatment resistant depression (Abdallah et al., 2015). When modeling an inherently human disorder, like schizophrenia, in animal models it is beneficial to recreate endophenotypes highly associated with the disorder. Endophenotypes are heritable biomarkers that cosegregate with the illness and include both behavioral and neurophysiological measures (Gottesman and Gould, 2003). For example, ketamine disrupts neurophysiological biomarkers in humans and rodents that are also disrupted in patients with schizophrenia such as auditory gating, mismatch negativity, and a positive deflection in the EEG for deviant auditory stimuli, known as the P300 (for a review, see Kocsis et al., 2013).

NMDAR antagonism may provide clues into a potential etiology of schizophrenia. Indeed, patients with anti-NMDAR encephalitis have symptoms that mimic schizophrenia (Fischer et al., 2016). NMDAR hypofunction leads to increased

extracellular glutamate and overall increased excitation in the brain (Löscher et al., 1991; Moghaddam et al., 1997; Stone et al., 2012). NMDAR hypofunction may help to explain atrophy and reduced GAD67 and PV expression in interneurons of postmortem brains from patients with schizophrenia (for a review, see Frohlich and Van Horn, 2014). Furthermore, postmortem evidence reveals decreased NR2A mRNA in interneurons of the prefrontal cortex of patients with schizophrenia (Woo et al., 2008a), with increased NR2A expression in specific sets of calbindin expressing interneurons (Woo et al., 2008b). Taken together, NMDAR signaling in interneurons may be important for producing schizophrenia symptoms.

Oscillatory alterations accompany all pharmacological manipulations that produce psychotomimetic behavior (Pittman-Polletta et al., 2015; Rosen et al., 2015a). An acute subanesthetic dose of ketamine increases cortical gamma power (30-80Hz) in humans (Anticevic et al., 2015; Hong et al., 2010; Shaw et al., 2015) and rodents (Ehrlichman et al., 2009; Kulikova et al., 2012; Lazarewicz et al., 2009; Meltzer et al., 2013; Pinault, 2008; Shaffer et al., 2014). Ketamine also impairs the acquisition and manipulation of working memory as well as verbal learning and attention in healthy human volunteers (for a review, see Gilmour et al., 2012). Similarly, NMDAR antagonism using MK-801 causes significant impairments in spatial memory, sensory gating, and synaptic plasticity in rats (Blot et al., 2015; Manahan-Vaughan et al., 2008; Nikiforuk et al., 2016; Smith et al., 2011). In rodents, ketamine also reduces the signal-to-noise ratio of evoked gamma oscillations (Saunders et al., 2012), as observed in patients with schizophrenia. Many studies have explored the effects of ketamine in rodent models in an effort to gain further

insight into schizophrenia and the treatment of depression (Lodge and Mercier, 2015). One recent study suggests that the effects of ketamine on evoked gamma oscillations, and specifically the signal-to-noise ratio of gamma oscillations have more predictive power for potential therapeutics than ketamine's effects on ongoing gamma oscillations (Hudson et al., 2016). Interestingly, long-term, but not acute treatment with neuroleptics that target dopamine signaling decreases ketamine-induced positive and cognitive symptoms in healthy human volunteers (Krystal et al., 1999; Lipschitz et al., 1997; Malhotra et al., 1997). Likewise, long-term, but not acute treatment with neuroleptics that target dopamine signaling decreases ketamine-induced increases in gamma power and motor activity in rodents (Anderson et al., 2014; Jones et al., 2012). Taken together, these finding provide support that the ketamine model has predictive validity in testing drugs for pro-cognitive potential in schizophrenia and other psychiatric disorders (Gilmour et al., 2012).

Increasing evidence suggests that effects of ketamine on gamma oscillation power are independent from its antidepressant-like effects. First, other NMDAR antagonists, such as MK-801 and phencyclidine (PCP) increase gamma power without exerting antidepressant effects (Autry et al., 2011; Zanos et al., 2016). Second, NR2B antagonists alone recapitulate ketamine's antidepressant effects without altering gamma power or extracellular glutamate *in vivo* (Jiménez-Sánchez et al., 2014; Kocsis, 2012; Li et al., 2010; Miller et al., 2016). Intriguingly, a recent study implicates hydroxynorketamine (HNK), a ketamine metabolite, as mediating the acute antidepressant effects of ketamine independent of NMDAR inhibition. HNK still induces increases in gamma power, but

without increasing motor activity (Zanos et al., 2016). Thus, it is possible that the antidepressant properties of ketamine, or its metabolite could be separated from its psychotomimetic properties by increasing its target specificity.

1.3.2 Ketamine pharmacology

While multiple NMDAR antagonists increase gamma power, ketamine binds many receptors, and one of these targets may also influence the circuit to increase gamma power. Ketamine is an noncompetitive antagonist of NMDARs which binds to NR2A and NR2B containing NMDARs equally (Frohlich and Van Horn, 2014). Of ketamine's two enantiomers, S-ketamine has four times higher affinity for the NMDAR PCP binding site and produces more psychiatric disturbances than R-ketamine (Oye et al., 1992). Ketamine also acts as a partial agonist of the dopamine D2 receptor and has weak affinity for serotonin 5HT2A receptors (Kapur and Seeman, 2002), both of which have been used as targets in antipsychotic treatments. Furthermore, ketamine has weak affinity for sigma-1 receptors, which have been implicated in cognition and cerebral metabolism (Oye et al., 1992). Interestingly, subchronic NMDAR antagonist administration reduced sigma 1 receptor expression in the frontal cortex and hippocampus of mice (Kunitachi et al., 2009), and patients with schizophrenia have reduced sigma 1 receptor expression in the cortex (Weissman et al., 1991). Finally, studies have observed weak affinity for ketamine to kappa receptors and muscarinic acetylcholine receptors as well (Frohlich and Van Horn, 2014). Additionally, at anesthetic doses, ketamine blocks sodium channels and I_h currents (Frohlich and Van Horn, 2014).

Ketamine has a significant influence on dopaminergic neurotransmission. Ketamine increases the firing rates of dopamine neurons in the VTA (Belujon and Grace, 2014) and NMDAR antagonists increase extracellular dopamine (Löscher et al., 1991). Intriguingly, the $GABA_A$ receptor agonist muscimol reduces NMDAR antagonist induced increases in extracellular dopamine in the mPFC (Yonezawa et al., 1998), suggesting that NMDAR antagonism increases extracellular dopamine at least in part by the inhibition of GABA release from cortical interneurons. Furthermore, a PET study showed that the severity of ketamine-induced positive symptoms is correlated with dopamine release in the anterior cingulate cortex and lateral prefrontal cortex of healthy volunteers (Aalto et al., 2005), further establishing the relationship between NMDAR antagonism and dopamine.

1.3.3 Ketamine's effects on local neural circuits

While it is well known that acute application of an NMDAR antagonist increases gamma power in the cortex, hippocampus, and other subcortical regions (Kocsis et al., 2013), chronic application of NMDAR antagonists, and *in vitro* preparations have yielded mixed results. For example, *in vitro* ketamine decreases the power of kainate-induced gamma oscillations in the medial entorhinal cortex (Cunningham et al., 2006), but increases the power of kainate-induced gamma oscillations in the primary auditory cortex (Roopun et al., 2008). Chronic ketamine administration (2-4 weeks of 30mg/kg/day) causes decreases in gamma oscillation power and reduced number of PV+ interneurons (Kittelberger et al., 2012). These mixed results further complicate our understanding of how NMDAR antagonism increases gamma power.

Two hypotheses have been proposed to explain how NMDAR antagonism leads to increased excitation in the cortex. The *disinhibition hypothesis* proposes that low doses of ketamine selectively inhibit excitatory neurotransmission on cortical inhibitory interneurons, which in turn leads to the disinhibition of cortical pyramidal neurons. In the competing *direct hypothesis*, direct antagonism of NMDARs on pyramidal neurons induces a cell-autonomous form of homeostatic plasticity resulting in increased excitation (for a review, see Miller et al., 2016).

In support of the *disinhibition hypothesis*, the NMDAR antagonist MK801 increases the frequency of regular spiking putative pyramidal neurons in the PFC (Homayoun and Moghaddam, 2007a; Jackson et al., 2004) and reduces the firing rates of putative fast-spiking interneurons (FSIs) *in vivo* (Homayoun and Moghaddam, 2007a). However, in a similar study in the orbitofrontal cortex, ketamine decreased the firing rate of putative interneurons, but had little effect on the firing rates of putative pyramidal neurons (Quirk et al., 2009). Contradicting this hypothesis, however, NMDAR antagonists actually increase the levels of extracellular GABA in the mPFC of rats (Chowdhury et al., 2012), indicating greater inhibitory neurotransmission after NMDAR antagonist application. More recent experimental evidence calls this hypothesis into question.

In order for the *disinhibition hypothesis* to be valid, tonically active NMDARs on interneurons must excite these neurons enough to maintain inhibitory synaptic tone and limit action potentials in pyramidal neurons (Miller et al., 2016). Indeed bath application of NMDA increases interneuron excitability in the CA1 and CA3 of the hippocampus in

acute slices (Mann and Mody, 2010; Xue et al., 2011). Under the *disinhibition hypothesis*, excitatory synapses onto interneurons should show higher dependence on NMDAR activation than pyramidal neurons. In support, NMDAR antagonists act with greater affinity on LTP in interneurons of the hippocampus than pyramidal neurons (Grunze et al., 1996). Furthermore, a GluN2B selective NMDAR antagonist reduced synaptic NMDAR-mediated currents and excitability in interneurons more than in pyramidal neurons (Hanson et al., 2013). However, even more experimental evidence suggests that NMDAR contribution to synaptic currents is stronger in pyramidal neurons than in PV+ interneruons (Hull et al., 2009; Rotaru et al., 2011; Wang and Gao, 2009). Indeed, *in vitro* electrophysiological studies suggest that AMPA receptor (AMPAR)-mediated currents contribute at least three times more excitation to PV+ interneurons than NMDAR-mediated currents (Angulo et al., 1999; Carlén et al., 2012; Korotkova et al., 2010; Rotaru et al., 2011; Wang and Gao, 2009). Additionally, quantitative electron microscopy revealed the highest expression of NMDARs in spine synapses onto pyramidal neurons and the lowest expression of NMDARs on PV+ interneurons in the hippocampus (Nyíri et al., 2003). Low concentrations of extracellular glutamate can provide a tonic depolarizing current via extrasynaptic NMDARs that increases the excitability of cells. It was further hypothesized that this tonic NMDAR-mediated current increase the excitability of PV+ interneurons more than pyramidal neurons; however, experimentally, it was shown that pyramidal neurons and interneurons have similar levels of basal activation (Povysheva and Johnson, 2012). Nevertheless, computation modeling studies suggest that non PV+ interneurons may actually play a greater role in NMDAR

antagonist induced disinhibition than PV+ basket cells (Neymotin et al., 2011). However, taken together, it appears that NMDAR-mediated currents are stronger in pyramidal neurons than in PV+ interneurons; therefore, the *disinhibition hypothesis* seems highly flawed.

According to the *direct hypothesis*, direct antagonism of constitutively active NMDARs on pyramidal neurons induces increased cell-intrinsic excitation. One explanation for this is that NMDAR activation increases the synaptic expression of GIRK channels, which hyperpolarize cells and reduce spike frequency (Chung et al., 2009a, 2009b). Therefore inhibiting NMDA receptors on pyramidal neurons would increase the excitability of those pyramidal neurons because GIRK channels would remain internalized. A second explanation involves tonic glutamatergic currents. Ambient glutamate produces a tonic current mediated mostly by NR2B-containing NMDARs (Miller et al., 2014). These receptors have a higher sensitivity to NMDAR agonists, a decreased sensitivity to Mg^{2+} block, and dominate the extrasynaptic receptor pool (Miller et al., 2016). In fact, selective gene deletion of NR2B- containing NMDARs from cortical pyramidal neurons increased the frequency of glutamate release onto pyramidal neurons in layers 2&3 of the PFC (Miller et al., 2014), indicating increased excitatory drive. Furthermore, blocking extrasynaptic ligand-gated ion channels such as NMDARs can influence the cable properties of dendrites modifying the spatial and temporal summation within pyramidal interneurons (Harnett et al., 2013; Makara and Magee, 2013). It follows from the *direct hypothesis* that NR2B-containing NMDARs are responsible for

ketamine's effects on neuronal firing rates, but these changes are independent from the NR2A-mediated circuit that increases gamma oscillation power.

Another recent hypothesis suggests that the NMDA/AMPA receptor-mediated current ratio in pyramidal neurons is responsible for changes in excitability and gamma power after ketamine administration. NMDAR antagonists require NR2A receptor inhibition to increase gamma power (Kocsis, 2012). Inhibition of the NR2A receptor also mediates the increase in extracellular glutamate after NMDAR antagonist administration (Jiménez-Sánchez et al., 2014). These two findings, taken together, implicate a change in proportion of glutamatergic signaling through the AMPAR vs. the NMDAR. Instead of merely reducing excitatory drive to neurons, NMDAR antagonism appears to excite these neurons through elevated extracellular glutamate signaling through AMPARs (Maeng et al., 2008). Further supporting this hypothesized mechanism, ketamine requires AMPAR activity to increase gamma power (Zanos et al., 2016). Additionally, ketamine increases AMPAR mediated activity in unstimulated hippocampal slices (Nosyreva et al., 2013) and increases AMPAR mediated activity in the prefrontal cortex (Moghaddam et al., 1997). Together, these results indicate that ketamine increases gamma power by increasing the glutamatergic signaling through AMPARs. Recent evidence suggests that kainate receptors and metabotropic glutamate receptors may actually play an even larger role in generating and maintaining gamma oscillations in the absence of NMDA receptor-mediated signaling (Lladó-Pelfort et al., 2016). Intriguingly, the majority of NMDARs on PV+ interneurons express NR2A, and these receptors have faster temporal dynamics than NMDARs on pyramidal neurons (Kim et al., 2005; Kinney et al., 2006), leaving

open the possibility that PV+ interneurons may be essential in mediating the rise in extracellular glutamate. Furthermore, selective reduction of AMPAR-mediated currents in PV+ interneurons reduced kainate-induced gamma power *in vitro* (Fuchs et al., 2007), further hinting that AMPAR signaling in PV+ interneurons may be vital for ketamine's effects on gamma power.

An additional approach for testing the role of NMDARs in specific populations of neurons *in vivo* involves directed gene deletion using cell-type specific promoters driving the expression of recombinase enzymes and conditional knockout alleles. Genetic ablation of NMDARs from PV+ interneurons increases ongoing gamma power and decreases stimulus-evoked gamma power (Carlén et al., 2012; Korotkova et al., 2010), again reproducing the endophenotype of reduced signal-to-noise ratio in gamma power observed after NMDAR antagonist administration. Similarly, in mouse models of NMDAR hypofunction in a mixed population of interneurons, ongoing local field potentials (LFPs) also show an increase in gamma power (Nakao and Nakazawa, 2014). Removing NR1-containing NMDARs from PV+ interneurons late in development increases the firing rates of putative pyramidal neurons and decreases synchrony with surrounding neurons (Belforte et al., 2010). Interestingly, genetic removal of NR1-containing NMDA receptors from forebrain pyramidal neurons produced the same gamma oscillation pattern observed when NMDA receptors were removed from PV+ interneurons (Tatard-Leitman et al., 2015). Specifically, these mice displayed increased ongoing/spontaneous gamma power and decreased evoked gamma power (Tatard-Leitman et al., 2015). Furthermore, pyramidal neurons from these mice spiked more

often, and increased the spontaneous EPSC frequency (Tatard-Leitman et al., 2015), suggesting that removing NMDA receptor-mediated currents from pyramidal neurons actually makes these cells more excitable. Overall, the endophenotypes observed after genetic removal of NMDA receptors from PV+ interneurons lends support to the *disinhibition hypothesis*, and the endophenotypes observed after genetic removal of NMDA receptors from pyramidal neurons lends support to the *direct hypothesis*. Surprisingly, both genetic manipulations decrease the signal-to-noise ratio of gamma power and increase the excitability of pyramidal neurons, so it remains unclear which cell type is more important for mediating the effects of ketamine.

It remains an open question how the spiking of individual neurons contributes to NMDAR antagonist induced gamma power. Ensemble recordings in freely moving rats have shown that the NMDAR antagonist MK-801 increases the firing rates, decreases burst activity, and disorganizes the spiking of putative pyramidal neurons (Jackson et al., 2004; Molina et al., 2014), all of which may reduce the efficiency of information transmission. In fact, the correlation between spike rate and gamma oscillations was reduced after MK801 administration (Wood et al., 2012), with spiking becoming more random (Molina et al., 2014). Therefore it is plausible that changes in firing rate make little, if any contribution to changes in low gamma-range local field potential. Increases in firing rates may still contribute to increases in high gamma power over a large range (Ray and Maunsell, 2011).

1.3.4 Ketamine's effects systems-level circuits

While the majority of research has focused on high frequency gamma oscillations, low frequency oscillations are also disturbed after NMDAR antagonism and in schizophrenia. Ketamine reduces delta, theta, and alpha oscillations in response to auditory clicks in humans (Hong et al., 2010). Patients with schizophrenia frequently show enhanced delta frequency (1-5Hz) activity (Galderisi et al., 2009; Itil et al., 1972). Interestingly, NMDAR antagonists applied to the mediodorsal thalamus generate irregular, low frequency (0.5-1.5Hz) delta rhythms in the medial prefrontal cortex (Kiss et al., 2011a, 2011b). Furthermore, locally applied NMDAR antagonists do not modify delta oscillations in the mPFC when applied there, but increase mPFC delta rhythms when applied to the thalamus (Kiss et al., 2011b). Additionally, theta-gamma cross frequency coupling is impaired by acute NMDAR blockade, specifically through the antagonism of NR2A-containing NMDARs (Kocsis, 2012). Further work is needed to understand the relationship between ketamine-induced changes in low frequency oscillations and high frequency oscillations, and the relationship between NMDAR antagonism in the thalamus and cortex.

Ketamine influences brain connectivity in a variety of ways. In human fMRI, patients with schizophrenia show hyperconnectivity during the early stages of the illness while chronic schizophrenia is marked by dysconnectivity (Anticevic et al., 2015). Indeed, patients with schizophrenia typically show decreased functional connectivity between thalamic and cortical regions (Lynall et al., 2010). At rest, some groups have observed that ketamine increases functional connectivity in healthy human volunteers

(Anticevic et al., 2015; Driesen et al., 2013a); while, other groups have observed reductions in connectivity between the mPFC and default mode network and affective network (Scheidegger et al., 2012). This suggests that ketamine may be a better model of early stage schizophrenia at the systems level.

In healthy volunteers, working memory tasks activate a task-related network and reduce the activity of the default mode network. After ketamine administration, this anti-correlated relationship between the two circuits is greatly reduced (Anticevic et al., 2012), reflecting a reduced signal-to-noise ratio in the relationship between these networks. Furthermore, during a working memory task, ketamine bilaterally decreases functional connectivity in the dorsolateral prefrontal cortex connectivity (Driesen et al., 2013b). Together with ketamine-induced hyperconnectivity during rest, this finding suggests that ketamine reduces signal-to-noise in circuit pathways.

Results from metabolism studies complicate findings from MRI studies. Ketamine increases metabolism in the mPFC while decreasing metabolism in the dorsal reticular thalamic nucleus, a major source of inhibitory innervation to the mediodorsal thalamus (Dawson et al., 2013). Additionally, ketamine increases the functional connectivity of the prelimbic PFC to the dorsal reticular thalamic nucleus and concurrently decreases the functional connectivity of the PFC to the mediodorsal thalamus (Dawson et al., 2013). However, a later study by the same investigators found increased functional connectivity between the PFC and MD thalamus (Dawson et al., 2014). Further work is necessary to elucidate ketamine –induced changes in functional connectivity and determine how these changes relate to schizophrenia.

1.3.5 Dose-related effects of ketamine

NMDAR antagonists have dramatically different functions depending on dose. At low doses, ketamine evokes psychotomimetic behavior and acts as an antidepressant (Abdallah et al., 2015; Berman et al., 2000; Krystal et al., 1994; Zarate et al., 2006). Interestingly, the exact same doses of ketamine (0.3-0.5mg/kg in humans, 5-10mg/kg in rodents) are used to induce the symptoms of early stage schizophrenia in healthy volunteers and rapidly treat depression and reduce suicidal idealization resistant to antidepressant treatment (Abdallah et al., 2015; Belujon and Grace, 2014; Carreno et al., 2015; Corlett et al., 2013; Frohlich and Van Horn, 2014). Ketamine also reduces depressive symptoms in rodent models of depression, and blunts the effects of uncontrollable stress (Amat et al., 2016; Belujon and Grace, 2014; Carreno et al., 2015; Li et al., 2010). Although street use of ketamine is illegal, racemic ketamine is also used recreationally at unknown doses for its psychomimetic effects (Lodge and Mercier, 2015). At higher doses (5-10mg/kg in humans, 70-100mg/kg in rodents), ketamine induces anesthesia. Ketamine is mostly used as an anesthetic in children due to its short half-life (Rowland, 2005; Shaffer et al., 2014). In both humans and rodents, therapeutic doses of ketamine are ~15% of the anesthetic dose. These dose-dependent effects of ketamine provide support for the *direct hypothesis* as stated above because at low levels, ketamine acts predominantly on extrasynaptic GluN2B-containing receptors, which are much more likely to be basally active, and at higher concentrations ketamine acts predominantly on synaptic NMDARs, which are less active, but appear to be responsible for changes in oscillations, and potentially its dissociative effects.

1.4 Overview of dopamine in the PFC

1.4.1 Dopaminergic innervation and modulation of the prefrontal cortex

The PFC integrates sensory, motor, and affective information to perform executive control of goal-directed behaviors (Fuster, 2001; Miller and Cohen, 2001), and it has long been appreciated that the dopamine system plays an important role in modulating information processing in the PFC (Goldman-Rakic, 1995; Robbins and Arnsten, 2009). Anatomically, three major dopaminergic projections emanate from the ventral mesencephalon, which have been named as mesostriatal, mesolimbic, and mesocortical pathways (Björklund and Dunnett, 2007). These pathways originate from a fairly small number of neurons with extensive collateralization in their respective target areas, such as striatum, amygdala and the PFC (Björklund and Dunnett, 2007). Within the mesocortical pathway, frontal cortical areas receive much denser innervation compared to posterior primary sensory areas (Berger et al., 1991; Björklund and Dunnett, 2007). The dopaminergic projection neurons that send long-range axons to innervate target neurons in the prefrontal cortical regions are mostly located in the ventral tegmental area (VTA) of the midbrain (Björklund and Dunnett, 2007; Lammel et al., 2008), and they comprise the mesoprefrontal dopaminergic circuit. Early on, the dopamine system was thought to be generally overactive in schizophrenia, as drugs targeting dopamine receptors acted as antipsychotics. However, this hypothesis was later refined to account for results from imaging and genetic studies suggesting hypofrontality and hypofunction of the prefrontal dopamine system (Davis et al., 1991; Meyer-Lindenberg et al., 2002). This revised dopamine hypothesis of schizophrenia posits that hyperactivity of the mesostriatal

pathway and hypofunction of the mesoprefrontal dopamine system occur simultaneously, although their causal relationship is a matter of current debate (Simpson et al., 2010)

Although the growth of the mesoprefrontal dopaminergic axons is initiated prenatally (Kalsbeek et al., 1988; Verney et al., 1982), studies in both non-human primates and rodents indicate that this innervation matures much later in life. In particular, prefrontal dopaminergic axons continue to develop throughout adolescence, reaching a higher level of innervation density in early adulthood compared to that in the preadolescent period (Benes et al., 2000; Kalsbeek et al., 1988; Lambe et al., 2000; Rosenberg and Lewis, 1995).

A key structural feature of the mesoprefrontal dopaminergic innervation is the density of axonal boutons of the VTA projection neurons (Benes et al., 2000; Berger et al., 1985; Kalsbeek et al., 1988; Lambe et al., 2000; Rosenberg and Lewis, 1995). Axonal boutons on the mesoprefrontal dopaminergic axons have enriched expression of the dopamine-synthesizing enzyme tyrosine hydroxylase (TH) and contain synaptic vesicles for dopamine release (Goldman-Rakic et al., 1989; Miner et al., 2003; Séguéla et al., 1988). Some of these boutons form synaptic contacts with excitatory or inhibitory neurons in the PFC, while others may simply serve as dopamine release sites without any apposition to post-synaptic specializations (Descarries and Mechawar, 2000; Goldman-Rakic et al., 1989; Séguéla et al., 1988; Smiley and Goldman-Rakic, 1993). The existence of synaptic and non-synaptic dopaminergic boutons suggests both synaptic and diffuse volume transmission by dopamine neurons, although the exact proportions of these types

of boutons appear to be highly variable across species and regions (Descarries and Mechawar, 2000).

Dopamine release from axonal boutons is triggered by the firing activities of dopamine neurons (Schultz, 2007). The dopamine neurons normally fire in two distinct activity patterns that have been characterized as being either tonic or phasic (Schultz, 2007). Tonic firing consists of regular or irregular spiking at frequencies less than 10 Hz, typically 3-4 Hz, and are prevalent in dopamine neurons when animals are in the resting state (Grace et al., 2007; Hyland et al., 2002; Robinson et al., 2004). In contrast, phasic firing consists of bursts of action potentials at frequencies higher than 10 Hz, are often correlated with reward-predicting, novelty or motivationally salient events (Bromberg-Martin et al., 2010; Cohen et al., 2012; Schultz, 2007). Tonic extracellular dopamine concentrations are estimated between 5 and 50 nM at the dopamine terminals, and phasic dopamine release increases this concentration by 30 to 100 nM (Lavin et al., 2005; Wightman and Robinson, 2002).

Throughout the brain, D1Rs and D2Rs are widely distributed, while D3Rs, D4Rs and D5Rs display considerably weaker or more restricted expression (Bentivoglio and Morelli, 2005). Unlike in the striatum, dopamine receptor expression in cortical areas generally does not exhibit clear cell type or pathway-specific patterns. Evidence from different approaches suggests that both D1- and D2-type receptors occur presynaptically and postsynaptically on pyramidal neurons and interneurons (Bentivoglio and Morelli, 2005). Dopamine receptors are expressed most prominently in the deep cortical layers where the dopamine innervation is densest, but can be found in the superficial layers as

well. Furthermore, based on mRNA distribution, D1R and D2R expressing cells tend not to overlap except in layer 5, suggesting some regional or laminar selectivity of dopamine receptor expression (Santana et al., 2009). Interestingly, although more pyramidal neurons than GABAergic interneurons express the D1R, a greater proportion of interneurons express D1R, because of the prevalence of pyramidal neurons relative to interneurons (Santana et al., 2009).

1.4.2 Dopamine and cognition

Dopamine neuron activity modulates the activity of PFC neurons during cognitive tasks and motivational behaviors (Goldman-Rakic, 1995; Grace et al., 2007; Robbins and Arnsten, 2009), whereas deficiencies in mesoprefrontal dopaminergic circuits in humans are associated with major psychiatric disorders in humans such as schizophrenia, attention deficit/hyperactivity disorders (ADHD), and addiction (del Campo et al., 2011; Goldstein and Volkow, 2011; Winterer and Weinberger, 2004). A major cognitive function mediated by the PFC is working memory, which allows for the active maintenance of relevant information to guide subsequent actions (Brozoski et al., 1979). Prefrontal dopamine effects are concentration-dependent, such that both too little and too much dopamine lead to reduced cognitive performance (Sawaguchi and Goldman-Rakic, 1994; Vijayraghavan et al., 2007). Subjects with low prefrontal dopamine levels due to a Met-to-Val substitution in the catechol-O-methyltransferase (COMT) gene show reduced performance in working memory and executive function tasks (Goldberg et al., 2003). Furthermore, amphetamine administration, which increases dopamine levels, improves prefrontal efficiency in Val homozygotes but decreases efficiency in Met homozygotes

(Mattay et al., 2003). These findings have led to the proposal of an inverted U-shaped functional response curve to increasing dopamine in the PFC.

1.4.3 Cellular effects of dopamine

At the cellular level, working memory is encoded by the persistent activities of stimulus-selective neuronal assemblies in the PFC (Goldman-Rakic, 1995), and dopamine signaling plays an important role in optimizing the signal-to-noise ratio in prefrontal neural representations (Vijayraghavan et al., 2007; Williams and Goldman-Rakic, 1995). Transient increases in extracellular dopamine enhance evoked repetitive firing and suppress spontaneous firing for an extended period in pyramidal neurons in anesthetized animals (Lavin et al., 2005). In contrast, rapid dopamine reduces the firing activity of interneurons from the PFC in anesthetized animals (Tierney et al., 2008). More recent work using different combinations of optogenetic stimulation of dopaminergic fibers suggests that tonic dopamine may have opposite effects from phasic dopamine at the synaptic level (Rosen et al., 2015b). In vitro, dopamine can increase the excitability of FSIs and the frequency of GABA release, but has mixed effects on pyramidal neuron glutamatergic synapses and excitability (Gonzalez-Islas and Hablitz, 2003; Gulledge and Jaffe, 2001; Kröner et al., 2007; Penit-Soria et al., 1987; Tseng and O'Donnell, 2004; Zhou and Hablitz, 1999). By modulating cortical inhibition, dopamine decreases noise and has the potential to modulate excitation/inhibition balance and network oscillations.

Despite a plethora of research, there is no unified view on the effects of dopamine on PFC neuron function (Seamans and Yang, 2004). This is in part due to the challenges in interpreting data derived through the use of dopamine itself or general dopamine

agonists that broadly activate dopamine receptor signaling in different cell types and subcellular compartments and thereby trigger complex and frequently opposing cellular and circuit effects. Receptor-specific agonists and antagonists, used at selective concentrations, have therefore been instrumental in dissecting the effects of distinct dopamine receptor types on neuronal function.

D1R activation increases the excitability of both FSI and pyramidal neurons and increases $GABA_AR$ and NMDAR-mediated currents in pyramidal cells (Cepeda et al., 1992; Gao and Goldman-Rakic, 2003; Seamans et al., 2001; Trantham-Davidson et al., 2008, 2014; Tseng and O'Donnell, 2004; Yang and Seamans, 1996; Zheng et al., 1999); but see (Gorelova et al., 2002). Therefore, enhanced inhibition keeps spontaneous firing low and enhanced excitability keeps recurrent network activity high when pyramidal neurons receive stimulation. In contrast, activation of D2-type receptors decreases NMDA, AMPA and $GABA_A$ receptor mediated currents in pyramidal neurons, allowing more spontaneous firing, and weakening connections between cells (Li et al., 2009; Rosen et al., 2015b; Seamans et al., 2001; Trantham-Davidson et al., 2008; Tseng and O'Donnell, 2007a; Zheng et al., 1999); but see (Gonzalez-Islas and Hablitz, 2003). Selective D2R activation makes it easier to release the contents of working memory and redirect attention to new rules (Floresco et al., 2006). Notably, rapid (<1s) application of small localized doses of D1- and D2-type receptor agonists by iontophoresis elicits effects on pyramidal neuron excitability that are opposite to those observed with treatments applied on a longer time scale, providing more evidence for the fundamental differences in cellular responses to phasic and tonic modes of receptor activation (Moore

et al., 2011). Furthermore, phasic dopamine appears to increase shaeffer collateral pathway responses via D1R activation whereas low levels of dopamine simulating tonic dopamine neuron firing depress shaeffer collateral pathway responses via a D4R-dependent mechanism (Rosen et al., 2015b). Although activation of D1- and D2-type receptors typically act through opposing signaling pathways, they often synergize in the modulation of neuronal properties. For instance, D1-type and D2-type receptors work synergistically to enhance spike-timing dependent LTP (t-LTP) (Xu and Yao, 2010). T-LTP enhances the storage of information in neural networks in which pyramidal neurons fire infrequently (Singer, 1993). Specifically, D2-type receptor activation suppresses GABA release from local interneurons that typically gate the induction of t-LTP, and D1-type receptor activation at excitatory synapses allows t-LTP at an extended time window (Xu and Yao, 2010). Therefore, dopamine facilitates synaptic potentiation in cortical circuits. Gamma oscillations also may serve as a temporal template for t-LTP (Axmacher et al., 2006). Thus dopamine may also enhance t-LTP through the modulation of gamma oscillations.

1.4.4 Dopamine and gamma oscillations

Rhythmic oscillations are a basic feature of neural networks, and reflect the temporal and spatial integration of large numbers of neurons within and across brain regions. A large number of psychiatric and neurological disorders, including schizophrenia, ADHD, autism, epilepsy and Alzheimer's disease, display altered gamma frequency oscillations within the PFC and cortico-subcortical networks (Herrmann and Demiralp, 2005). While the importance of network oscillations for cognitive function has

long been known, only a few studies have examined the role of dopamine in PFC oscillations.

Available evidence from human and rodent EEG studies suggests that dopamine increases the power of neural oscillations in the PFC, but has little effect on their induction or frequency. Persons with prolonged event-related increases in dopamine due to polymorphisms in the dopamine transporter gene *DAT1* show an increase in evoked gamma power in response to target stimuli (Demiralp et al., 2007). In healthy subjects, antagonizing D2R with haloperidol reduces gamma power in response to attended stimuli in the contralateral hemisphere (Ahveninen et al., 2000). Similarly, the increase in gamma power in the mPFC observed during a treadmill walking task which requires attention is dependent on dopamine (Delaville et al., 2015). A 6-hydroxydopamine (6-OHDA) lesion to the substantia nigra eliminates this peak for ~3 weeks. Surprisingly, it later returns, perhaps due to another compensatory mechanism (Delaville et al., 2015). Additionally, rats with ketamine-induced gamma oscillations show a reduction in gamma power in the cortex when given either clozapine or haloperidol, both antipsychotics that target D2-type receptors (Anderson et al., 2014; Jones et al., 2012). Dopamine is also important for increased coherence of gamma rhythms between the internal globus pallidus and the motor cortex, a process known as ‘motor binding’ that underlies the organization of normal voluntary movement (Engel et al., 2005).

Theta oscillations are a predominant frequency in the hippocampus during active behavior, and depleting dopamine in the hippocampus decreases theta activity (Nakagawa et al., 2000), while injecting dopamine or apomorphine into the medial

septum increases hippocampal theta oscillations (Miura et al., 1987). Moreover, direct infusion of dopamine into the PFC of anesthetized rats increases theta oscillation coherence between the PFC and the hippocampus, a process that is believed to underlie reward prediction (Benchenane et al., 2011). These findings suggest that dopamine can augment the power of theta and of gamma oscillations, and increase the coherence of distributed networks oscillating at theta frequencies.

In slices with intact dopaminergic projections, exogenous dopamine can dose-dependently modulate cyclical changes in resting membrane potential called up-and down-states (Kroener et al., 2009). Gamma oscillations can be induced in slices by electrical stimulation or by agonists for kainate or metabotropic acetylcholine receptors. Dopamine increases the power and duration of stimulation-induced gamma oscillations in hippocampal area CA1 (Wójtowicz et al., 2009), but decreases the power and duration of carbachol induced oscillations in CA1 (Weiss et al., 2003) and kainate-induced oscillations in CA1 and CA3 (Wójtowicz et al., 2009), but see (Andersson et al., 2012b). These variances might be partly explained by differences in the mechanisms underlying each type of oscillation, and by differences in dopamine receptor activation. Nonetheless, pharmacological analysis of the involvement of dopamine in *in-vitro* gamma oscillations has proven informative. For example, antipsychotics including clozapine and haloperidol inhibit cholinergic hippocampal CA3 gamma oscillations (Schulz et al., 2012). Clozapine also suppresses synchronized pyramidal network activity in layer 5 of the PFC (Gao, 2007). Furthermore, activation of the D1-type receptors decreases carbachol-induced gamma oscillation power (Weiss et al., 2003), while D4R activation increases gamma

oscillation power in the hippocampus in kainate-induced oscillations(Andersson et al., 2012a; see also Section 1.5.7). These findings show that dopamine effects on oscillations are complex and depend on a large number of factors.

1.4.5 Modulation of fast-spiking interneuron properties by dopamine

Even small changes in interneuron function can produce large changes in gamma oscillations (Kopell et al., 2000; Whittington et al., 2011). Three key determinants of the power and frequency of gamma oscillations are 1) the magnitude and 2) kinetics of synaptic inhibition between interneurons, and 3) the driving excitatory current onto interneurons (Traub et al., 1996). Networks of FSI interconnect through chemical and electrical synapses that augment gamma activity by increasing FSI sensitivity to coherent excitatory inputs. Nonselective stimulation of dopamine receptors by exogenous dopamine appears not to change the electrical coupling of interneurons through gap junctions (Towers and Hestrin, 2008). However, selective activation of D1-type receptors reduces coupling (Hampson et al., 1992) while activation of D2-type receptors increases coupling (Onn and Grace, 1994), suggesting opposing effects of different dopamine receptor types. Moreover, dopamine acting through D1-type receptors decreases the amplitude of IPSCs in FSI (Towers and Hestrin, 2008). Dopamine also changes the intrinsic properties of FSI by increasing the firing rate of PV+ FSIs *in vivo* (Tseng et al., 2006), and *in vitro* (Gao and Goldman-Rakic, 2003; Gorelova et al., 2002; Kröner et al., 2007; Trantham-Davidson et al., 2008; Zhou and Hablitz, 1999); but see (Tierney et al., 2008).

By reducing spontaneous firing in PV+ interneurons, dopamine augments temporal precision and thereby sharpens the spike timing of FSI (Gao and Goldman-Rakic, 2003; Tierney et al., 2008). Furthermore, D1-type and D2-type receptors increase the amplitude and opening kinetics of the h-current, an inwardly rectifying hyperpolarization-activated nonselective cation current, in interneurons (Wu and Hablitz, 2005). Likewise, dopamine activation reduces potassium currents, increasing the probability of repetitive firing (Gorelova et al., 2002; Schreiber et al., 2004). Computational modeling suggests that D4Rs may modify potassium currents to increase gamma power (Kuznetsova and Deth, 2008), although experimental verification is still pending. See sections 1.5.6 and 1.5.7 for a detailed discussion of D4R effects on synaptic and intrinsic properties and on gamma oscillations.

1.4.6 Maturation of dopamine signaling

As discussed earlier, PFC circuits finish maturing during adolescence and early adulthood, a period of high vulnerability to first psychotic episode in persons with schizophrenia. Maturation involves concomitant changes in responses to dopamine, receptor composition in FSI, and gamma-band activity during cognitive performance. From childhood to early adolescence, gamma frequency oscillations dominate most cortical regions, and their power correlates with increases in cognitive performance (Uhlhaas et al., 2009). Strikingly, gamma oscillations ebb during adolescence then increase dramatically in early adulthood (Uhlhaas et al., 2009). At the end of this period, dopamine exerts strong control over excitation/inhibition balance and thereby aids in the

selection of adequate behavioral responses and the suppression of poor behavioral choices (O'Donnell, 2011).

Dopamine receptor expression and signaling change with age in rodents (O'Donnell, 2011) . D1Rs, D2Rs, and D4Rs increase in density in the PFC through adolescence, and then show a reduction in adult animals (Andersen et al., 2000; Brenhouse et al., 2008; Naneix et al., 2012); but see (Tarazi and Baldessarini, 2000). Furthermore, the D1-type receptor agonist SKF38393 increases the intrinsic excitability of FSI in slices from both adult (PD>50) and juvenile (PD<35) rats, while the D2-type receptor agonist quinpirole increases FSI excitability in post- but not pre-pubertal slices (Tseng and O'Donnell, 2007b). Similarly, in slices from prepubertal rats, co-administration of a D1-type agonist and NMDA only excites pyramidal neurons for tens of milliseconds, but in adults it creates plateau depolarizations lasting several hundred of milliseconds (Tseng and O'Donnell, 2005).

Mature FSI have faster membrane oscillations and spikes, less adaptation, and less NMDAR contribution (Belforte et al., 2010; Goldberg et al., 2011; Okaty et al., 2009; Rotaru et al., 2011; Wang and Gao, 2009, 2010). Dopamine innervation and signaling might play a role in the development of FSI and in shaping this mature phenotype. Treatment with dopamine or coculture with mesencephalic slices accelerates PV+ interneurons maturation in rat organotypic slices from the frontorbital cortex and increases the density of PV+ cells in deep cortical layers (Porter et al., 1999; Ross and Porter, 2002). Moreover, elevation of prenatal dopamine levels by intrauterine cocaine exposure increases the ramification of PV+ interneurons in the anterior cingulate, a

cortical area receiving dense dopaminergic innervation, but not the primary visual cortex, an area that receives little dopaminergic innervation (Wang et al., 1995). Conversely, 6-OHDA lesions in the medial forebrain bundle cause a reduction of the density of PV expressing cells in the zona incerta of the diencephalon without reducing the total number of cells, suggesting that dopamine is required for the maintenance of a mature FSI phenotype (Heise and Mitrofanis, 2005). These findings are consistent with the notion that the dopamine system is a critical modulator of GABAergic interneurons during postnatal maturation of cortical connectivity (O'Donnell, 2011), and that persons with schizophrenia exhibit reduced PV and GAD67 immunoreactivity (Lewis et al., 2011). Hence, one possible treatment goal in schizophrenia might be the preservation or restoration of normal FSI function.

1.5 Properties of the dopamine D4 receptor

1.5.1 Historical identification of the D4R

Following the cloning of the genes and cDNAs for the prototypical D2R and D1R, the gene for the human dopamine D4R (gene symbol: *DRD4*) was isolated in 1991 by homology cloning in an effort to identify additional D2-related receptors (Van Tol et al., 1991). Similar to the other D2-type receptors, it contains short amino-terminal extracellular and carboxyl-terminal intracellular tail domains, and a fairly long third intracellular loop. *DRD4* orthologs in humans and other higher primates additionally contain a polymorphic (2-10) number of tandem 48 nucleotide repeats located in the sequence encoding the third cytoplasmic loop (Van Tol et al., 1992), with 4 and 7 repeats being the most common variants overall but with substantial regional and ethnic

differences in frequencies (Chang et al., 1996). D4R variants show different potencies for dopamine. Using the amplitude of G protein-induced inwardly rectifying potassium currents to determine receptor activation, dopamine was 5 times more potent at the D4.2 and D4.7 receptor variants than the D4.4 receptor variant (Wedemeyer et al., 2007). However, the D4.7 receptor is two times less effective than the D4.2 or D4.4 receptor at inhibiting cyclic AMP production (Asghari et al., 1995). The D4.7 variant is associated with increased risk for ADHD (see Section 1.5.2), and altered cortical gamma oscillation power (Demiralp et al., 2007).

1.5.2 Pharmacological properties and involvement in psychiatric disorders

Initial pharmacological analyses indicated that D4R has a higher affinity for clozapine than the closely related D2R, and was therefore proposed to consitute the main pharmacological target of this efficacious atypical antipsychotic receptors (Van Tol et al., 1991). In contrast to typical or first-generation antipsychotics, extrapyramidal effects are observed to a lesser extent, or not at all, in patients treated with clozapine. While these findings generated excitement early on, subsequent studies argued against the possible utility of D4R-targeting drugs to treat the positive symptoms of schizophrenia. Most importantly, novel, more selective D4R antagonists such as L-745,870 and sonepiprazole were largely ineffective as neuroleptics in clinical trials (Bristow et al., 1997; Corrigan et al., 2004; Kramer et al., 1997). Consistent with this, clozapine is known to target numerous other receptor systems with low nanomolar affinities, including serotonergic (5-HT2), muscarinic and β-adrenergic receptors (Baldessarini and Frankenburg, 1991), and it was concluded that its efficacy as a neuroleptic reflected a much more complex

multi-target pharmacology with a significant contribution from serotonergic receptors (Meltzer and Huang, 2008). These findings, taken together with genetic association studies that largely failed to identify *DRD4* polymorphic variants as risk factors (Jonsson et al., 2003), dampened enthusiasm to pursue the D4R as a promising antipsychotic drug target for schizophrenia.

However, the D4R soon re-emerged as a genetic risk factor for ADHD, a heterogeneous but highly heritable syndrome characterized by a variable combination of persistent, pervasive and developmentally inappropriate levels of inattention, hyperactivity and impulsiveness that typically lead to poor academic performance (APA, 1994). Perturbations of catecholaminergic pathways are a leading hypothesis in ADHD, and dopaminergic drugs such as methylphenidate are clinically efficacious. Consistent with this, numerous ADHD candidate genes including *DRD4*, *DAT1*, *COMT*, *MAOA* and *DBH* are integral parts of the catecholaminergic neurotransmission system. Both case-control and family-based association studies reported increased transmission of the polymorphic *DRD4.7* variant (for example, LaHoste et al., 1996; Rowe et al., 1998; Smalley et al., 1998; Swanson et al., 1998) and other polymorphisms (Arcos-Burgos et al., 2004; Barr et al., 2000) in children diagnosed with the syndrome. Subsequent meta-analyses supported a linkage between the *DRD4.7* allele and ADHD (for example, Faraone et al., 2001; Maher et al., 2002).

1.5.2.1 Cognitive effects of acute D4R activation

Although D4R antagonists proved ineffective as antipsychotics, D4R targeting drugs have been examined in cognitive tasks in monkeys and rodents. For the most part,

D4R agonists increase working memory performance and fear acquisition according to an inverted U-shaped response curve (Bernaerts and Tirelli, 2003; Browman et al., 2005; Murai et al., 2014; Nakazawa et al., 2015; Woolley et al., 2008); but see (Nayak and Cassaday, 2003). Interestingly, D4R antagonists have paradoxical promnesic effects at low doses (Zhang et al., 2004). Specifically, low doses of D4R antagonists reverse working memory deficits induced by stress or chronic PCP administration in monkeys (Arnsten et al., 2000; Jentsch et al., 1999). Furthermore, rats with low baseline memory performance showed the greatest improvements to low doses of the D4R antagonist L-745,870 and impairments at high doses, while rats with high baseline memory performance were impaired by administration of L-745,870 at every concentration (Zhang et al., 2004).. In the rat, intra-mPFC injection of L-741,741, another highly selective D4R inhibitor, blocks the acquisition (but not expression) of fear conditioning and the encoding of emotional memory by mPFC neurons (Laviolette et al., 2005). Conversely, mPFC injection of the D4R agonist PD168077 increases the salience of sub-threshold foot shocks while it blocks the acquisition of fear conditioning in response to supra-threshold foot shocks (Lauzon et al., 2009; Tye et al., 2009). Additionally, the D4R agonists A-412997 and PD168077 enhance memory for aversive stimuli according to an inverted U-shaped curve (Browman et al., 2005), but have also shown linear increases in working memory performance in a similar procedure and a novel object recognition paradigm (Bernaerts and Tirelli, 2003; Woolley et al., 2008). Taken together, these results suggest that the D4R mediates memory consolidation of both normal and emotionally salient experiences, and that the intensity of the stimulus interacts with

dopamine signaling through D4Rs.

1.5.3 D4R expression in fast-spiking PV+ interneurons

A number of studies have found D4R mRNA and protein in PV+ interneurons of both the PFC and the hippocampus. Expression in these neurons was first observed in the monkey by double immunohistology using a carefully characterized polyclonal antibody against the extracellular aminoterminus of the receptor (Mrzljak et al., 1996). Immunoreactive cells were found in PFC layers III-V and in hippocampal area CA1. In both areas, strongly labeled PV-interneurons were accompanied by lightly labeled pyramidal neurons. This study also found intense D4R immunoreactivity in the rodent globus pallidus (homologous to the primate external globus pallidus), and thalamic reticular nucleus, which are both made up entirely of GABAergic projection neurons. Evidence for D4R expression in PV-positive interneurons also comes from a single-cell RT-PCR study of acutely isolated rat PFC neurons (Vysokanov et al., 1998). Moreover, reporter gene expression was detected in PFC pyramidal neurons and interneurons, some of them expressing PV, in mice harboring a bacterial artificial chromosome (BAC) transgene in which the green fluorescent protein was expressed under the transcriptional control of the *Drd4* locus (Noain et al., 2006). Two groups additionally investigated D4R expression in GABAergic interneurons using double-in situ hybridization for D4R and GAD67, and identified co-expressing cells in layer V of the monkey PFC (de Almeida and Mengod, 2010; de Almeida et al., 2008) and in the mouse hippocampus (Andersson et al., 2012b). The latter study also employed double-immunohistochemistry using an antibody raised against the extracellular amino-terminus of the rat D4R (Ariano et al.,

1997) and found that the majority (71%) of D4R+ neurons in areas CA1 and CA3 co-express PV and that conversely 21% of PV-interneurons co-express D4R. In aggregate, what emerges from all these findings is the notion that in the PFC, both local GABAergic interneurons and pyramidal neurons express D4R transcript and protein while in the hippocampus the evidence favors D4R expression largely in GABAergic interneurons.

1.5.4 Behavioral phenotypes of mice lacking D4R function

1.5.4.1 Locomotor effects

An initial behavioral analysis of mixed-background *Drd4*$^{-/-}$ mice revealed locomotor hypoactivity and increased sensitivity to locomotor-stimulating effects of acute ethanol, cocaine and methamphetamine injections, indicative of deficits in nigrostriatal function (Rubinstein et al., 1997). Amphetamine hypersensitivity was confirmed in a subsequent study using *Drd4*$^{-/-}$ mice congenic on the C57Bl/6J background, and expanded to also include altered behavioral sensitization to repeated amphetamine injections (Kruzich et al., 2004). At the neurochemical level, *Drd4*$^{-/-}$ mice exhibit altered striatal dopamine metabolism (Rubinstein et al., 1997), and lower baseline and KCl-evoked extracellular striatal dopamine levels (Thomas et al., 2007). In contrast, dopamine synthesis and turnover in the PFC of mutant mice is not different (Rubinstein et al., 2001). Evidence in favor of a role of the D4R in regulating motor activity also comes from studies reporting that D4R antagonism restores normal locomotor activity in periadolescent rats rendered transiently hyperactive by neonatal 6-OHDA lesions (Zhang et al., 2001). These lesions reduce dopaminergic projections to the forebrain and serve as a neurodevelopmental model of ADHD with good face validity, reproducing a number of

its core symptoms. Strikingly, 6-OHDA-mediated hyperactivity is absent in *Drd4*$^{-/-}$ mice (Avale et al., 2004). Although these findings strongly suggest a role for the D4R in mediating behavioral responses to perturbed dopamine function in the striatum, it remains unclear if these effects originate, as suggested, in a hyperexcitable PFC or elsewhere, and what molecular and cellular D4R-dependent processes underlie them.

1.5.4.2 Cognitive effects

The involvement of the D4R in cognitive functions, in particular avoidance behavior and emotional learning, has been analyzed in both mutant mice as well as in acute pharmacological paradigms (see Section 1.5.2.1). Dulawa and colleagues found that novelty-induced behavioral responses were reduced in *Drd4*$^{-/-}$ mice compared to wild-type controls with little effect on anxiety (1999). While this report concluded that D4R deficiency did not affect avoidance behavior, a different study found *Drd4*$^{-/-}$ mice exhibit heightened anxiety in the elevated plus maze and light/dark preference exploration tests that was ameliorated by ethanol and the benzodiazepine midazolam (Falzone et al., 2002). The fact that these anxiolytic drugs work by increasing GABAergic transmission, taken together with prominent D4R expression in the PFC, striatal dopamine dysregulation and increased excitability of PFC neurons from mutant mice (Rubinstein et al., 2001), was interpreted as indicative of altered PFC control of striatal dopamine release in *Drd4*$^{-/-}$ mice. On the other hand, acute pharmacological inhibition of D4R in the rat medial PFC by L-745,870 injection was shown to be anxiolytic in the elevated plus maze and shock-probe burial test (Shah et al., 2004). Taken together, these findings suggest that the D4R is involved in emotional learning, but that the effects of receptor

interference depend on the experimental approach utilized (acute/local/pharmacological vs. chronic/global/genetic). Consistent with this notion, studies have found secondary changes in *Drd4*$^{-/-}$ mice, including upregulation of D1- and NMDAR expression and increased striatal glutamate that might reflect compensatory responses to a lack of D4R function in mutant mice (Gan et al., 2004; Thomas et al., 2009).

Consistent with the notion of altered PFC function, micro-PET imaging experiments indicate reduced baseline PFC glucose metabolism in *Drd4*$^{-/-}$ mice (Michaelides et al., 2010). Moreover, methylphenidate decreases PFC glucose metabolism in normal mice but increases it in mutants (Michaelides et al., 2010). It is unclear to what extent these metabolic changes are directly linked to the lack of D4R function in these mice, or to compensatory changes like the ones mentioned above. Interestingly, while *Drd4* homozygous mice are normal in behavioral tests of attention and impulsivity (Helms et al., 2008; Young et al., 2011), *Drd4* heterozygous mice exhibit less response inhibition in the 5 choice – continuous performance task (Young et al., 2011). This observation is consistent with a lack of secondary neurochemical changes in *Drd4*$^{+/-}$ mice (Thomas et al., 2007) and might therefore represent a true hypomorphic D4R phenotype that is not occluded by compensatory neural adaptations observed in the full mutants.

1.5.5 Synaptic effects of D4Rs

1.5.5.1 Effects on cortical microcircuits

Cellular effects of D4R signaling in neurons have mostly been studied using electrophysiological recordings in brain slices, acutely dissociated neurons or long-term

neuron cultuResearch Importantly, many of the effects discussed below were observed using high concentrations of the D4R agonist PD168077 that may also activate adrenergic α1A and α2C as well as serotonergic 5HT1A receptors (Moreland et al., 2005). At the local circuit level, Onn and colleagues found that in PFC slices with intact synaptic connections between axon collaterals and recorded neurons, D4R inhibition causes complex evoked spike discharges in pyramidal neurons, but only with intact GABAergic transmission (2006). The authors suggest that dopamine signaling bi-directionally regulates PFC pyramidal neuron excitability via D1R and D4R-dependent pathways, respectively, and that D4Rs reduce pyramidal neuron excitability through their tonic activity by low ambient levels of dopamine. Consistent with these results, *Drd4*$^{-/-}$ mice exhibit hyperexcitability of PFC pyramidal neurons and are more sensitive to bicuculline (Rubinstein et al., 2001). Although these findings indicate a possible role of D4Rs in promoting GABAergic transmission onto PFC pyramidal neurons, acute assessments of the effects of pharmacological D4R perturbations on GABAergic interneuron function have yielded mixed results (Gao, 2007; Gorelova et al., 2002). The possibility that D4R effects might vary between different cortical areas has to be considered as well, as pharmacological data from the prelimbic cortex suggest that D4Rs actually facilitate pyramidal neuron firing (Ceci et al., 1999). A different study in the mPFC found the D4R activation did not significantly influence the intrinsic excitability of pyramidal neurons, but increased the excitability of FS PV+ interneurons (Trantham-Davidson et al., 2014). These increases in excitability after D4R activation were mediated by the Kv3.1/3.2 channel, and were not observed in animals with chronic alcohol

exposure during development. Despite increases in PV+ interneuron excitability after D4R activation, evoked IPSCs measured on pyramidal neurons decreased after bath application of the D4R agonist (Trantham-Davidson et al., 2014).

1.5.5.2 Inhibition of ionotropic receptors

Various studies using neuronal preparations from the PFC, the hippocampus and the rodent globus pallidus have consistently found pharmacological D4R activation to decrease postsynaptic currents and surface expression of both excitatory and inhibitory ionotropic receptors (see Tables 1 and 2). GABA current amplitude and surface expression of $GABA_AR$ $\beta_{2/3}$ clusters are decreased in PFC pyramidal neurons after treatment with relatively high concentrations (30 μM) of the D4R agonist PD168077 (Graziane et al., 2009; Wang et al., 2002). Agonist treatment also reduces $GABA_A$ IPSCs in globus pallidus GABAergic neurons in wild-type mice but not in *Drd4*$^{-/-}$ mice (Shin et al., 2003). However, D4R activation does not affect GABA current amplitude in hippocampal pyramidal neurons during ongoing kainate-induced oscillations (Andersson et al., 2012a). These data correlate with the expression of D4Rs on PFC pyramidal and globus pallidus GABAergic neurons (Ariano et al., 1997; Mrzljak et al., 1996), but not in hippocampal pyramidal neurons (Andersson et al., 2012b), and suggest that effects on GABAergic transmission are cell-autonomous.

D4R stimulation also reduces NMDA and AMPA receptor-mediated currents. NMDAR-mediated currents and surface expression decrease in acutely isolated PFC and hippocampal pyramidal neurons in response to agonist treatment (Beazely et al., 2006; Kotecha et al., 2002; Wang et al., 2003), although the downstream signaling pathways

may differ between the PFC and hippocampus (see Section 1.5.6). Similar effects were reported in pyramidal neurons from acute PFC slices (Trantham-Davidson et al., 2014), in projection neurons of the lateral amygdala (Martina and Bergeron, 2008), and in hippocampal area CA1 where NMDAR-dependent induction of LTP induction in *stratum oriens* was inhibited by D4R activation (Herwerth et al., 2012). Intriguingly, in PFC slices from animals treated with the NMDAR antagonist PCP, a psychotomimetic drug that can elicit effects remarkably similar to the symptomology of schizophrenia (Jentsch et al., 1999), D4R activation no longer inhibits NMDAR-mediated currents, although the cellular mechanisms underlying this effect are not known (Wang et al., 2006).

In pyramidal neurons of the PFC, but not the hippocampus, acute D4R activation was also shown to reduce baseline AMPAR-mediated currents and surface expression in pyramidal neurons (Andersson et al., 2012a; Kwon et al., 2008; Yuen et al., 2010); but see (Gu et al., 2006; Rubinstein et al., 2001). High concentrations of PD168077 also reduce baseline AMPAR-mediated currents and surface expression in PFC interneurons (Graziane et al., 2009). Furthermore, recent data suggest that D4R effects on AMPARs may at least in part be state-dependent. In cultured hippocampal neurons expressing the D4R, agonist treatment has no effect of baseline AMPAR surface expression but internalizes GluA1-containing AMPARs following a chemical form of LTP (Kwon et al., 2008). In PFC pyramidal cells, PD168077 decreases AMPAR-mediated currents when slices are pretreated with bicuculline to increase overall activity but increases AMPAR-mediated currents in slices pretreated with TTX to reduce overall activity (Yuen and Yan, 2011; Yuen et al., 2010). D4Rs also reverse early LTP at Schaeffer collateral-to-CA1

glutamatergic synapses by reversing AMPAR EPSCs back to pre-LTP levels (Kwon et al., 2008). New evidence suggests that this may be a circuit-based effect. Dopamine released from VTA fibers increases the EPSPs from the Schaeffer collateral pathway onto PV+ interneurons in the pyramidal layer through the activation of D4 receptors (Rosen et al., 2015b). This produces feedforward inhibition which suppresses the EPSPs from the Schaeffer collateral pathway onto pyramidal neurons in the CA1 (Rosen et al., 2015b). Intriguingly, brief dopamine release via optogenetic dopaminergic fiber stimulation decreased EPSPs at Schaeffer collateral-to-CA1 glutamatergic synapses, whereas tonic dopamine bath application, or bursts of optogenetic activity increased EPSPs at these synapses (Rosen et al., 2015b), demonstrating that tonic and phasic dopamine produce different circuit-level responses via the D4 receptor. Taken together, with the observation that *Drd4*$^{-/-}$ mice have dramatic increases in glutamatergic signaling (Rubinstein et al., 2001), these data suggest that the D4R is involved in homeostatic processes that serve to maintain overall glutamatergic excitability within a physiological range.

postsynaptic current	**Increase/ Decrease**	**Cell Type**	**Region**	**Citations**
AMPA	↑at low synaptic activity	Pyramidal	PFC	Yuen and Yan, 2011; Yuen et al., 2010; but see Rubinstein et al., 2001; Onn et al., 2006
AMPA	↓ at high synaptic activity	Pyramidal	PFC, Hippocampus	Kwon et al., 2008; Yuen et al., 2010; Yuen and Yan, 2011
AMPA	↓	Interneuron	PFC	Yuen and Yan, 2009; Yuen et al., 2010
NMDA	↓	Pyramidal	PFC,	Kotecha, Oak, et al., 2002;

			hippocampus, lateral amygdala	Wang, Zhong, et al., 2003; Beazely et al., 2006; Wang et al., 2006; Martina and Bergeron, 2008; Herwerth et al., 2012, Trantham-Davidson et al., 2014
GABA	↓	Pyramidal, various others	PFC, hippocampus, septal nucleus, thalamus, globus pallidus, subthalamic nucleus, substantia nigra	Wang et al., 2002; Shin et al., 2003; Florán et al., 2004a, 2004b; Asaumi et al., 2006; Acosta-García et al., 2009; Graziane et al., 2009; Gasca-Martinez et al., 2010; Govindaiah et al., 2010; Andersson et al., 2012a, Trantham-Davidson et al., 2014
VGCC	↓	Pyramidal, granule cells	PFC, cerebellum	Mei et al., 1995; Wang et al., 2006
K^+ channel: inward rectifying	↑		Cultured Neurons	Werner et al., 1996; Pillai et al., 1998; Lavine et al., 2002; Wedemeyer et al., 2007
K^+ channel: outward current	↓	Fast-spiking interneurons	Hippocampus	Andersson et al., 2012a
K+ channel: delayed rectifier	↑	Fast-spiking interneurons	PFC	Trantham-Davidson et al., 2014

Table 1. Postsynaptic effects of D4R activation on evoked and mini amplitudes, and changes in firing rate.

Presynaptic release	**Increase/ Decrease**	**Cell Type**	**Region**	**Citations**
AMPA	↓	Pyramidal	PFC	Rubinstein et al., 2001
AMPA	No change	Interneuron	PFC, hippocampus	Yuen and Yan, 2009; Andersson et al., 2012a
GABA	↓	Various	Hypothalamus,	Azdad et al., 2003;

			septal nucleus, thalamus	Baimoukhametova et al., 2004; Asaumi et al., 2006; Gasca-Martinez et al., 2010

Table 2. Presynaptic effects of D4R receptor activation (PSP frequency).

1.5.5.3 Effects on ion channels

D4R activation decreases voltage-gated calcium channel currents in acute PFC slices and cultured cerebellar granule cells (Mei et al., 1995; Wang et al., 2006). Heterologously expressed D4Rs also couple to GIRK channels in *Xenopus* oocytes (Wedemeyer et al., 2007; Werner et al., 1996) through a Gβγ-dependent mechanism (Pillai et al., 1998). In principle, both activities are well suited to reduce neurotransmitter release from presynaptic nerve terminals. Consistent with this notion, the D4R agonist PD168077 reduces the frequency of mIPSCs onto layer 5 pyramidal neurons indicative of reduced GABA release from local interneurons (Gao, 2007). Moreover, D4Rs modulate transmitter release in various midbrain regions receiving GABAergic projections from the globus pallidus (Acosta-García et al., 2009; Asaumi et al., 2006; Baimoukhametova et al., 2004; Florán et al., 2004a, 2004b; Gasca-Martinez et al., 2010). As mentioned earlier, globus pallidus GABAergic neurons express high levels of D4R (Mrzljak et al., 1996). Ablation of globus pallidus neurons by kainate injection prevents the inhibitory effects of PD168077 in the thalamic reticular nucleus and the substantia nigra (Acosta-García et al., 2009; Gasca-Martinez et al., 2010). Effects on presynaptic calcium currents may also contribute to reduced glutamate release (Romo-Parra et al., 2005; Rubinstein et al., 2001; Yuen et al., 2010).

1.5.6 D4R signaling partnerships

Dopamine receptors were initially classified according to their ability to positively or negatively couple to adenylyl cyclase to promote the production of the intracellular second messenger cAMP. Additionally, D2-type receptors mediate many of their physiological functions via liberation of Gβγ subunits and subsequent modulation of effectors such ion channels and receptors either by direct binding or by activation of intracellular signaling pathways such as phospholipase C and MAP kinase. For general reviews on dopamine signaling pathways downstream of heterodimeric G-proteins the reader is referred to a number of excellent earlier reviews on the subject (Beaulieu and Gainetdinov, 2011; Gainetdinov et al., 2004; Greengard et al., 1999; Missale et al., 1998). I will instead focus on signaling partnerships of the D4R with other G-protein coupled receptors (GPCR) and with receptor tyrosine kinases (RTK) in the regulation of neuronal function, as many of the described D4R effects in the central nervous system are tightly linked to the functional association with other receptor systems. These synergistic partnerships encompass both direct and functional interactions between receptors.

1.5.6.1 Partnerships with G-protein coupled receptors

It is now widely accepted that dopamine receptors and other GPCRs can form homomeric and heteromeric structures, and that these multimolecular aggregates can affect both ligand binding as well as signaling characteristics of their constituent subunits (Ferre et al., 2007, 2009). Recent studies have shown that the D4R heteromerizes with the both the long and the short forms of the D2R (Borroto-Escuela et al., 2011; González et al., 2012a). Furthermore, neurochemical evidence suggests that interactions between D4R

and D2S receptors mediate dopamine modulation of neurotransmitter release from corticostriatal glutamatergic projections where these receptors are co-expressed (González et al., 2012a). Intriguingly, heteromerization with D2S receptors was observed with D4R variants harboring 2 or 4, but not 7 tandem repeats, and engineered mice with the human 7-repeat version knocked into the mouse *Drd4* locus failed to show increased glutamate release in the striatum in response to co-activation of D2Rs and D4Rs (González et al., 2012a). These findings are especially relevant in light of the implication of the 7-repeat allele of the human *DRD4* gene in psychiatric disorders. A second interaction was recently reported between the D4R and α_{1B} or β1 adrenergic receptors in the pineal gland where these receptors synergize to regulate circadian melatonin synthesis (González et al., 2012b).

1.5.6.2 D4R partnerships with receptor tyrosine kinases

Functional interactions between GPCRs and RTKs have been known for many years (Daub et al., 1996). These interactions are typically functional, rather than physical, and mostly manifest as transactivation of a RTK by a GPCR (Ferguson, 2003). An early example of transactivation of a dopamine receptor involves the regulation of NMDAR function and surface expression by D4Rs (see Section 1.5.5.2). The downstream signaling pathway linking D4R activation in PFC neurons involves protein kinase A inhibition and activation of protein phosphatase 1, effects typically attributed to canonical inhibitory G-protein signaling (Wang et al., 2003). However, D4R-mediated NMDAR internalization in hippocampal neurons depends not on PKA inhibition, but rather on transactivation of the platelet-derived growth factor receptor (PDGFR), and involves

activation of a phospholipase C / IP3 / Ca^{2+} signaling pathway (Kotecha et al., 2002). Interestingly, NMDAR internalization in the PFC in response to PDGFR transactivation by dopamine is mediated by D2Rs but not D4Rs (Beazely et al., 2006). This is one of many examples of a significant region-specific difference in the intracellular signaling of the D4R. The D4R is also tightly linked to the acute effects of the NRG/ErbB4R signaling pathway in the central nervous system (see Section 1.6.4 and 1.6.5).

1.5.7 D4R and gamma oscillations

D4R activation simultaneously increases gamma-frequency LFP power and measures of cognition. The D4R agonist A-412,997 increases gamma power in prefrontal, occipital and parietal cortices in awake, behaving rodents (Kocsis et al., 2014). Furthermore, a partial D4R agonist, Ro 10-5824 concurrently increases frontal cortical gamma power and performance on the object retrieval detour task in marmosets (Nakazawa et al., 2015). Moreover, indirect evidence already exists that D4Rs in the human cortex modulate gamma oscillations. Carriers of the 7-repeat *DRD4* allele (*DRD4.7*) show enhanced evoked and induced gamma oscillations in the frontal and association cortices in response to auditory stimuli (Demiralp et al., 2007). This increase in evoked gamma oscillations does not discriminate between target and filler stimuli, suggesting that it is harder for subjects to distinguish between salient and distracting stimuli, a finding that is consistent with the association of the *DRD4.7* allele with ADHD and potentially cognitive function in other psychiatric disorders (see Section 1.5.2). Importantly, the 7R variant has half the potency of more common third-loop repeat variants for inhibiting cAMP (Asghari et al., 1995) and less effectively forms

heterodimers with the long and short variants of the D2R (Borroto-Escuela et al., 2011; González et al., 2012a). If the modulation of gamma rhythms in individuals carrying the *DRD4.7* polymorphism is indeed compromised, the prediction would be that normal D4R function enhances signal-to-noise ratios by suppressing gamma rhythms in response to non-salient sensory stimuli. At least in principle, the finding that D4Rs decrease AMPAR-mediated currents in interneurons in the PFC (Yuen and Yan, 2009), and that decreased excitatory drive onto PV+ interneurons reduces gamma oscillation power (Rotaru et al., 2011), correlates well with increases in gamma in subjects carrying the *DRD4.7* allele.

As touched upon previously, patients with schizophrenia have elevated ongoing gamma power and reduced sensory-evoked or task-related gamma power (see Section 1.2.1). It follows that lowering the ongoing gamma power in a patient with schizophrenia would increase the signal-to-noise ratio of the evoked oscillations during sensory perception and cognitive tasks. Given that fact that the D4R agonist increases gamma power in normal animals (Kocsis et al., 2014), and it is hypothesized that lowering baseline gamma power will have pro-cognitive effects in schizophrenia patients (Gilmour et al., 2012), the D4R antagonist may actually be a better pro-cognitive target, as the D4R antagonist could be expected to lower ongoing gamma oscillation power in schizophrenia patients. On the other hand, humans with a subsensitive variant of the D4R, which in principle may mimic the effects of D4R antagonism, have reduced signal-to-noise ratios for gamma oscillations in response to auditory stimuli (Demiralp et al., 2007). It remains

to be seen whether a D4R agonist or antagonist will have a greater effect on gamma oscillations in an animal model of schizophrenia.

An investigation into the cellular effects of D4R signaling revealed that PD168077 enhances spike coherence and phase-coupling of action potentials to gamma oscillations in FSI, suggesting that D4R activation enhances gamma power by augmenting the synchronized inhibition of pyramidal neurons (Andersson et al., 2012a). Notably, pharmacological activation of other dopamine receptors, or direct application of dopamine, had no effect on gamma power *per se*. However, an enhancement of gamma power by dopamine was unmasked by simultaneous application of the D1-type receptor blocker SCH23390, indicating that D1-type receptors antagonize the effects of D4Rs on gamma oscillations (Andersson et al., 2012b).

Interestingly, D4R-mediated augmentation of gamma power is sensitive to blockade of NMDARs by AP5, although AP5 has no effect on gamma power *in vitro* per se (Andersson et al., 2012b). NMDARs on FSI have long been considered critical for normal excitation/inhibition balance in cortical microcircuits, and have been at the center of the glutamate hypofunction theory of schizophrenia (Coyle et al., 2006; Lisman et al., 2008; Nakazawa et al., 2012). Indeed, compelling evidence from gene targeting studies suggest an important role of NMDARs on FSI for the proper maturation of cortical circuits and the emergence of gamma oscillations during development that diminishes in the mature brain (Belforte et al., 2010; Korotkova et al., 2010). Likewise, electrophysiological studies in wild-type mice show that excitatory postsynaptic potentials (EPSPs) on FSI have large contributions from NMDARs in juveniles that

diminish during maturation (Rotaru et al., 2011; Wang and Gao, 2009). In mature FSI, excitatory drive is dominated by AMPARs to ensure high temporal precision between excitation and spiking (Rotaru et al., 2012). Notably, since NMDARs have slower kinetics than AMPARs, the summating properties of excitatory synapses with a large NMDAR contribution make them less suitable to support gamma rhythms. Given that D4Rs internalize NMDARs (see Section 1.5.5.2), a simple explanation might be that D4R improves excitation-spiking coupling by removing NMDARs from excitatory synapses of FSI to increase gamma power. Indeed, blockade of NMDARs increases gamma power *in vivo* (Pinault, 2008), and this is not observed if AMPARs are simultatneously inhibited (Zanos et al., 2016). Yet, if this were true, blocking NMDARs would occlude rather than inhibit the D4R effect on gamma power, and would increase gamma power even in the absence of D4R agonist. However, as mentioned earlier, this was not observed *in vitro* (Andersson et al., 2012a). I performed a similar experiment *in vivo* and observed that ketamine occluded the effect of D4R agonists on gamma power in the mPFC, but not the MD thalamus. Further work is necessary to explore this region-specific difference.

1.6 Overview of neuregulin-ErbB signaling

Neuregulins (NRGs) comprise a family of secreted and membrane bound factors characterized by the presence of an epidermal growth factor-like motif and that signal through ErbB RTKs to regulate a diverse array of developmental and acute processes in the peripheral and central nervous systems (Buonanno and Fischbach, 2001; Mei and Nave, 2014). Moreover, genes for both neuregulin 1 (NRG1) and ErbB4Rs have been identified as risk factors for schizophrenia (Mei and Xiong, 2008;Buonanno, 2010).

1.6.1 Genetic association with schizophrenia

Small mutations in the genes encoding NRGs and ErbB receptors endow an increased risk for developing schizophrenia. Single nucleotide polymorphisms (SNPs) in the NRG1 gene have been associated with schizophrenia in many, but not all population and genome-wide association (GWAS) studies (for excellent reviews, see Buonanno, 2010; Mei and Xiong, 2008). Indeed, people with the "schizophrenia risk" haplotype of NRG1 show many of the endophenotypic traits involved in schizophrenia including reduced paired-pulse inhibition (PPI), abnormal gamma oscillation activity, reductions in IQ, and a higher risk for the development of psychosis or unusual thoughts (Hall et al., 2006; Hong et al., 2008; Krug et al., 2008). Furthermore, the mRNA for NRG1 types 1, 2, and 4 are enriched in the PFC and hippocampus of brains from schizophrenia patients (Hashimoto et al., 2004; Parlapani et al., 2010). Additionally, cortical slices from patients with schizophrenia have higher levels of phosphorylated ErbB4R and enhanced NRG1 effects reducing NMDAR activity (Hahn et al., 2006). SNPs in ErbB4 have also been genetically associated with schizophrenia (Agim et al., 2013; Nicodemus et al., 2006, 2010; Silberberg et al., 2006). Indeed, ErbB4R transcript and protein expression is higher in the PFC of patients with schizophrenia (Joshi et al., 2014; Silberberg et al., 2006). This elevated ErbB4R expression is associated with reductions in PFC interneurons (Joshi et al., 2014). These findings highlight the relative importance of NRG1/ErbB signaling in interneurons as compared to pyramidal neurons in conferring disease risk.

1.6.2 NRG/ErbB receptor role in development

In the developing cortex, most glutamatergic neurons differentiate in the ventricular and subventricular zones and migrate laterally whereas interneurons differentiate in the ganglionic eminences and migrate tangentially to their final destinations. After migration, both types of neurons generate axons and dendrites to form neural circuits (Mei and Nave, 2014). Furthermore, NRG1 regulates myelination of nerves in the peripheral nervous system, but not the central nervous system, indicating that it promotes the activity of Schwann cells, but may not play a role in oligodendrocytes (Brinkmann et al., 2008).

NRG1-ErbB4Rsignaling is critical for the migration, maturation and synaptogenesis onto interneurons. Interneurons express ErbB4Rs as early as embryonic day 13 in the mouse (Yau et al., 2003), and these receptors appear to guide interneurons to their final destinations (Flames et al., 2004). Interestingly, deletion of the ErbB4R reduces the number of cortical interneurons, but not when the deletion happens after embryonic day 13.5 (Fazzari et al., 2010; Flames et al., 2004). Similarly, deletion of NRG1 has no effect on cortical or hippocampal development (Brinkmann et al., 2008). Furthermore, NRG1 and ErbB4R signaling promotes the formation and maturation of excitatory synapses on interneurons. Specifically, mice with genetic deletion of ErbB4R from interneurons have reduced mEPSC frequency, and fewer puncta with glutamatergic signaling markers such as vGlut-1, PSD-95 and GluA1 (del Pino et al., 2013; Fazzari et al., 2010; Ting et al., 2011). Indeed, ErbB4Rs stabilize PSD-95, which promotes the maturation of glutamatergic synapses (Ting et al., 2011). Additionally,

ErbB4Rexpression is critical in the synaptogenesis of PV+ chandelier cells, but not basket cells onto pyramidal neurons (del Pino et al., 2013; Fazzari et al., 2010). Similarly, overexpressing NRG1 type 3 in pyramidal neurons increased the density of chandelier cell axonal boutons onto pyramidal neurons (Fazzari et al., 2010). Finally, ErbB4R signaling is not essential for the formation of synapses between interneurons. Indeed, GABAergic synapses onto PV+ basket cells formed appropriately in the absence of ErbB4Rsignaling in interneurons (Yang et al., 2013b).

In excitatory neurons, NRG1-ErbB4R signaling still plays a role in proper development, even though it is likely that ErbB4 is not expressed in these cells. NRG1 signaling through ErbB4R stimulates neurite outgrowth in hippocampal neurons and cerebellar granule cells (Cahill et al., 2012; Krivosheya et al., 2008). Genetic deletion of ErbB2Rs and ErbB4Rs in the central nervous system reduced the density of dendritic spines in cortical and hippocampal pyramidal neurons (Barros et al., 2009), but deletion of ErbB4Rs specific to pyramidal neurons did not alter mEPSC frequency or the density of dendritic spines (Fazzari et al., 2010). Interestingly, mEPSC frequency and the density of dendritic spines on pyramidal neurons were reduced in mice lacking ErbB4Rs on PV+ interneurons (del Pino et al., 2013; Yin et al., 2013a), providing evidence that interneurons express ErbB4, but pyramidal neurons do not. Indeed, multiple studies suggest that ErbB4Rs are restricted to GABAergic neurons in the developing and adult brain (Fazzari et al., 2010; Neddens and Buonanno, 2010; Vullhorst et al., 2009; Woo et al., 2007). Changes in dendritic spine density in pyramidal neurons are most likely the result of compensatory effects related to the lack of ErbB4Rs in PV+ interneurons.

NRG-ErbB signaling also may modify the expression of ionotropic receptors. Genetic removal of ErbB2 and ErbB4 receptors had no effect on the expression of NMDA of $GABA_A$ receptors *in vivo* (Gajendran et al., 2009). In contrast, NRG-β isoform increased NR2C mRNA more than 100-fold in cerebellar granule cells, and this effect was blocked by the NMDAR antagonist AP5 *in vitro* (Ozaki et al., 1997).

1.6.3 Synaptic effects of ErbB4R

1.6.3.1 Ionotropic receptors

Neuregulin 1 modulates GABA receptor (GABAR)-mediated currents and the excitability of interneurons, but has mixed effects on basal AMPAR-mediated and NMDAR-mediated currents. In general, NRG1 does not change glutamatergic currents in hippocampal CA1 neurons (Chen et al., 2010; Huang et al., 2000; Iyengar and Mott, 2008; Kwon et al., 2005). Mice lacking ErbB4Rs on PV+ interneurons show increased sEPSC frequency in pyramidal neurons and PV+ interneurons (del Pino et al., 2013), suggesting that NRG1 signaling through ErbB4R typically decreases glutamate release onto pyramidal neurons in normal animals. Interestingly, NRG2 signals through ErbB4Rs in cortical interneurons to internalize NMDARs and decrease NMDAR-mediated currents (Vullhorst et al., 2015). Notably, while one group observed that NRG1 attenuates NMDAR-mediated currents in PFC pyramidal neurons (Gu et al., 2005), this has never been reproduced (Vullhorst et al., 2015). Soluble NRG1 signaling through ErbB4Rs promotes GABA release (Chen et al., 2010; Woo et al., 2007), and both pharmacological inhibition and genetic removal of the ErbB4R reduces GABA transmission, increases the firing of pyramidal neurons and enhances LTP in slices (Chen et al., 2010; Kwon et al.,

2005; Pitcher et al., 2008), indicating that ErbB4R signaling is important in generally inhibiting brain activity. Furthermore, ErbB4R promotes the endocytosis of $GABA_AR_{\alpha 1}$ in cultured hippocampal interneurons, which decreases the amplitude and decay kinetics of inhibitory signaling in these interneurons (Mitchell et al., 2013). This ErbB4R-mediated endocytosis of GABA occurs without ErbB4's receptor tyrosine kinase activity (Mitchell et al., 2013).

1.6.3.2 Effects on ion channels

NRG1 indirectly decreases the firing rate of PFC pyramidal neurons (Wen et al., 2010), and has mixed effects on interneurons. Both endogenous and exogenous NRG1 signals through ErbB4Rs to increase the excitability of PV+ interneurons in mouse cortical layers 2-3, and has similar effects in the hippocampus, but with much smaller magnitudes (Li et al., 2012). Specifically, NRG1 hyperpolarizes the action potential threshold by inhibiting $K_{v1.1}$ channels (Li et al., 2012). In contrast, genetic deletion of ErbB4Rs from PV+ interneurons increases the spontaneous firing of hippocampal PV+ interneurons at resting membrane potentials, increases evoked spiking using current ramps, and decreases rheobase currents (del Pino et al., 2013), indicating that ErbB4Rs in PV+ interneurons normally decreases intrinsic excitability. However, these changes in excitability occur in the absence of significant changes in action potential threshold or latency, suggesting a potential indirect effect. Also, a different study showed that genetic deletion of ErbB4Rs from PV+ interneurons decreases the spontaneous and evoked firing of cortical PV+ interneurons (Yang et al., 2013b). Furthermore, in dissociated hippocampal ErbB4-expressing neurons or cerebellar granule cells NRG1 does not

increase intrinsic excitability (Janssen et al., 2012; Yao et al., 2013). In fact, NRG1 reduces the excitability of hippocampal interneurons by decreasing voltage-gated sodium currents (Janssen et al., 2012) in ErbB4-expressing neurons, and chronic, but not acute NRG1 increases transient outward potassium currents in immature, but not adult neurons (Yao et al., 2013). These findings could imply that NRG1 requires intact neural circuits to increase the excitability of PV+ interneurons, which leaves open the possibility that modified dopamine levels may play a role in the effects of NRG1 on excitability.

1.6.4 Long-term potentiation

NRG1/ErbB4R signaling inhibits the induction, and reverses the early expression, of long-term potentiation (LTP) at CA3->CA1 glutamatergic synapses (Huang et al., 2000;Kwon et al., 2005;Shamir et al., 2012). Furthermore, neutralizing endogenous NRG1 pharmacologically or genetically removing ErbB4Rs promotes the establishment of LTP, revealing that NRG1 regulates synaptic plasticity (Agarwal et al., 2014; Chen et al., 2010; Pitcher et al., 2008). Interestingly, established LTP cannot be reversed by NRG1, suggesting a time-dependence of LTP reversal (Pitcher et al., 2011). A possible mechanism for LTP reversal is that NRG1 reduces AMPAR mediated EPSCs at potentiated synapses and stimulates the internalization of surface AMPARs, but not in the presence of ErbB receptor tyrosine kinase inhibitors, suggesting that NRG1 signaling through ErbB receptors help neurons internalize AMPARs at potentiated synapses (Kwon et al., 2005). However, this does not directly explain how glutamatergic synapses depotentiate because when ErbB4Rs are removed from pyramidal neurons, NRG1 still reverses LTP (Chen et al., 2010). In accordance with the evidence that ErbB4R signaling

is specific to interneurons, acute NRG1 treatment does not suppress LTP in the hippocampus of mice with a genetic deletion of ErbB4R from PV+ interneurons (Chen et al., 2010; Shamir et al., 2012). Surprisingly, acute LTP reversal by NRG1 is still observed when $GABA_A$ receptor signaling is blocked (Kwon et al., 2005; Pitcher et al., 2011). Exactly how ErbB4R signaling on PV+ neurons reduces LTP without $GABA_A$ receptor signaling remains a mystery.

An alternative explanation for ErbB4R-mediated LTP reversal includes a role for changes in tonic dopamine levels. LTP reversal by NRG1 critically depends on the activation of D4Rs (Kwon et al., 2008). Taken together with the finding that NRG1 infusion in the dorsal hippocampus triggers dopamine release, this suggests that NRG1/ErbB4R signaling regulates hippocampal LTP via a dopamine/D4R pathway (Kwon et al., 2008). There are two established mechanisms by which D4R activation can depotentiate synapses. First, D4R activation can reduce NR2B-containing NMDAR-mediated currents during LTP in the presence of $GABA_A$ receptor inhibitors (Herwerth et al., 2012). Second, D4Rs can increase the EPSPs from stimulation of the Shaeffer's collateral pathway onto PV+ interneurons which in turn decreases the EPSPs recorded from pyramidal neurons due to feedforward inhibition (Rosen et al., 2015b). However, it is not known if the ErbB4 and D4 receptor systems interact in the same or across different cell types, or which signaling pathways link their activation to the removal of synaptic AMPARs that seems to underlie LTP reversal by NRG1 and D4R agonists.

Three hypotheses emerge for the interaction of D4Rs and ErbB4Rs: (1) D4Rs and ErbB4Rs interact directly on PV+ interneurons, but not pyramidal neurons. (2) ErbB4Rs

are not expressed on pyramidal neurons, but help mediate an increase in tonic dopamine so that D4Rs on pyramidal neurons are activated. (3) D4Rs and ErbB4Rs interact within dopaminergic fibers, which would explain why D4R antagonists and NRG1 can both increase extracellular dopamine (Broderick and Piercey, 1998; Kwon et al., 2008). In support of the first hypothesis, ErbB4Rs are undetectable in pyramidal neurons (Vullhorst et al., 2009;Neddens et al., 2011) while both ErbB4Rs and D4Rs are expressed in GABAergic cells including PV+ interneurons (Mrzljak et al., 1996;Andersson et al., 2012b). Additionally, inhibition of LTP induction and reversal of LTP are absent from mice with targeted deletions of ErbB4Rs in PV+ interneurons (Chen et al., 2010;Shamir et al., 2012), and absent in the pharmacological blockade of D4Rs. Finally, both receptors synergize in the modulation of hippocampal gamma oscillations (Andersson et al., 2012b) that critically depend on PV+ interneurons. In support of the second hypothesis, others have observed effects of D4R activation in pyramidal neurons, including the regulation of LTP through NR2B-containing NMDARs (Herwerth et al., 2012). One major criticism of this hypothesis is that dopamine increases LTP through D1-type receptors (Huang and Kandel, 1995; Otmakhova and Lisman, 1996), so it is unclear why a D4R mediated effect would overpower this D1-type receptor mediated effect. Dopamine neurons shift from tonic (1-4Hz) to phasic (10-30Hz) firing rates in response to salient and rewarding stimuli (Schultz, 2007). Recent work has shown that phasic dopamine (as mimicked by 25 seconds of light bursts that optogenetically stimulated dopamine release) increases Shaeffer's collateral pathway EPSP through D1R signaling while tonic dopamine release (as mimicked by short bursts of optogenetically stimulated

dopamine release, or bath application of dopamine) decreases Shaeffer's collateral pathway EPSP via feedforward inhibition from increased PV+ neuron activity mediated by D4R signaling (Rosen et al., 2015b). Therefore, given that NRG1 increases the extracellular dopamine in a manner that reflects a rise in tonic dopamine, it follows that D4R-mediated dopaminergic signaling would predominate.

1.6.5 Effects on gamma oscillations

Early studies in acute rodent slices showed that NRG signaling via ErbB4 potently augments kainate-induced gamma oscillations in hippocampal area CA3 (Fisahn et al., 2009). Additionally, mice with a full genetic ErbB4R deletion have reduced gamma LFP power compared to wildtype mice *in vitro* (Fisahn et al., 2009). Furthermore, NRG1 increases the spiking synchrony of pairs of PFC pyramidal neurons or interneurons, but not when GABAergic signaling is inhibited (Hou et al., 2014). Additionally, NRG1 does not increase the gamma power in mice with FSI-specific ablation of ErbB4R (Hou et al., 2014). Given that NRG/ErbB4R effects on LTP reversal in CA1 critically depend on D4R signaling, it was plausible to hypothesize that NRG1 effects on gamma oscillation power also depend on D4R signaling. Indeed, D4R inhibition by L-745,870 largely blocks the potentiating effects of NRG1 on gamma oscillations (Andersson et al., 2012b). Conversely, PD168077 increases gamma power, albeit to a lesser extent than ErbB4R activation by NRG1, suggesting that NRG1/ErbB4R signaling engages multiple signaling systems that synergistically augment gamma oscillations. Neither PD168077 nor NRG1 induce gamma oscillations in naïve slices, indicating that their modulatory effects impinge on ongoing oscillations (Fisahn et al.,

2009;Andersson et al., 2012b). Interestingly, *in vivo*, genetic deletion of ErbB4Rs from FSIs increases gamma power (31-100Hz) recorded in the pyramidal layer of hippocampus CA1 during locomotion compared to wild type mice (del Pino et al., 2013). Furthermore, this conditional ErbB4R deletion reduces the theta (4-8Hz) coherence and cross-correlation between the CA1 of the hippocampus and the mPFC of anesthetized mice (del Pino et al., 2013). Finally, PV+ interneuron-specific ablation of ErbB4Rs leads to an increase in spontaneous seizures (Tan et al., 2012). Taken together, endogenous NRG signaling through the ErbB4 receptor appears to participate in the generation of gamma oscillations.

1.6.6 Effects on behavior

Too much or too little NRG/ErbB signaling causes behavioral changes that mimic symptoms of schizophrenia in rodents. Specifically, mice with genetic deletion of ErbB4Rs from interneurons display hyperactivity and deficits in fear conditioning, paired-pulse inhibition (PPI), and working memory (Chen et al., 2010; del Pino et al., 2013; Shamir et al., 2012; Wen et al., 2010). Moreover, mice lacking NRG1 processing enzymes have similar behavioral impairments (Tamura et al., 2012). Surprisingly, an increase in NRG1 signaling by transgenically overexpressing NRG1 type 1 causes similar behavioral deficits as well (Agarwal et al., 2014; Deakin et al., 2012; Luo et al., 2014; Yin et al., 2013b), suggesting that NRG/ErbB signaling may follow an inverted u-shaped curve, like that seen for dopamine signaling.

Conversely, NRG1 treatment has the potential to reduce behavioral and glutamatergic effects in the ketamine-model of schizophrenia. Acute ICV or systemic

administration of NRG1 ECD has no effect on spontaneous behavior, but prevents PCP-induced hyperactivity and deficits in PPI (Engel et al., 2015). Interestingly, NRG1 treatment again followed a U-shaped dose response curve with too little or too much NRG1 having only a small effect on PCP-induced hyperactivity. Furthermore, reverse microdialysis of 10nM NRG1 reduces extracellular glutamate in the PFC and hippocampus and reduces PCP-induced increases in GABA in the hippocampus (Engel et al., 2015).

1.7 Specific Aims

Although D4R antagonists are not efficacious antipsychotics, D4R targeting drugs still hold potential as adjunct therapies to ameliorate the cognitive deficits seen in schizophrenia (see, for example Furth et al., 2013). If the effects of D4R stimulation on pharmacologically induced gamma oscillations in vivo are indeed indicative of a potentiating effect on induced or evoked oscillations in other neocortical areas, one might speculate that agonists may actually be more effective than antagonists at improving cognitive function in individuals with schizophrenia, as evidenced by some animal studies. However, if these changes in gamma power better reflect ongoing oscillations, then an antagonist may be more effective at improving cognitive function.

In the following studies, I examine the effects of D4R activation and inhibition on ionotropic receptors in PV+ interneurons and pyramidal neurons in an attempt to construct the mechanisms by which D4Rs modulate gamma oscillations (Chapter 2). I then compare treadmill-walking-induced gamma oscillations with those induced by ketamine at the LFP and single neuron level in the rat mPFC and MD thalamus. I then

test the D4R agonist and antagonist's ability to modulate gamma oscillations and single neuron activity in each brain region before and after ketamine administration (Chapter 3). Finally, I systemically inject a pan-ErbB antagonist, JNJ-28871063 and observe changes in LFP and single neuron activity before and after ketamine administration (Chapter 4). Together, these studies increase our understanding of how D4R and ErbB activity modulate gamma power *in vivo*, with the hope that this can guide drug discovery for better treatment of the cognitive symptoms of schizophrenia.

These findings offer new and exciting avenues to think about the involvement of dopamine neurotransmission in network activity. However, one must be mindful of the many complexities of D4R signaling when designing and interpreting meaningful experiments. These include the likelihood that the cellular D4R expression pattern varies in different cortical regions, that drug effects on D4R function might be dose-dependent and that the receptor might engage in different signaling partnerships in different cells or subcellular compartments. With proper consideration for these important issues, I believe that these investigations into the role of dopamine and ErbB signaling hold great promise for a better understanding of the relationship between neuromodulators and rhythmic network activity that underlies cognitive processes.

CHAPTER TWO: The effects of dopamine D4 receptor agonism and antagonism *in vitro*

2.1 Introduction

Parvalbumin-expressing interneurons (PV+ interneurons) are essential for the generation and maintenance of gamma oscillations (Bartos et al., 2007). Indeed, optogenetic silencing of PV+ interneurons suppresses gamma power (Sohal et al., 2009), and random optogenetic excitation of PV+ interneurons induces gamma oscillations via feedback inhibition (Cardin et al., 2009). Gamma oscillations arise in networks of FSIs interconnected by chemical and electrical synapses (see Bartos et al., 2007). Most FSIs are PV-expressing basket cells that form inhibitory connections with ~60 other PV-expressing basket cells and form perisomatic connections with hundreds of pyramidal neurons (Sik et al., 1995), allowing them to coordinate the spike timing of hundreds of neurons. Furthermore, PV+ interneurons faithfully release GABA in response to depolarization (Hefft and Jonas, 2005), and generate action potentials about once per gamma cycle during the ascending phase of the oscillation, both *in vitro* (Gloveli et al., 2005; Hájos et al., 2004) and *in vivo* (Tukker et al., 2007). Surprisingly, an early study that used tetanic stimulation to evoke gamma oscillations in the CA1 of the hippocampus *in vitro* revealed that gamma oscillations can be maintained without ionotropic excitatory transmission (Whittington et al., 1995). Idealized computational models revealed how gamma oscillations can be generated by mutual inhibition between mildly excited interneurons (called I-cells) in ING models, or through I-cells responding to synchronous

excitatory volleys from pyramidal neurons (called E-cells) in PING models (Tiesinga and Sejnowski, 2009).

However, brain networks do not exist in isolation, and PV+ interneurons are not the only neurons involved in gamma oscillations. The three key determinants of the power and frequency of gamma oscillations are (1) the magnitude and (2) kinetics of synaptic inhibition between interneurons, and (3) the driving excitatory current onto interneurons (Traub et al., 1996). In most ING or PING computational models , gamma power is determined by excitation onto PV+ FSIs (Jadi et al., 2015), and pyramidal neurons provide the greatest source of excitation onto PV+ interneurons (Gulyás et al., 1999). However, activation through gap junctions plays an excitatory role as well (Tamás et al., 2000). Although PV+ interneurons are highly interconnected, the majority of inhibitory innervation from PV+ interneurons onto other PV+ interneurons is dendritic, while the majority of somatic inhibitory innervation onto PV+ interneurons is from vasoactive intestinal peptide (VIP)-expressing interneurons (Hioki et al., 2013). Furthermore, ~25% of the dendritic inhibition onto PV+ interneurons is from somatostatin (SOM)-expressing interneurons (Hioki et al., 2013). Therefore, focusing solely on PV+ interneurons fails to capture the entire picture of the excitation-inhibition balance involved in neural synchrony. Given that the dynamics of network inhibition is fundamental in setting the power and frequency of gamma oscillations, I examined inhibitory currents in pyramidal neurons and both PV+ and non-PV expressing interneurons, as well as the intrinsic excitability of interneurons themselves.

Dopamine directly influences FSIs to affect neural synchrony. For instance, activation of D1 and D4 receptors (D4Rs) reduce gap junction coupling between interneurons (Hampson et al., 1992; Li et al., 2013; Onn and Grace, 1994), and exogenous dopamine increases the evoked firing rate of FSIs *in vivo* (Tseng et al., 2006) and *in vitro* (Gorelova et al., 2002; Trantham-Davidson et al., 2008). Dopamine also acts through D1 receptors to decrease inhibitory postsynaptic currents (IPSCs) in FSIs (Towers and Hestrin, 2008). Activation of the D4R also directly affects neural synchrony, potentially through its activity in PV+ interneurons (Furth et al., 2013). The D4R has a high affinity for dopamine (Rondou et al., 2010) and may be activated at low concentrations of the endogenous dopamine present in the brain slice (Acosta-García et al., 2009; Onn et al., 2006; Rubinstein et al., 2001). Furthermore, basal levels of dopamine may activate D4Rs on PV+ interneurons to influence long-term potentiation (Rosen et al., 2015b). Therefore, it is important to examine both the effects of D4R antagonism and D4R agonism on GABAergic signaling, as D4Rs may be constitutively active.

Dopamine D4R expression is sparse in the hippocampus *cornu ammonis* 1 (CA1) and *cornu ammonis 3* (CA3). Only 25% of PV+ interneurons contain the D4R in CA1 and CA3 (Andersson et al., 2012b), but 71% of D4R-expressing neurons are PV+ interneurons in the same areas (Andersson et al., 2012b). Therefore, the majority of the effects of D4R activation may arise through its effects on PV+ interneurons. It is also possible, however, that the D4R has more widespread localization than we can currently detect. Radioligand binding studies suggest that there may be more D4Rs than can be

easily detected by immunohistochemistry or in situ hybridization. In fact, a quantitative radioligand study estimated that putative D4Rs represent about half of all D2-type receptors in the prefrontal cortex and hippocampus (Tarazi et al., 1997). Further evidence suggesting a more widespread expression of D4Rs is the fact that small molecule D4R agonists and antagonists work at nanomolar concentrations in the slice (Andersson et al., 2012a, 2012b; Kwon et al., 2008) and in mediating cognitive effects *in vivo* (Bernaerts and Tirelli, 2003; Clifford and Waddington, 2000; Patel et al., 1997; Zhang et al., 2004). Despite the rich literature regarding the modulation of PV+ interneurons by dopamine, the function of the dopamine D4R in regulating voltage-gated and ligand-gated ion channels in interneurons is mostly unknown.

The dorsal hippocampus is also critically involved in spatial working memory and other cognitive tasks, while the ventral hippocampus is critically involved in stress and emotions (Fanselow and Dong, 2010). Previous research in our lab focused on dopamine D4 receptor (D4R) activation in O-LM interneurons from the *stratum oriens* of the dorsal hippocampus (CA1) for three reasons: (1) These interneurons are easy to identify; (2) the dorsal hippocampus receives dopaminergic innervation from the VTA (Jay, 2003); (3) pharmacological manipulations in the dorsal hippocampus may play a significant role in the therapeutic efficacy of cognitive enhancers. This previous work revealed that D4R activation decreased the amplitude of evoked AMPA-mediated currents on a select group of interneurons (n=5 of 8 cells) from the *stratum oriens* of CA1 of the hippocampus (Buonanno lab, unpublished results). Furthermore, dopamine D4R activation increased the frequency of both spontaneous and miniature inhibitory postsynaptic currents (sIPSCs

and mIPSCs respectively; sIPSCs, n=6 cells; mIPSCs, n=6 cells) in pyramidal neurons from the pyramidal layer of the CA1 of the hippocampus, and this effect was blocked by D4R antagonists (Buonanno lab, unpublished results). Miniature IPSCs are recorded in the presence of the voltage-gated sodium channel blocker tetrodotoxin; therefore, changes in frequency observed after D4R activation reflect presynaptic changes in the release probability that is independent from action potential activity. These results indicate that the dopamine D4R acts presynaptically in interneurons to increase the probability of release of GABA vesicles at synapses onto pyramidal neurons. Finally, activation of the dopamine D4R resulted in one of two patterns in mIPSC activity recorded from interneurons from the *stratum oriens* of CA1 of the hippocampus. Dopamine D4R activation either increased the frequency of mIPSCs on interneurons (n=3 of 6 cells) or decreased the mIPSC amplitude in a separate population of interneurons (n=3 of 6 cells; Buonanno lab, unpublished results). As both evoked AMPA receptor mediated amplitudes and miniatute GABA-ergic amplitudes decreased in some interneurons, but not others, it became important to classify these interneurons. However, the original recordings were performed in wild-type mice and the cells were not filled with any intracellular markers, such as biocytin. Therefore, it was neither possible to further distinguish the interneurons using morphological characteristics, nor using their expression of calcium binding proteins and neuropeptides. Therefore, I recorded from mouse lines (PV/Tom) with red fluorescent marker TOMATO expressed in PV+ interneurons to distinguish PV+ interneurons from non-PV expressing interneurons.

To better understand how dopamine D4R activation and inhibition can modulate network activity both *in vitro* and *in vivo*, I examined how D4R agonists and antagonists alter synaptic inhibition onto both excitatory pyramidal neurons and inhibitory interneurons, and I examined how D4R agonists and antagonists influence the intrinsic excitability of PV+ interneurons. Specifically, I applied D4R agonists and antagonists separately to PV+ interneurons, non-PV+ interneurons, and pyramidal neurons and recorded mIPSCs to look specifically at the pre- and post-synaptic influence of the D4R, rather than those determined by action potential related activity. I also examined how D4R activation and inhibition influenced the intrinsic excitability of PV+ interneurons by recording action potentials evoked by somatic current injections to determine changes in the action potential threshold, rheobase currents, and spike shape. Because all neurons in the *stratum oriens* of the CA1 are interneurons, I recorded from neurons in PV/Tom mice to distinguish PV+ interneurons from non-PV expressing interneurons to determine whether the effects of the D4R are specific to PV+ interneurons. Furthermore, as I was planning to make *in vivo* recordings from layers 3-5 of the medial prefrontal cortex (mPFC), I investigated whether D4R activation in PV+ interneurons of the mPFC would have the same effects that it had on interneurons of the *stratum oriens* of the dorsal hippocampus CA1 (dhCA1).

2.2 Materials and Methods

2.2.1 Animals

The PV-Cre mouse line ***Pva1b***$^{tm1(cre)Arbr}$, expressing Cre recombinase from the ***Pva1b*** locus by insertion of the gene into its 3′ untranslated region, and a mouse line

expressing tdTomato fluorescent protein from the Rosa26 locus (***Ai14***) were obtained from The Jackson Laboratory (Hippenmeyer et al., 2005). Both lines were received on a mixed 129×C57BL/6J background, backcrossed in our facility for two generations to C57BL/6J wild type mice and have thus been maintained inbred. Mice were kept on a 12/12 hour light/dark schedule with access to food and water ***ad libitum***. Animals were treated in accordance with the National Institutes of Health Animal Welfare guidelines. All procedures were approved by the NIH animal care and use committee. Every effort was made to minimize the number of animals used and their discomfort.

2.2.2 Drugs

CNQX (6- cyano-7-nitroquinoxaline-2,3-dione) disodium salt, DL-D-2-amino- 5-phosphonopentanoic acid (AP5), tetrodotoxin (TTx) citrate, the D4R agonist PD168077, and the D4R antagonist L745870 were all purchased from Tocris (Ballwin, MO) and dissolved in water. About half of the D4R agonist was dissolved in DMSO, before it became known that it would also dissolve in water. All stock solutions were stored at 4 °C, −20 °C, or −80 °C according to the manufacturer's suggestions, and diluted on the day of use. Stock solutions and picrotoxin (Tocris) were diluted in ACSF immediately before bath application.

2.2.3 Slice preparation

Coronal prefrontal and hippocampal slices (300 µm) from 4-7 week-old male and female mice were prepared in ice-cold ACSF containing (in mM): 124 NaCl, 25 Na_2HCO_3, 11 glucose, 2.5 KCl, 1.3 $MgCl_2$, 2.5 $CaCl_2$, 1.25 NaH_2PO_4, bubbling with

95% O_2, 5%CO_2 (carbogen). Slices were incubated in a holding chamber at 32 °C for 1 h in ACSF saturated with carbogen, and then transferred to 23 °C ACSF and kept for at least 1 h before recording. Slices were transferred to a submerged recording chamber continuously perfused at 2mL/min at 32- 35°C with ACSF.

2.2.4 Electrophysiology

Whole cell patch-clamp recordings were performed with borosilicate glass microelectrodes (2-8 MΩ). A multiclamp 700A amplifier equipped with a Digidata 1322A data acquisition board and pClamp10 software (Molecular Devices) was used. Recorded data were sampled at 20-50kHz and filtered at 10kHz using pClamp and analyzed with Clampfit (Molecular Devices) or AxoGraph. Bridge balance and access resistance were monitored during recordings and experiments with >20% change were discarded. Data was also discarded if action potentials did not overshoot 0mV throughout the length of the recording.

2.2.5 Current clamp

To examine intrinsic excitability, membrane potential was set at -70mV before current injection protocols, and neurons were held in a membrane test protocol in voltage clamp between current clamp recordings. Synaptic currents were blocked with CNQX (10 μM), AP5 (25 μM), and picrotoxin (100 μM). Glass recording electrodes were filled with a potassium gluconate-based internal solution (in mM): 125 K-gluconate, 20 KCl, 10 HEPES, 0.5 EGTA, 4 Mg-ATP, 0.3 Na-GTP, 10 phosphocreatine, at pH 7.2 adjusted with KOH (290mOsm). After recording an initial baseline for 10–12 min, a D4R agonist

or D4R antagonist was bath-applied until a stable response was attained (10-12 min). The rheobase current was measured with a series of 500ms, 50pA hyperpolarizing and depolarizing current steps (-200 to +700pA), and defined as the smallest current injection needed to elicit an action potential. Action potentials were identified from current clamp recordings using a threshold of 50mV/ms in the first derivative membrane voltage. To measure AP waveform, a suprathreshold depolarizing current was injected for 5 ms. Action potential amplitude was measured as the absolute difference between the action potential peak and the voltage threshold of action potential initiation. AP duration was measured at the half-maximal amplitude. After-hyperpolarization amplitude was calculated as the difference between the average voltage in the 1ms preceding the action potential, and the minimum voltage in the 5ms after the action potential peak using the average of the first 25 action potentials in a recording. Latency, rise-time, half-width, decay, and inter-event interval were also extracted.

2.2.6 Voltage clamp

To examine inhibitory synaptic currents, sIPSCs and mIPSCs were recorded at a holding potential of -70mV throughout the experiment. Inhibitory postsynaptic currents were collected in the presence of 10μM CNQX and 25 μM DL-AP5 to block AMPA and NMDA receptors respectively. mIPSCs were collected in the presence of 1μM TTX to block action potential initiated neurotransmitter release. After recording an initial baseline for 10–12 min, a D4R agonist or D4R antagonist was bath-applied until a stable response was attained (10-12 min). Glass recording electrodes were filled with a cesium-chloride based internal solution (in mM): 130 CsCl, 8 NaCl, 10 HEPES, 0.5 EGTA, 4

Mg-ATP, 0.3 Na-GTP, 10 phosphocreatine, 5 QX-314 (pH 7.2, 290 mOsm). For each recording, IPSCs were identified using template-based detection software (Clampfit 10) and were visually confirmed. Events with amplitudes less than 2.5 times the noise (root mean square) were excluded from the analysis. Miniature IPSC averages were based on more than 200 events. Decay kinetics were analyzed from non-overlapping events and determined with a single-exponential curve fitting.

2.2.7 Statistics

Data are represented as mean ± SEM. Statistical analyses were performed using GraphPad Prism 6. All data were analyzed with paired Student's *t* test when comparing two groups, unless otherwise noted. P values below 0.05 were considered statistically significant.

2.2.8 Immunohistochemistry

Following recordings, biocytin-filled neurons were fixed in 4% PFA-PBS containing 4% sucrose overnight at 4° C, followed by blocking with 10% donkey serum PBS for an additional 2 hours. Slices were washed several times with PBS and incubated in the same blocking buffer overnight with the addition of 0.1% Triton-X 100 to permeabilize the cell membrane and block intracellular unreacted aldehydes. Following this blocking step, primary mouse monoclonal antibody against parvalbumin (Sigma) was applied at 1:500 in the same blocking buffer. Slices were washed in PBS several times, followed by incubation with fluorescently labeled secondary antibodies (Texas Red dye-conjugated Goat anti-Mouse IgG, Jackson Laboratories for parvalbumin, Alexa 488,

Sigma for biocytin) in the blocking buffer at room temperature for 1 hour. Slices were then washed with PBS, incubated in a 10% glycerol cryoprotective solution for more than 45 minutes and recut to 70 µm on a freezing microtome. Slices were washed and mounted on slides in MOWIOL (CalBiochem). Laser scanning confocal images were acquired using an LSM510 (Zeiss) and all channels set to an airy unit of 1. Fast-spiking cells are either chandelier cells, or basket cells (Markram et al., 2004), and were morphologically classified accordingly.

2.3 Results

2.3.1 GABA receptor-mediated currents in pyramidal neurons

The D4R has the ability to modify presynaptic GABA release. In the hypothalamus, thalamic reticular nucleus, or septal nucleus, D4R agonists decreased the frequency of GABA release (Asaumi et al., 2006; Baimoukhametova et al., 2004; Gasca-Martinez et al., 2010). However, in the hippocampus, D4R agonists increased the frequency of GABA release onto pyramidal neurons (unpublished results, Buonanno lab). D4R agonists also decrease postsynaptic GABA-mediated currents (Graziane et al., 2009; Shin et al., 2003; Wang et al., 2002) (but see Andersson et al., 2012a), and acute inhibition of the D4R increases total GABA release from *globus pallidus* into the *substantia nigra* (Acosta-García et al., 2009). Therefore, I examined GABA-mediated currents in pyramidal neurons of the mPFC to determine whether the D4R effect was region specific. The D4R agonist (PD168077 100nM) did not significantly influence the frequency (+2%) or amplitude (-1%) of spontaneous IPSCs (both $p>0.05$, paired *t*-test, n=4) in layer 5 of the mPFC (data not shown). Therefore, I recorded from the dorsal

hippocampus CA1 (dhCA1) pyramidal layer to reproduce earlier results. In the pyramidal layer of the dhCA1, the D4R agonist (PD168077 100-200nM) also did not significantly influence the frequency (-7%) or amplitude (-4%) of miniature IPSCs (both $p>0.05$, paired *t*-test, n=6, data not shown). I ordered fresh reagents, recorded from pyramidal neurons in the CA1 again, and still found no significant differences (both $p>0.05$, paired *t*-test, n=3, data not shown).

To determine whether D4R antagonists modified synaptic inhibition onto pyramidal neurons in dhCA1, I recorded mIPSCs from these neurons before and after bath application of the D4R antagonist. The D4R antagonist (L-745,870 50nM) increased the GABA release probability from interneurons onto pyramidal neurons by about 2.0 Hz (+17%, $p<0.05$, paired *t*-test) and increased the amplitude of these currents in the pyramidal neurons by 6.0 pA in a manner that trends toward significance (+22%, $p=0.054$, paired *t*-test, n=4, Fig2.1). This indicates that D4R inhibition increases presynaptic GABA release onto pyramidal neurons, and suggests a postsynaptic change in GABA receptor signaling within pyramidal neurons.

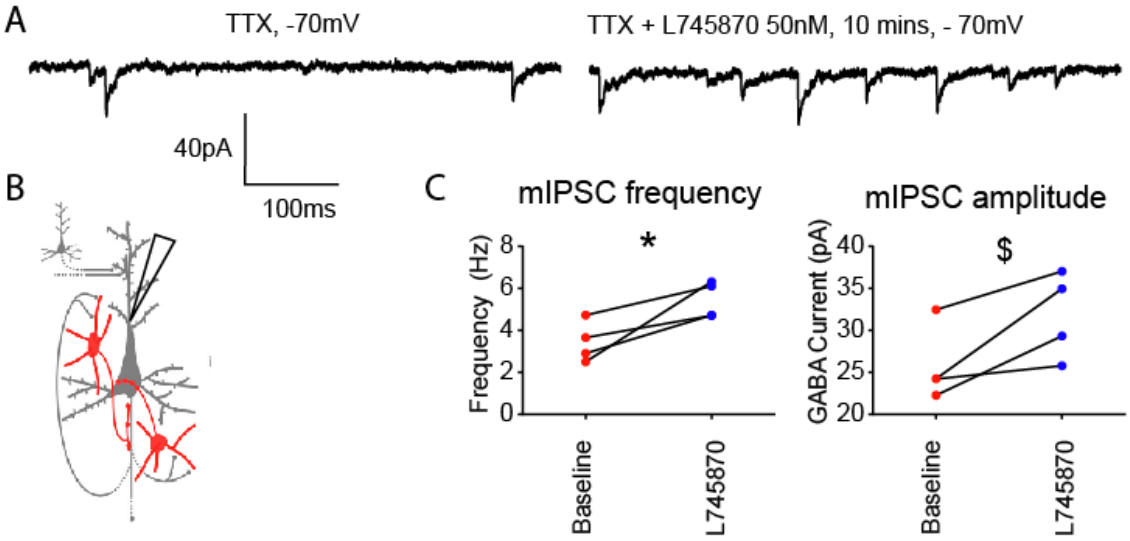

Figure 2.1: D4R inhibition increases presynaptic GABA release onto pyramidal neurons in dorsal hippocampus. (**A**) Representative trace before and 10 minutes after administration of L745870 (50nM). All recordings were made at 32 degrees in the presence of CNQX (10µM) and DL-AP5 (25 µM) to block AMPA and NMDA receptors respectively. (**B**) Schematic representation of the experiment. (**C**) Graphs show the mIPSC frequency and amplitude before drug application (baseline) and 10 minutes after administration of the D4R antagonist. *:p<0.05, $:p<0.1, paired t-tests, n=4.6.

2.3.2 GABA receptor-mediated currents in interneurons

To understand how D4R activation modulates GABAergic neurotransmission onto interneurons themselves, I recorded mIPSCs from PV+ interneurons and non PV-expressing interneurons from the dhCA1 in PV/Tom mice before and after bath application of the D4R agonist PD168077 (200nM). Activation of the D4R reduced the frequency of GABA release onto PV+ interneurons by 3.9Hz (+30%, $p<0.05$) and reduced the amplitude of GABAR-mediated currents by 5.5pA ($p<0.01$, n=5, paired *t*-tests, Fig2.2A&D). Reductions in average amplitude may arise from a decrease in high amplitude events, an increase in events near the detection threshold, or both. Plotting the cumulative distribution function of each IPSC event revealed a decrease in high

amplitude events and an increase in the density of the events near the threshold detection (near 10 pA, Fig2.2D). If the amplitude of some events decreased below the detection threshold, this could also explain the apparent reduction in event frequency. Averaging 200 IPSCs together and measuring the kinetics revealed that IPSCs tend to decay more slowly after D4R activation (p=0.06, n=3, Fig2.2C). This suggests a possible shift in the composition of synaptic $GABA_A$Rs, such as the internalization of receptors with rapid decay kinetics, like α1-subunit containing receptors (Okada et al., 2000). In contrast, D4R activation had no significant influence on the amplitude of GABA-mediated currents in non-PV expressing interneurons (+6%, p>0.05, paired t-test, n=4), but reduced the frequency of GABA release onto these neurons by 1.3Hz (-25%, p<0.05, paired t-test, n=4). This suggests a presynaptic effect of D4R activation that decreases GABA release at synapses between interneurons. Surprisingly, in PV+ interneurons in layer 5 of the mPFC the D4R agonist, PD168077 (100nM), did not significantly influence the frequency (+6%) or amplitude (+7%) of mIPSCs (both p>0.05, paired t-test, n=7, data not shown). This indicates that the effect of D4R activation is brain-region specific.

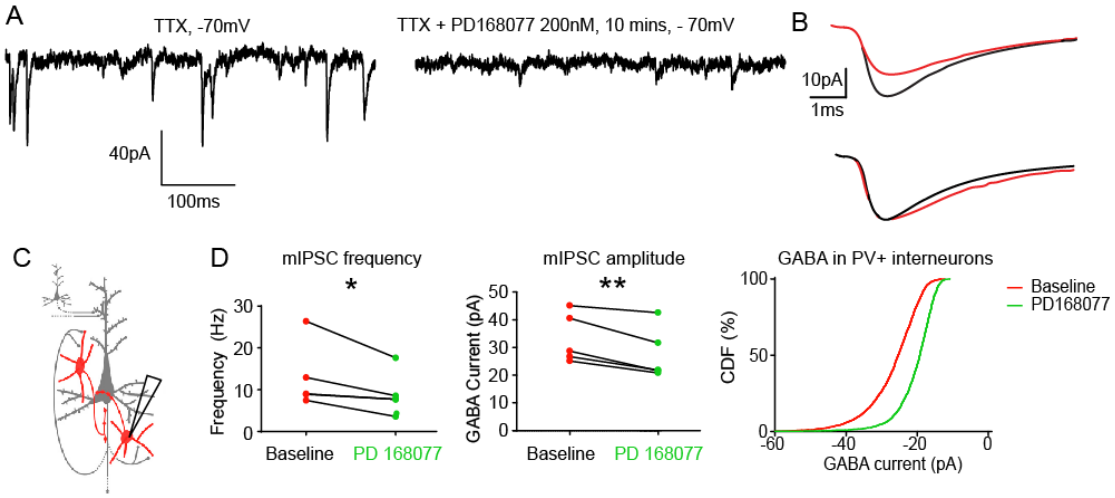

Figure 2.2: D4R activation decreases presynaptic GABA release onto PV+ interneurons in the dorsal hippocampus CA1. (**A**) Representative trace before and 10 minutes after administration of PD168077 (200nM). All recordings were made at 32 degrees in the presence of TTX (1 µM), CNQX (10µM) and DL-AP5 (25 µM) to block action potentials, AMPA and NMDA receptors respectively. (**B, Top**) 200 representative IPSCs averaged before (black) and 10 minutes after (red) bath application of PD168077 (200nM). **Bottom**, same mIPSCs normalized by amplitude to show the differences in decay kinetics. (**C**) Schematic representation of the experiment. (**D**) Graphs show the mIPSC frequency and amplitude before drug application (baseline) and 10 minutes after administration of the D4R agonist. Right, cumulative distributive function reveals that a smaller percentage of high amplitude events after D4R agonist administration. *:$p<0.05$, **:$p<0.01$, paired *t*-tests, n=6.

To determine whether D4R antagonists modified synaptic inhibition onto PV+ interneurons in the mPFC, I recorded mIPSCs from PV+ interneurons before and after bath application of the D4R antagonist. The D4R antagonist, L745870 (50nM), did not significantly influence the frequency (+1%) or amplitude (+4%) of mIPSCs (both $p>0.05$, paired t-test, n=3). There were not enough artifact-free recordings from the interneurons in the dhCA1 to make any conclusions about the effects of D4R antagonists on GABAergic neurotransmission in this region.

2.3.3 Excitability of PV+ interneurons

To determine whether D4R inhibition affected the intrinsic excitability or action potential characteristics of PV+ neurons, I somatically injected current into PV+ neurons in layer 5 of the mPFC of PV/Tom mice. In layer 5 PV+ neurons, the D4R antagonist hyperpolarized the action potential voltage threshold by 5.06mV ($p<0.05$), decreased the amplitude by 10.19mV ($p<0.05$), and decreased the afterhyperpolarization amplitude by 2.15mV ($p<0.01$) compared to baseline (Fig2.3, paired *t*-tests). The antagonist also increased excitability (Fig2.3C), by shortening the latency to the first action potential at

each current injection by an average of 0.93ms (starting with the current injection 50pA after the rheobase for each cell, $p<0.001$, paired *t*-test). Additionally, the average interspike interval decreased by 1.5ms (starting with the current injection 50pA after the rheobase for each cell, $p<0.05$, paired *t*-test). These changes suggest that D4Rs modify sodium (Na^+) and potassium (K^+) currents with endogenous levels of dopamine in the slice. Vehicle recordings from PV+ interneurons did not show significant changes in voltage threshold or action potential shape over time ($p>0.05$), indicating that these effects were not artifacts. Unlike recordings performed with the agonist and vehicle, PV+ interneurons receiving the D4R antagonist rarely required a more negative holding current later in the recording (0/7 vs. 6/22). There were no significant changes in input resistance (average change antagonist -4.1% vs. vehicle & agonist -1.5%, both $p>0.05$), indicating no significant changes in leak currents at -70mV. Taken together, the D4R antagonist increases the cell-intrinsic excitability of PV+ interneurons in layer 5 of the mPFC.

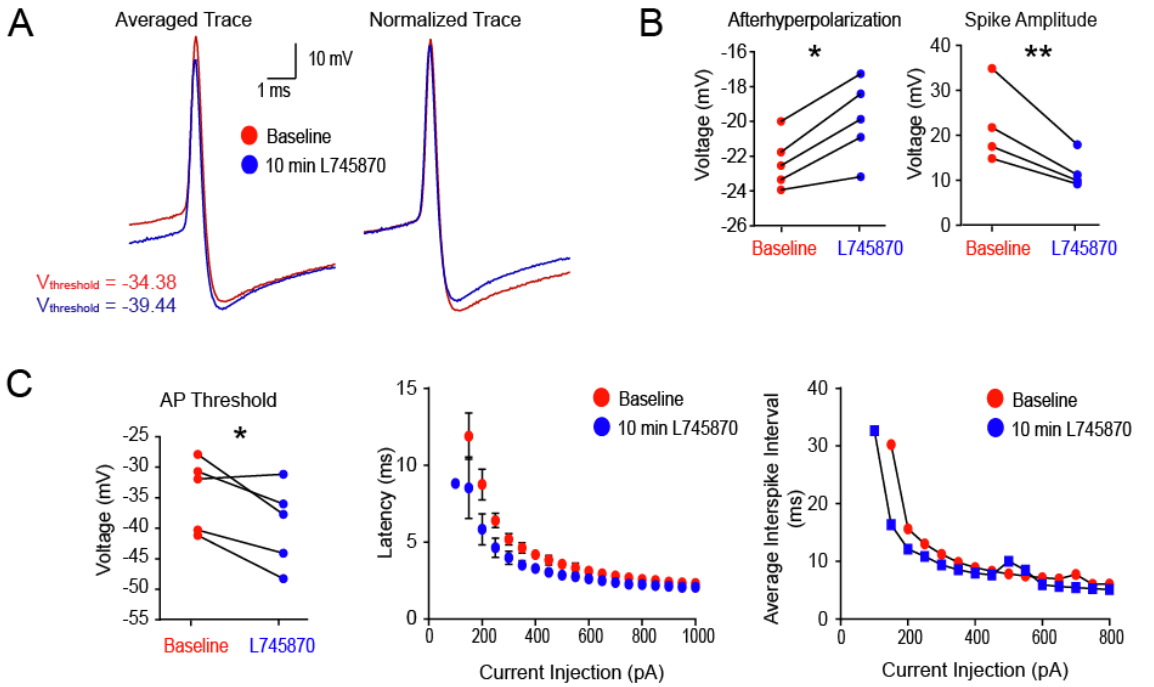

Figure 2.3: D4R antagonists increase the excitability of PV+ interneurons in layer 5 of the mPFC. A, A representative average of the first 25 action potentials at baseline (red) and after 10 minutes of L745870 (50nM) bath application (blue) in a PV+ interneuron from layer 5 of the mPFC. The normalized trace sets traces equal at $V_{threshold}$. **B**, Significant reduction in afterhyperpolarization (left) and spike amplitude (right) suggest possible changes in Na^+ or K^+ conductances. **C**, Action potential threshold (left), average latency (middle) and interspike interval (right) all reveal an increase in overall neuron excitability (n=5, **p*<0.05, ***p*<0.01, paired *t*-test).

In contrast, application of the D4R agonist, PD168077 (200nM), did not significantly alter action potential half-widths or afterhyperpolarization amplitudes produced from hippocampal PV+ interneurons (*p*>0.05, n=6, paired *t*-test) in agreement with Andersson *et al* (2012a). However, I observed subtle changes in spike amplitudes and decay times. Spike amplitude decreased by 3.49mV (*p*<0.05, n=6, paired *t*-test) and decay time increased by 22.89µs (*p*<0.01, n=6, paired *t*-test).

2.4 Discussion

In the current study, I administered a D4R agonist or D4R antagonist to slices from the dhCA1, or mPFC, and recorded from PV+ or non-PV expressing interneurons and pyramidal neurons. I analyzed the effects of dopamine D4R activation on PV+ interneurons and determined that the D4R reduced GABAR-mediated currents postsynaptically, and slowed the decay kinetics of mIPSCs. These confirmed previous findings in the lab showing that a subpopulation of interneurons had decreased postsynaptic GABAR-mediated currents, and suggests that this subpopulation was in fact PV+ interneurons. I also observed that D4R antagonism increased the frequency and amplitude of GABAR-mediated currents in pyramidal neurons, contrary to previous findings from our lab demonstrating that D4R agonism increased the frequency of GABAR-mediated currents in pyramidal neurons. While this might suggest a potential U-shaped curve, such that D4R agonism or antagonism increases the frequency of GABA release onto pyramidal neurons, I failed to reproduce earlier findings that the D4R agonist increased the frequency of GABAR-mediated currents in pyramidal neurons. I also failed to reproduce previous findings in the lab that D4R agonism increased the frequency of GABA-mediated currents in a separate population of interneurons. Finally, I observed that D4R agonism had little effect on the intrinsic excitability of PV+ interneurons, but D4R antagonism increased their intrinsic excitability.

2.4.1 Expression patterns

D4R agonists decreased the frequency and amplitude of IPSCs in PV+ interneurons in the dhCA1, but not from PV+ interneurons in layer 5 of the mPFC.

Dopamine receptor expression patterns vary between brain regions. While dopamine projections in layer 5 of the mPFC are relatively plentiful, these projections into the hippocampus are difficult to detect (Björklund and Dunnett, 2007). Therefore, the hippocampus may have lower endogenous levels of dopamine, resulting in more D4Rs with free ligand-binding sites. However, D4R mRNA expression is highest in layer 5 of the prefrontal cortex (de Almeida and Mengod, 2010; Lidow et al., 1998), while only 21% of PV-expressing interneurons express D4R at levels high enough to detect via *in situ* hybridization in the hippocampus (Andersson et al., 2012b). It is probable that many of the neurons involved in this study simply did not express the D4R. While many PV+ interneurons do not express the D4R, there is no reliable way to determine whether a cell expresses the D4R. The D4R is hard to detect with an antibody because it is expressed at low levels and does not form obvious puncta. We have attempted to use single cell PCR and post-hoc immunohistochemistry to determine whether a cell express the D4R, but currently we were unable to detect the D4R at the single cell level.

Furthermore, the expression and intracellular function of the D4R depends on brain region and cell type. While pyramidal neurons from the hippocampus decreased NMDA currents after D4R activation with a high dose of agonist (10μM PD168077), pyramidal neurons from the prefrontal cortex showed no change in NMDAR-mediated current amplitude (Beazely et al., 2006). Even within brain regions, dopamine may have differential effects. For instance, dopamine increases pyramidal neuron excitability in the prelimbic cortex, but not in the neighboring infralimbic cortex or cingulate gyrus (Ceci

et al., 1999). Further research is needed to better understand why D4R activation dichotomous effects on PV+ interneurons in the mPFC versus the dhCA1.

2.4.2 GABAergic currents

Careful examination of the concentrations of the D4R agonist used in other investigations is important, as it would be easy to ascribe off-target effects of pharmacological agents to the D4R's mechanism of action. D4R agonists and antagonists work in the nanomolar range; however, most studies using these drugs have used concentrations well above the EC_{50} for other related receptors (Tocris website). For instance, the D4R agonist PD168077, binds to 5HT1A receptors at ~250nM and binds to α2c receptors at ~440nM in HEK cells (Moreland et al., 2005). While I used 100-200nM of the D4 agonist PD-168077, the concentrations used in other studies in slice are between 10 and 50μM. Unfortunately, agonists have rarely been used in conjunction with antagonists or in knockout animals (for an exception see Yuen et al., 2010), so it is unclear which effects ascribed to the D4R may actually be related to off-target drug activity. Furthermore, rapid release of dopamine from dopaminergic fibers can produce the opposite effects of bath-applied dopamine (Rosen et al., 2015b). It is important, therefore, to remain cautious about how the effect of long-term D4R activation due to bath application relates to phasic dopamine release *in vivo*.

No clear picture emerged about how D4R activation influences GABAergic signaling onto pyramidal and interneurons. I found no significant difference in the amplitude of mIPSCs in pyramidal neurons or non-PV expressing interneurons after D4R activation. This confirmed a previous study using low concentrations of the D4R agonist

in the hippocampus (Andersson et al., 2012a), but contrasted with two studies using higher agonist concentrations in the globus pallidus and prefrontal cortex (Shin et al., 2003; Wang et al., 2002). GABAR-mediated currents in PV+ interneurons in the dhCA1 decreased with D4R activation. Previous studies suggest that GABAR-mediated current reductions in other neuronal types involves the internalization of $GABA_AR_{\beta 2/3}$ receptors (Graziane et al., 2009). Additionally, I observed no significant change in IPSC frequency in pyramidal neurons in the mPFC after D4R activation. Although previous work in our lab showed that D4R activation increases mIPSC frequency in pyramidal neurons, other literature revealed a decrease in IPSC frequency in the hypothalamus, thalamus, and septal nucleus (Asaumi et al., 2006; Azdad et al., 2003; Baimoukhametova et al., 2004; Gasca-Martinez et al., 2010). Therefore, the D4R appears to have different presynaptic activity in different brain regions. Furthermore, I observed that D4R activation decreased the frequency of GABA release onto PV+ and non-PV interneurons in the dhCA1. This may arise from synapse-specific differences in D4R expression and release probability. In pyramidal neurons, the probability of release from a given axon depends on the postsynaptic contact (Scanziani et al., 1998), therefore synapses between two PV+ neurons may act differently from PV+ interneuron synapses onto pyramidal neurons.

D4R inhibition presented an equally perplexing picture as to its influence on GABAergic signaling. While D4R activation had little effect on GABA-mediated currents in pyramidal neurons, the D4R antagonist increased the frequency and amplitude of GABA-mediated currents in pyramidal neurons in the dhCA1, suggesting both a presynaptic and postsynaptic effect of D4R activation. However, D4R inhibition had little

effect on GABA-ergic currents in PV+ interneurons in the mPFC. Three possible explanations for these findings emerge: 1) D4Rs are mainly expressed in PV+ interneurons where they stay active at low levels, decreasing interneuron excitability and mIPSC frequency through two unique mechanisms, such as the modification of potassium channels in the interneuron soma (Bean, 2007), and modification of quantal release at the presynaptic terminal (Borisovska et al., 2013). 2) D4Rs are mainly expressed in astrocytes where they regulate intracellular calcium levels and GABA uptake to modulate extracellular GABA concentration to influence the frequency of mIPSCs (Kang et al., 1998) and where they are able to influence mIPSC amplitude onto interneurons more strongly than on pyramidal neurons (Shigetomi et al., 2012). 3) D4Rs are scattered at low levels throughout many cell types and brain areas. When activated, these receptors maintain a homeostatic balance (Yuen et al., 2010), therefore, either activation or inactivation of these receptors in a relatively quiescent preparation causes a plethora of changes which enhance the overall activity of the network.

2.4.3 Excitability

Inhibition of D4Rs increases PV+ interneuron excitability in one of two ways: it may work through an intrinsic mechanism, or it may increase extracellular dopamine in the slice. One recent study showed that D4Rs increased FSI excitability through Kv3.1/3.2 channels (Trantham-Davidson et al., 2014). However, these recordings were performed at non-specific doses of the D4R agonist PD 168077 (40μM instead of 100 nM). A study using more appropriate agonist concentrations also observed that D4R activation decreased an outward rectifying potassium current recorded from FSIs, but

only at voltages above -10mV (Andersson et al., 2012a). Given that outward K^+ currents repolarize the membrane during an action potential, reducing these currents will increase the half-width of the action potential more than modifying action potential voltage threshold. The action potentials of PV+ interneurons did not widen significantly with D4R activation; however, with the D4R antagonist, there was a trend toward narrower action potentials (half-width = 44.5 μs faster, p=0.08). D4R agonists have also been shown to decrease G-protein inwardly-rectifying potassium (GIRK) currents (Wedemeyer et al., 2007), so inhibiting these receptors may increase GIRK currents to influence neuronal excitability. Earlier recordings from FSIs suggested that inhibition of D4Rs had no effect on their excitability as revealed by membrane depolarization (Gorelova et al., 2002). However, this measure fails to capture the effects of the D4R on voltage-gated ion channels and instead focuses on the leak currents active near the neuron's resting potential. The faster latencies, reduced afterhyperpolarizations and changes in AP amplitude such as those I have observed (Fig2.3) often reflect changes in voltage-gated Na^+ and K^+ currents.

The hypothesis that inhibition of D4Rs increase PV+ interneuron excitability by increasing extracellular dopamine in the slice is attractive because it provides a potentially common pathway for both NRG1 and D4R to increase intrinsic excitability. Dopamine levels increase in the PFC after application of a D4R antagonist (Broderick and Piercey, 1998) and in the hippocampus after application of NRG1 (Kwon et al., 2008). Dopamine alone increases FSI excitability in the prefrontal cortex through the activation of D1-type receptors (Gorelova et al., 2002), and increases the excitability of

pyramidal neurons (Ceci et al., 1999). Dopamine's effect on pyramidal neurons was reversed by 10 μM of the D4R antagonist L745870; although the specificity of the drug at this concentration is questionable. Likewise, D2-type dopamine receptors regulate calcium currents (Bender et al., 2010), axonal potassium currents (Kole et al., 2007; Yang et al., 2013a), Na^+ currents (Maurice et al., 2001), and I_h currents (Campanac and Hoffman, 2013), all of which contribute to a neuron's excitability (Bean, 2007). Furthermore, NRG1 increases FSI excitability in slices through the phosphorylation of a Kv1 channel (Li et al., 2012), but decreases the excitability of ErbB4-expressing cultured hippocampal neurons by reducing Na^+ currents (Janssen et al., 2012). More signaling pathways are intact in slices than in cultured neurons, therefore NRG1 activation may increase dopamine levels in a slice, but not a cultured set of neurons thereby influencing excitability via dopamine in the slice, and via intrinsic properties in the culture. Finally, PV+ interneurons lacking ErbB4Rs have greater spontaneous activity than PV+ interneurons with ErbB4Rs (del Pino et al., 2013). This suggests that ErbB4R activation may inhibit the intrinsic excitability of PV+ neurons at baseline.

Two aspects of the recording methods are worthy of discussion. 1) Before each recording, I reset the membrane potential to -70mV (± 3 mV) in order to cancel out changes in tonic GABA or NMDA receptor mediated currents. This also allowed me to examine changes in the same set of ionic currents. Although I did not see a significant change in holding current (8± 8pA at baseline vs. 0± 41pA 10 minutes after the antagonist), resetting the membrane potential to -70mV may have masked a significant depolarization or voltage-gated current (Owen et al., 2013). However, there was no

significant change in membrane resistance, as would be expected if tonic currents were changing. 2) Cells often display different excitability patterns when stimulated extrasynaptically versus somatically. I chose to only examine somatic current injections to avoid potential confounds with changes in glutamatergic signaling.

I consistently experienced problems reproducing the results of a senior electrophysiologist. In attempts to standardize our recordings, I made recordings from the brain region that she did. I also tried using her set of reagents, making new reagents, using mice of different age ranges and sexes, and doubling the doses of the D4R agonist, but I was unable to replicate her findings. I went through and re-analyzed her data to ensure that we used the same data analysis techniques. Her recordings showed clear effects while mine did not. The only variable not tested was the recording apparatus itself. Due to the inability to replicate previous findings, I focused my efforts on *in vivo* recordings of single neurons and gamma frequency local field potential (LFP).

CHAPTER THREE: Neuronal correlates of ketamine and walking induced gamma oscillations in the medial prefrontal cortex and mediodorsal thalamus

3.1 Introduction

In the mPFC, neural synchrony in the gamma frequency range (30-80Hz) is thought to play an important role in cognitive flexibility, working memory, and attention (Cannon et al., 2014; Gregoriou et al., 2015). Indeed, optogenetic inhibition of mPFC interneurons inhibits both gamma local field potential (LFP) power and cognitive flexibility while activation of mPFC interneurons at gamma frequencies restores cognitive flexibility in cognitively impaired mice (Cho et al., 2015). Previous work from our lab has shown increases in gamma LFP power in the rodent mPFC during a treadmill walking task that requires attention (Delaville et al., 2015). Gamma power increases have also been observed during locomotion and arousal in the visual cortex (McGinley et al., 2015a; Niell and Stryker, 2010; Vinck et al., 2015). Additionally, it has been proposed that impairments in gamma oscillations play a key role in producing the cognitive deficits observed in psychiatric disorders such as schizophrenia (Pittman-Polletta et al., 2015; Sakurai et al., 2015). Cognitive deficits often precede the onset of psychosis, and show the least improvement after antipsychotic treatment (Green, 2006; Minzenberg and Carter, 2012). Specifically, many studies find that patients with schizophrenia have elevated ongoing cortical gamma power, and exhibit task-related deficits in gamma power modulation during sensory perception and cognitively demanding tasks (Cho et al., 2006; Jadi et al., 2015; Minzenberg et al., 2010).

Ketamine-induced gamma power in rodents has been used as a physiological correlate of psychosis and possible biomarker for investigating the efficacy of antipsychotics (Gilmour et al., 2012; Hudson et al., 2016). In healthy humans, an acute, subanesthetic dose of ketamine induces the symptoms of early stage schizophrenia, such as cognitive impairments, perceptual distortions and hallucinations (Krystal et al., 1994) and increases ongoing gamma power (Anticevic et al., 2015; Hong et al., 2010; Muthukumaraswamy et al., 2015; Shaw et al., 2015). Similarly, in rats, an acute, subanesthetic dose of ketamine increases motor activity, incoordination, and ongoing cortical and thalamic gamma power (Hakami et al., 2009; Kocsis et al., 2013; Saunders et al., 2012). Further insight into the mechanisms by which ketamine increases gamma power within cortical local circuits and within the thalamus may be useful for understanding its clinical relevancy. Therefore, this study seeks to further characterize gamma oscillations induced by ketamine by comparing these oscillations to physiological gamma oscillations induced by walking in the mPFC and one of its major sources of innervation, the MD thalamus, at the LFP and single neuron levels.

Given that reduction of ketamine-induced cortical gamma power has been proposed to predict antipsychotic drug efficacy, we also tested the ability of a dopamine D4 receptor (D4R) agonist to decrease ketamine-induced gamma power. The D4R has emerged as a potential pro-cognitive target in schizophrenia due to its expression in the mPFC (Mrzljak et al., 1996), and the ability of D4R agonists to increase gamma power and cognitive performance (for a review, see Furth et al., 2013; Nakazawa et al., 2015). Furthermore, D4R antagonists reverse cognitive deficits induced by stress or chronic

NMDAR antagonism in monkeys (Arnsten et al., 2000; Jentsch et al., 1999). Finally, the D4R antagonist can prevent other neuromodulators, such as neuregulin 1, which has repeatedly been genetically associated with the risk for schizophrenia (Buonanno, 2010), from increasing gamma power (Andersson et al., 2012b). Consequently, the D4R may constitute a potential target for modulating gamma oscillation power in the ketamine model of schizophrenia.

The present study examined the effects of an acute subanesthetic dose of ketamine on the LFP and single neuron activity of the mPFC and MD thalamus of a rat performing a treadmill walking task. We analyzed the effects of ketamine on spike-LFP relationships in each structure to provide insight into the ways in which neuronal spiking correlates with changes in locally synchronized gamma oscillations and to ascertain whether ketamine increases gamma power through a distinct mechanism in the MD thalamus versus the mPFC. Finally, we tested the influence of a dopamine D4R agonist and antagonist on ketamine-induced gamma.

3.2 Materials and Methods

All experimental procedures were conducted in accordance with the NIH Guide for Care and Use of Laboratory Animals and approved by NINDS Animal Care and Use Committee. We attempted to minimize the number of animals used and their discomfort.

3.2.1 Rats and behavioral paradigm

Male Long Evans rats (Charles River, Frederick, MD, USA), weighing 280–300 g, were housed with ad libitum access to chow and water in environmentally controlled conditions with a 12:12 h light:dark cycle (lights off at 9:00h). Rats were handled daily

the week before surgery and trained to walk on a circular treadmill as previously described (Avila et al., 2010). The treadmill walking task requires attentiveness, as the rats have to maintain a consistent walking speed in order to avoid being pushed by a stationary paddle placed on the treadmill (Fig 3.1B).

3.2.2 Surgical procedures

Two electrodes were implanted for recording LFP and spikes from the left prelimbic mPFC, and the left MD thalamus during the same surgery (Fig 3.1A). Rats were anesthetized with 75 mg/kg ketamine and 0.5 mg/kg medetomidine (i.p.) and placed in a stereotaxic frame (David Kopf Instruments, Tujunga, CA, USA), with head-fixed with atraumatic ear bars. Holes were drilled in the skull above the target coordinates for the mPFC (AP: +3.6 mm from the bregma, ML: +0.6 mm from the sagittal suture and DV: 3.6 mm from the skull surface), and MD thalamus (AP: -2.5 mm from the bregma suture, ML: +0.5 mm from the sagittal suture and DV: 5.8 mm from the skull surface; Fig3.1A). Electrode bundles consisted of 8 stainless steel teflon-insulated microwires plus an additional 9^{th} wire with no insulation on the distal ~1 mm of the recording tip with lower impedance serving as a local reference (Brazhnik et al., 2012; Delaville et al., 2015; Dupre et al., 2016). They were implanted in the target regions and secured to the skull with screws and dental cement. Ground wires from each set of electrodes were wrapped around a screw located above the cerebellum. After completion of surgeries, 0.15% of ketoprofen in 0.9% NaCl solution was given subcutaneously (s.c.), and atipamezole (0.3-0.5 mg/kg, s.c.) was administered to reverse the effect of medetomidine.

During the first week of postoperative recovery, the rat's diet was supplemented with fruit and bacon treats. Rats were retrained at the circular treadmill walking task after the fourth postoperative day.

3.2.3 Behavioral analysis

A web camera (Logitech) was mounted next to the circular treadmill in order to provide behavioral data synchronized with the electrophysiological recordings. To quantify how ketamine affected behavior, an independent experimenter assessed the rodent's behavior using 50-second video epochs with treadmill-off and treadmill-on. Behavior with the treadmill-on was scored from before the ketamine injection (baseline) and 15 minutes after the ketamine injection, and behavior with the treadmill-off was scored from baseline and 13 minutes after the ketamine injection.

When the treadmill was off, the rat was still inside the circular treadmill track and the paddle was down so that it could not walk the treadmill freely. In this condition, untreated rats entered states of attentive or inattentive rest, but ketamine-treated rats were either hyperactive, or ataxic. To evaluate motor activity, we measured the number of seconds that the rat spent moving his trunk or limbs (but not its head). Ataxia was scored according to the following scale (adapted from Cho et al., 1991; Cui et al., 2014): (0) inactive or coordinated movements, (1) awkward or jerky movements or loss of balance while rearing, (2) frequent falling or partial impairment of antigravity reflexes, (3) the inability to move beyond a small area and to support body weight and (4) inability to move except for twitching movements. The stereotypic rating scale was also adapted from (Cho et al., 1991). Briefly, we quantified the number of head-bobs, turns, and the

number of seconds spent backpedaling. Head-bobs included side-to-side or vertical head movements, and turns involved a 180 degree turn so that the rat's direction in the treadmill had changed.

During treadmill-on epochs, an independent experimenter recorded the number of turns, the number of times that the rat hit the paddle, and the duration the rat spent being pushed by the paddle. Paddle hits counted for any of the rat's body parts other than the tip of his tail. Comparisons between baseline and ketamine treatment were made using paired t-tests for each behavioral measure.

3.2.4 Electrophysiological recordings

Extracellular spike and LFP recordings were collected for every experiment using Plexon (Dallas, TX) and Spike2 (CED, Cambridge, UK) systems as described in (Delaville et al., 2015). Both spikes and LFPs were referenced to the scraped 9^{th} wire. Spikes were sampled at 40kHz and LFPs were sampled at 2kHz. Action potentials were amplified (10,000x) and band pass filtered (0.3-8 kHz). LFPs were amplified (2000x) and band pass filtered (0.7-150 Hz). Discriminated spike and LFP signals were digitized, stored and analyzed using Spike2 data acquisition and analysis software.

Baseline recordings consisted of at least two five-minute epochs of counterclockwise walking and two 40 second epochs of inattentive rest without artifacts. After drug injections, the rat repeated a pattern of walking for 4 minutes and treadmill-off for one minute for the first 25 minutes, then the treadmill was turned off for the final 4 minutes before the next injection. Direct observation and videotaped motor behavior were used to identify artifact-free 100-second intervals within the treadmill walking epochs

and 40 to 100 second intervals from treadmill-off epochs. Any epoch of either behavior showing artifacts was excluded. The circular treadmill‘s speed was set at 9 to 11 rotations per minute.

3.2.5 Experimental conditions and drugs

Starting one week after the surgery, recording sessions were conducted once a week with at least six days between each recording. Table 3 shows the order of the three experiments and Table 4 shows the time course of each experiment. Treadmill on and off recordings at post-surgical day 7 were obtained from 15 rats. Ten rats participated in the experiments described in Table 3 and the remaining five rats were used in a separate study.

Rats that participated in the D4R dose response curve experiments were randomly assigned to receive the vehicle or D4R agonist first (n=6). The D4R agonist A-412997 (Tocris, MN) and antagonist L-745,870 (Tocris) were dissolved in saline and injected at 1mL/kg subcutaneously. Doses of the agonist were chosen based on Kocsis and colleagues (2014) so that the final cumulative dose was 3mg/kg of A-412997. Injections were given every 30 minutes in ascending order from 0.3mg/kg through 1.5mg/kg A-412997, as described in Table 4.

The second experiment (Ascending doses of ketamine, n= 8, Table 4) consisted of two consecutive 5mg/kg doses of racemic ketamine-hydrochloride (Akorn, IL) administered subcutaneously one hour apart. This paradigm was chosen because ketamine has long-term effects on behavior, and 5 and 10 mg/kg ketamine are the two most commonly used doses in other rodent studies (Amat et al., 2016; Li et al., 2010;

Pinault, 2008). The two-dose paradigm allowed us to probe whether a cumulative dose of 10mg/kg ketamine would have similar effects to a single 10mg/kg dose. This experiment was performed on a different day from the final anesthetic dose, although all three doses are compared.

In the final experiment, we employed a drug testing paradigm similar to the one used by Jones and colleagues (2012) in which a pretreatment was administered 30 minutes before an injection of ketamine (n=6, Table 4). In short, we recorded 30 minutes of baseline, followed by an injection of one of three pretreatments – saline, 3mg/kg A-412997, the D4R agonist, or 5mg/kg L-745,870, the D4R antagonist. Each drug was administered according to a random design. Thirty minutes after the pretreatment, a single injection of 10mg/kg ketamine was given subcutaneously, and recordings continued for the next 100 minutes. Therefore every rat was his own control. The final anesthetized recording was combined with the last experimental recording in about half of the rats and started 100 minutes after the ketamine injection. If the rat had already received 10mg/kg ketamine, then the final dose was 90mg/kg. Otherwise 100mg/kg of ketamine was administered subcutaneously as the final ataxia-inducing dose.

Group	Week 1	Week 2	Week 3	Week 4	Week 5	Week 6
N= 4 rats	D4R/vehicle dose response curves: rats randomly assigned to receive vehicle of D4R agonist first		D4R antagonist dose response (data not shown)	Ascending doses of ketamine	Sacrificed	
N= 2 rats	D4R/vehicle dose response curves: rats randomly assigned to receive vehicle of D4R agonist first		Vehicle, A412997, or L745870 pretreatment 30 minutes before ketamine injection: order of treatments randomly assigned			Sacrificed
N= 4 rats	Ascending doses of ketamine	Vehicle, A412997, or L745870 pretreatment 30 minutes before ketamine injection: order of treatments randomly assigned			Sacrificed	

Table 3. Experimental design. Randomized drug delivery schedules for each group of rats, with 1 week washout between recordings. Rats in the first two groups were randomly assigned to receive the D4R agonist or the vehicle dose response curve on week 1, and rats in the second two groups received the ketamine pretreatments, 1mL/kg saline, the D4R agonist 3mg/kg A-412997, and the D4R antagonist 5mg/kg L-745870 in a randomized order.

Experiment	Injection 1, Time = 0 minutes	Injection 2, Time = 30 minutes	Injection 3, Time = 60 minutes	Injection 4, Time = 90 minutes
D4R dose response curve	0.3mg/kg A-412997	1.2 mg/kg A-412997	1.5 mg/kg A-412997	5 mg/kg L-745,870
Vehicle dose response curve	1mg/mL saline	1 mg/mL saline	1mg/mL saline	5 mg/kg L-745,870
Ascending doses of ketamine	5mg/kg ketamine	1mg/mL saline*	5mg/kg ketamine	
Vehicle pretreatment + Ketamine	1mg/mL saline	10mg/kg ketamine		
L-745,870 pretreatment + Ketamine	5 mg/kg L-745,870	10mg/kg ketamine		
A-412997 pretreatment + Ketamine	3mg/kg A-412997	10mg/kg ketamine		
Final ketamine	100mg/kg ketamine	0.15 mg medetomidine#		

Table 4. Time course of each recording. Each recording consisted of a 30 minute drug-free baseline followed by a 125 minute post injection period. The time course of the injections is indicated in the table. *: injected at 45 minutes, # injected between 20 and 30 minutes.

3.2.6 Spectral analysis of local field potential recordings

LFP power was measured by fast Fourier transform (FFT) with a frequency resolution of ~1 Hz and normalized by dividing the power at each frequency by the sum of power between 250 and 300Hz in order to compensate for any instrumental

fluctuations over time (Brazhnik et al., 2016). For each structure, total power in the low gamma (40-59Hz) and high gamma (70-120Hz) frequency ranges was calculated using a spike2 script. Additionally, if a significant peak was found between 40 and 70Hz, the power was summed from 7Hz below and above the peak to find the total low gamma power. A peak was considered significant if its relative maximum was greater than the surrounding 14 frequency bins in the low gamma range, the first derivative of the spectrum was positive to the left of the peak and negative to the right of the peak, and the second derivative at the peak was negative, indicating a downward concavity. LFP power from two wires per electrode bundle during two epochs was averaged for each behavioral condition. Spectral coherence was calculated for the same set of wires between the mPFC and MD thalamus using a Spike2 script and FFT-based spectral coherence. Coherence was calculated as in Delaville and colleagues (2015). Using 100 second epochs, any coherence over 0.015 was considered significant. Data are reported as mean ± SEM.

To visualize spectral power changes over time for the selected epochs, time-frequency wavelet spectra were constructed using continuous wavelet transforms. The Morlet wavelet was applied to the LFPs using 128 frequency scales and a time resolution of approximately 750 ms (Time-Frequency Toolbox (http://tftb.nongnu.org). Time-frequency mPFC-MD thalamus coherence was calculated using FFT-based coherence over a 10 second (s) sliding window (Chronux: http://chronux.org). The multitaper coherence analysis introduced a bias determined by the following formula:

$$B = \frac{1}{\sqrt{\nu}}$$

B is the bias introduced by the analysis and v represents the degrees of freedom, equivalent in this case to the number of tapers used. This multitaper calculation utilized 19 tapers, resulting in a bias of about 0.23. To compensate for this, the smallest coherence values in the plot were adjusted to 0.23 and the largest to 1.23, rather than 0 and 1, respectively (Bokil et al., 2007).

In order to analyze the effects of the different drugs on the LFPs compared to baseline recordings, percent change from baseline walk in each frequency bin (for data visualization), or for each frequency range (for specific frequency range analysis) was used. Percent change was calculated using the formula:

$$Percent\ Change = \frac{P_{f,t} - P_{f,baseline}}{P_{f,baseline}} \times 100\%$$

P is power in the frequency range (f) at a given time (t). Outlier time points for power were removed using the ROUT (robust nonlinear regression combined with outlier removal) test with Q set to 1% (Motulsky and Brown, 2006) and the average of the other rats was used as a replacement value (Dupre et al., 2016).

The effects of various drug treatments on coherence and power over time within specific frequency ranges were assessed during treadmill walking using two-way repeated measures analysis of variance (ANOVA) following by Holm-Sidak's multiple comparisons with the level of significance: $\alpha = 0.05$.

To test for a bimodal distribution within the firing rates, angular phases and half-widths of interneurons, a dip test (Hartigan and Hartigan, 1985) was used. When showing that mean STWA ratios were significantly different from a randomly ordered spike train (with a theoretical value of 1), a permutation test was used.

3.2.7 Cell sorting and STWA analysis

Spike waveforms from the mPFC and the MD thalamus were sorted using principal component analysis (PCA) in Spike2. To assess effective sorting for single cells, inter-spike interval (ISI) histograms were generated and inspected to ensure that sorted cell clusters did not exhibit multiunit behavior by firing within the assumed refractory period (1.2 ms). Putative pyramidal neurons and interneurons were separated using trough-to-peak intervals (Azouz et al., 1997; Brazhnik et al., 2012; Wilson et al., 1994). Units with trough-to-peak intervals greater than 0.5ms were classified as putative pyramidal neurons (112/147), and those with intervals less than 0.4ms were classified as interneurons (31/147). Four neurons did not fit into either category and were left unclassified. In this paper, the terms pyramidal neuron and interneuron refer to putative pyramidal and putative interneurons, respectively. MD thalamus neurons with narrow waveforms were excluded if the recovery phase of the action potential was less than 0.293ms (mean-2.5SD, n=9 cells) to ensure a homogeneous population of neurons. . These 9 neurons showed significant walking-induced increases in firing rate and spike-gamma LFP relationships (both $p<0.05$, ratio paired t-tests), similar to those observed in the other MD thalamus neurons.

To assess the temporal relationship between the spiking activity of individual neurons and LFPs from the same structure, spike-triggered waveform averages (STWA) were calculated for epochs of 100 to 200 seconds. LFPs from the recording wire or one of two neighboring wires were band-pass filtered between 40 and 59Hz. For each wire with a usable spike train, we calculated its coherence between 40Hz and 59Hz with all the

other wires, and ranked each wire from the one with the maximum to the minimum coherence. We selected the wire with the maximum coherence and the median coherence as the neighboring wires, and refer to them as the maximum wire and median wire, respectively. Peak-to-trough amplitudes of the STWAs at or around the spike (zero time) were obtained as a measure of correlation between the spike train and dominant gamma oscillation. Twenty shuffled STWAs for the same epochs were created by shuffling the interspike intervals of each spike train and used to create 20 normally distributed peak-to-trough values. The extent of correlation between spikes and gamma-filtered LFPs after ketamine or D4R drug treatments during epochs of walking was compared to baseline walk epochs using the mean ratio of unshuffled/shuffled peak-to-trough amplitudes (mean STWA ratio). Comparisons of firing rate and mean STWA ratio between baseline and ketamine administration were assessed using repeated measures one-way ANOVAs with Holm-Sidak's multiple comparisons: $\alpha = 0.05$. Outlier neurons were removed using the ROUT (robust nonlinear regression combined with outlier removal) test with Q set to 0.1%(Motulsky and Brown, 2006).

3.2.8 Histology

After recordings were completed, rats were deeply anesthetized with ketamine (100mg /kg, s.c.) and 0.15mg medetomidine and recording sites were marked by passing a 10 μA positive current for 15-17 seconds via 3 microwires and 9 seconds via the reference electrode. Rats were perfused intracardially with 200 mL cold saline followed by 200 mL 4% paraformaldehyde in phosphate buffer solution (PBS). Brains were post-fixed in paraformaldehyde solution overnight and then immersed in 10% sucrose in

phosphate buffered saline (0.1 M, pH 7.4). Coronal sections of 35 μm were collected on slides. Sections for electrode placement verification were mounted on glass slides and stained with cresyl violet and 5% potassium ferricyanide-9% HCl to reveal the iron deposited at the electrode tips. Rats were only included in the analysis if the electrodes were properly placed in the prelimbic mPFC and/or the core or shell of the MD thalamus.

3.3 Results

To investigate the effects of ketamine on the relationships between behavior, gamma power, and neuronal activity in the mPFC and the MD thalamus, the major thalamic source of mPFC innervation (Mitchell and Chakraborty, 2013), we recorded simultaneously from these two structures during different behavioral states before and after ketamine administration (10 mg/kg, Fig 3.1). It has been shown that ketamine administration induces a state of hyperactivity and increases cortical gamma activity (Hakami et al., 2009). Previous work in our lab has shown that treadmill walking also induces an increase in mPFC gamma activity (Delaville et al., 2015). To compare the effects of locomotion alone with ketamine's effects on gamma power, we first examined the effects of treadmill walking on LFP activity in rats; then we examined the effects of ketamine administration on LFP activity and motor behavior during treadmill walking.

3.3.1 Effects of treadmill-walking and ketamine on gamma power

The present results confirmed previous observations showing that treadmill walking induced an increase in mPFC gamma power (Delaville et al., 2015). Seven days post-electrode implantation, during treadmill-off epochs, there was no significant spectral

peak in the low gamma range (40-70Hz). During treadmill-on, the power spectra of the mPFC showed an increase in LFP power in a relatively narrow band with a mean peak of 51.1±0.8Hz (Fig 3.1C,E,G). The LFP power in a 15Hz range surrounding this significant gamma peak (see Section 3.2.6) increased by 23.8% relative to treadmill-off (p<0.01, paired t-test; Fig Fig 3.1F). To gain insight into whether projections from the MD thalamus contribute to walking-induced gamma activity in the mPFC during walking, we examined its LFP activity. Interestingly, in the MD thalamus, the low gamma power increased by 17.5% during treadmill walking in a broader band than observed in the mPFC with a mean peak at 48.6 ±0.5 Hz (p<0.01, paired t-test; Fig 3.1C,E-G). Thus, treadmill walking induced increases in gamma power in both the MD thalamus and mPFC.

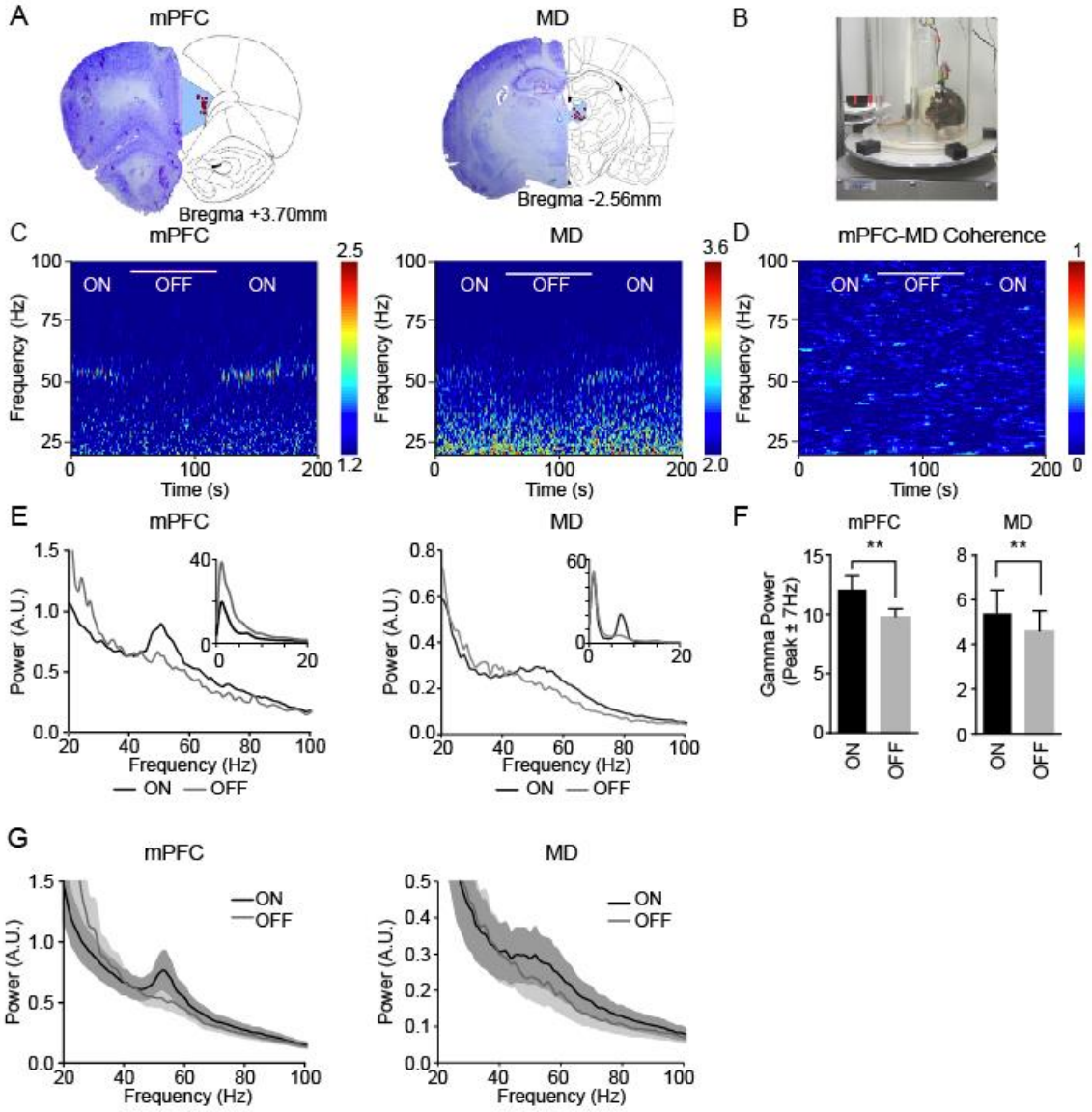

Figure 3.1. Walking-induced gamma power on the first recording day. A, Histological reconstruction (**left**) and electrode placements marked as red dots (right) of the recording electrodes in the prelimbic mPFC (**left**), and MD thalamus (**right**). **B,** Photograph of the rotating circular treadmill. The treadmill rotated at 9-11 rotations per minute for recording epochs and the paddle in the back ensured that the rat continued walking. **C,** Representative wavelet-based scalograms represent the time-frequency plots of LFP spectral power in the mPFC (**left**) and MD thalamus (**right**) from post-surgical day 7 during epochs with the treadmill off (white bar) and on. Warmer colors indicate higher power. **D,** Representative FFT-based spectrogram shows coherence between the mPFC and MD thalamus from the first recording day. **E, G,** Representative (**E**) or averaged (**G**) LFP power spectra for epochs with treadmill on (black) or off (grey) at the first recording day (n=12 rats). Power spectra from 0-20Hz shown in the inset (**E**). Colored shadows indicate SEM (**G**). **F,** Mean total gamma LFP power with the treadmill on and off from the first recording day. The frequency range of the gamma power was determined by finding the significant gamma peak (see methods) between 40 and 70Hz in each epoch during treadmill walking ±7Hz, and kept constant between

epochs with the treadmill on and off for each rat. Values are reported as mean ± SEM. **: $p<0.01$, paired t-tests.

The present results also confirmed observations that ketamine administration increases motor activity (Table S2; Hakami et al., 2009). Rats became significantly more active for the first 30 minutes after ketamine administration ($p<0.05$, t-tests). Furthermore, rats exhibited more differences in behavior before and after ketamine with the treadmill off, than during epochs of treadmill walking. Indeed, with the treadmill off, after ketamine administration, rats became more active, more likely to walk backwards, turn within the track, and show stereotypic behaviors, or appear more ataxic compared to baseline (all $p<0.05$, paired t-tests; Table 5). With the treadmill on, ketamine administration did not significantly affect the treadmill walking behavior (all $p>0.05$, paired t-tests; Table 5). However, following ketamine administration, it appears that rats were more attentive to the walking task, as they made contact with the paddle less often ($p<0.05$, paired t-test; Table 5). Taken together, the rat's behavior was more consistent before and after ketamine administration when the treadmill was on.

	Behaviors	Pre-ketamine	Post-ketamine
Treadmill-OFF Behaviors			
Hyperactivity	Time moving trunk or limbs (seconds)	1.3±0.7	45.8±0.9***
	Turns	0.1±0.1	2.4±0.6**
	Time walking backwards (seconds)	0±0	2.0±0.7*
Stereotypy	Head-bobs	0.3±0.2	3.3±0.8**
Ataxia	Ataxia Score (0-4)	0±0	1.3±0.2***
Treadmill-ON Behaviors			
Hyperactivity	Turns	0±0	0.6±0.3
Attentiveness	Paddle Hits	8.7±2.0	3.0±0.6*
	Time touching paddle (seconds)	9.9±2.4	4.8±1.7
	Time per paddle hit (seconds)	0.9±0.2	2.0±0.9

Table 5. Behavioral measures before and after ketamine during treadmill on and off epochs. Quantified measures of behavior from ~15 minutes before and after ketamine administration. Values are reported as percentage or mean ± SEM. *: $p<0.05$, **: $p<0.01$, ***: $p<0.001$, paired t-tests.

During treadmill-off epochs, ketamine administration increased gamma power by 371% relative to the same day's treadmill-off epochs before ketamine (gamma power=42.4±8.7 vs 9.0±0.4, $p<0.05$, paired t-test; Fig 3.2A,C-E). Specifically, the power spectra of the mPFC showed an increase in LFP power in a relatively narrow band with a mean peak of 55.9±1.0 Hz (Fig 3.2C,E). Ketamine also induced an increase in gamma range activity in the MD thalamus with two significant peaks: 55.2±2.3Hz and 80.6±1.6Hz (Fig 3.2A,C-E). Power centered around the low gamma peak increased by 41% after ketamine (from 2.4±0.2 to 3.4±0.4, $p<0.05$, paired t-test), and power centered around the 80Hz peak increased by 79% (from 1.2± 0.1 to 2.1±0.3, $p<0.05$, paired t-test). Thus, as previously shown (Pinault, 2008), ketamine administration increased gamma power.

To investigate whether ketamine-induced gamma power in the mPFC and MD thalamus is correlated with motor activity, we examined gamma LFP oscillations before and after ketamine administration during epochs of treadmill walking. With the treadmill on, ketamine administration induced an increase in gamma power in the mPFC and MD thalamus of 254% and 31% respectively compared to baseline (both $p<0.05$, Holm-Sidak's multiple comparisons; Fig 3.2A,C-E). Ketamine-induced gamma power was not significantly greater in the mPFC or the MD thalamus when the treadmill was on compared to off ($p>0.05$, paired t-test; Fig 3.2D). Furthermore, in the mPFC , during treadmill-on epochs, there was no difference in the ketamine-induced gamma peak's frequency (55.8 ± 1.4Hz) or the total power surrounding this peak (gamma power=43.1±9.5) compared to treadmill-off (both $p>0.05$, paired t-tests). Likewise, in the MD thalamus, neither the frequency of the ketamine-induced gamma peaks (52.4±1.4Hz and 80.7Hz ± 1.1Hz), nor the power of the gamma peaks (low gamma power = 3.3±0.4 and high gamma power = 2.3±0.4) showed significant differences between treadmill-on and treadmill-off epochs ($p>0.05$, paired t-test; Fig 3.2A,C,E).

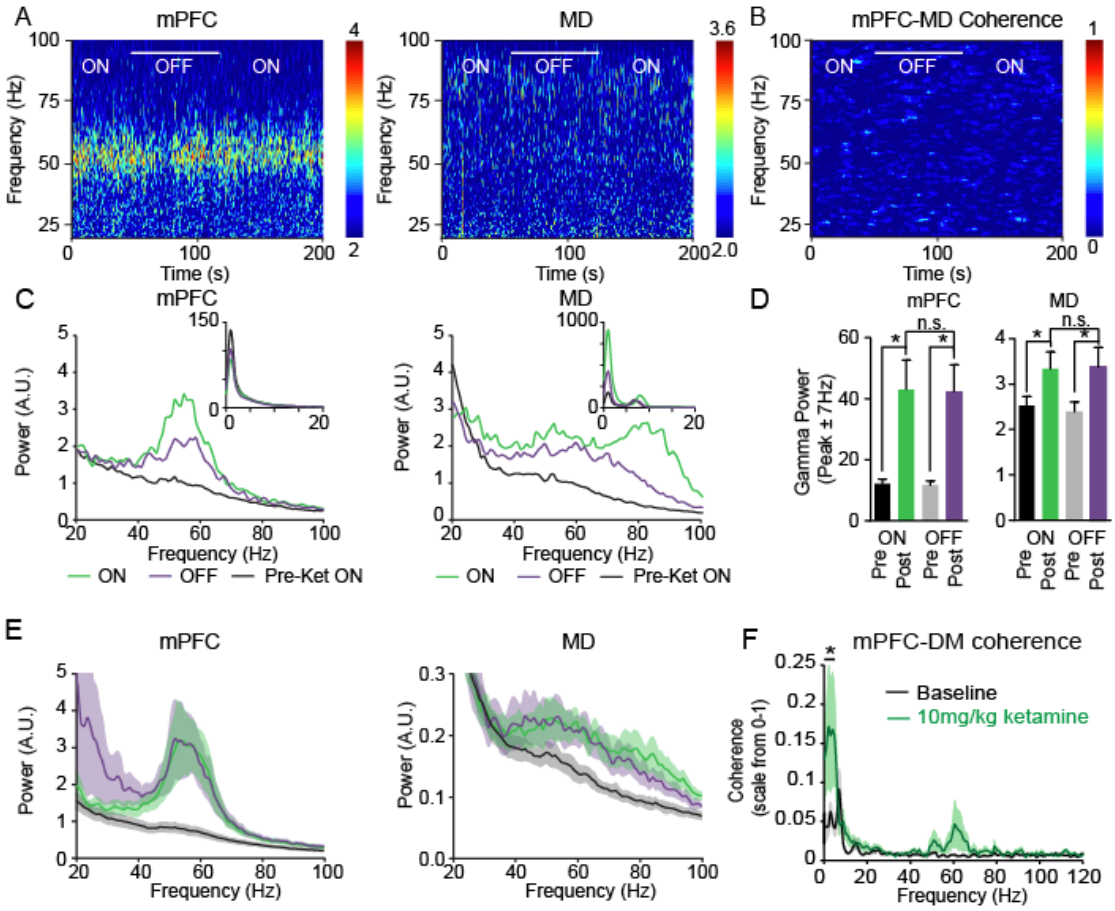

Figure 3.2. Comparison between walking-induced gamma power and ketamine-induced gamma power in the medial prefrontal cortex (mPFC) and mediodorsal thalamus (MD). A, Representative wavelet-based scalograms represent the time-frequency plots of LFP spectral power in the mPFC (**left**) and MD thalamus (**right**) 13-17 minutes after 10mg/kg ketamine s.c. during epochs with the treadmill off (white bar) and on. Warmer colors indicate higher power. **B,** Representative FFT-based spectrogram shows coherence between the mPFC and MD thalamus 13-17 minutes after 10mg/kg ketamine s.c. **C,E,** Representative (**C**) and averaged (**E**) LFP power spectra for epochs 13-17 minutes after 10mg/kg ketamine for epochs with the treadmill off (purple) and on (green), and the baseline treadmill walking power from the same recording day (black, n=6 rats). Power spectra from 0-20Hz shown in the inset (**C**). **D,** Mean total gamma LFP power with the treadmill on and off from before (PRE) and 13-17 minutes after 10mg/kg ketamine s.c (**J,** POST). The frequency range of the gamma power was determined by finding the significant gamma peak (see methods) between 40 and 70Hz in each epoch during treadmill walking ±7Hz, and kept constant between epochs with the treadmill on (ON) and off (OFF) for each rat. **F,** Ketamine increases coherence between the MD thalamus and the mPFC from 0-6Hz. Linear graph shows averaged LFP coherence at baseline walk (black) and 15 minutes after 10mg/kg ketamine (green) (n=5 rats). Colored bands indicate SEM. The bar with the star indicates a significant difference at this frequency range using multiple t-tests with false-detection rate set to 1%. Values are reported as mean ± SEM. *: $p<0.05$, paired t-tests.

Our behavioral and electrophysiological results show that treadmill walking did not significantly modify ketamine-induced gamma power and allowed us better control of the rat's behavior. Therefore, all further analyses examined epochs with the treadmill on.

Although increases in low gamma LFP power were seen in a similar frequency range in the mPFC and MD thalamus during treadmill walking, coherence between the mPFC and MD thalamus (peak between 40-70 Hz ± 7 Hz) did not reach the statistically predetermined levels of significance (Rosenberg et al., 1989), nor was there any change between epoch with the treadmill on versus off (n=9 rats; Fig 3.2F). Likewise, average LFP coherence between mPFC and MD thalamus in the low gamma frequency range (peak between 40-70Hz ± 7 Hz) did not reach significance after ketamine administration (n= 5, Fig 3.2F). We analyzed the relationship between low (theta) and high (gamma) frequencies within the MD thalamus LFP. Gamma activity sometimes occurs at a specific phase in theta oscillations. Measures of phase-amplitude coupling (PAC) can also be used to determine if low frequency activity in one structure influences high frequency activity in a separate structure. Within the MD thalamus, no PAC was observed before ketamine administration, but after ketamine gamma oscillations centered ~85Hz nested within theta oscillations of 7-9Hz in every rat examined (Fig 3.3A). This suggests that in the MD thalamus, a shared mechanism modulates theta and gamma oscillations. Furthermore, low frequency oscillations in the MD thalamus (2-6Hz) modulated gamma power in the mPFC between 50Hz and 65Hz after ketamine administration, but not before (Fig 3.3B). This indicates that the MD thalamus influences

the gamma frequency activity of the mPFC through modulation of low frequency oscillations.

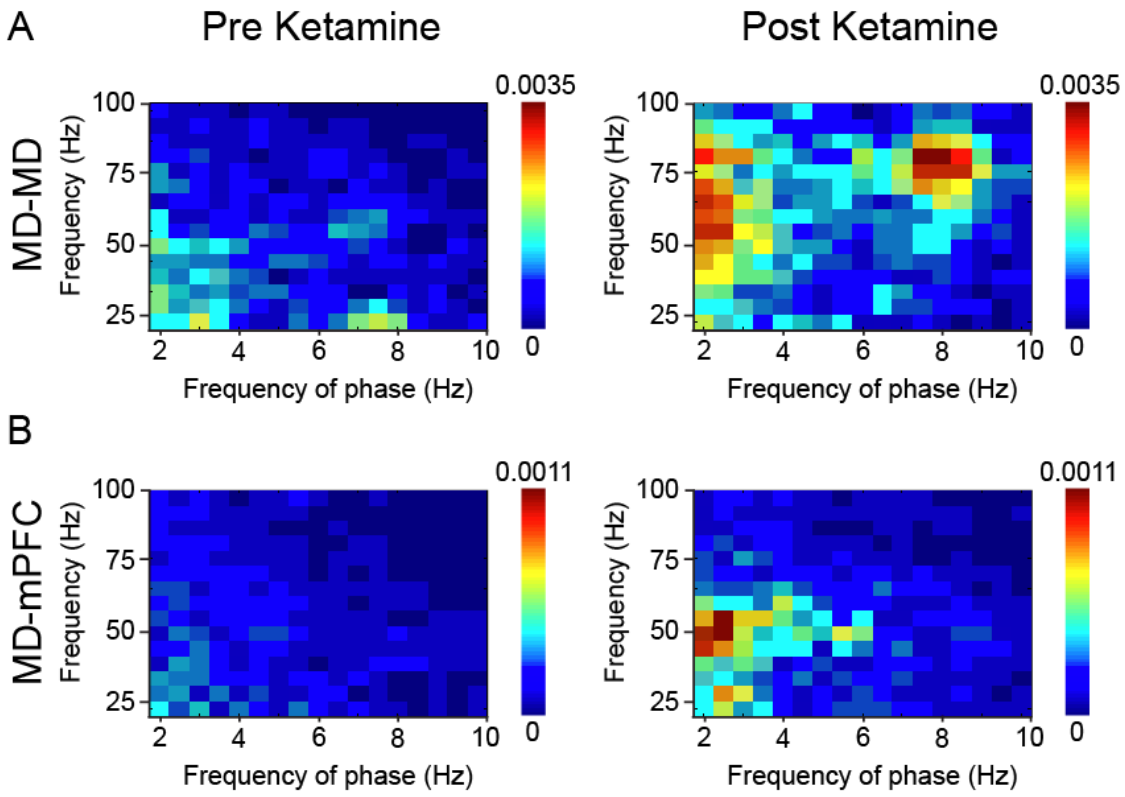

Figure 3.3. Ketamine increases phase-amplitude coupling within the MD thalamus and between MD thalamus and mPFC.(**A**) Representative comodulograms plot the analytic amplitude of the LFP from the MD thalamus (y-axis, 20-100Hz) as a function of the phase of the LFP from the MD thalamus (x-axis, 2-10Hz) before (**left**) and 15 minutes after 10mg/kg ketamine injection (**right**). Warmer colors indicate stronger cross-frequency coupling. (**B**) Same as in (**A**) except the analytic amplitude of the LFP from the mPFC (y-axis) is plotted as a function of the phase of the LFP from the MD thalamus (x-axis).

3.3.2 Spike-LFP correlations in walking-induced gamma power

To further investigate the neuronal correlates of the increases in LFP gamma activity associated with treadmill walking, we examined changes in the firing rates of neurons in the mPFC and MD thalamus. Putative pyramidal neurons and interneurons from the mPFC were separated using waveform shape and firing rates (Fig 3.4A&B). Interneurons were further divided into fast-spiking interneurons, with firing rates above

8Hz (n=8) and slower interneurons, with firing rates below 8Hz (n=22). Other than rate, we observed no statistically significant differences between the groups in other parameters, such as spike-LFP relationships, so all cortical interneurons were analyzed as one group for the rest of the analyses. Overall, the firing rates of mPFC pyramidal and interneurons, as well as MD thalamus neurons increased during walking relative to treadmill-off (Fig 3.4C). The firing rates of pyramidal neurons in the mPFC increased by 12% from 4.2±0.3Hz to 4.7±0.3Hz with the treadmill-on compared to treadmill-off ($p<0.05$, n=112, paired t-test; Fig 3.4C). Although this increase is modest, 40% of pyramidal neurons in the mPFC showed more than a 20% increase in firing rate, while 16% showed more than a 20% decrease with the treadmill on compared to off (Fig 3.4D). Furthermore, the firing rates of interneurons in the mPFC increased by 33% when the treadmill was turned on (from 2.7±0.5Hz to 3.6±0.6Hz, $p<0.01$, paired t-test; Fig 3.4C). When examined in detail, 70% of interneurons in the mPFC showed more than a 20% increase in firing rate, whereas10% showed more than a 20% decrease with the treadmill on compared to off (Fig 3.4D). Similarly, the firing rate of MD thalamus neurons also increased by 32% from 3.4±0.5Hz to 4.5 ±0.5Hz during treadmill walking ($p<0.001$, paired t-test; Fig 3.4C). In fact, 56% of MD thalamus neurons showed more than a 20% increase in firing rate, while 14% showed more than a 20% decrease with the treadmill on compared to off (Fig 3.4D). In summary, increases in the firing rate of neurons in both the mPFC and MD thalamus complement walking-induced increases in gamma power.

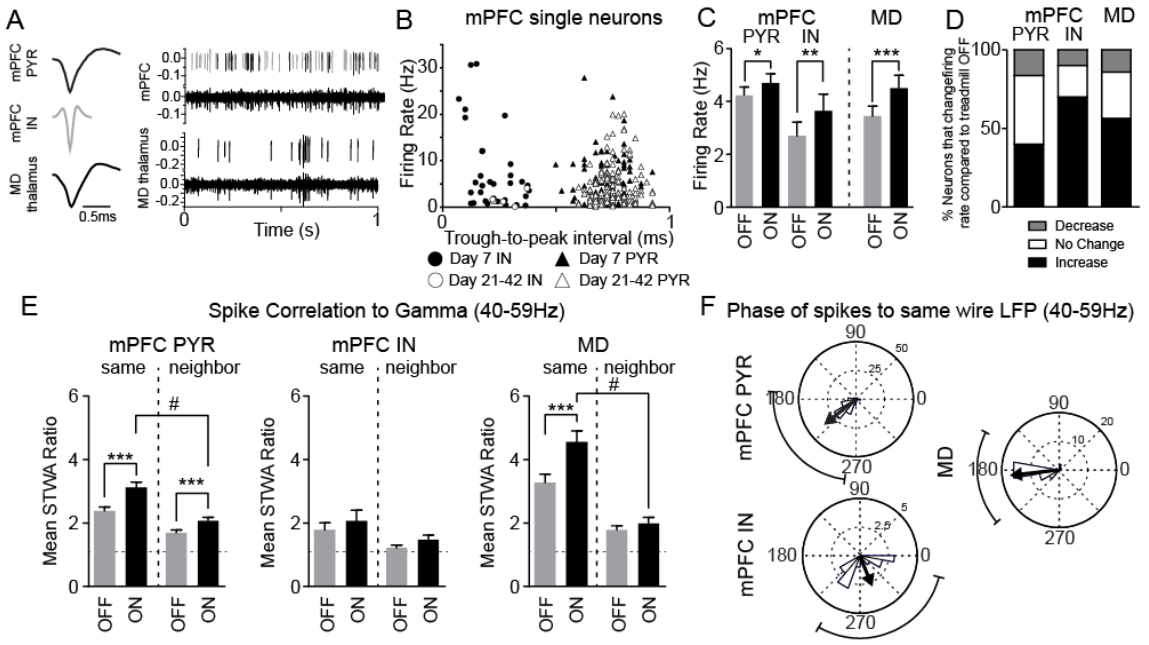

Figure 3.4. Effects of treadmill walking on firing rates and spike-LFP correlation.A, Average waveforms, raw signals, and spiketrains from the mPFC (top) and MD thalamus (bottom) with the treadmill on. **B**, Interneurons and pyramidal neurons were separated using trough-to-peak intervals. More interneurons were detected on post-surgical day 7 than days 21-42. **C**, Firing rates of pyramidal neurons (PYR; n=112 neurons from 12 rats, **left**) and interneurons (IN; n=25 neurons from 9 rats, **middle**) from the mPFC and neurons from the MD thalamus (n= 64 neurons from 12 rats, **right**). **D,** Percentage of neurons showing an increase (black, >20%), decrease (grey, <-20%), or no change (white) of rate with treadmill on compared to off. **E,** Mean ratios between peak to trough amplitudes of unshuffled/shuffled spike triggered waveform average (STWA) for LFPs recorded from the same wire (**left**) or the maximum (neighbor) wire (**right**, see methods) filtered from 40-59Hz for mPFC pyramidal neurons (**left**) and mPFC interneurons (**middle**) and MD thalamus neurons (**right**). A ratio of 1 (dashed horizontal line) indicates no difference between shuffled and unshuffled values. **F,** Phase plots showing the distributions of phase-relationships between mPFC spikes and LFPs from the same wire filtered between 40 and 59Hz for spike trains showing significant correlation to the gamma LFP during epochs of treadmill walking in pyramidal (PYR, n=74 neurons from 13 rats) and interneurons (n=12 neurons from 9 rats) from the mPFC and MD thalamus (n=31 neurons from 12 rats). Spikes were significantly oriented to gamma LFPs, Rayleigh test: $p<0.05$. Values are reported as mean ± SEM. *: $p<0.05$, **: $p<0.01$, ***: $p<0.001$, paired t-tests. #: $p<0.001$, unpaired t-tests.

To gain insight into the extent to which spiking activity correlated with gamma power in the mPFC and MD thalamus, we examined spike-gamma LFP correlations, a measure of synchronization between spike trains and gamma oscillations. Peak-to-trough values of the spike triggered waveform averages (STWA) were used to evaluate the extent of the correlation between the spike and the simultaneously recorded oscillation filtered at 40-59Hz (gamma LFP). Interspike intervals from the same epochs were

shuffled 20 times, and after each shuffle, an additional STWA was generated (see methods). Spike trains were considered significantly correlated with LFP oscillations when the peak-to-trough amplitude of the unshuffled spike train STWA exceeded the mean shuffled peak-to-trough amplitude by 3 standard deviations (for an example, see Fig 3.6A).

Figure 3.4E shows a comparison of the mean ratios of the unshuffled to shuffled STWA peak-to-trough amplitudes (mean STWA ratio) of pyramidal neurons and interneurons from the mPFC, as well as neurons from the MD thalamus referenced to gamma LFPs. The spiking of mPFC pyramidal neurons and MD thalamus neurons was more correlated to the 40-59Hz oscillation with the treadmill on (mPFC:70%, MD: 72% significantly correlated) compared to off (mPFC: 54%, MD: 63% significantly correlated, $p<0.05$, paired t-tests; Fig 3.4E). Specifically, mPFC pyramidal neuron spike-gamma LFP correlations increased during walking (mean STWA ratio increased from 2.38±0.12 to 3.12±0.17, $p<0.001$, paired-t-test; Fig 3.4E). Additionally, MD thalamus spike-gamma LFP correlations increased with the treadmill on versus off (mean STWA ratio =4.67±0.46 and 3.59±0.44 respectively, $p<0.001$, paired t-test; Fig 3.4E). In contrast, spikes from mPFC interneurons were not significantly more correlated to the gamma LFP during treadmill walking ($p>0.05$, paired t-test). However, 36% and 33% of the mPFC interneurons were significantly correlated to the gamma LFP during treadmill on and treadmill off respectively.

To obtain a measure of the distribution of the LFP oscillations in the area around an individual neuron, we referenced a single neuron's spiking activity to the LFP of a

neighboring wire within the recording electrode bundle. For each wire with a usable spike train, we calculated its coherence between 40Hz and 59Hz with all the other wires, and ranked each wire from the one with the maximum to the minimum coherence. We selected the wire with the maximum coherence (average coherence of 0.71±0.03 in the mPFC and 0.69±0.02 in the MD thalamus), and the median coherence (average coherence of 0.42±0.03 in the mPFC and 0.36±0.03 in the MD thalamus) as the neighboring wires, and refer to them as the maximum wire and median wire, respectively. Selecting the wire with median coherence prevented selection of a wire that had splayed away from the bundle during implantation. During treadmill walking the spike-gamma LFP correlation was lower when mPFC pyramidal neurons (-33% $p<0.01$) or MD thalamus neurons (-56%, $p<0.001$), but not interneurons ($p>0.05$) were referenced to the maximum wire compared to the recording wire (t-tests; Fig 3.4E). Furthermore, fewer mPFC pyramidal neurons and MD thalamus neurons were significantly correlated to the gamma LFP (40-59Hz) when referenced to the maximum wire versus the recording wire (mPFC: 42% vs. 70%; DM: 42% vs. 72%, $p<0.01$, Fisher's exact test). This suggests that walking-induced gamma power within both the mPFC and MD thalamus is relatively localized.

In order to quantify the temporal relationships between the three different neuron populations and ongoing gamma oscillations, we determined the phase preference of those spike trains significantly correlated to the gamma LFP from the recording wire. Pyramidal neurons in the mPFC spiked during the ascending phase of the 40-59Hz filtered LFP oscillation with a preferred angle of 219 degrees (both $p<0.01$, Rayleigh test;

Fig 3.4F, n=74). mPFC interneurons spiked at one of two preferred angles, 238 degrees or 344 degrees (dip test revealed a trend towards a bimodal distribution, $p = 0.074$). MD thalamus neurons spiked during the ascending phase of the 40-59Hz filtered LFP oscillation with a preferred angle of 207 degrees ($p<0.001$, Rayleigh test; Fig 3.4F). Accordingly, MD thalamus neurons and mPFC pyramidal neurons have similar phase relationships to the LFP during walking-induced gamma power.

3.3.3 Effects of 10mg/kg ketamine on single neurons in the mPFC and MD thalamus

To further investigate the neuronal correlates of the increases in synchronized gamma activity associated with ketamine administration, LFPs and spike trains recorded from the mPFC and MD thalamus were examined for changes in power, firing rate and spike-gamma LFP correlation. First, we examined the time-course of changes in low gamma power during treadmill walking in a predetermined frequency band (40-59Hz) matching the frequency used for the spike-gamma LFP correlation analysis. Low gamma power (40-59Hz) was significantly higher 15 minutes after a 10mg/kg ketamine injection in both the mPFC (+170%) and MD thalamus (+30%) compared to baseline ($p<0.05$, Holm-Sidak's multiple comparisons; Fig 3.5). Gamma power returned to baseline 75 minutes after ketamine administration ($p>0.05$, Holm-Sidak's multiple comparisons; Fig 3.5).

We also examined the gamma-range coherence between the wires to study the spatial distribution of gamma oscillations. In both the mPFC and MD thalamus, ketamine significantly increased the intra-electrode bundle coherence to both the median and

maximum wires (all $p<0.05$, paired t-test), but had a greater influence over the coherence to the median wire (both $p<0.001$, paired t-test, data not shown). Specifically, in the mPFC the coherence values of each wire to the median wire increased from 0.42 ±0.03 before ketamine to 0.51 ±0.03 after ketamine ($p<0.001$, paired t-test) and the maximum wire increased slightly from 0.71 ±0.03 to 0.74 ±0.03 ($p<0.05$, paired t-test). Additionally, in the MD thalamus the coherence values of each wire to the median wire increased from 0.36 ±0.03 before ketamine to 0.45 ±0.03 after ketamine ($p<0.001$, paired t-test) and the maximum wire increased slightly from 0.69 ±0.02 to 0.72 ±0.02 ($p<0.01$, paired t-test). Together it appears that ketamine increases the conduction of gamma oscillations across a broader spatial scale after ketamine treatment.

We then examined the firing rates of neurons from the mPFC and MD thalamus. Only two mPFC interneurons were detected during ketamine treatments, perhaps due to the fact that these recordings were performed several weeks after surgery. Fifteen minutes after 10mg/kg ketamine, the mean firing rate of mPFC pyramidal neurons was 33% higher than after saline injection ($p<0.05$, Holm-Sidak's multiple comparisons; Fig 3.5A). Seventy-five minutes after ketamine injection firing rates returned to baseline levels ($p>0.05$, Holm-Sidak's multiple comparisons; Fig 3.5A). In contrast, the firing rates of neurons in the MD thalamus decreased by 46% fifteen minutes after ketamine administration ($p<0.01$, Holm-Sidak's multiple comparisons; Fig 3.5B) despite a concurrent, significant increase in low gamma power. Firing rates returned to baseline levels 75 min after ketamine injection ($p>0.05$, Holm-Sidak's multiple comparisons; Fig 3.5B). The results show that NMDAR antagonism through ketamine has significant, yet

opposite effects on the mean firing rates of mPFC pyramidal neurons and MD thalamus neurons.

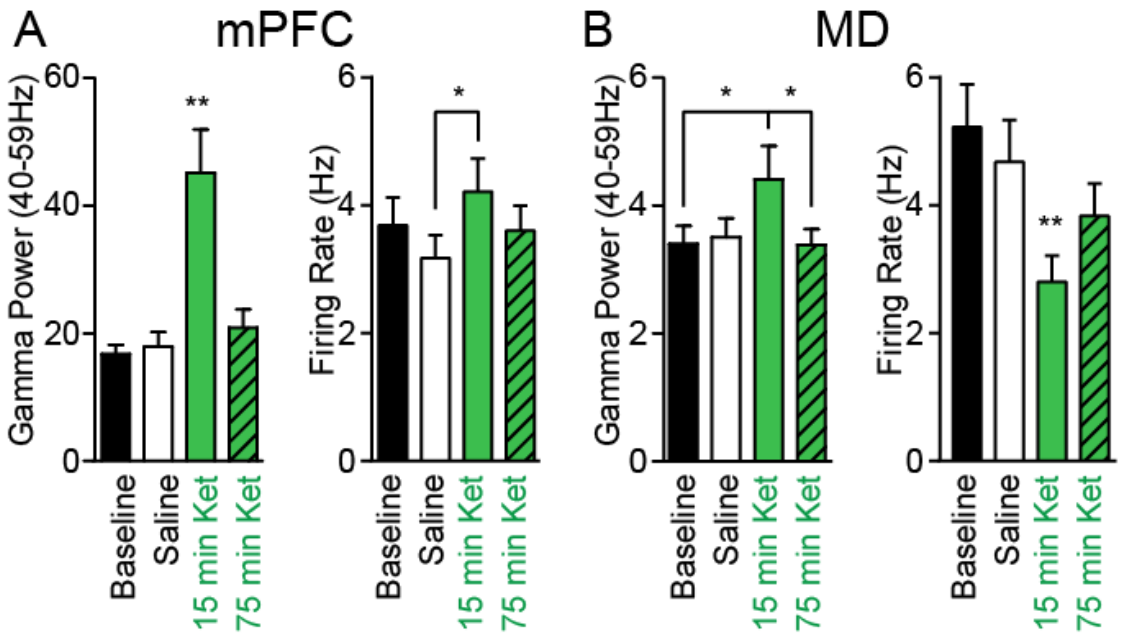

Figure 3.5. Although ketamine administration induces increases in low gamma power in both the MD thalamus and mPFC, it induces increased firing rates in the mPFC and decreased firing rates in the MD thalamus.A-B, left, Low gamma (40-59Hz) power in the mPFC (**A**, n=10 rats) and the MD thalamus(**B**, n=6 rats) during treadmill walking at baseline (black), 15 minutes after saline injection (white), 15 minutes (green) or 75 minutes after 10mg/kg ketamine (green with diagonal stripes). **A-B, right**, Firing rate of pyramidal neurons in the mPFC (**A**, n=44 neurons from 6 rats) and the MD thalamus (**B**, n=37 neurons from 6 rats). Values are reported as percentage or mean ±SEM. *:$p<0.05$, **:$p<0.01$, repeated-measures one-way ANOVA with Holm-Sidak's multiple comparisons test.

Next, we examined the relationship between spikes and gamma oscillations. Representative unshuffled and shuffled STWAs shown in figure 3.6A from the mPFC and MD thalamus demonstrate that spike-gamma LFP correlations increased after ketamine administration in the mPFC, but decreased in the MD thalamus. The spike-gamma LFP correlation of mPFC pyramidal neurons increased 15 minutes after ketamine, relative to baseline or saline injection (both $p<0.01$, Holm-Sidak's multiple comparisons), and returned to baseline 75 minutes after ketamine administration ($p>0.05$,

Holm-Sidak's multiple comparisons; Fig 3.6B). After ketamine administration, pyramidal neurons in the mPFC were more correlated to gamma LFPs from the same wire, the maximum wire, and the median relative to baseline (same wire mean STWA ratio = 5.05±0.46 vs 2.94±0.20; maximum wire mean STWA ratio = 4.62±0.48 vs 2.23±0.17,median wire mean STWA ratio = 3.77±0.34 vs 1.81±0.15, all $p<0.001$, Holm-Sidak's multiple comparisons; Fig 3.6B). In contrast to decreases in mean STWA ratios between the recording and maximum wire observed during walking-induced gamma, no decrease was observed during ketamine-induced gamma ($p>0.05$, t-test). This substantiates the idea that the ketamine-induced gamma is less localized around the neuron than walking-induced gamma. Interestingly, while there was no significant difference in the percentage of pyramidal neurons significantly correlated to the gamma LFP when referenced to the recording wire ($p>0.05$), a difference between epochs before and after ketamine administration became apparent when referenced to the wire with the maximum coherence ($p<0.01$), or the wire with the median coherence ($p<0.001$, Fig 3.6B, Chi-Square tests). This was mainly driven by a decrease in the proportion of neurons significantly correlated to gamma-filtered LFPs at baseline in both neighboring wiResearch Thus it appears that ketamine increases spike-LFP correlations across a broader spatial array, and this was accompanied by increases in the average coherence between wires in the bundle as well ($p<0.05$, repeated measures one-way ANOVA). In both walking and ketamine-induced gamma power, as gamma power increases, spike-gamma LFP correlations increase in the mPFC.

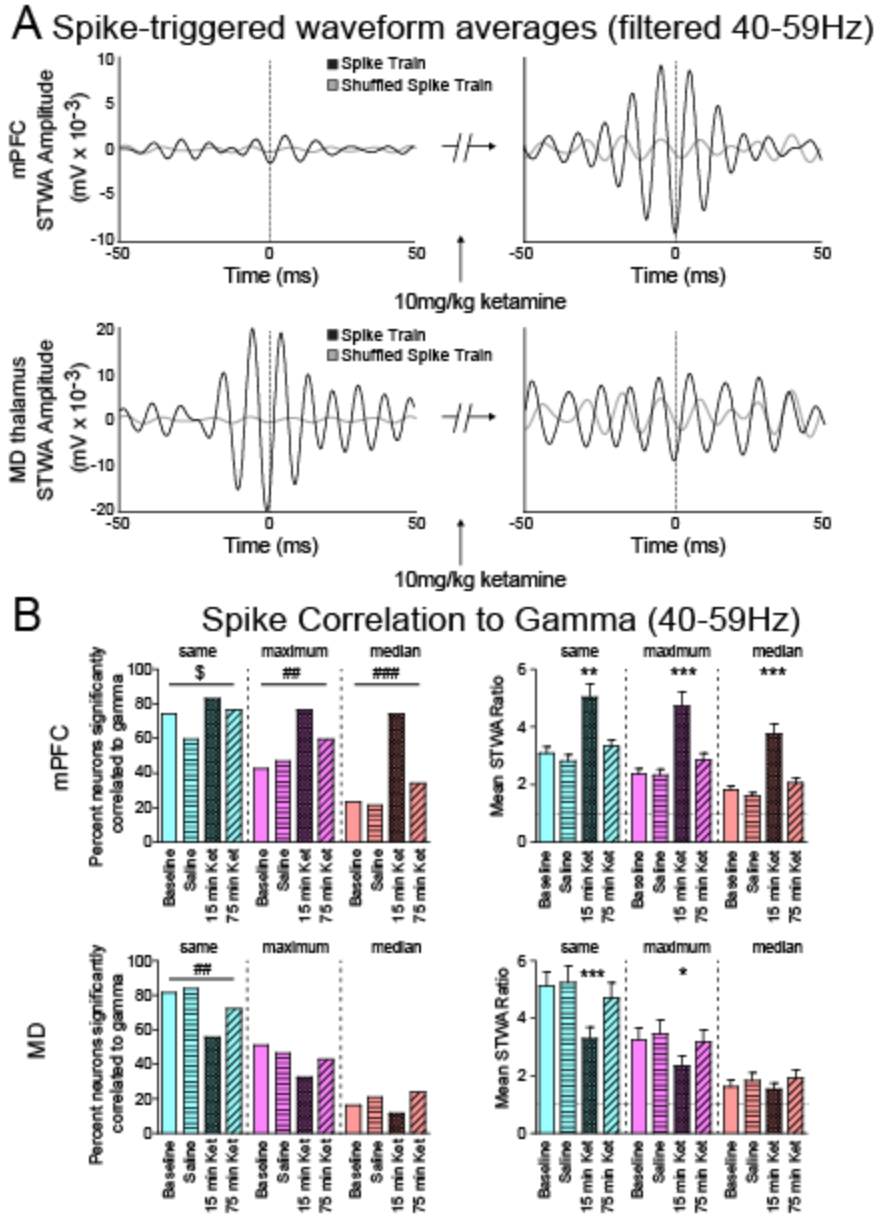

Figure 3.6. Ketamine increases the spike-gamma LFP correlation in the mPFC and decreases it in the MD thalamus.A, Representative spike-triggered waveform averages (STWAs) of an mPFC pyramidal neuron (**top**) and neuron from the MD thalamus (**bottom**) with LFPs from the recording wire filtered from 40-59Hz 15 minutes before and after ketamine administration. **B,** The percentage of neurons significantly correlated to low gamma oscillations (40-59Hz, **left**) from the mPFC (**top**) and the MD thalamus (**bottom**), when the spike train was referenced to the recording wire (same, blue), and neighboring wires with the maximum (purple) and median (coral) coherence (see Section3.2.7). Mean ratios (**right**) between peak to trough amplitudes of the original STWA and the mean of 20 shuffled STWAs for LFPs filtered from 40-59Hz recorded from the same wire, maximum, or median wire for putative mPFC pyramidal neurons (**top**) and MD thalamus neurons (**bottom**). A bar with significance stars over it indicates that this bar is significantly different from all the other conditions. A ratio of 1 (dashed horizontal line) indicates no difference between shuffled and unshuffled values. Values are reported as percentage or mean ±SEM.

*:$p<0.05$, **:$p<0.01$, ***:$p<0.001$, repeated-measures one-way ANOVA with Holm-Sidak's multiple comparisons test, $:$p<0.1$, ##:$p<0.01$, ###:$p<0.001$, chi-square test.

A very different picture emerged in the MD thalamus after ketamine administration. As gamma power increased, neurons in the MD thalamus were less correlated to gamma LFPs from the same wire and the neighboring wiResearch MD thalamus neurons were ~34% less correlated to the MD thalamus gamma LFPs 15 minutes after 10mg/kg ketamine than at baseline walk when the spikes were referenced to the same wire or a neighboring wire (same wire mean STWA ratio = 3.63±0.42 vs 5.54±0.51; maximum wire mean STWA ratio = 1.63±0.19 vs 2.48±0.33, both $p<0.001$, Holm-Sidak's multiple comparisons; Fig 3.6B). Spike-gamma LFP correlations 15 minutes after ketamine were lower than baseline, 15 minutes after saline injection, or 75 minutes after ketamine (all $p<0.01$, Holm-Sidak's multiple comparisons; Fig 3.6B). However, when referenced to the median wire, there was no significant difference in spike-gamma LFP correlation before and after ketamine administration ($p>0.05$, Holm-Sidak's multiple comparisons, Fig 3.6B). Furthermore, while the percentage of MD thalamus neurons significantly correlated to the gamma LFP decreased when referenced to the recording wire ($p<0.05$), this was not observed when referenced to either neighboring wire ($p>0.05$, Chi-Square tests). This is driven by the decrease in the percentage of neurons significantly correlated at baseline, and suggests that the LFP of each wire in the bundle in the thalamus may be more influenced by spiking activity than the LFP in the mPFC. Taken together, gamma power in the MD thalamus arises from a separate mechanism from that observed in the mPFC.

To gain further insight into the relationship between the mPFC and MD thalamus, we performed STWAs of spike trains from the MD thalamus referenced to the mPFC LFPs and vice versa. Less than 5% of MD thalamus spike trains were significantly correlated to gamma oscillations in the mPFC and less than 5% of mPFC pyramidal spike trains were significantly correlated to MD thalamus LFP before or after ketamine (n=42 and n= 73 respectively, Fig 3.7). Similarly, neither the correlation of mPFC pyramidal spikes referenced to MD thalamus gamma oscillations, nor the correlation of MD thalamus spikes referenced to mPFC gamma oscillations were significantly different from the mean STWA ratio of random spike trains before or after ketamine (all $p>0.05$, permutation test, Fig 3.7). In conjunction with the absence of coherence between mPFC and MD thalamus, these results suggest that mPFC neurons are not driving gamma oscillations in the MD thalamus or vice versa.

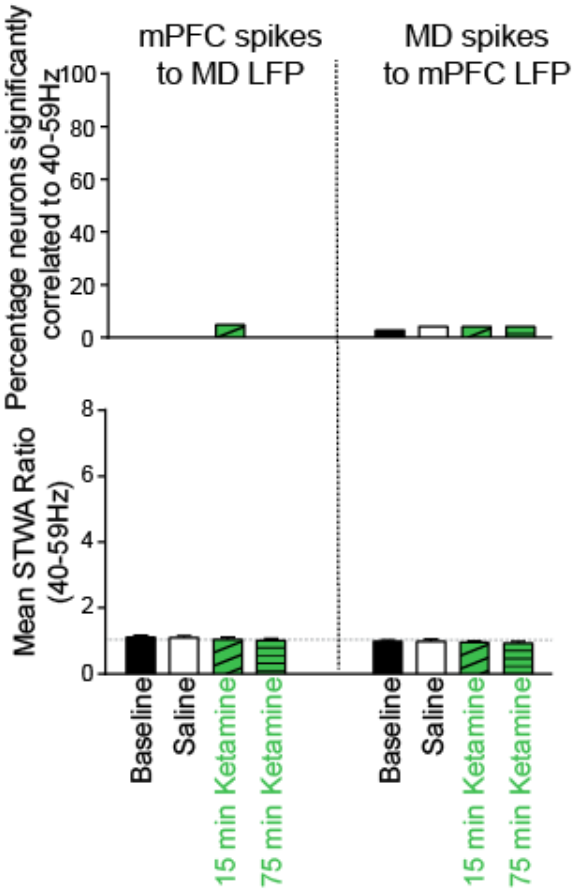

Figure 3.7. Effects of ketamine on spike-LFP correlations between mPFC and MD thalamus. Bar graphs show the percentage of neurons significantly correlated to the LFP recorded on the same wire from 40-59Hz (**top**), and mean STWA ratio (**bottom**). The percent of mPFC neurons phase-locked the MD thalamus LFP is shown on the left, and the percent of MD neurons phase-locked to the mPFC LFP and the STWA ratios of the MD thalamus neurons to mPFC LFP is shown on the right. A ratio of 1 (dashed horizontal line) indicates no difference between shuffled and unshuffled values. There were no significant differences.

To further explore the relationship between spiking and the high gamma peak in the MD thalamus, we performed STWAs of spike trains from the MD thalamus to LFPs filtered in the high gamma range from 70-115Hz. As observed in the lower gamma frequency range, MD thalamus neurons were less correlated to the MD thalamus high gamma LFPs 15 minutes after 10mg/kg ketamine than at baseline walk when the spikes were referenced to the same wire or a neighboring wire (same wire mean STWA ratio =

5.65±0.62 vs 9.02±0.72; maximum wire mean STWA ratio = 2.98±0.35 vs 3.92±0.43, both $p<0.001$, Holm-Sidak's multiple comparisons; Fig 3.8). Again, when referenced to the median wire, there was no significant difference in spike-high gamma LFP correlations before and after ketamine ($p>0.05$, Holm-Sidak's multiple comparisons; Fig 3.8). On a cautionary note, when spike artifacts are not fully filtered from the LFP, the trough of spike and the trough of the cycle will align at 180 degrees (Ray, 2015). The average phase and cycle of these MD thalamus neurons was 180.7 degrees and 82Hz signifying that these data may contain spike-noise contamination rather than real changes in spike-high gamma LFP relationships. Furthermore, there is evidence that spiking increases high gamma power between 80Hz and 100Hz (Ray and Maunsell, 2011).However, our results likely do not fit this explanation as firing rates declined in the thalamus, gamma power was enhanced.

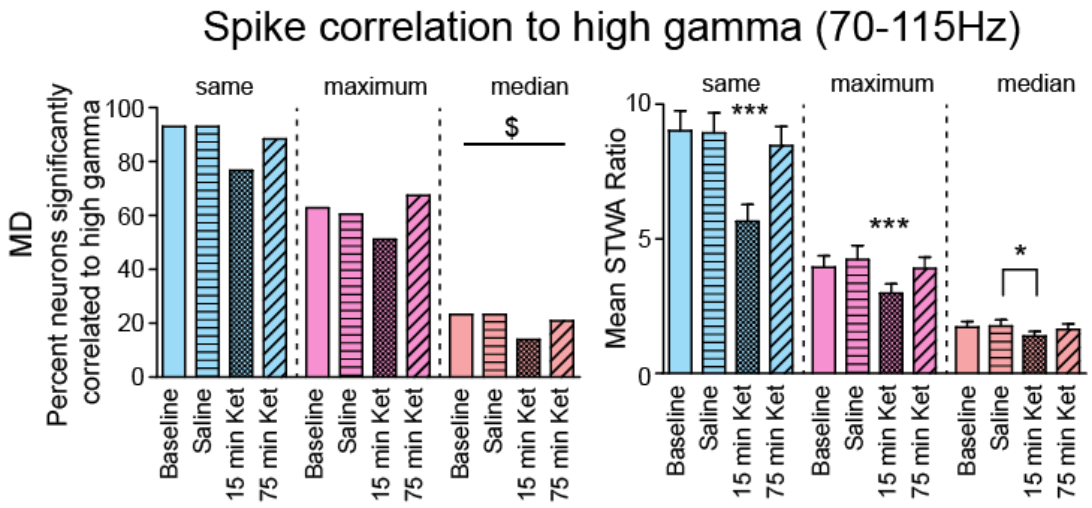

Figure 3.8. Ketamine decreases the spike-high gamma LFP correlation in the MD thalamus.Left, The percentage of MD thalamus neurons significantly correlated to high gamma oscillations (70-115Hz) from the MD thalamus, when the spike train was referenced to the recording wire (same, blue), maximum (purple) and median (coral) wires (see Section 3.2.7). Mean ratios (**right**) between peak to trough amplitudes of the original STWA and the mean of 20 shuffled STWAs for LFPs filtered from 70-115Hz recorded from the same wire, maximum, or median wire for MD thalamus neurons. A bar with significance

stars over it indicates that this bar is significantly different from all the other conditions. Values are reported as percentage or mean ±SEM. *:$p<0.05$, **:$p<0.01$, ***:$p<0.001$, repeated-measures one-way ANOVA with Holm-Sidak's multiple comparisons test, $:$p<0.1$, chi-square test.

3.3.4 Effects of different doses of ketamine in the mPFC

3.3.4.1 Dosage effects on gamma power

To gain further perspective on how a single dose of ketamine may potentiate the effects of further ketamine administration, and to compare the two most common doses of ketamine used in previous work in this field (5mg/kg and 10mg/kg) the effects of two consecutive subanesthetic doses of 5mg/kg ketamine given one hour apart were compared to a single 10mg/kg dose. Both doses induced an increase in gamma power in low (peak between 40-70Hz ± 7Hz) and high (70-120Hz) gamma frequency ranges. However, significant spectral peaks were only evident in the low gamma range (Fig 3.9C) as shown by representative wavelet-based scalograms of LFP recordings and gamma-filtered LFPs (Fig 3.9A-B). Interestingly, during treadmill walking, the gamma peak frequency increased from 48.9±0.9Hz before ketamine to 56.4±1.2Hz after 5mg/kg ketamine and to 54.9±1.3Hz after the second 5 mg/kg dose ($p<0.001$, Holm-Sidak's multiple comparisons; Fig 3.9D).

LFP power increased from baseline in both low (peak between 40-70±7Hz) and high (70-120Hz) gamma frequency bands and remained elevated from the first injection of ketamine until 65 minutes after the second injection of ketamine ($p<0.05$; RM one-way ANOVA; Fig 3.9E-F). The increase in low gamma power was greater after the second 5mg/kg dose than the first 5mg/kg dose ($p<0.01$, paired t-test; Fig 3.9E). With 5mg/kg ketamine, the low gamma power increased by 96.4±18.1% and with the cumulative dose of 10mg/kg low gamma power increased by 158±24.8% (Fig 3.9E). A single injection of

10mg/kg ketamine increased low gamma power significantly more than two consecutive doses of 5mg/kg ketamine (+ 262% vs. +158%, $p<0.05$, t-test). In contrast, in the high gamma range, the power increased by ~40% from baseline walking with both injections, and there was no difference between the two doses ($p>0.05$, paired t-test; Fig 3.9F). Furthermore, there was no significant difference between the increases in high gamma power after a single injection of 10mg/kg ketamine and after two consecutive doses of 5mg/kg ketamine ($p>0.05$, t-test). This indicates that one dose of ketamine potentiates the effects of further ketamine administration within the same hour on low gamma power, but not high gamma power in the mPFC. Furthermore, this reveals that a single dose of ketamine has greater effects on low gamma power than two consecutive ketamine injections that add up to the same dose.

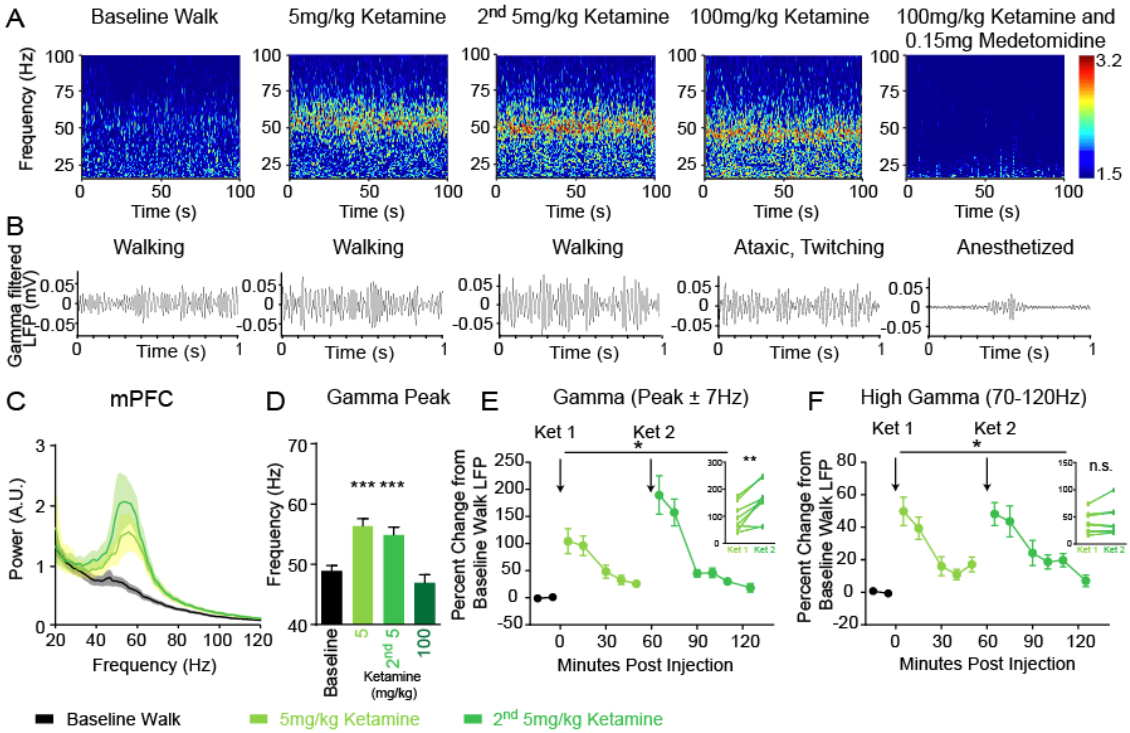

Figure 3.9. Increasing doses of ketamine influence low gamma power, not high gamma power.A, Representative wavelet-based scalograms show the time-frequency plots of LFP spectral power in the

mPFC during treadmill walking before ketamine injection (baseline), 15 minutes after 5mg/kg ketamine, 15 minutes after a 2nd dose of 5mg/kg ketamine, and with the treadmill-off at 10 minutes after a cumulative dose of 100mg/kg ketamine, and 5 minutes after 0.15mg of medetomidine, a myorelaxant, administered 20-25 minutes after the cumulative dose of 100mg/kg ketamine. **B,** Examples of gamma-band pass filtered LFP (40-70Hz) in the mPFC at each of the time points mentioned above. **C,** Averaged LFP power spectra 15 minutes after each 5mg/kg injection of ketamine (n=8 rats). Colored shadows indicate SEM. Legend appears at the bottom. **D**, Frequency of the spectral peak in the gamma-band (40-70Hz) at each dose of ketamine. There was no peak 5 minutes after 0.15mg of medetomidine. **E-F,** For each rat, the power within the low gamma band (**E**, maximum peak between 40 and 70Hz ±7Hz) or high gamma band (**F**, 70-120Hz) were summed at baseline walk using the average of four 40 to 100 second epochs of artifact-free walking. Percent change from baseline power over time is displayed in the low gamma (**E**), and high gamma (**F**) frequency ranges. Arrows indicate injections of 5mg/kg ketamine. The bar with the star indicates a significant change from baseline walking for every time point under the bar. The percent change in low gamma power (**E, inset**) or high gamma power (**F, inset**) from baseline walking is shown at 15 minutes after the first and second 5mg/kg injection of ketamine with lines connecting the doses in each rat. Values are reported as percentage or mean ± SEM. *: $p<0.05$, **: $p<0.01$, ***: $p<0.001$, repeated measures one-way ANOVA with Holm-Sidak's multiple comparison tests.

3.3.4.2 Dosage effects on neuronal correlates

As observed with 10mg/kg ketamine, 5mg/kg ketamine increased the firing rate of neurons from 4.4±0.6Hz at baseline to 5.4± 0.8Hz ($p<0.01$, Holm-Sidak's multiple comparisons; Fig 3.10). Furthermore, 5mg/kg ketamine significantly increased the spike-gamma LFP correlation of pyramidal neurons referenced to the maximum wire relative to baseline (mean STWA ratio increased from 1.7±0.1 to 2.3±0.2, $p<0.01$), but not when referenced to the recording wire ($p>0.05$, Holm-Sidak's multiple comparisons; Fig 3.10). Changes in firing rate were comparable after a single dose of 5mg/kg ketamine (+25%) and 10mg/kg ketamine (+33%), but the changes in spike-gamma LFP correlation to the maximum wire were more sizable after 10mg/kg ketamine (+109%) than after 5mg/kg ketamine (+35%).

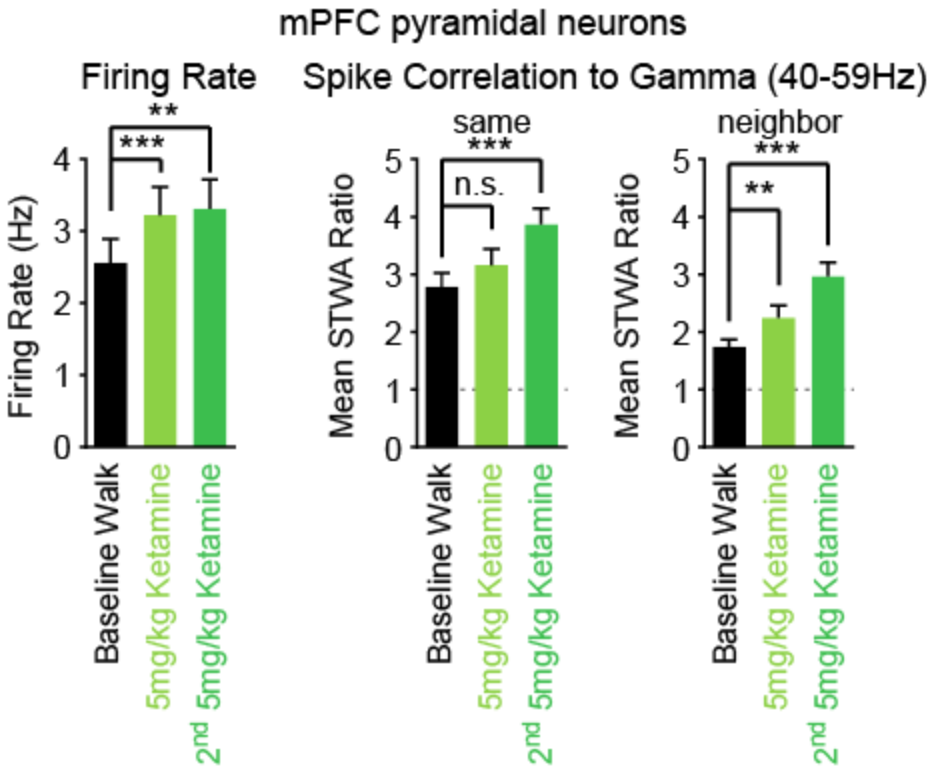

Figure 3.10. 10mg/kg ketamine has more consistent effects on the spiking of mPFC pyramidal neurons than 5mg/kg ketamine. Bar graphs show the effects of ketamine dose on the firing rate of putative pyramidal neurons in the mPFC (**left**), and the spike-LFP relationship of single neurons to the gamma band using the mean STWA ratio from 40-59Hz calculated from the LFP on the recording wire (**middle**), and to the maximum wire (**right**, n= 49 neurons). STWA ratios are the ratio of the peak-to-trough amplitude of the unshuffled STWA/shuffled STWA of mPFC spike trains to mPFC LFPs. Spike trains were shuffled 20 times. Values are reported as percentage or mean ± SEM. **:p<0.01, ***:p<0.001, repeated measures one-way ANOVA followed by Holm-Sidak's multiple comparison test.

3.3.5 Effects of anesthetic doses of ketamine

3.3.5.1 Dosage effects on gamma power

At high doses, ketamine is used as an analgesic and anesthetic in animals and children (Lodge and Mercier, 2015). We next examined an ataxia-inducing dose of 100 mg/kg ketamine to determine the effect of a high dose of ketamine on gamma power and further investigate the connection between motor activity and gamma power. Although 100mg/kg ketamine induced severe ataxia by 10 min after injection, this dose induced a

robust increase in low gamma power (peak between 40-70Hz ±7Hz) in the mPFC (+277%) compared to baseline (p<0.01, Holm-Sidak's multiple comparisons, Fig 3.11A). Intriguingly, one rat became fully ataxic after 100mg/kg ketamine, but showed less than a 20% increase in mPFC gamma power. The gamma peak frequency of 46.9±1.3Hz was not significantly different from baseline but lower than the peak frequencies observed after both 5mg/kg and 10mg/kg ketamine (p<0.001, Holm-Sidak's multiple comparisons; Fig 3.9D). 100mg/kg ketamine also doubled gamma power in the high gamma range (70-120Hz, p<0.05, Tukey's multiple comparisons). Subsequent administration of the α2a adrenergic agonist and muscle relaxant medetomidine eliminated the gamma peak while deeply anesthetizing the rat (Fig 3.11A&C). Five minutes after administration of medetomidine mPFC power had increased over 400% in both the theta (4-8Hz) and alpha (8-12Hz) frequency ranges compared to baseline (both p<0.001, Tukey's multiple comparisons).

Although 100mg/kg ketamine appeared to increase gamma power in the MD thalamus more than 10mg/kg ketamine (+101% vs. +24%); this increase was not significant, perhaps because fewer animals could be included in the analysis (n=5, p>0.05, Tukey's multiple comparisons, Fig 3.11B). Successive administration of medetomidine increased gamma power by 130% compared to baseline (p<0.05, Tukey's multiple comparisons, Fig 3.11C). A dose of 100mg/kg ketamine more than doubled gamma power in the high gamma range (70-120Hz) in the MD thalamus (p<0.05, Tukey's multiple comparisons, Fig 3.11D), and high gamma power remained elevated 5 minutes after medetomidine administration (+66% of baseline high gamma power,

p<0.05, Tukey's multiple comparisons, Fig 3.11D). As in the mPFC, medetomidine increased MD thalamus power ~400% in both the theta (4-8Hz) and alpha (8-12Hz) frequency range compared to baseline (both p<0.001, Tukey's multiple comparisons). These observations reveal a lack of correlation between motor activity and increased gamma LFP power after ketamine administration. They also reveal a strong correlation between low frequency power and anesthesia.

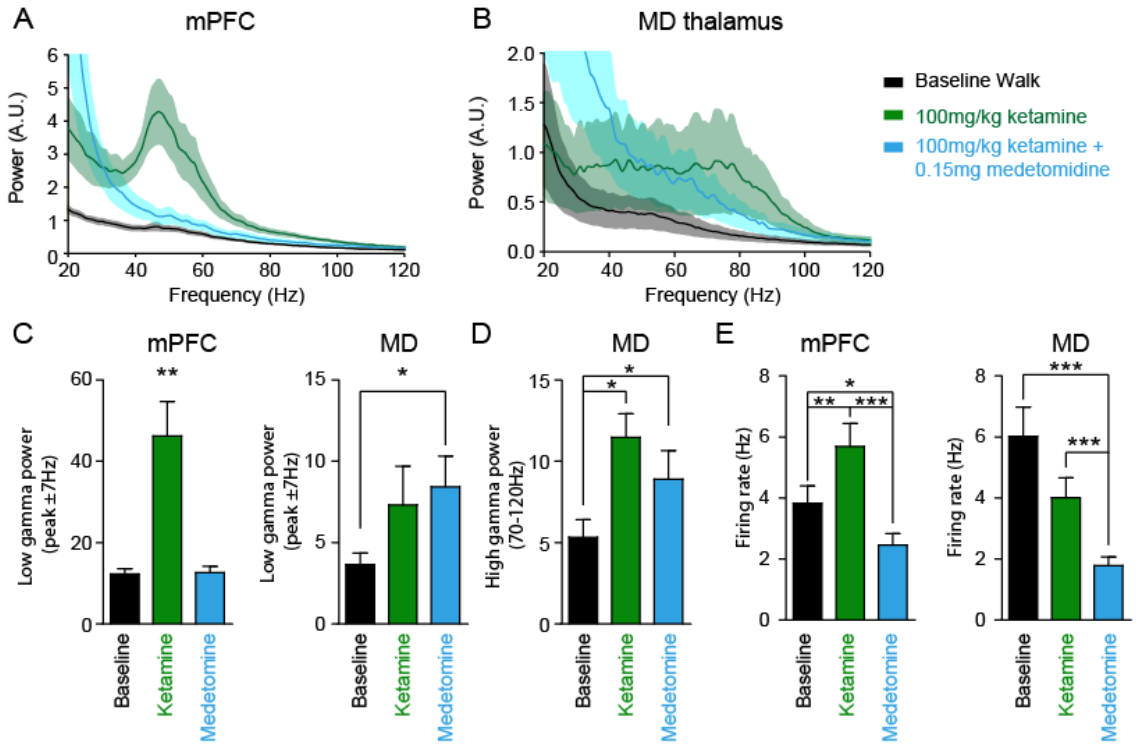

Figure 3.11. Ataxia-inducing doses of ketamine increase gamma power, and subsequent medetomidine eliminates the induced gamma peak. Averaged LFP power spectra in the mPFC (n= 8 rats, **A**) and MD thalamus (n=5 rats, **B**) during untreated treadmill walking, 10 minutes after 100mg/kg ketamine (green), and 5 minutes after subsequent 0.15mg medetomidine administration (blue). Colored shadows indicate SEM. Legend appears at the right. **C**, Low gamma power (peak between 40 and 70 Hz ±7Hz) in the mPFC (**left**) and MD thalamus (**right**) at time points from **A-B**. **D,** High gamma power (70-120Hz) in the MD thalamus at time points from **A-B**. **E,** Average firing rates of neurons in the mPFC and MD thalamus at time points from **A-B.** Values are reported as percentage or mean ± SEM. *:p<0.05, **:p<0.01, ***:p<0.001, repeated measures one-way ANOVA followed by Holm-Sidak's multiple comparison test.

3.3.5.2 Dosage effects on neuronal correlates

To gain further insight into neural correlates associated with changes in gamma oscillations after high doses of ketamine and anesthesia, we examined the firing rates of neurons from the mPFC and MD thalamus. In the mPFC, 100mg/kg ketamine increased the average firing rates of pyramidal neurons by 49% compared to baseline, and subsequent medetomidine administration decreased the average firing rates of pyramidal neurons by 36% compared to baseline (n=48, both $p<0.05$, Tukey's multiple comparisons test, Fig 3.11E). In the MD thalamus, unlike after 10mg/kg ketamine, 100mg/kg ketamine did not decrease the average firing rates of neurons ($p>0.05$, Tukey's multiple comparison's test). However, successive medetomidine administration decreased average firing rates by 70% compared to baseline ($p<0.001$, Tukey's multiple comparisons test). Taken together, these results indicate that medetomidine greatly decreases the spiking activity of neurons in multiple brain regions, and this may be related to its anesthetic properties.

Next, we examined the relationship between spikes and gamma oscillations in the mPFC using STWAs. Again, we used the LFP from the wire on which the spike train was recorded, as well as the maximum and median wire. In every combination of spike trains and wires, the mean STWA ratios significantly increased after 100mg/kg ketamine, and decreased after 0.15mg medetomidine (all $p<0.01$, Holm-Sidak's multiple comparisons, Fig 3.12A). The spike-gamma LFP correlation with ketamine and medetomidine together was still higher than baseline in every combination of spike trains and wires (all $p<0.01$, Holm-Sidak's multiple comparisons, Fig 3.12A). Specifically, when referenced to the

recording wire, 66% of putative pyramidal neurons were significantly correlated to the gamma-filtered LFP (40-59Hz) at baseline. This percentage increased to 91% after 100mg/kg ketamine, and 72% after ketamine and medetomidine together ($p<0.01$, Chi-Square test). Similarly, the spike-gamma LFP correlation increased by 155% after 100mg/kg ketamine compared to baseline, then decreased by 41% after 0.15mg medetomidine ($p<0.01$, n= 48, Holm-Sidak's multiple comparisons). Nevertheless, while the animal was anesthetized with 100mg/kg ketamine and 0.15mg medetomidine the spike-gamma LFP correlation was still 49% higher than at baseline, even though the low gamma power was not significantly different between these conditions. When referenced to the maximum wire, 42% of putative pyramidal neurons were significantly correlated to the gamma-filtered LFP (40-59Hz) at baseline. This percentage increased to 85% after 100mg/kg ketamine (a 202% increase in mean STWA ratio), and 69% after ketamine and medetomidine together (a 38% decrease in mean STWA ratio, all $p<0.01$, Chi-Square test, Holm-Sidak's multiple comparisons, Fig 3.12A). Still, the spike-gamma LFP correlation was 86% higher than baseline when the animal was anesthetized with 100mg/kg ketamine and 0.15mg medetomidine ($p<0.01$, Holm-Sidak's multiple comparisons). Only 17% of putative pyramidal neurons were significantly correlated to the gamma-filtered LFP (40-59Hz) from the median wire at baseline. This percentage increased to 75% after 100mg/kg ketamine, and 58% after ketamine and medetomidine together ($p<0.001$, Chi-square test). Similarly, the spike-gamma LFP correlation increased by 227% after 100mg/kg ketamine compared to baseline, and then decreased by 38% after 0.15mg medetomidine ($p<0.01$, n=48, Holm-Sidak's multiple comparisons,

Fig 3.12A). Nevertheless, while the animal was anesthetized with 100mg/kg ketamine and 0.15mg medetomidine the spike-gamma LFP correlation was still 104% higher than at baseline. Overall, these findings reveal greater ketamine-induced increases in spike-gamma LFP correlation across a broader spatial scale than a narrower spatial scale because increases were more pronounced when referenced to a median wire rather than the recording wire.

Next, we examined the relationship between spikes and gamma oscillations in the MD thalamus during anesthesia. With both 100mg/kg ketamine, and subsequent 0.15mg medetomidine the spike-gamma LFP correlations were significantly reduced compared to baseline when referenced to the recording, or maximum wire (all $p<0.05$, Holm-Sidak's multiple comparisons), but not the median wire (both $p>0.05$, Holm-Sidak's multiple comparisons), perhaps because baseline spike-gamma LFP correlations were so low in the median wire. Specifically, when referenced to the recording wire, 88% of neurons were significantly correlated to the gamma-filtered LFP (40-59Hz) at baseline. This percentage decreased to 72% after 100mg/kg ketamine, and 59% after subsequent administration of medetomidine ($p<0.01$, Chi-Square test). Similarly, the spike-gamma LFP correlation decreased by 38% after 100mg/kg ketamine compared to baseline ($p<0.001$, n=32), but were not significantly affected by subsequent injection of 0.15mg medetomidine (+14%, $p>0.05$, Holm-Sidak's multiple comparisons, Fig 3.12A). Nonetheless, while the animal was anesthetized with 100mg/kg ketamine and 0.15mg medetomidine the spike-gamma LFP correlation was 29% lower than at baseline ($p<0.01$), even though the power in the low gamma frequency range was greater than at

baseline. When referenced to the maximum wire or the median wire, the percentage of neurons significantly correlated to the gamma-filtered LFP (40-59Hz) at baseline did not change significantly (p>0.05, Chi-square test,Fig 3.12A). However, the spike-gamma LFP correlation decreased by 38% after 100mg/kg ketamine compared to baseline when referenced to the maximum wire (p<0.01, Holm-Sidak's multiple comparisons), but was not significantly affected by subsequent injection of 0.15mg medetomidine (+19%, p>0.05, n= 32, Holm-Sidak's multiple comparisons). Furthermore, while the animal was anesthetized with 100mg/kg ketamine and 0.15mg medetomidine together the spike-gamma LFP correlation was still 25% lower than at baseline (p<0.05). Lastly, there were no significant differences in the spike-gamma LFP correlations when referenced to the median wire (p>0.05, n= 32, Holm-Sidak's multiple comparisons, Fig 3.12A). Taken together, these data show a striking spatial decay in gamma oscillations in the MD thalamus. This provides evidence that individual spikes may cause a short resonant oscillation at gamma frequencies, but for the most part, gamma oscillations are not emanating from local circuits in this region.

Finally, we examined the spike-LFP correlations to high gamma oscillations between 70-115Hz in the MD thalamus since there is a spectral "bump" in this range. As observed in the low gamma range, there were no significant differences in the spike-gamma LFP correlations referenced to the median wire. In contrast, significant decreases in spike-high gamma LFP correlation were observed when referenced to the recording wire and the wire with maximum coherence (all p<0.05, n= 32, Holm-Sidak's multiple comparisons, Fig 3.12B). Specifically, when referenced to the recording wire, 94% of

neurons were significantly correlated at baseline. This percentage decreased to 72% and 53% after 100mg/kg ketamine and 0.15mg medetomidine respectively (p<0.01, Chi-square test). Additionally, the spike-high gamma LFP correlation decreased from baseline (mean STWA ratio: 5.33 ± 0.48) by 38% after 100mg/kg ketamine (mean STWA ratio: 3.30 ± 0.31) and decreased from baseline 29% during ketamine and medetomidine induced anesthesia (mean STWA ratio: 3.76 ± 0.50) when referenced to the recording wire (both p<0.01, n=32, Holm-Sidak's multiple comparisons). When referenced to the wire with the maximum coherence, there was no significant difference in the percentage of neurons significantly correlated to the high gamma filtered LFP (p>0.05, Chi-square test). Examining spike-high gamma LFP correlations using mean STWA ratios increases the accuracy of differences examined and gives greater statistical power. When referenced to the wire with the maximum coherence in the 70-115Hz range, the spike-gamma LFP correlation decreased from baseline (mean STWA ratio: 3.19 ± 0.40) by 37% after 100mg/kg ketamine (mean STWA ratio: 1.98 ± 0.22), and decreased from baseline 26% after 100mg/kg ketamine and 0.15mg medetomidine together (mean STWA ratio: 2.37 ± 0.30, both p<0.05, Holm-Sidak's multiple comparisons, Fig 3.12B). Taken together, ketamine has the greatest influence on spike-LFP correlations to gamma when referenced to the recording wire in the MD thalamus and the median wire in the mPFC.

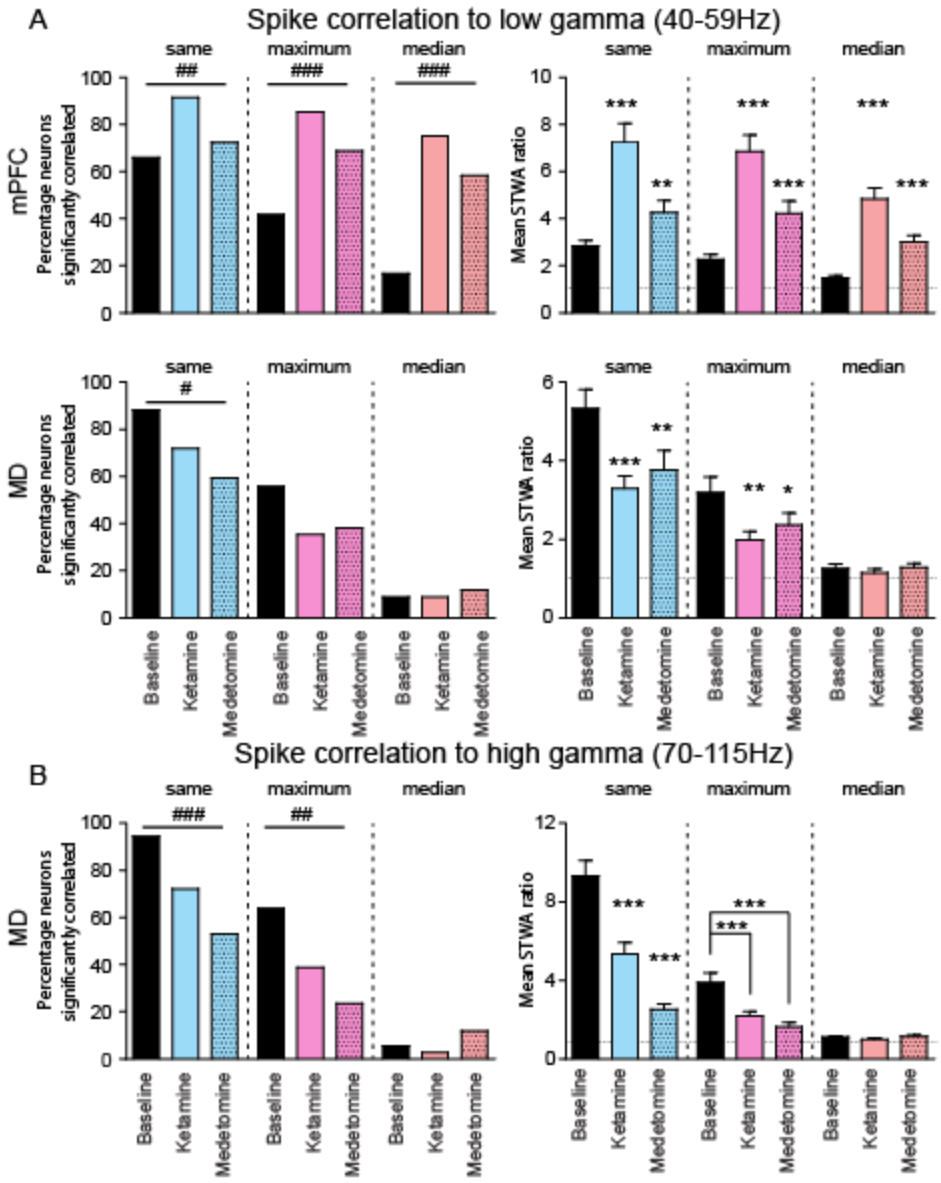

Figure 3.12. Comparison of recording wires to neighboring wires in the mPFC and MD thalamus reveal different spatial relationships in each structure.A, The percentage of neurons significantly correlated to low gamma oscillations (40-59Hz, **left**) from the mPFC (**top**) and the MD thalamus (**bottom**), when the spike train was referenced to the recording wire (same, blue), maximum (purple) and median (coral) wires (see Section 3.2.7) 10 minutes after 100mg/kg ketamine (**ketamine**) or 5 minutes after subsequent administration of medetomidine (**medetomidine**). Mean ratios (**right**) between peak to trough amplitudes of the original STWA and the mean of 20 shuffled STWAs for LFPs filtered from 40-59Hz recorded from the same wire, maximum, or median wire for putative mPFC pyramidal neurons (**top**) and MD thalamus neurons (**bottom**). **B**, Same as in **A** except the spike trains were referenced to LFPs filtered in the high gamma range (70-115Hz). A bar with significance stars over it indicates that this bar is significantly different from all the other conditions. A ratio of 1 (dashed horizontal line) indicates no difference between shuffled and unshuffled values. Values are reported as percentage or mean ±SEM.

*:$p<0.05$, **:$p<0.01$, ***:$p<0.001$, repeated-measures one-way ANOVA with Holm-Sidak's multiple comparisons test, $:$p<0.1$, ##:$p<0.01$, ###:$p<0.001$, chi-square test.

3.3.6 Effects of the D4R agonist on gamma power

Dopamine D4R agonists concurrently increase gamma power and cognitive performance in normal animals (Nakazawa et al., 2015) and D4R antagonists reverse cognitive deficits induced by chronic NMDAR antagonism (Arnsten et al., 2000). As it has been suggested that a drug's ability to modulate ketamine-induced increases in gamma power reflects its therapeutic potential (Jones et al., 2012), we were interested in exploring the effects of these D4R-targeting drugs on ketamine-induced increases in gamma activity during treadmill walking in the mPFC and MD thalamus.

To examine the effect of the D4R agonist A-412997 on gamma power during treadmill walking in the absence of ketamine, either three ascending doses or three vehicle injections were administered 30 minutes apart followed by a 5mg/kg dose of the D4R antagonist L-745,870 (see Section 3.2.5). In the mPFC, a cumulative dose of 1.5mg/kg A-412997 induced a modest but significant 12.1±2.4% increase in gamma power ($p<0.05$, Holm-Sidak's multiple comparisons; Fig 3.14A). This was not further increased by a subsequent 1.5mg/kg injection ($p>0.05$, Holm-Sidak's multiple comparisons). Indeed a cumulative dose of 3mg/kg A-412997 increased gamma power by 11.2±1.8% compared to baseline ($p<0.05$, Holm-Sidak's multiple comparisons; Fig 3.13). Likewise, in the MD thalamus, the cumulative dose of 3mg/kg A-412997 increased gamma power by 9.4±5.5% ($p<0.05$), but the other doses had no significant effect ($p>0.05$, Holm-Sidak's multiple comparisons; Fig 3.14C). These increases in gamma power were reduced by the D4R antagonist in the mPFC (-8.9%, $p<0.05$, paired t-test;

Fig 3.13& 3.14A, and the MD thalamus (-8.8%, $p<0.05$, paired t-test; Fig 3.14C). However, the D4R antagonist did not significantly change gamma power after vehicle injections ($p>0.05$, paired t-tests; Fig 3.14&C). These results are consistent with previous findings showing an increase in gamma power with D4R agonists (Kocsis et al., 2014), and indicate that walking-induced gamma oscillations are not dependent on D4R activity.

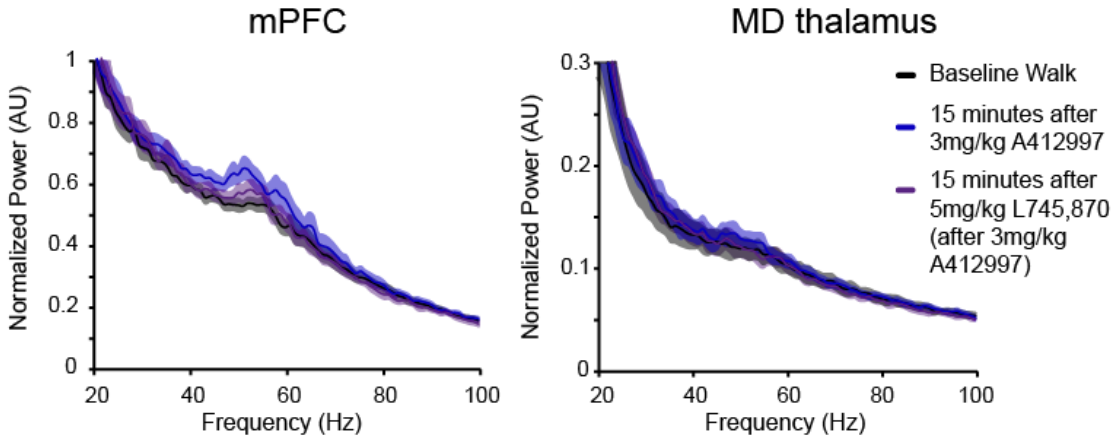

Figure 3.13. D4R agonists increase gamma power and D4R antagonists reverse this effect. Averaged LFP power spectra for the mPFC (**left**) and MD thalamus (**right**), during treadmill walking at baseline (black), 15 minutes after a cumulative dose of 3mg/kg A-412997(blue), and 15 minutes after a subsequent dose of 5mg/kg L745870 (purple). Colored shadows indicate SEM.

3.3.7 The D4R agonist and antagonist influence ketamine-induced neurophysiological changes

We next assessed the effects of the D4R agonist (3mg/kg A-412997) and antagonist (5mg/kg L-745,870) administered 30 minutes before a ketamine injection on ketamine-induced behaviors and gamma power. Neither the D4R agonist nor the D4R antagonist had significant influences on measures of attentiveness, hyperactivity, stereotypic behaviors, or ataxia after ketamine injection while the treadmill was off or on (all $p>0.05$, one-way ANOVA, n=12 rats). Moreover, in the mPFC, the D4R

pretreatments neither influenced the low gamma power (peak between 40 and 70Hz ±7Hz) 15 minutes after ketamine administration, nor influenced the time course of gamma power recovery (p>0.05, RM two-way ANOVA; Fig 3.14E-F). In contrast, in the MD thalamus ketamine-induced increases in gamma power were enhanced by the D4R agonist pretreatment as compared to the saline pretreatment (Fig 3.14G-H). Fifteen minutes after the ketamine injection, low gamma power had increased by an average of 86.1±20.2% after the D4R agonist pretreatment as compared to 36.9±14.8% after saline pretreatment (p<0.001, Tukey's multiple comparisons; Fig 3.14G-H) . Similarly, 35 minutes after the ketamine injection, low gamma power had increased by an average of 37.3±16.1% after the D4R agonist pretreatment as compared to 11.9±8.8% after saline pretreatment (p<0.05, Tukey's multiple comparisons; Fig 3.14H). The D4R antagonist neither influenced low gamma power nor the time course of recovery after ketamine (both p>0.05, RM two-way ANOVA; Fig 3.14E-H). Taken together, these data show that the D4R pretreatments influence ketamine-induced gamma power in the MD thalamus, but not the mPFC.

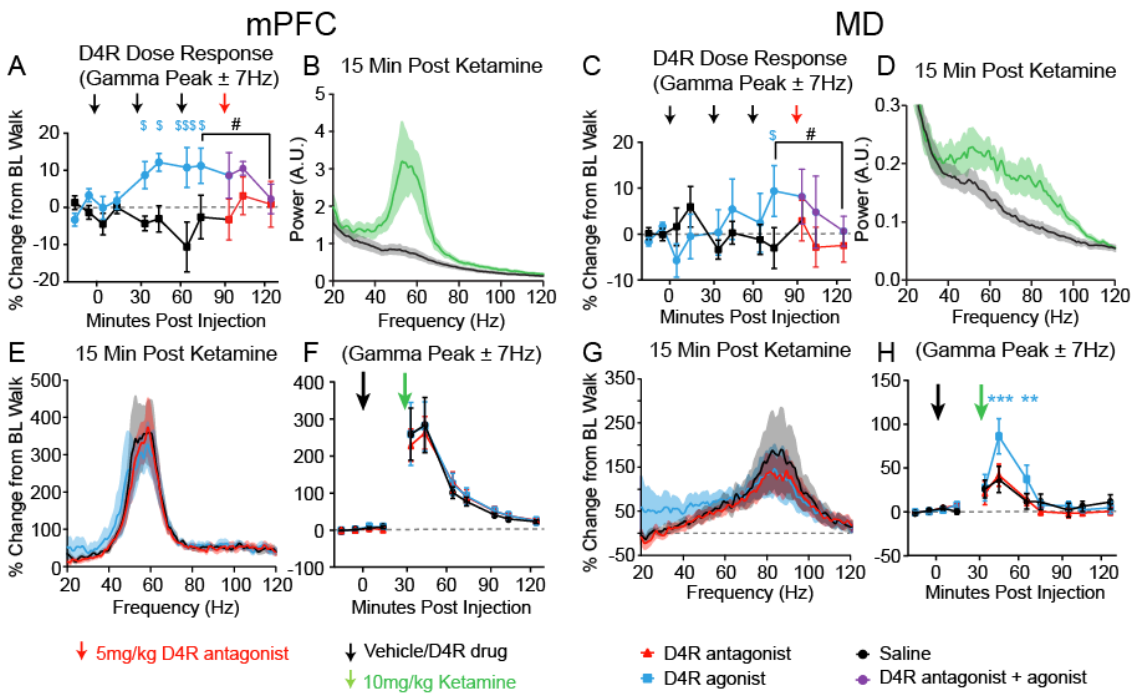

Figure 3.14. Effects of the dopamine D4 receptor agonist and antagonist on gamma power in the presence and absence of ketamine. Gamma power during treadmill walking in the mPFC (**A,B,E,F**) and MD thalamus (**C,D,G,H**). (**A&C**) Percent change in gamma power (peak between 40-70Hz ±7Hz) in rats without ketamine treatments. Black arrows indicate injections of saline (black curve) or A-412997, the D4R agonist, injected at 0.3mg/kg at the 1st arrow, 1.2mg/kg at the 2nd arrow, and 1.5mg/kg at the 3rd arrow (blue curve). The cumulative dose was 3mg/kg A-412997. The red arrow indicates an injection of 5mg/kg L-745,870, the D4R antagonist. Red curve shows the effect of the antagonist after saline and purple curve indicates the effect of the antagonist after the agonist (n=6 rats). **B, D,** Averaged LFP power spectra in the mPFC (**B**) and MD thalamus (**D**) at baseline (black) and 15 minutes after 10mg/kg ketamine (green) with saline injection 30 minutes prior (n=6 rats). Colored shadows indicate SEM. **E, G,** Average percent change in LFP power spectra from baseline walking power 15 minutes after 10mg/kg ketamine for each frequency in the mPFC (**C**) and MD thalamus (**G**). The red trace indicates pretreatment with the antagonist (5mg/kg L-745,870), the blue trace indicates the pretreatment with the agonist (3mg/kg A-412997), and the black trace indicates the pretreatment with saline. **F,H,** Changes in low gamma (peak between 40-70Hz± 7Hz) power in the mPFC (**F**) and MD thalamus (**H**) over time. Data is presented as percent change from the rats's baseline walking power on the recording day. The black arrow indicates the injection of the pretreatment (D4R agonist and antagonist or saline), and the green arrow indicates the injection of 10mg/kg ketamine. Blue stars indicate a significant change from saline pretreatment with the agonist (n=6 rats). The frequency range of the gamma power was determined by finding the frequency of the maximum gamma peak between 40 and 70Hz in each epoch and summing power from the surrounding 15Hz range. Values are reported as percentage ±SEM. *: $p<0.05$, **: $p<0.01$, ***: $p<0.001$, two-way repeated measures ANOVA with Tukey's multiple comparisons. $: $p<0.05$, $$$: $p<0.001$, significant difference from vehicle injections, Holm-Sidak's multiple comparisons test; #: $p<0.05$, paired t-test comparing percent change in power 15 minutes after 3mg/kg A-412997 and 35 minutes after 5mg/kg L-745,870.

To assess whether the D4R agonist and antagonist influenced ketamine-induced changes in firing rate, we examined neurons in the mPFC and MD thalamus after each pretreatment. As described above, ketamine increased firing rates in the mPFC and decreased firing rates in the MD thalamus (Fig 3.5B). In mPFC pyramidal neurons, no significant differences in ketamine-induced increases in firing rates were observed between pretreatments with saline, the D4R agonist, or the D4R antagonist ($p>0.05$, one-way ANOVA; Fig 3.15A). Only 6 mPFC interneurons were recorded after any of the three pretreatments, so they were not analyzed further. Interestingly, in the MD thalamus, the D4R agonist pretreatment attenuated the ketamine-induced decrease in neuronal firing rates ($p>0.05$, RM one-way ANOVA; Fig 3.15B). In contrast, ketamine still reduced the firing rates of MD thalamus neurons by 2.1±0.6Hz after saline pretreatment and 2.2±0.7Hz after the D4R antagonist pretreatment (both $p<0.01$, Holm-Sidak's multiple comparisons; Fig 3.15B). Likewise, both the saline pretreatment and the D4R antagonist pretreatment alone induced a modest yet significant decrease in the MD thalamus neuronal firing rate of 0.4±0.2Hz (both $p<0.05$), but the D4R agonist alone does not ($p>0.05$, Holm-Sidak's multiple comparisons; Fig 3.15B). Overall, the D4R pretreatments had no effect on ketamine-induced changes in firing rate in the mPFC, but the D4R agonist modified firing rates before and after ketamine in the MD thalamus.

The D4R pretreatments had no obvious effect on spike- gamma LFP correlations referenced to the same wire in the mPFC or the MD thalamus. As described above, ketamine increased spike-gamma LFP correlations in the mPFC and decreased spike-gamma LFP correlations in the MD thalamus (Fig 3.6). In the mPFC, the D4R-targeting

pretreatments neither influenced ketamine-induced increases in spike-gamma LFP correlation, nor influenced spike-gamma LFP correlation per se (both $p>0.05$, one-way ANOVAs; Fig 3.15C). Furthermore, in the MD thalamus, none of the pretreatments influenced ketamine-induced decreases in spike-gamma LFP correlation, or affected spike-gamma LFP correlation per se (both $p>0.05$, one-way ANOVA; Fig 3.15D). Taken together, these data suggest that the D4R agonist may influence the effect of ketamine on gamma power and firing rates in the MD thalamus without influencing relationships between individual neurons and gamma oscillations.

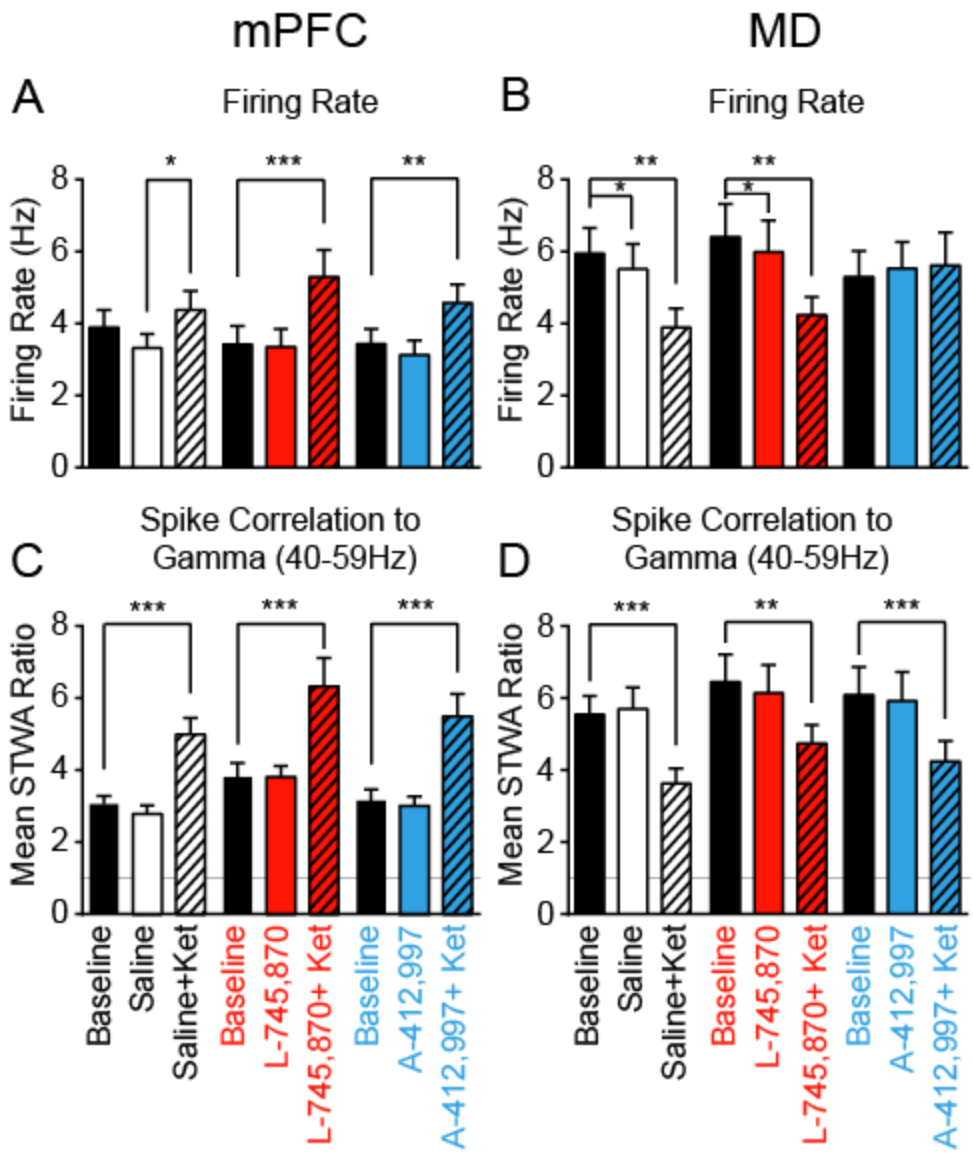

Figure 3.15. Effects of dopamine D4R agonist and antagonist on ketamine induced changes in single neuron activity.A-B, Firing rates of putative pyramidal neurons in the mPFC (**A**) and neurons in the MD thalamus (**B**) at baseline (black), 15 minutes after the pretreatment injection (solid color), and 15 minutes after 10mg/kg ketamine (striped) with saline pretreatment (white, mPFC*:* n=47 neurons from 6 rats, MD thalamus*:* n=39 neurons from 6 rats), the antagonist pretreatment, L-745,870 (5mg/kg, s.c., red, mPFC*:* n=34 neurons from 6 rats, MD thalamus*:* n=36 neurons from 6 rats), or the agonist pretreatment, A-412997 (3mg/kg, s.c., blue, mPFC: n= 42 neurons from 6 rats, MD thalamus*:* n= 32 neurons from 6 rats). **C-D,** Mean ratios between peak to trough amplitudes of the original STWA and the mean of 20 shuffled STWAs for LFPs filtered from 40-59Hz recorded from the same wire in the mPFC (**C**) and MD thalamus (**D**). There were no significant differences between pretreatment groups on ketamine-induced firing rates or spike-LFP correlations (p>0.05, one-way ANOVAs). Values are reported as mean ± SEM. *:p<0.05, **:p<0.01, ***:p<0.001, repeated measures one-way ANOVAs were used for each pretreatment group followed by Holm-Sidak's multiple comparisons test.

3.4 Discussion

In the current study, subanesthetic doses of ketamine were administered to rats to examine the relationships between increases in gamma power and spiking activity in mPFC and MD thalamus. Ketamine induced a striking increase in gamma power in both structuResearch Ketamine also increased the firing rate and correlation between mPFC spiking and gamma oscillations. In contrast, in the MD thalamus, ketamine reduced the firing rate and correlation between spiking and gamma oscillations. As ketamine-induced increases in gamma power, firing rate, and spike-LFP correlation in the mPFC were observed in conjunction with an increase in motor activity, the effects of increases in motor activity induced by treadmill walking were examined. Treadmill walking alone also increased gamma power in both mPFC and MD thalamus, but to a lesser extent than ketamine administration and these effects were not additive. In the mPFC, walking concurrently increased the firing rates of pyramidal neurons and interneurons and increased synchronization between pyramidal neuron spikes and gamma oscillations. Moreover, unlike the effect of ketamine in the MD thalamus, walking concurrently increased the firing rate and synchronization between spikes and gamma oscillations, suggesting a different circuit is responsible for increasing thalamic gamma power induced by walking compared to ketamine.

Dopamine D4R-targeting drugs may have potential for treating cognitive deficits in schizophrenia (Furth et al., 2013). As it has been proposed that a drug's ability to modulate gamma power might reflect its therapeutic potential (Anderson et al., 2014; Celada et al., 2013; Hudson et al., 2016; Jones et al., 2014; Ma and Leung, 2014), we

examined the effects of these D4R-targeting drugs on ketamine-induced gamma activity. Neither the D4R agonist nor antagonist significantly influenced ketamine-induced gamma oscillations or firing rates in the mPFC. However, in the MD thalamus, the D4R agonist increased ketamine-induced gamma and modified neuronal firing rates.

3.4.1 Neurophysiological correlates of ketamine and locomotion

Many studies have used ketamine to gain further insight into schizophrenia and the treatment of depression (Lodge and Mercier, 2015). In clinical experiments low doses of the NMDAR antagonist ketamine (~15% of the anesthetic dose) increase cortical gamma power while inducing symptoms of early stage schizophrenia (Anticevic et al., 2015; Corlett et al., 2013; Driesen et al., 2013b; Krystal et al., 1994; Stone et al., 2008, 2012). Interestingly, long-term, but not acute treatment with neuroleptics decreases ketamine-induced positive and cognitive symptoms in healthy human volunteers (Krystal et al., 1999; Lipschitz et al., 1997; Malhotra et al., 1997). Likewise, in rodents, low doses of ketamine (~15% of the anesthetic dose) increase cortical gamma power and motor activity (Ehrlichman et al., 2009; Kulikova et al., 2012; Lazarewicz et al., 2009; Meltzer et al., 2013; Nikiforuk et al., 2016; Pinault, 2008; Saunders et al., 2012; Shaffer et al., 2014), and long-term, but not acute treatment with neuroleptics decreases ketamine-induced increases in gamma power and motor activity (Anderson et al., 2014; Jones et al., 2012). While the circuit by which NMDAR antagonists increase gamma power is still mysterious, it is likely that gamma power increases by increases in fast AMPAR-mediated currents relative to slower NMDAR-mediated currents (Maeng et al., 2008). Three pieces of evidence support this idea. (1) Inhibiting NR2A-expressing NMDARs

leads to increases in both extracellular glutamate and gamma power (Jiménez-Sánchez et al., 2014; Kocsis, 2012) that are not seen when NR2B is inhibited. (2) Ketamine no longer increases gamma power when AMPARs are inhibited (Zanos et al., 2016). (3) D4R activation reduces NMDAR-mediated currents more than AMPAR currents (Furth et al., 2013), and the effects of D4R activation are occluded by ketamine administration. Interestingly, in the MD thalamus, AMPAR expression is low compared to NMDAR expression (Salt and Eaton, 1996), while in the cortex AMPA currents predominate glutamatergic signaling (Rotaru et al., 2011). This may help explain why ketamine has opposite effects on the MD thalamus and mPFC at the single neuron level.

Notably, ketamine is currently used to rapidly treat depression and reduce suicidal idealization resistant to antidepressant treatment at the same doses that that are used to induce psychomimetic symptoms in healthy volunteers (Abdallah et al., 2015; Berman et al., 2000; Zanos et al., 2016). A recent study implicates (2R,6R)-hydroxynorketamine (HNK), a ketamine metabolite, as mediating the acute antidepressant effects of ketamine. (2R,6R)-HNK still induces increases in gamma power, but without increasing motor activity (Zanos et al., 2016). Increasing evidence suggests that effects of ketamine on gamma oscillation power are independent from its antidepressant-like effects. First, other NMDAR antagonists, such as MK-801 and PCP increase gamma power without exerting antidepressant effects (Autry et al., 2011; Zanos et al., 2016). Second, NR2B antagonists alone recapitulate ketamine's antidepressant effects without altering gamma power or extracellular glutamate *in vivo* (Jiménez-Sánchez et al., 2014; Kocsis, 2012; Li et al., 2010; Miller et al., 2016).

One recent study suggests that the effects of ketamine on evoked gamma oscillations have more predictive power for potential therapeutics than ketamine's effects on ongoing gamma oscillations (Hudson et al., 2016). Given that ketamine induced similar increases in gamma power whether the rat was walking, or in the stationary treadmill, it is likely that ketamine-induced gamma oscillations during treadmill walking better reflect ongoing gamma oscillations than evoked gamma oscillations, although more work is needed. Even though we did not examine behavioral correlates of schizophrenia, we observed that rats avoided colliding with the paddle within the treadmill more effectively after 10mg/kg ketamine, suggesting that gamma power and attention are correlated even when induced by ketamine. This confirmed a recent study showing that ketamine increases attention in young rodents (Guidi et al., 2015).

The present study provides two lines of evidence supporting the hypothesis that walking and ketamine induced gamma oscillations in the mPFC are locally generated by a common pyramidal-interneuron generated gamma (PING) circuit (Cannon et al., 2014; Jadi et al., 2015). While power in both low (40-70Hz) and high (70-120Hz) gamma ranges increased after ketamine administration, only the increase in low gamma power around the significant spectral peak was dose-dependent, and this peak frequency (~55Hz) was similar to that observed during the gamma generated by locomotion (~51Hz). This confirmed previous work from our lab and others that has shown increases in gamma LFP power in the rodent mPFC and visual cortex during locomotion (Delaville et al., 2015; Niell and Stryker, 2010) and arousal (McGinley et al., 2015a; Vinck et al., 2015). This finely tuned increase in gamma activity could reflect activity in

a local circuit with precise temporal dynamics, such as a PING circuit (Womelsdorf et al., 2014). The second line of evidence involved measuring synchronization through investigation of the peak-to-trough amplitudes of spike triggered waveform averages (STWAs). Traditionally, STWAs are thought to reveal relationships between postsynaptic currents that generate a spike or local resonance produced by a spike (Einevoll et al., 2013; Moca et al., 2014; Reimann et al., 2013). They may also reveal network oscillations that bias spike timing (Ray, 2015). As observed in the visual cortex (Munk et al., 1996; Vinck et al., 2015), mPFC pyramidal neurons showed increased spiking synchronization to gamma oscillations during walking epochs concurrent with increases in gamma power, as would be expected in a circuit where power is enhanced by the rhythmic activation of pyramidal neurons (Lee and Jones, 2013). On a cautionary note, though interneurons did not show increased spiking synchronization to gamma oscillations during walking, as might be predicted in a PING model.

Other evidence suggests a more complex mechanism of gamma generation after ketamine administration than PING. Acute application of NMDAR antagonists increase gamma power, increase the firing rates of pyramidal neurons, but decrease the firing rates of interneurons over a similar time course (Homayoun and Moghaddam, 2007a; Jackson et al., 2004; for a review, see Miller et al., 2016). In order for the disinhibition of pyramidal neurons to directly increase gamma power, one would expect these neurons to exhibit synchronization with gamma oscillations. In agreement with this, our results showed that 5 and 10mg/kg ketamine each increased the firing rates and spike-gamma LFP correlations of mPFC pyramidal neurons. However, the magnitude of these increases

was not proportional. While pyramidal neurons showed similar increases in firing rate induced by ketamine or walking (33% vs. 11%), increases in gamma power induced by ketamine were substantially larger than those induced by walking in the mPFC (254% vs. 23.8%). Wood and colleagues (2012) also observed a lower correlation between firing rates and gamma power in the frontal cortex after administration of the NMDAR antagonist MK-801 than before. This would suggest that mechanisms generating gamma power differ when gamma power is induced by NMDAR antagonism rather than locomotion. In untreated humans, spike-gamma LFP correlations tend to be high when neuronal spiking becomes synchronized (Nir et al., 2007); however, MK-801 treatment in rats desynchronizes spiking while increasing gamma power in the prefrontal cortex (Molina et al., 2014). Thus, the relationship between the pyramidal neuron firing rate and abnormal gamma power after ketamine administration remains complex.

We observed that ketamine significantly increased gamma oscillations in the MD thalamus, comparable to increases observed in the rodent ventrolateral thalamus of rodents (Hakami et al., 2009), and human thalamus (Rivolta et al., 2015). Increases in gamma in the MD thalamus emerged over a broader range than in the mPFC, with two spectral peaks, centered at 55Hz and 81Hz. Although mPFC and MD thalamus are reciprocally connected (Mitchell and Chakraborty, 2013) and both show spectral peaks around 55Hz, we neither observed gamma frequency coherence between these structures, nor observed spiking synchronized to gamma oscillations between these structuResearch This confirms a finding in healthy humans that ketamine administration did not significantly alter prefrontal-MD thalamus functional connectivity (Höflich et al., 2015),

although ketamine appears to increase thalamocortical connectivity using different measures (Anticevic et al., 2015; Dawson et al., 2013; Driesen et al., 2013a). Furthermore, acute NMDAR antagonists administered in the MD thalamus induced increases in the delta (0-4Hz) range LFP of the mPFC similar to those induced by systemic administration (Kiss et al., 2011a). Contrary to effects seen in the mPFC, ketamine simultaneously decreased firing rates and reduced correlations between spikes and gamma oscillations in both gamma ranges in the MD thalamus, suggesting that gamma power in the MD thalamus may be driven by external inputs rather than locally generated resonance (Buzsáki et al., 2012; Kezunovic et al., 2012).

Spike trains from mPFC pyramidal neurons as well as MD thalamus neurons show increased synchronization to gamma range oscillations during walking when spikes were referenced to the recording wire. However, this was not observed when MD thalamus neurons were referenced to a neighboring wire. One explanation for these results is that the LFP around the MD thalamus neurons is more localized than that around the mPFC pyramidal neurons (Buzsáki et al., 2012; Reimann et al., 2013). After ketamine administration, mPFC pyramidal neurons showed increased synchronization to gamma oscillations when referenced to the recording wire or a neighboring wire. This suggests that the relationship between spiking activity and gamma is spatially localized in walking-induced gamma (Sirota et al., 2008) and more widespread during ketamine-induced gamma.

The question remains: how does ketamine increase gamma power in the MD thalamus yet decrease the firing rates of neurons in this structure and decrease the

correlation between spikes and gamma power? A few possible explanations emerge. First, different types of glutamatergic innervation establish different types of anatomical connections with thalamic relay neurons (Sherman, 2013). Corticothalamic inputs may activate group I metabotropic glutamate receptors (mGluRs) to prolong EPSPs, inactivating T-type calcium channels and switching neurons from burst firing, which may be highly aligned with gamma oscillations, to tonic firing, which may not align with gamma oscillations (Sherman, 2013). Gamma power in this region would thus result from coordinated glutamatergic EPSPs, perhaps originating from the basal ganglia or amygdala, which both show a prominent increase in gamma power after ketamine administration (Hakami et al., 2009; Nicolás et al., 2011). 2) Second, thalamic output is sensitive to spatial and temporal dynamics. For instance, low frequency stimulation of corticothalamic afferents suppresses the spiking activity of thalamic relay neurons while high frequency stimulation of these afferents increases the spiking activity of thalamic relay neurons (Crandall et al., 2015). This occurs because monosynaptic excitatory corticothalamic input onto thalamic relay cells is relatively weak compared to robust disynaptic inhibition from thalamic reticular neurons. NMDA receptor mediated currents dominate the majority of excitatory corticothalamic inputs (Deleuze and Huguenard, 2016), and are responsible for enhancing the excitability of thalamic relay neurons after high frequency stimulation (Crandall et al., 2015), supporting the *direct hypothesis* in the thalamus. Therefore, after inhibiting NMDA receptors in thalamic relay neurons, repetitive stimulation to these neurons would become inhibitory, further explaining why NMDA receptor antagonism decreases the firing rates of MD thalamus neurons.

Importantly, gamma oscillations in the barrel cortex induce rhythmic IPSCs in the ventral posterior medial nucleus, followed by rhythmic EPSCs (Crandall et al., 2015). With NMDA receptor-mediated currents blocked, it is likely that the switch from IPSCs to EPSCs never occurs. Thus the gamma power detected in the MD thalamus may simply arise from subthreshold currents within relay cells. Finally, it is important to note, that in contrast to our findings with ketamine the NMDA receptor antagonist PCP increases the spiking of the MD thalamus (Santana et al., 2011) via the preferential reduction in the activity of the thalamic reticular nucleus, the major source of inhibitory innervation to the MD thalamus (Troyano-Rodriguez et al., 2014). Under normal conditions, the average cell in the thalamic reticular nucleus is GABAergic and spikes 10 times faster than the average cell in the MD thalamus, which is glutamatergic (Troyano-Rodriguez et al., 2014). PCP directly reduces the firing rate of thalamic reticular neurons to a greater extent than it reduces the firing rate relay neurons, lending support to the *disinhibition hypothesis* in the thalamus.

3.4.2 Relevance of the D4R

The dopamine D4 receptor (D4R) emerges as a potential target for enhancing cognition in psychiatric disorders due to the ability of D4R agonists to increase gamma power and cognitive performance (Andersson et al., 2012a, 2012b; Bernaerts and Tirelli, 2003; Kocsis et al., 2014; Nakazawa et al., 2015; Nayak and Cassaday, 2003; Woolley et al., 2008). Interestingly, D4R antagonists have paradoxical promnesic effects at low doses (Zhang et al., 2004), but decrease task performance when co-administered with an antipsychotic (Murai et al., 2014). However, low doses of D4R antagonists reverse

working memory deficits induced by stress or chronic PCP administration in monkeys (Arnsten et al., 2000; Jentsch et al., 1999). Furthermore, humans with a subsensitive allelic variant of the D4R (D4.7) show abnormal gamma oscillatory activity during a task requiring attention (Demiralp et al., 2007), and are more likely to have ADHD (Swanson et al., 1998). These findings suggest that D4R activity is finely-tuned to promote optimal gamma oscillations and cognitive performance.

While it has been suggested that basal levels of dopamine may activate D4Rs (Rosen et al., 2015b), our results showed that the D4R antagonist had little effect on gamma power or firing rates during treadmill walking in the mPFC or MD thalamus. However, as observed by Kocsis and colleagues (2014), a D4R agonist increased gamma power in both structuResearch Unlike during walking-induced gamma, during D4R agonist-induced gamma the correlation between mPFC pyramidal spikes and gamma oscillations did not increase, even though the increase in gamma power is similar (24% vs. 12%, respectively This may suggest that increases in gamma power after D4R activation arose from a different mechanism than walking-induced increases in gamma power, but could simply reflect the smaller change in power.

As ketamine have been shown to increase extracellular dopamine in the cortex of rodents (Moghaddam et al., 1997), and the D4R has the highest affinity for dopamine of any dopaminergic receptor(Rondou et al., 2010), we predicted that D4Rs would be active after ketamine administration, and therefore the D4R antagonist would diminish ketamine's effects on behavior or neurophysiological measures in the mPFC or MD thalamus. However, pretreatment with the D4R antagonist had little effect. In contrast,

pretreatment with the D4R agonist augmented ketamine's effects on gamma power and reduced ketamine's effects on firing rates in the MD thalamus. Other investigators have shown changes in cortical ketamine-induced gamma power using chronic pretreatment with antipsychotics, but not acute (Anderson et al., 2014; Jones et al., 2012, 2014). Thus, it remains to be seen whether chronic treatment with D4R-targeting drugs could reduce ketamine-induced gamma power.

The D4R agonist had a greater effect on ketamine-induced gamma power in the MD thalamus than in the mPFC. These region specific differences could be explained by differences in D4R expression. Indeed, in the cortex (Mrzljak et al., 1996) and the hippocampus (Andersson et al., 2012b), D4R expression is highest in parvalbumin-positive fast-spiking interneurons, but D4R is also sparsely expressed in pyramidal neurons (Mrzljak et al., 1996). Less D4Rs are found in the MD thalamus; however, the thalamic reticular nucleus, which inhibits dorsal thalamic nuclei, has high D4R expression (Ferrarelli and Tononi, 2011; Mrzljak et al., 1996), and inputs into the thalamus have presynaptic D4Rs (Gasca-Martinez et al., 2010; Govindaiah et al., 2010).

3.4.3 Conclusion

Ketamine increases cortical gamma power and produces cognitive impairments in healthy humans similar to the impairments observed in patients with schizophrenia (Hong et al., 2010; Krystal et al., 1994). Multiple psychotomimetic drugs and rodent models of schizophrenia increase cortical gamma power (Rosen et al., 2015a) and desynchronize spiking from oscillations (Wood et al., 2012). In contrast, our results show increased spike-gamma LFP correlations in the mPFC and decreased spike-gamma LFP

correlations in the MD thalamus. Our results show that gamma oscillations induced by walking and ketamine are similar in the mPFC, hinting at a common circuit underlying both oscillations. However, the differences in neuronal correlates of walking- and ketamine-induced gamma oscillations in the MD thalamus suggest that these oscillations arise from different mechanisms. Thus, walking-induced 51Hz gamma oscillations are more similar between the mPFC and MD thalamus, while ketamine-induced 55Hz gamma oscillations show region-specific differences.

CHAPTER FOUR: ErbB receptor signaling *in vivo*

4.1 Introduction

Patients with schizophrenia show deficits in neural oscillation activity and local synchrony in the mPFC (Sakurai et al., 2015; Spellman and Gordon, 2015). Furthermore, animal models of schizophrenia show impaired synchrony in the gamma frequency range (for example, Carlson et al., 2011; Goto and Grace, 2006), or impaired oscillatory coherence between the prefrontal cortex and other brain regions such as the hippocampus (for example, Sigurdsson et al., 2010). These animal models encompass multiple possible etiologies, including genetic manipulation, perinatal infection or stress, and pharmacological insults (Rosen et al., 2015a). Altered neural oscillations have been proposed as a potential endophenotype observed in both animal models and human patients (Spellman and Gordon, 2015). Often these altered oscillations are directly linked to behavioral deficits. For example, impaired thalamic-prefrontal coherence correlates with deficits in working memory (Parnaudeau et al., 2013). Thus it is important to have better understanding of which neurotransmitter systems have a direct influence on gamma oscillation frequency and power.

Neuregulin 1 and neuregulin 2 are neurotrophic factors that activate the tyrosine kinase of ErbB receptors (Buonanno, 2010). Exogenous neuregulin 1β increases kainate-induced gamma oscillation power in hippocampal slices (Fisahn et al., 2009); however, this effect is not observed in the presence of the pan-ErbB antagonist PD158780, or in slices from full ErbB4 knockout mice (Fisahn et al., 2009). Additionally, over 50% of GABAergic PV+ interneurons, thought to be pivotal in the generation and maintenance

of gamma oscillations (Bartos et al., 2007), express ErbB4 receptors. These data make ErbB4 a likely candidate for the modulation of gamma oscillations. Moreover, in ErbB4 knockout mice, PV+ interneuron expression is ~31% lower than in wildtype animals, and kainate-induced gamma oscillations have ~60% less power (Fisahn et al., 2009). Furthermore, while ErbB4 receptors are expressed in most types of interneurons in a layer specific and region specific manner, these receptors have very low expression in somatostatin or calbindin positive neurons (Neddens and Buonanno, 2010). Interestingly, these same calbindin-expressing interneurons are mostly spared in the brains of SCZ patients, while many other interneuron types are reduced (Lewis et al., 2005), indicating that correct ErbB4 signaling may be important for the development of interneurons and preventing schizophrenia.

Mice with transgenic overexpression of NRG1 type 1 show hippocampus-specific working memory deficits in adulthood (Deakin et al., 2012) which may be related to deficits in neural synchrony. In hippocampal slices from these transgenic mice, the peak frequency of carbachol-induced gamma oscillations is reduced by ~4Hz without any significant change in power (Deakin et al., 2012). In this preparation, pyramidal neurons fired preferentially near the start of the gamma cycle (Deakin et al., 2012), and slices show a greater tendency towards epileptiform activity with 60% ending in epileptiform activity as compared to 9% of slices from wild-type mice ending in epileptiform activity (Deakin et al., 2012). This suggests that inhibitory neurotransmission in mice with transgenic overexpression of NRG1 type 1 is impaired.

Given the importance of understanding the connection between neuregulin and ErbB signaling pathways and the generation of gamma oscillations, other research groups have examined the effects of NRG1 and ErbB signaling *in vivo*. Mice with ErbB4 genetically removed from all interneurons show higher power in every frequency range from theta to gamma in the hippocampus during urethane-anesthesia recordings compared to littermate controls (del Pino et al., 2013). Gamma power was also increased in the infralimbic region of the prefrontal cortex of these genetically modified mice. Interestingly, when anesthetized using ketamine instead of urethane, 50% of the animals showed epileptic hypersynchrony (del Pino et al., 2013), similar to the increase in epileptiform activity observed in hippocampal slices from mice overexpressing NRG1 type 1 (Deakin et al., 2012). In awake behaving mice, gamma power was dramatically higher in mice lacking ErbB4 receptors in interneurons compared to their littermate controls, but all other frequency ranges were not different (del Pino et al., 2013). These mice also show cognitive deficits, paired-pulse inhibition deficits, and hyperactivity, which all may be related to changes in inhibitory neurotransmission and gamma synchrony. As in *in vitro* preparations, gamma oscillations can also be induced *in vivo* through the systemic injection of kainic acid. In wild type mice with kainic acid-induced gamma oscillations, an infusion of 6mM NRG1 into the lateral ventricle triples gamma power recorded from prefrontal EEG (Hou et al., 2014). Moreover, this increase is not observed in mice with genetic ablation of ErbB4 from interneurons, and kainic acid increased gamma power to a lesser extent in these mice (Hou et al., 2014). Hou and colleagues examined slices from the prefrontal cortex and observed an increase in

synchrony between pairs of pyramidal neurons, or pairs of interneurons after bath application of 5 or 10nM NRG1 (Hou et al., 2014). These changes in synchrony relied on intact GABAergic signaling and ErbB4 signaling, because neither effect was observed when recorded in the presence of the GABA receptor inhibitor picrotoxin, or in mice with genetic ablation of ErbB4 from interneurons (Hou et al., 2014).

Overall, both overexpression of NRG1 and underexpression of its receptor ErbB4 can modulate gamma oscillation power. Furthermore, both overexpressing NRG1 and genetic deletion of ErbB4 receptors on interneurons induces behavioral deficits (Agarwal et al., 2014; Deakin et al., 2012; del Pino et al., 2013; Shamir et al., 2012). While NRG1 and ErbB4 have both been implicated in schizophrenia (Mei and Xiong, 2008; Stefansson et al., 2002), it is unclear whether manipulation of this receptor system may have therapeutic effect in the treatment of the cognitive symptoms, or endophenotypes of schizophrenia, such as impaired gamma oscillations. To help clarify the role of ErbB receptors, in this study, I examine the effects of an antagonist that inhibits multiple ErbB receptors on gamma oscillation power before and after ketamine injection. The ketamine injection recapitulates the signal-to-noise problems in gamma oscillation power in a similar way to that observed in schizophrenia patients during sensory and cognitive tasks (Cho et al., 2006; Saunders et al., 2012).

4.2 Materials and Methods

All experimental procedures were conducted in accordance with the NIH Guide for Care and Use of Laboratory Animals and approved by NINDS Animal Care and Use Committee. We attempted to minimize the number of animals used and their discomfort.

4.2.1 Rats and behavioral paradigm

Male Long Evans rats (Charles River, Frederick, MD, USA), weighing 280–300 g, were housed with ad libitum access to chow and water in environmentally controlled conditions with a 12:12 h light:dark cycle (lights off at 9:00h). Rats were handled daily the week before surgery and trained to walk on a circular treadmill as previously described (Avila et al., 2010).

4.2.2 Surgical procedures

A single guide cannula attached to an electrode was implanted for recording LFP and spikes from the left prelimbic medial prefrontal cortex (mPFC). The cannula was placed so that when the infusion cannula was inserted into the guide cannula, the infusion would occur at the recording site. Rats were anesthetized with 75 mg/kg ketamine and 0.5 mg/kg medetomidine (intraperitoneal, i.p.) and placed in a stereotaxic frame (David Kopf Instruments, Tujunga, CA, USA), with head-fixed with atraumatic ear bars. Holes were drilled in the skull above the target coordinates for the mPFC (AP: +3.6 mm from the bregma, ML: +0.6 mm from the sagittal suture and DV: 3.6 mm from the skull surface). The electrode bundle consisted of 8 stainless steel teflon-insulated microwires plus an additional 9^{th} wire with no insulation on the distal ~1 mm of the recording tip with lower impedance serving as a local reference (Brazhnik et al., 2012; Delaville et al., 2015; Dupre et al., 2016). It was implanted in the target region and secured to the skull with screws and dental cement. A ground wires from the electrode was wrapped around a screw located above the cerebellum. After completion of surgery, 0.15% of ketoprofen in 0.9% NaCl solution was given subcutaneously (s.c.), and atipamezole (0.3-0.5 mg/kg,

s.c.) was administered to reverse the effect of medetomidine. During the first week of postoperative recovery, the rat's diet was supplemented with fruit and bacon treats. Rats were retrained at the circular treadmill walking task after the fourth postoperative day.

4.2.3 Behavioral analysis

A web camera (Logitech) was mounted next to the circular treadmill in order to provide behavioral data synchronized with the electrophysiological recordings. To quantify how the pan-ErbB antagonist affected ketamine-induced behaviors, an independent experimenter assessed the rodent's behavior using 50-second video epochs with treadmill-off and treadmill-on. Behavior with the treadmill-on was scored from before the ketamine injection (baseline) and 15 minutes after the ketamine injection, and behavior with the treadmill-off was scored from baseline and 13 minutes after the ketamine injection.

When the treadmill was off, the rat was inside the stationary circular treadmill track and the paddle was down so that it could not walk the treadmill freely. In this condition, untreated rats entered states of attentive or inattentive rest, but ketamine-treated rats were either hyperactive, or ataxic. To evaluate motor activity, we measured the number of seconds that the rat spent moving his trunk or limbs (but not its head). Ataxia was scored according to the following scale (adapted from Cho et al., 1991; Cui et al., 2014): (0) inactive or coordinated movements, (1) awkward or jerky movements or loss of balance while rearing, (2) frequent falling or partial impairment of antigravity reflexes, (3) the inability to move beyond a small area and to support body weight and (4) inability to move except for twitching movements. The stereotypic rating scale was also

adapted from (Cho et al., 1991). Briefly, we quantified the number of head-bobs, turns, and the number of seconds spent backpedaling. Head-bobs included side-to-side or vertical head movements, and turns involved a 180 degree turn so that the rat's direction in the treadmill had changed.

During treadmill-on epochs, an independent experimenter recorded the number of turns, the number of times that the rat hit the paddle, and the duration the rat spent being pushed by the paddle. Paddle hits counted for any of the rat's body parts other than the tip of his tail. Comparisons between baseline and ketamine treatment were made using paired t-tests for each behavioral measure.

2.4 Electrophysiological recordings

Extracellular spike and LFP recordings were collected for every experiment using Plexon (Dallas, TX) and Spike2 (CED, Cambridge, UK) systems as described in (Delaville et al., 2015). Both spikes and LFPs were referenced to the scraped 9^{th} wire. Spikes were sampled at 40kHz and LFPs were sampled at 2kHz. Action potentials were amplified (10,000x) and band pass filtered (0.3-8 kHz). LFPs were amplified (2000x) and band pass filtered (0.7-150 Hz). Discriminated spike and LFP signals were digitized, stored and analyzed using Spike2 data acquisition and analysis software.

Baseline recordings consisted of at least two five-minute epochs of counterclockwise walking and two 40 second epochs of inattentive rest without artifacts. After drug injections, the rat repeated a pattern of walking for 4 minutes and treadmill-off for one minute for the first 25 minutes, then the treadmill was turned off for the final 4 minutes before the next injection. Direct observation and videotaped motor behavior were

used to identify artifact-free 100-second intervals within the treadmill walking epochs and 40 to 100 second intervals from treadmill-off epochs. Any epoch of either behavior showing artifacts was excluded. The circular treadmill‘s speed was set at 9 to 11 rotations per minute.

2.5 Experimental conditions and drugs

Three of the five rats with proper electrode placement received cannula infusions of 10nM neuregulin 2 (source) diluted in ACSF seven days after surgery, and cannula infusions of sterile saline diluted in ACSF 10 days after surgery. The infusion volume was 400nL administered over 5 minutes, with one minute of rest before pulling out the infusion cannula. In the following three weeks, these rats received one of three pretreatments, saline (5mL), 5% DMSO (5mL), or 5mg/kg JNJ-28871063 dissolved in 5% DMSO thirty minutes prior to a 10mg/kg ketamine injection (at 1mL/kg, s.c.). A different drug was used each week and recordings were always more than 6 days apart. The order of pretreatments was randomized for each rat according to a latin-square design. Rats were anesthetized with 100mg/kg ketamine, followed by 0.15 mg medetomidine administered 30 minutes later, and then sacrificed. In one rat, the grounding electrode broke partway through the experimental recordings, so the intrabundle coherence and single neuron data was excluded from this rat after the break.

Two of the five rats with proper electrode placement received one of five pretreatments: 25% DMSO, 5mg/kg JNJ-28871063 dissolved in 25% DMSO, 3mg/kg A-412997, 5mg/kg L-745,870, 5mg/kg clozapine administered subcutaneously at ~1mL/kg. Thirty minutes after the pretreatment injection, 10mg/kg ketamine was injected (at

1mL/kg, s.c.) Recordings were performed one week apart. A different drug was used each week and the order of pretreatments was randomized for each rat according to a latin-square design. For both rats, the first recording used in this analysis was more than three weeks after the surgery, and the recordings were performed third and fifth in the order of pretreatments. Rats were given a cocktail of D1 and D2 antagonists prior to ketamine injection, then anesthetized using a total of 100mg/kg ketamine and 0.15mg medetomidine, then sacrificed.

2.6 Spectral analysis of local field potential recordings

LFP power was measured by fast Fourier transform (FFT) with a frequency resolution of ~1 Hz and normalized by dividing the power at each frequency by the sum of power between 250 and 300Hz in order to compensate for any instrumental fluctuations over time (Brazhnik et al., 2016). For each structure, total power in the low gamma (40-59Hz) and high gamma (70-120Hz) frequency ranges was calculated using a spike2 script. Additionally, if a significant peak was found between 40 and 70Hz, the power was summed from 7Hz below and above the peak to find the total low gamma power. A peak was considered significant if its relative maximum was greater than the surrounding 14 frequency bins in the low gamma range, the first derivative of the spectrum was positive to the left of the peak and negative to the right of the peak, and the second derivative at the peak was negative, indicating a downward concavity. LFP power from two wires per electrode bundle during two epochs was averaged for each behavioral condition.

To visualize spectral power changes over time for the selected epochs, time-frequency wavelet spectra were constructed using continuous wavelet transforms. The Morlet wavelet was applied to the LFPs using 128 frequency scales and a time resolution of approximately 750 ms (Time-Frequency Toolbox (http://tftb.nongnu.org).

In order to analyze the effects of the different drugs on the LFPs compared to baseline recordings, percent change from baseline walk in each frequency bin (for data visualization), or for each frequency range (for specific frequency range analysis) was used. Percent change was calculated using the formula:

$$Percent\ Change = \frac{P_{f,t} - P_{f,baseline}}{P_{f,baseline}} \times 100\%$$

P is power in the frequency range (f) at a given time (t). Outlier time points for power were removed using the ROUT (robust nonlinear regression combined with outlier removal) test with Q set to 1% (Motulsky and Brown, 2006) and the average of the other rats was used as a replacement value (Dupre et al., 2016).

The effects of various drug treatments on coherence and power over time within specific frequency ranges were assessed during treadmill walking using two-way repeated measures analysis of variance (ANOVA) following by Holm-Sidak's multiple comparisons with the level of significance: $\alpha = 0.05$.

2.7 Cell sorting and STWA analysis

Spike waveforms from the mPFC and the MD thalamus were sorted using principal component analysis (PCA) in Spike2. To assess effective sorting for single cells, inter-spike interval (ISI) histograms were generated and inspected to ensure that sorted cell clusters did not exhibit multiunit behavior by firing within the assumed

refractory period (1.2 ms). Putative pyramidal neurons and interneurons were separated using trough-to-peak intervals (Azouz et al., 1997; Brazhnik et al., 2012; Wilson et al., 1994). Units with trough-to-peak intervals greater than 0.5ms were classified as putative pyramidal neurons (19/20), and those with intervals less than 0.4ms were classified as interneurons (1/20). Given the low occurrence of interneurons in this data set, statistics could not be safely generalize from the behavior of this neuron to the entire population, so the behavior of this neuron is not reported.

To assess the temporal relationship between the spiking activity of individual neurons and LFPs from the same structure, spike-triggered waveform averages (STWA) were calculated for epochs of 100 to 200 seconds. LFPs from the recording wire or a neighboring wire were band-pass filtered between 40 and 59Hz. The coherence between each wire and every other wire in the frequency range of 40-59Hz was calculated during baseline walk. For each wire, the other wires were ranked from the wire with the most coherence to the least coherence. One of the two neighboring wires the wire within the electrode bundle with the maximum coherence to the wire on which the spike train was recorded. The second neighboring wire was selected by finding the wire with the median coherence to the wire on which the spike train was recorded. Peak-to-trough amplitudes of the STWAs at or around the spike (zero time) were obtained as a measure of correlation between the spike train and dominant gamma oscillation. Twenty shuffled STWAs for the same epochs were created by shuffling the interspike intervals of each spike train and used to create 20 normally distributed peak-to-trough values. The extent of correlation between spikes and gamma-filtered LFPs after ketamine or D4R drug

treatments during epochs of walking was compared to baseline walk epochs using the mean ratio of unshuffled/shuffled peak-to-trough amplitudes (mean STWA ratio). Comparisons of firing rate and mean STWA ratio between baseline and ketamine administration were assessed using repeated measures one-way ANOVAs with Holm-Sidak's multiple comparisons: $\alpha = 0.05$. Outlier neurons were removed using the ROUT (robust nonlinear regression combined with outlier removal) test with Q set to 0.1%(Motulsky and Brown, 2006).

4.2.8 Histology

After recordings were completed and the animal was anesthetized, recording sites were marked by passing a 10 μA positive current for 15-17 seconds via 3 microwires and 9 seconds via the reference electrode. Rats were perfused intracardially with 200 mL cold saline followed by 200 mL 4% paraformaldehyde in phosphate buffer solution (PBS). Brains were post-fixed in paraformaldehyde solution overnight and then immersed in 10% sucrose in phosphate buffered saline (0.1 M, pH 7.4) for 1 week. Coronal sections of 35 μm were collected on slides. Sections for electrode placement verification were mounted on glass slides and stained with cresyl violet and 5% potassium ferricyanide-9% HCl to reveal the iron deposited at the electrode tips. Rats were only included in the analysis if the electrodes were properly placed in the prelimbic mPFC, and gliosis around the cannula and electrode was not pervasive into the recording site.

4.3 Results

We attempted to examine the effects of both the activation and inhibition of ErbB receptors on low gamma power. However, technical difficulties related to the cannula

administration of NRG1β and NRG2 at the recording site precluded any reasonable analysis of ErbB4 activation. To determine the effects of NRG/ErbB inhibition on gamma oscillations, we systemically injected the pan-ErbB antagonist JNJ-28871063 (5mg/kg s.c.) 30 minutes before an injection of 10mg/kg ketamine. The pan-ErbB antagonist had no significant effect on low gamma power (peak between 40 and 70Hz ±7Hz) or high gamma power (70-120Hz) during treadmill walking (both $p>0.05$, RM two-way ANOVA, Fig4.2). However, after the pan-ErbB antagonist, ketamine significantly increased the low gamma power more than after the DMSO vehicle injection recorded fifteen minutes after the ketamine injection (representative examples in Fig4.1., Ket-DMSO: +125% from baseline vs. Ket JNJ: +235% from baseline, n= 5, $p<0.05$, Holm-Sidak's multiple comparisons test), This potentiation of ketamine's increase in gamma power was also observed 5 minutes after the ketamine injection (Ket-DMSO: + 144% of baseline vs. Ket JNJ: 287% of baseline, n= 5, $p<0.05$, Holm-Sidak's multiple comparisons test), but not 35 minutes after the ketamine injection ($p>0.05$, Holm-Sidak's multiple comparisons test, Fig4.2). Furthermore, no significant differences between drug treatments were observed in the high gamma frequency range ($p>0.05$, Holm-Sidak's multiple comparisons test, Fig4.2). Taken together, these results show that inhibiting ErbB signaling actually increases the effects of ketamine on low gamma power, suggesting that inhibition of ErbB receptors could either cause or potentially exacerbate the symptoms of schizophrenia.

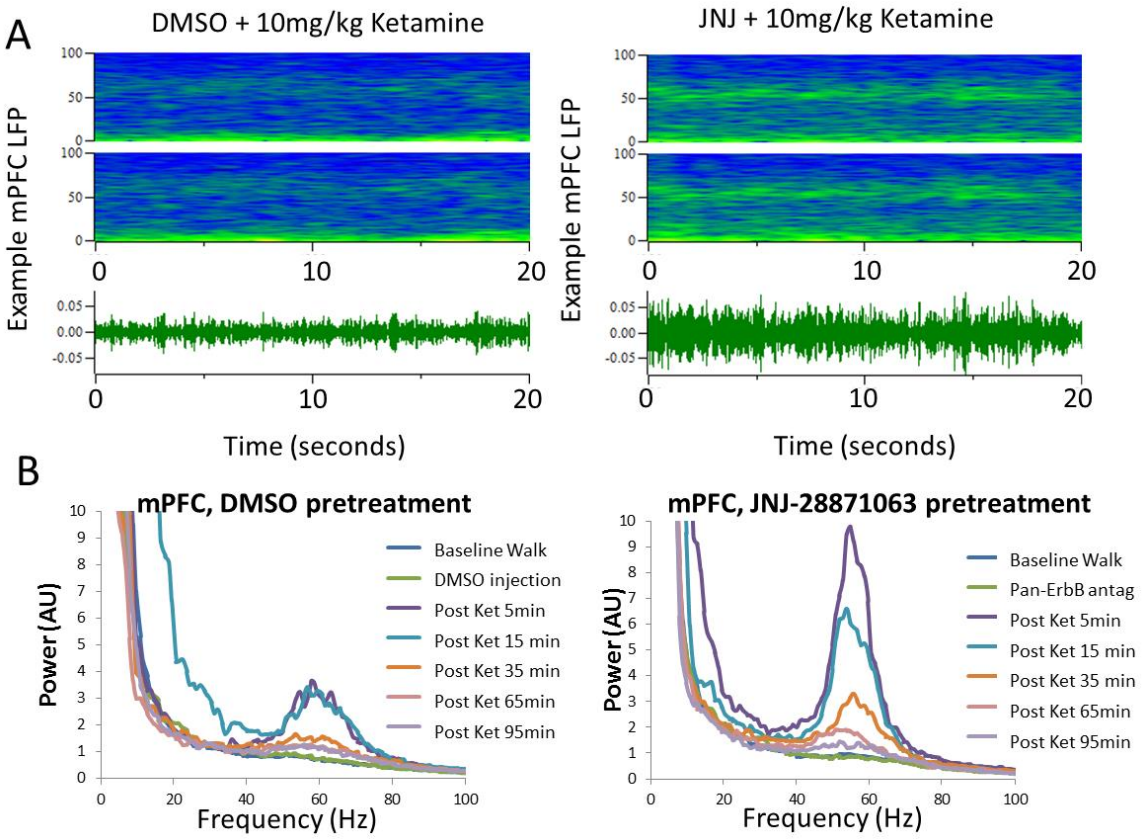

Figure 4.1. Representative example of the pan-ErbB antagonist potentiating ketamine-induced gamma power. (A) Representative power spectral density functions displayed over time from 15 minutes after 10mg/kg ketamine s.c. injection with DMSO pretreatment (**left**) and JNJ-28871063 (**right**) in two wires from the mPFC (**top**) from 0-100Hz. Note the narrow gamma band at 55Hz in each recording. Warmer colors indicate greater power. Gamma-filtered LFP waveform from 40-59Hz from the top channel in the figure (**bottom**). **(B)** Representative LFP power spectra in the mPFC for epochs with treadmill on at baseline (blue), 15 minutes after the DMSO (left) or JNJ injection (right, green), and 5, 15, 35, 65, and 95 minutes after the injection of ketamine.

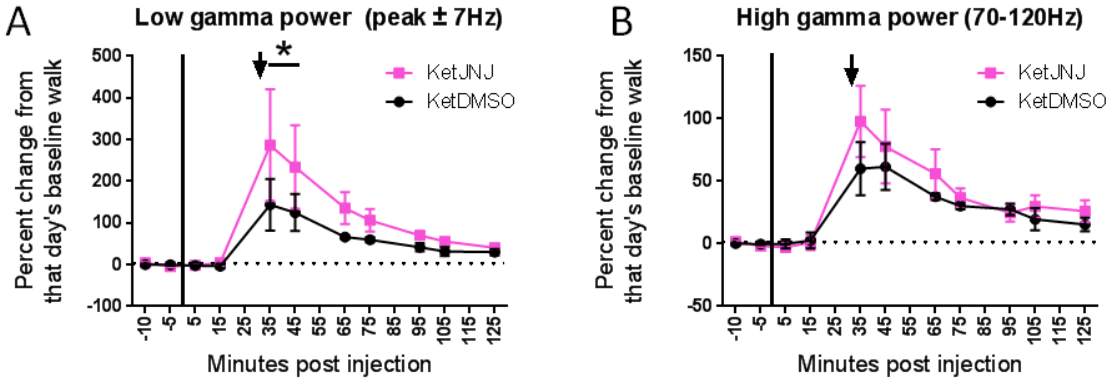

Figure 4.2. Pan-ErbB antagonist potentiates ketamine-induced gamma power (A) Percent change in gamma power (peak between 40-70Hz ±7Hz), and high gamma power (70-120Hz, **B**) in the mPFC of rats.

Black line indicates the injection of the pretreatment (5mg/kg JNJ-28871063 or DMSO), and black arrow indicates the injection of 10mg/kg ketamine. "Minutes post injection" indicates the time from the injection of the pretreatment. Pink curve shows the effect of the pan-ErbB antagonist and the black curve indicates the effect of DMSO (n=5 rats). The bar with the star indicates a significant change from baseline walking for every time point under the bar. Values are reported as mean ± SEM *:$p<0.05$, repeated measures one-way ANOVA with Tukey's multiple comparisons test.

To assess whether the pan-ErbB antagonist influenced ketamine-induced changes in firing rate, we examined neurons in the mPFC after each pretreatment. The pan-ErbB antagonist JNJ-28871063 reduced the average firing rates of pyramidal neurons in the mPFC by 23% during epochs of treadmill walking relative to epochs of treadmill walking before drug administration (1.11±0.24Hz vs. 1.44±0.31Hz, n=17, $p<0.05$, Dunnett's multiple comparisons test, Fig4.3). The diluted DMSO vehicle had no significant effect on the average firing rates of pyramidal neurons in the mPFC during treadmill walking ($p>0.05$, paired t-test). As described in Chapter 3, ketamine increases the firing rates of mPFC pyramidal neurons. Accordingly, ketamine increased the average firing rates of these neurons by 75% after the diluted DMSO vehicle injection (1.21±0.17Hz vs. 2.12±0.33Hz, n=17, $p<0.05$, Dunnett's multiple comparisons test, Fig4.3). Intriguingly, after pretreatment with the pan-ErbB antagonist, ketamine did not significantly increase the average firing rates of mPFC pyramidal neurons (+33%, $p>0.05$, paired t-test). This indicates that the pan-ErbB antagonist is capable of diminishing the effects of ketamine on single neurons *in vivo*. Seventy-five minutes after the ketamine injection, firing rates were not significantly different from baseline firing rates in either pretreatment condition (both $p>0.05$, Dunnett's multiple comparisons test).

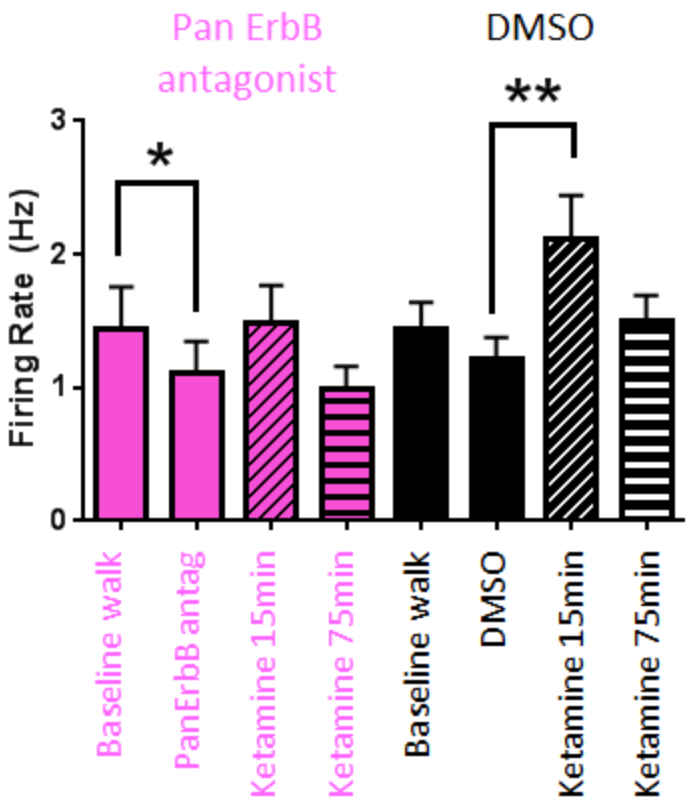

Figure 4.3. Pan-ErbB antagonist reduces baseline firing rates and reduces ketamine's effects on firing rates. Bar graph shows the mean and SEM of firing rates during the recordings from the pan-ErbB antagonist JNJ-28871063 (pink) and DMSO (black) pretreatments. The pretreatment values were measured 15 minutes after the injection. *: $p<0.05$, **: $p<0.01$, repeated-measures one-way ANOVA with Dunnett's multiple comparisons tests.

To investigate the spread of gamma oscillations around spiking neurons, the coherence between the wires within the bundle was examined. The coherence between each wire and every other wire in the frequency range of 40-59Hz was calculated during epochs of baseline walk, treadmill walking 15 minutes after the pretreatment injection, and treadmill walking 15 minutes after the ketamine injection. For each wire, the other wires were ranked from the wire with the most coherence to the least coherence. Overall, the coherence values of the maximum wire did not change before and after the pretreatments and ketamine injections (with one exception: pretreatment with JNJ: 0.76

was significantly lower than 15 minutes after ketamine: 0.82, $p<0.05$, Tukey's multiple comparisons, all other comparisons $p>0.05$). In contrast, the coherence values of each wire to the median wire significantly increased after ketamine with DMSO pretreatment (from an average of 0.46 to 0.52) and after ketamine with the pan-ErbB antagonist pretreatment (from 0.51 to 0.61, both $p<0.01$, Tukey's multiple comparisons). In summary, ketamine increases the gamma frequency coherence within the electrode bundle. Therefore, it appears that after ketamine, gamma oscillators influence the power and frequency of ongoing brain oscillations across a broader spatial scale than before ketamine treatment.

In Chapter 3, ketamine increased spike-gamma LFP correlations in the mPFC after saline pretreatments. However, after the dilute DMSO pretreatment, ketamine failed to significantly increase the spike-gamma LFP correlations in the recording wire, or either of two neighboring wires in the mPFC (Recording:+18%, Max: +16%, Median: +40% 15 minutes after ketamine vs. 15 minutes after pretreatment injection, n=17, all $p>0.05$, Holm-Sidak's multiple comparisons, Fig4.4). Furthermore, the pan-ErbB antagonist pretreatment had no obvious effect on spike-gamma LFP correlations referenced to the recording wire, or either of two neighboring wires in the mPFC (Recording:+2%, Max: +31%, Median: -26% 15 minutes after ketamine vs. 15 minutes after pretreatment injection, all $p>0.05$, Holm-Sidak's multiple comparisons). To directly compare the effect of the pan-ErbB antagonist pretreatment with the dilute DMSO vehicle, we computed the percent change in spike-gamma LFP correlation after ketamine injection relative to before the ketamine injection. There were no significant differences

in the percent change in spike-gamma LFP correlations between the pretreatment groups before or after ketamine, referenced to the recording wire (JNJ: +6% vs. DMSO: +44%) or one of two neighboring wires (Max JNJ: 57% vs. DMSO: +52%, Median JNJ: 42% vs. DMSO:57%, all $p>0.05$, Holm-Sidak's multiple comparisons, Fig4.4). Prior to ketamine injection, pyramidal neurons preferentially spiked in the falling phase of the gamma range LFP (~74% of all neurons, 148˚±15˚, $p<0.05$, Raleigh test). In contrast, after the ketamine injection, pyramidal neurons preferentially spiked in the ascending phase of the LFP (~64% of all neurons, 215˚±20˚, $p<0.05$, Raleigh test). These represented a significant shift in phase-preference after ketamine ($p<0.05$, Mardia-Watson Wheeler Test). In fact, 100% of the significantly correlated neurons spiked in the falling phase of the gamma range LFP before ketamine (n=1, phase preference = 148˚), and 100% of the significantly correlated neurons spiked in the ascending phase of the gamma LFP after ketamine (n= 4, phase preference = 312˚). Taken together, these data suggest that the DMSO pretreatment reduces the effects of ketamine on spike-gamma LFP correlation, and the pan-ErbB antagonist has little effect on spike synchronization to gamma oscillations. Furthermore, while the pan-ErbB antagonist increases ketamine-induced low gamma-power, the mechanism for this increase does not seem to involve local circuits of pyramidal neurons in the mPFC.

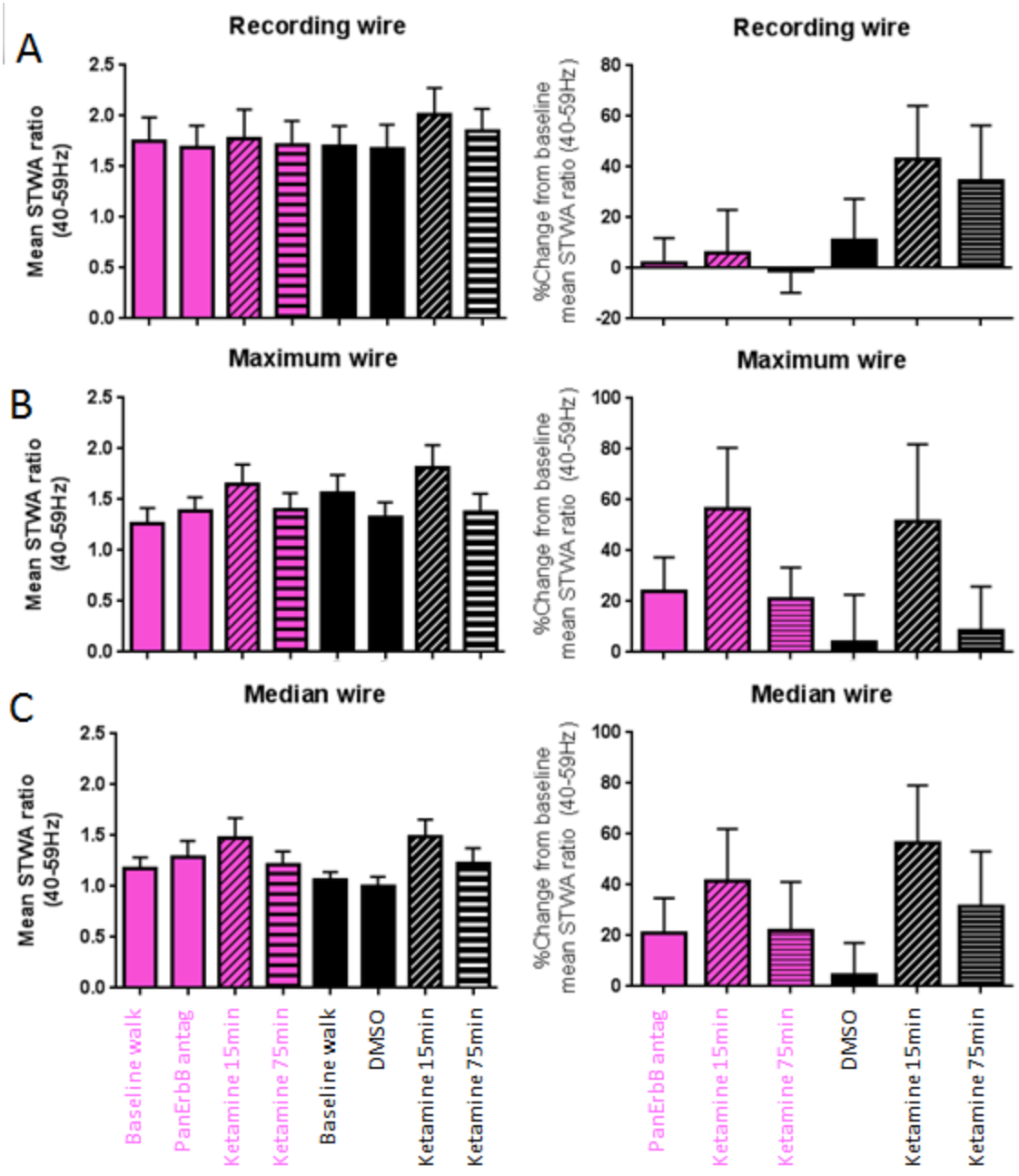

Figure 4.4. Pan-ErbB antagonist has no significant effect on spike-gamma LFP correlations. (Left) Mean ratios between peak to trough amplitudes of unshuffled/shuffled spike triggered waveform average (STWA) for LFPs recorded from the same wire (**A**) or the neighboring wire with maximum coherence in the bundle (**B**) or a neighboring wire with median coherence (**C**, see methods) filtered from 40-59Hz for mPFC pyramidal neurons. All pink bars are from the recording with the JNJ-28871063 pretreatment, and all black bars are from the DMSO vehicle pretreatment. The pretreatment measures were taken 15 minutes after the systemic injection of the DMSO or JNJ-28871063 injection. A ratio of 1 indicates no difference between shuffled and unshuffled values. (**Right**) For each neuron, the percent change from baseline mean

STWA ratio was calculated so that the different drug pretreatments could be directly compared. There were no significant differences in any of the groups tested.

4.4 Discussion

In the current study, I systemically administered a pan-ErbB antagonist and recorded from the mPFC of rats performing a treadmill walking task before and after an injection of ketamine that induces psychotomimetic effects. I analyzed the effects of ErbB antagonism on local field potentials and determined that ErbB antagonism potentiated the effects of ketamine on low gamma power, but not high gamma power. This confirmed previous results showing that NRG1 and ketamine administration only influenced low gamma power (Chapter 3, Fisahn et al., 2009). Given that ErbB4 is expressed selectively in interneurons (Vullhorst et al., 2009), and that genetic ablation of ErbB4 from interneurons increases hippocampal gamma power in awake behaving mice (del Pino et al., 2013), the increase in ketamine-induced gamma power was expected. Complicating this interpretation, however, is the fact that NRG1 infusion and therefore activation of ErbB4 receptors increases kainate-induced gamma power (Hou et al., 2014). One possibility is that endogenous NRG/ErbB signaling pathways are in homeostatic balance *in vivo,* so that either increasing or decreasing the activity of ErbB receptors will increase gamma power. Indeed it is important to remember that pan-ErbB antagonism had no significant influence on gamma power on its own. Together, these results demonstrate that either ErbB antagonism or NRG1 activation has the ability to increase chemically induced gamma power.

I also analyzed the activity of putative pyramidal neurons in the mPFC and observed that the pan-ErbB antagonist reduced the firing rates of these neurons compared

to baseline, unlike observations made from the hippocampus *in vitro* (Hou et al., 2014). The pan-ErbB antagonist also reduced the canonical ketamine-induced increase in the firing rate of pyramidal neurons such that it was no longer significantly different. In Chapter 3, I showed that ketamine increases the spike-gamma LFP correlation of mPFC pyramidal neurons. However, after DMSO or JNJ-28871063 pretreatment, this increase in synchronization was not observed in the recording wire or either of two neighboring wiResearch More work is needed to ascertain whether DMSO has a significant effect on the synchronization of mPFC pyramidal neurons to ongoing gamma oscillations.

A few key differences separate this study from previous studies. First, we recorded the LFP from chronically implanted electrodes in the mPFC so we could examine the differences between vehicle and pan-ErbB antagonist injections in the same animal, unlike the recordings made by Hou and colleagues (2014). Secondly, walking increases gamma oscillations, so we could examine the effects of the pan-ErbB antagonist on gamma oscillations in the absence of kainic acid or carbachol. To my knowledge, we were the first to observe the effects of pan-ErbB antagonism on physiological gamma power. Interestingly, ErbB4 deletion from interneurons increases gamma power (del Pino et al., 2013), whereas pan-ErbB antagonism had no significant effect on gamma power until ketamine was administered. Finally, most previous work has examined hippocampal oscillations evoked by carbachol or kainate *in vitro* (Andersson et al., 2012b; Deakin et al., 2012; Fisahn et al., 2009) whereas here I recorded *in vivo* from the mPFC, and examined both chemically induced oscillations, and physiologically induced oscillations.

The pan-ErbB antagonist reduced the firing rates of mPFC pyramidal neurons. In hippocampal and prefrontal slices, NRG1 increases the firing rates of PV+ interneurons (Li et al., 2012), but in cultured hippocampal neurons NRG1 decreases the firing rates of ErbB4-expressing interneurons (Janssen et al., 2012). Thus, ErbB antagonism may increase the firing rates of interneurons which in turn decreases the firing rates of mPFC pyramidal neurons. Unfortunately, we only recorded one interneuron, and this interneuron actually showed mild decreases in firing rate (<7%). Further investigations are needed to prove the involvement of interneurons. Moreover, the pan-ErbB antagonist is capable of reducing the effects of ketamine on pyramidal neuron firing rates *in vivo*. The mechanism underlying this effect remains unclear. JNJ-28871063 penetrates the blood brain barrier and inhibits the multiple ErbB receptors (Emanuel et al., 2008); therefore, it is possible that ErbB receptors other than ErbB4 are responsible for some of the changes observed after JNJ-28871063 administration. For instance ErbB2 and ErbB3 play important roles in myelination and behavior (Mei and Nave, 2014), although these have been rarely implicated in changing the activity of neurons. Furthermore, given that activation of ErbB4 can reduce NMDA currents (Vullhorst et al., 2015), inhibition of ErbB receptors may prevent the internalization of NMDA receptors at the synapse, allowing for more fully functional receptors after ketamine's noncompetitive antagonism. Finally, in Chapter 3, we observed that ketamine increased spike-gamma LFP correlations in the mPFC. In this study, we did not observe this increase after the pan-ErbB antagonist or DMSO. It is unclear how the DMSO administration could influence spike-gamma LFP correlations. Furthermore, because the same effect was observed with

the vehicle and the pan-ErbB antagonist, it is not safe to ascribe the reduction in ketamine-induced increases in spike-gamma LFP correlation to ErbB inhibition. Nevertheless, this data is similar to the finding that transgenic overexpression of NRG1 type 1 does not significantly influence the spike-gamma LFP correlation of pyramidal neurons from hippocampal slices with kainate-induced gamma oscillations (Hou et al., 2014). Although our results examine the inhibition of this NRG1/ErbB receptor system, instead of hyperactivation, we observed changes in firing rate, but not spike-gamma LFP correlation. Taken together, it appears that ErbB antagonism has unidirectional effects on firing rates, and no effect on spike-LFP correlations.

The mechanism underlying the potentiation of ketamine-induced gamma power after pan-ErbB antagonism is also unclear. NRG2 promotes ErbB4 clustering with GluN2B-containing NMDA receptors, followed by internalization of these receptors to decrease NMDA currents (Vullhorst et al., 2015). Similarly, ketamine antagonizes GluN2A and GluN2B containing NMDA receptors with equal affinity (Olney et al., 1999), and NMDAR antagonism increases gamma power. Therefore ErbB4 activation and not inhibition should potentiate ketamine-induced gamma oscillations. It is important to note that the real increase in gamma power may be related to GluN2A-containing NMDA receptors (Kocsis, 2012), or the relative contribution of AMPA currents to NMDA currents (see Chapter 1). Overall, these results indicate that the pan-ErbB antagonist does not seem to be a promising agent for the cognitive effects observed in schizophrenia because this drug does not reduce ketamine-induced gamma power (Anderson et al., 2014; Gilmour et al., 2012).

CHAPTER FIVE: Discussion

5.1 Major contributions of this thesis

Our work adds to the significant body of literature on the relationship between cortical gamma oscillations and attention (Benchenane et al., 2011; Cannon et al., 2014; Gregoriou et al., 2015). Low gamma power in the mPFC increased during treadmill walking, a task that requires attention. Similarly, low gamma power also increased in the mPFC after ketamine administration, which made our rats hyper vigilant. This corroborated findings by Guidi and colleagues (2015) that ketamine actually increases task attentiveness in rodents. Furthermore, we evaluated the utility of three novel agents to reduce ketamine-induced gamma power, and evaluated the utility of the acute ketamine model of schizophrenia (Gilmour et al., 2012). The importance of our findings, their interpretation and their relationship to existing data will be discussed below.

In Chapter 2, I administered a D4R agonist or D4R antagonist to slices from the dhCA1 or mPFC, and recorded inhibitory currents. I determined that D4R activation reduced miniature GABAR-mediated currents onto PV+ interneurons, D4R inhibition increased the frequency and amplitude of miniature GABAR-mediated currents onto pyramidal neurons, and D4R inhibition increased the intrinsic excitability of PV+ interneurons. These results suggest that endogenous dopamine activates D4Rs to restrain the intrinsic excitability of PV+ interneurons and lower the probability of GABA release onto pyramidal neurons. However, Rosen and colleagues observed that D4R activation increased excitatory glutamatergic currents onto PV+ interneurons (2015b), and Trantham-Davidson and colleagues observed that D4R activation increases the intrinsic

excitability of PV+ interneurons (2014). In these experiments, dopamine release was either stimulated optogenetically to simulate tonic dopamine signaling (Rosen et al., 2015b), or D4R agonists were bath applied at concentrations 200-400 times greater than the concentration that we used (Trantham-Davidson et al., 2014). Yet, aligning with these findings, activating D4Rs also reduced the inhibition onto PV+ interneurons (Chapter 2), which could potentially make these neurons more excitable. These results suggest that D4R activation is in homeostatic balance, and that increasing or decreasing its activation may increase the activity of PV+ interneurons to potentially increase gamma power. To test this hypothesis, we examined the effects of both the D4R agonist and antagonist on gamma oscillations *in vivo* in chapter 3. The agonist increased gamma power and the antagonist reversed this effect whether the animal was walking or not walking. However, neither effect was accompanied by firing rate changes *in vivo*. Therefore, even though the D4R agonist and antagonist both have effects *in vitro* that could result in increases in firing rates, and greater oscillatory power (Andersson et al., 2012b; Ceci et al., 1999; Onn et al., 2006; Trantham-Davidson et al., 2014), the agonist effectively increased gamma power, but the D4R antagonist only decreased gamma power if the D4R has been activated. The D4R is a G-protein coupled receptor that inhibits adenylyl cyclase to reduce cyclic-AMP (cAMP) production (Rondou et al., 2010). Because G-protein receptors use second messengers, the effects of the D4R activation can be expected to last minutes to hours. By inhibiting the D4R, other receptors may be able to couple to adenylyl cyclase and help restore basal levels of cAMP to reduce effects on gamma power. Interestingly, the D4R antagonist did not significantly decrease ketamine-induced

gamma power, even though ketamine increases extracellular dopamine concentrations (Moghaddam et al., 1997), and likely increases D4R activation. It follows that ketamine-induced gamma oscillations rely heavily on non-dopamine mediated mechanisms. As ketamine influences multiple receptors with different affinity (see Section 1.3.2), it is difficult to predict how ketamine influences second messenger systems. The primary mechanism underlying ketamine-induced gamma oscillations will be discussed in Section 5.4.

In chapter 3, anesthetic and subanesthetic doses of ketamine were administered to rats to examine the relationships between increases in gamma power and spiking activity in mPFC and MD thalamus. Gamma power increased substantially in both structures after ketamine administration. As observed previously, ketamine also increased the firing rate in the mPFC (Homayoun and Moghaddam, 2007a; Jackson et al., 2004), likely due to the increases in glutamatergic signaling through AMPARs after NMDAR antagonism (Maeng et al., 2008). We also observed an increase in the correlation between mPFC spiking and gamma oscillations. In contrast, in the MD thalamus, ketamine reduced the firing rate and correlation between spiking and gamma oscillations. This is likely a direct effect of removing NMDAR-mediated excitation from thalamic relay neurons. Due to the fact that ketamine-induced increases in gamma power, firing rate, and spike-LFP correlation in the mPFC were observed in conjunction with an increase in motor activity, we also examined the effects of motor activity and attention during a treadmill walking task. Treadmill walking alone also increased gamma power in the mPFC, as had been previously observed in our lab (Delaville et al., 2015), but to a lesser extent than after

ketamine administration. In the mPFC, walking concurrently increased the firing rates of pyramidal neurons and interneurons and increased synchronization between pyramidal neuron spikes and gamma oscillations. We added to the overall understanding of this walking-induced gamma by observing an increase in gamma power across a broader band in the MD thalamus during treadmill walking. Moreover, unlike the effect of ketamine in the MD thalamus, walking concurrently increased the firing rate and synchronization between spikes and gamma oscillations, suggesting a different circuit is responsible for increasing thalamic gamma power induced by walking compared to ketamine. In the MD thalamus, NMDAR mRNA expression is much greater than AMPAR mRNA expression within relay neurons (Salt and Eaton, 1996); therefore, after application of an NMDAR antagonist, these neurons become less excitable. Although extracellular glutamate levels still increase after ketamine, all of the AMPARs may quickly become occupied, preventing further changes in oscillatory activity. By contrast, during a treadmill walking task, the corticothalamic loop is important for sensory gating related to the rat's task performance (Guillery and Sherman, 2002).

As it has been proposed that a drug's ability to modulate gamma power might reflect its therapeutic potential (Anderson et al., 2014; Celada et al., 2013; Hudson et al., 2016; Jones et al., 2014; Ma and Leung, 2014), we examined the effects of two D4R-targeting drugs and a pan-ErbB antagonist on ketamine-induced gamma activity in Chapters 3 and 4. The D4R agonist and D4R antagonist significantly influenced neither ketamine-influenced gamma power nor ketamine-influenced firing rates in the mPFC. However, in the MD thalamus, the D4R agonist increased ketamine-induced gamma

power and modified neuronal firing rates. Furthermore, the pan-ErbB antagonist potentiated the effects of ketamine on low gamma power, but not high gamma power in the mPFC, while concurrently reducing ketamine's effects on firing rates. The pan-ErbB antagonist had no effect on gamma oscillations or single neuron activity before ketamine administration. This raises the question: why does exogenous NRG1/ErbB signaling affect chemically induced oscillations, as also observed by Hou and colleagues (2014), but not physiological oscillations? The most parsimonious explanation is that different neural circuits underlie chemically-induced gamma oscillations compared to walking-induced gamma oscillations, and our results fully support this hypothesis in the MD thalamus. In the mPFC, however, the story may be more complicated.

5.2 Comparison of gamma oscillations induced by walking and by ketamine administration

One of the main findings of this research is that gamma oscillations induced by walking and ketamine are similar in the mPFC and different in the MD thalamus. There is general consensus that there is ongoing rhythmic inhibition in the cortex that emerges from the activity of interneurons (Börgers et al., 2005; Ray, 2015). Almost any activation of interneurons can initiate rhythmic inhibition due to the highly interconnected nature of interneuronal networks (Bartos et al., 2007; Buzsaki and Wang, 2012; Cardin et al., 2009). In the mPFC, therefore, most gamma oscillations have local origins, even if the excitatory drive comes from afar, whereas in the MD thalamus, which in the rat lacks interneurons (Guillery and Sherman, 2002), most gamma power likely comes from synchronized activity projected from other locations (Tiesinga and Sejnowski, 2009).

Most previous work examining state-dependent gamma oscillations have focused on the primary motor and sensory cortices (for a review, see McGinley et al., 2015a), but our work focuses on the mPFC. Increases in arousal increase gamma band synchronization in both the relative membrane potential and local field potential power throughout the cortex (Delaville et al., 2015; Lee et al., 2014; McGinley et al., 2015b; Reimer et al., 2014; Vinck et al., 2015). These increases in power are accompanied by increases in gamma-frequency phase-locking in pyramidal neurons and interneurons (Munk et al., 1996; Vinck et al., 2015). This supports the predictions of the PING and ING compuational models showing that the spiking of pyramidal neurons and interneurons can produce gamma oscillations (Börgers et al., 2005). However, our results did not reveal significant increases in spike-gamma LFP correlations when the animal was completely aroused for the walking task compared to when the treadmill was off. This may be because we had less control over our periods of rest than some of the previous literature because we were not recording EMG and pupillometry to isolate periods of true quiet wakefulness. Therefore, periods of attentive rest, when spike-gamma correlations would already be high, may have contaminated the epochs that we used with the treadmill off, and therefore changes became harder to observe. Furthermore, a greater proportion of pyramidal neurons than interneurons were significantly correlated to gamma oscillations in the mPFC. This would support a model in which the firing of pyramidal neurons is potentially more important for the generation of gamma power than pyramidal neurons. Indeed, the amplitude of gamma oscillations depends in large part on the excitation of interneurons (Jadi et al., 2015), and the frequency is typically set by the

time constants of inhibitory current decay (Womelsdorf et al., 2014). Nevertheless, only one-third of our interneurons were significantly correlated to the ongoing gamma oscillation with the treadmill off, and though this percentage did not increase as the gamma power increased, these interneurons may be sufficient for the generation of gamma oscillations. Interneurons have less immediate influence on the voltage in a given location due to their small spherical soma shape as compared to the larger pyramidal somas which have a greater spatial distribution between the source and the sink (Einevoll et al., 2013).

We used spike-triggered waveform averages (STWAs) to measure the degree of spike correlation to LFPs. However, other studies examining arousal have used measures of pairwise phase consistency, or simple vector addition to determine spike-LFP relationships (Sigurdsson et al., 2010; Vinck et al., 2015). A few caveats of STWAs include the potential influence of extracellular transients related to the action potentials on the LFP, and the dependence on the frequency of the LFP band-pass filtering (Ray, 2015, my own observations). As the frequency range of the band-pass filtering increases, the probability that a spike train will significantly correlate with one of a frequencies within the band also increases. Finally, we have demonstrated repeatedly throughout this thesis that the patterns of spike-gamma LFP correlation change depending on which wire within the bundle is selected for the LFP. The wire from which the spike train was recorded consistently had higher spike-LFP correlations as measured by mean STWA ratio and the percentage of significantly correlated neurons compared to the neighboring wires with the maximum coherence or median coherence to the wire on which the spike

train was recorded. Therefore, STWAs may not be the most robust measure of spike-gamma LFP correlation, but actually reveal very fine-grained differences between LFPs across tens of microns.

Typically, reductions in delta frequency power, and increases in theta frequency power complement increases in gamma power induced by arousal (McGinley et al., 2015a). Interestingly, in humans, acute, subanesthetic ketamine increased gamma power and decreases delta power (Hong et al., 2010), supporting the hypothesis that gamma oscillations induced by arousal and acute, subanesthetic ketamine share a common mechanism. However, in some animal models, subanesthetic ketamine actually increased delta power (Kiss et al., 2011a, 2011b), which complicates this interpretation.

Finally, walking-induced gamma oscillations are dependent on intact dopamine neurotransmission (Delaville et al., 2015). Following a unilateral 6-hydroxydopamine lesion to the substantia nigra and most of the VTA, gamma, power no longer significantly increased during the treadmill walking task compared to the treadmill-off conditions (Delaville et al., 2015). Surprisingly, three weeks later, the walking-induced gamma band recovered, perhaps due to a compensatory mechanism (Delaville et al., 2015). Because the D4R has the highest affinity of all the dopamine receptors(Rondou et al., 2010) , we had predicted that dopamine signaling through the D4R would be responsible for the walking-induced increase gamma power. Therefore, we were surprised that the D4R antagonist had little effect on the walking-induced gamma power. Furthermore, the D4R antagonist increased the excitability of PV+ interneurons *in vitro*, which, according to the models (Jadi et al., 2015) should increase gamma power. Yet, this was not the case. It is

important to remember that endogenous dopamine is released in either tonic or phasic form, while D4R agonists and antagonists simply change the relative occupation of the different types of dopamine receptors. The importance of these two modes of signaling for understanding the data presented in this thesis will be discussed below.

5.3 Tonic versus phasic dopamine

NRG1/ErbB4R activation increased extracellular dopamine as detected by microdialysis (Kwon et al., 2008). The changes in dopamine concentration that can be detected by microdialysis better reflect the high tonic dopamine that activates D2-type receptors (Zheng et al., 1999) than the phasic dopamine that activates D1-type receptors (Zheng et al., 1999). *In vivo,* pharmacological activation of dopamine receptors using apomorphine, which mimics high tonic dopamine, enhanced gamma power slightly (<200%) and increased locomotion (Pinault, 2008). Although D4R activation increases gamma power *in vitro*, pharmacological activation of other dopamine receptors, or direct application of DA, had no effect on gamma power (Andersson et al., 2012b). In fact, when dopamine was applied simultaneously with the D1-type receptor blocker SCH23390, it increased gamma power *in vitro,* indicating that relative activity of D1-type receptors to D2-type receptors is critically important for generating gamma oscillations (Andersson et al., 2012b). Durstewitz and Seamans have proposed that imbalanced D1:D2-type receptor activation could be responsible for the cognitive, positive and negative symptoms observed in schizophrenia (2008). Mechanistically, low concentrations of bath-applied dopamine activate D1-type receptors which increase NMDAR-mediated currents whereas high concentrations of dopamine activate D2-type

receptors which decrease NMDAR-mediated currents (Yang and Seamans, 1996; Zheng et al., 1999). Bath applied dopamine acts more similarly to tonic extracellular dopamine, and until recently, it was difficult to mimic phasic dopamine release. However, optogenetic stimulation of dopaminergic fibers projecting through the hippocampus can induce a brief, and concentrated release of dopamine (Rosen et al., 2015b). These investigators determined that tonic dopamine increased the activity of PV+ interneurons via D4R receptors which in turn suppressed glutamatergic neurotransmission from the Schaeffer collateral pathway onto pyramidal neurons in the CA1 (Rosen et al., 2015b). In contrast, brief, highly concentrated dopamine release, simulating phasic dopamine increased glutamatergic neurotransmission in the Schaeffer collateral pathway via D1 receptor activation (Rosen et al., 2015b). As elaborated in section 1.2.1, patients with schizophrenia show reduced signal-to-noise ratios in terms of task-related gamma power. If tonic dopamine occupies a majority of the dopamine receptors at a given synapse, it can occlude the effects of phasic dopamine, which are related to salience and learning (Lauzon et al., 2009). Perhaps the deficits in signal-to-noise ratios could directly relate to the temporal signaling of dopamine. Overall, both the proportions of D1 and D4 receptor activation, as well as the proportion of tonic and phasic dopamine pathways are important to the excitation-inhibition balance, which underlies gamma oscillation generation. Just as individual notes, and the rhythm are equally important when playing the piano, both the timing of dopamine release, and the activation pattern of the various types of dopamine receptors are important for producing neuromodulation. Systemic drug administration, or bath application of dopamine are like playing the chords underneath

the music, and can obscure the melody if the melody requires hitting the same keys as those in the chords.

Dopamine D4R-targeting drugs have been proposed to have potential for treating cognitive deficits in schizophrenia (Furth et al., 2013); however, the present results found that these drugs show very limited ability to modulate ketamine-induced gamma activity. This raises the question: would these drugs really have little effect on cognition in schizophrenia patients, or is the acute ketamine model of schizophrenia not actually a useful tool for testing the cognitive benefits of pharmacological agents? Importantly, clinical trials to date have not supported the efficacy of the D4R antagonists as antipsychotics in the treatment of schizophrenia (Kramer et al., 1998; Bristow et al., 1998), so the lack of effect of the D4R-targeting drugs in modulating ketamine-induced gamma are not inconsistent with the use of this approach as a strategy for probing antipsychotic efficacy (Hudson et al., 2016; Jones et al., 2012). It remains to be seen whether the acute ketamine model has potential for developing treatments for the cognitive deficits related to schizophrenia, and if D4R-targeting drugs may still have pro-cognitive therapeutic potential in patients with schizophrenia.

5.4 Improvements over previous work and limitations

This thesis makes several improvements over existing literature. Firstly, using the treadmill walking task gives us better control over the rat's behavior than allowing the rat to roam freely in an open field (del Pino et al., 2013; Hakami et al., 2009). Secondly, by using chronic recording electrodes, each rat can be used in multiple recordings, and can become his own control. Our microelectrodes have finer spatial resolution than rodent

EEG and allowed us to simultaneously probe the activity of single neurons and local field potential (Delaville et al., 2015; Homayoun and Moghaddam, 2007b). We also developed a novel measure of attention by counting the number of times that the rat hits the paddle within the treadmill. Due to the fact that the rats became hyperactive as they improved at the treadmill-walking task it is hard to tease apart whether ketamine reduced the number of paddle hits by increasing attention, or simply by increasing the rat's activity. However, as the rat became more active, it increased its overall touching of the walls of the treadmill and decreased the number of times that it touched the paddle (Chapter 3). Therefore it is likely that the ketamine actually improved the rat's attention to the task, as had been observed previously by Guidi and colleagues (2015).

There are many animal models of the phenotypes present in schizophrenia, but we chose to use an acute, subanesthetic dose of ketamine to examine the effects of various drugs on gamma power. We had three key reasons for choosing this model: (1) This model has been used previously to test antipsychotic treatments (Anderson et al., 2014; Hudson et al., 2016; Jones et al., 2012, 2014; Ma and Leung, 2014). (2) This model has been well-established and is commonly used in both rodents and humans, yet the mechanisms underlying its effects are largely unknown (Frohlich and Van Horn, 2014; Kocsis et al., 2013). We hoped to increase the understanding of the mechanisms underlying this model, especially as ketamine is becoming more prevalent for the treatment of depression as well. (3) This model is easily reproducible and multiple experiments can be performed in the same rats, unlike after chronic NMDAR antagonist administration (Kittelberger et al., 2012; Wang et al., 2006). Whereas chronic ketamine

administration recapitulates more of the effects of chronic schizophrenia, such as parvalbumin depletion (Behrens et al., 2007; Kinney et al., 2006), acute ketamine mimics more of the diagnostic endophenotypes, such as cognitive, positive, and negative symptoms, and decreased signal to noise in gamma power (Cho et al., 2006; Hong et al., 2010; Krystal et al., 1994; Saunders et al., 2012). Furthermore, to my knowledge, there are no controlled studies of chronic ketamine use in humans, perhaps due to ethical considerations. As such data from the acute ketamine model in rodents can directly inform hypotheses about acute ketamine in humans, whereas the chronic ketamine model does not directly relate to human studies. Furthermore, there is also a multitude of genetic models of the phenotypes present schizophrenia (Rosen et al., 2015a), but these studies are limited to one specific etiology, and are restricted by breeding capacity, and species. Genetic models are typically generated in mice and all of our equipment was designed for rats.

5.5 A unifying hypothesis for mechanisms underlying increased gamma power

To conclude this thesis I will attempt to bring together the evidence reviewed in Chapter 1 and experimental results from chapters 3 and 4 into a coherent theory on how ketamine, D4R activation, and ErbB4R activation all increase cortical gamma oscillations.

I propose that increasing the synaptic AMPA/NMDA current ratio increases cortical gamma power, specifically by decreasing NMDAR activity. Activation of ErbB4Rs and D4Rs both promote the internalization of NMDARs (Beazely et al., 2006; Vullhorst et al., 2015). The two predominant types of NMDARs in the adult

hippocampus and prefrontal cortex are those that contain NR2A and NR2B subunits. NMDARs with NR2A subunits have faster deactivation kinetics than NMDARs with NR2B subunits (Kim et al., 2005), and AMPAR s have the fastest decay kinetics. Notably, ErbB4R activation decreases NR2B-containing NMDAR-mediated currents (Vullhorst et al., 2015), and D4R activation reduces long-term potentiation of AMPAR-mediated currents via a NR2B-containing NMDAR mediated mechanism (Herwerth et al., 2012). NR2B-containing NMDARs are typically extrasynaptic (although they can move to the synapse during LTP and LTD, and are also synaptic in early postnatal development), and are not responsible for increasing gamma power, or extracellular glutamate when antagonized (Jiménez-Sánchez et al., 2014; Kocsis, 2012; Miller et al., 2016). NR2B and NR2A have opposite effects on the surface expression of AMPARs as well: NR2A-NMDARs promote the surface expression of GluR1 whereas NR2B-NMDARs inhibit GluR1 surface expression (Kim et al., 2005). Thus, by internalizing NR2B-NMDARs, more AMPARs can stably remain at the membrane. NMDAR antagonists also appear to increase gamma power by increasing the AMPA/NMDA current ratio. NMDAR antagonists excite pyramidal neurons (Jackson et al., 2004) by elevating extracellular glutamate transmission through AMPARs (Maeng et al., 2008). Inhibiting NR2A-NMDARs also increases extracellular glutamate and gamma power (Jiménez-Sánchez et al., 2014; Kocsis, 2012). Additionally, ketamine increases AMPAR-mediated currents in hippocampal slices (Nosyreva et al., 2013). Finally, AMPAR signaling is essential for gamma oscillations, as NMDAR antagonists have little effect on gamma power in the presence of an AMPAR antagonist (Zanos et al., 2016).

If the AMPA/NMDA current ratio is pivotal for setting gamma power, and the D4R agonist augments gamma power by reducing NMDAR-mediated currents in hippocampal pyramidal neurons (Beazely et al., 2006) and prefrontal cortical pyramidal neurons (Trantham-Davidson et al., 2014; Wang et al., 2003, 2006), then D4R agonists would have little to no effect on gamma oscillations after ketamine administration, since this pharmacological manipulation already increased the AMPA/NMDA current ratio. Indeed, the D4R agonist did not increase gamma power after an NMDAR antagonist *in vitro* (Andersson et al., 2012a), nor *in vivo* (Chapter 3). Along these lines, acute or chronic treatment with the NMDAR antagonist phencyclidine blocked the effect of the D4R on NMDARs in cortical pyramidal neurons (Wang et al., 2006). Interestingly, inhibiting the D4R increased evoked NMDAR-mediated currents in pyramidal neurons of the hippocampus (Kotecha et al., 2002), indicating that the D4R has a small ongoing effect that can increase with increased receptor activation. To my knowledge, no one has studied the effects of D4R activation on NMDAR-mediated currents in PV+ interneurons. Moreover, it remains unclear whether modulation of NMDAR or AMPAR-mediated currents must occur in pyramidal neurons, fast-spiking interneurons, or combinations of these neuronal types to generate changes in local field potentials. Previous work has examined the effects of NMDAR antagonism on mice with interneuron-specific deletion of NMDARs (Belforte et al., 2010; Korotkova et al., 2010). However, this fails to account for secondary effects, such as the extracellular increase in glutamate over a longer time scale. In future experiments, glutamate uncaging could be coupled with mice with cell-type specific ablation of NMDARs to determine whether the AMPA/NMDA

current ratio in PV+ interneurons, pyramidal neurons, or both types of neurons is important for determining the power of gamma oscillations.

BIBLIOGRAPHY

Aalto, S., Ihalainen, J., Hirvonen, J., Kajander, J., Scheinin, H., Tanila, H., Någren, K., Vilkman, H., Gustafsson, L.L., Syvälahti, E., et al. (2005). Cortical glutamate-dopamine interaction and ketamine-induced psychotic symptoms in man. Psychopharmacology (Berlin) *182*, 375–383.

Abdallah, C.G., Sanacora, G., Duman, R.S., and Krystal, J.H. (2015). Ketamine and Rapid-Acting Antidepressants: A Window into a New Neurobiology for Mood Disorder Therapeutics. Annual Review of Medicine *66*, 509–523.

Acosta-García, J., Hernández-Chan, N., Paz-Bermúdez, F., Sierra, A., Erlij, D., Aceves, J., and Florán, B. (2009). D4 and D1 dopamine receptors modulate [3H]GABA release in the substantia nigra pars reticulata of the rat. Neuropharmacology *57*, 725–730.

Agarwal, A., Zhang, M., Trembak-Duff, I., Unterbarnscheidt, T., Radyushkin, K., Dibaj, P., Martins de Souza, D., Boretius, S., Brzózka, M.M., Steffens, H., et al. (2014). Dysregulated expression of neuregulin-1 by cortical pyramidal neurons disrupts synaptic plasticity. Cell Reports *8*, 1130–1145.

Agim, Z.S., Esendal, M., Briollais, L., Uyan, O., Meschian, M., Martinez, L.A.M., Ding, Y., Basak, A.N., and Ozcelik, H. (2013). Discovery, validation and characterization of Erbb4 and Nrg1 haplotypes using data from three genome-wide association studies of schizophrenia. PloS One *8*, e53042.

Ahveninen, J., Kähkönen, S., Tiitinen, H., Pekkonen, E., Huttunen, J., Kaakkola, S., Ilmoniemi, R.J., and Jääskeläinen, I.P. (2000). Suppression of transient 40-Hz auditory response by haloperidol suggests modulation of human selective attention by dopamine D2 receptors. Neuroscience Letters *292*, 29–32.

de Almeida, J., and Mengod, G. (2010). D2 and D4 dopamine receptor mRNA distribution in pyramidal neurons and GABAergic subpopulations in monkey prefrontal cortex: implications for schizophrenia treatment. Neuroscience *170*, 1133–1139.

de Almeida, J., Palacios, J.M., and Mengod, G. (2008). Distribution of 5-HT and DA receptors in primate prefrontal cortex: implications for pathophysiology and treatment. Progress in Brain Research *172*, 101–115.

Amat, J., Dolzani, S.D., Tilden, S., Christianson, J.P., Kubala, K.H., Bartholomay, K., Sperr, K., Ciancio, N., Watkins, L.R., and Maier, S.F. (2016). Previous Ketamine Produces an Enduring Blockade of Neurochemical and Behavioral Effects of Uncontrollable Stress. Journal of Neuroscience *36*, 153–161.

Andersen, S.L., Thompson, A.T., Rutstein, M., Hostetter, J.C., and Teicher, M.H. (2000). Dopamine receptor pruning in prefrontal cortex during the periadolescent period in rats. Synapse *37*, 167–169.

Anderson, P.M., Pinault, D., O'Brien, T.J., and Jones, N.C. (2014). Chronic administration of antipsychotics attenuates ongoing and ketamine-induced increases in cortical γ oscillations. International Journal of NeuropsychoPharmacology Official Scientific Journal Collective International Neuropsychopharmacology CINP *17*, 1895–1904.

Andersson, R., Johnston, A., and Fisahn, A. (2012a). Dopamine D4 Receptor Activation Increases Hippocampal Gamma Oscillations by Enhancing Synchronization of Fast-Spiking Interneurons. PLoS ONE *7*, e40906.

Andersson, R.H., Johnston, A., Herman, P.A., Winzer-Serhan, U.H., Karavanova, I., Vullhorst, D., Fisahn, A., and Buonanno, A. (2012b). Neuregulin and dopamine modulation of hippocampal gamma oscillations is dependent on dopamine D4 receptors. Proceedings of the National Academy of Science U. S. A. *109*, 13118–13123.

Angulo, M.C., Rossier, J., and Audinat, E. (1999). Postsynaptic glutamate receptors and integrative properties of fast-spiking interneurons in the rat neocortex. Journal of Neurophysiology *82*, 1295–1302.

Anticevic, A., Gancsos, M., Murray, J.D., Repovs, G., Driesen, N.R., Ennis, D.J., Niciu, M.J., Morgan, P.T., Surti, T.S., Bloch, M.H., et al. (2012). NMDA receptor function in large-scale anticorrelated neural systems with implications for cognition and schizophrenia. Proceedings of the National Academy of Science U. S. A. *109*, 16720–16725.

Anticevic, A., Corlett, P.R., Cole, M.W., Savic, A., Gancsos, M., Tang, Y., Repovs, G., Murray, J.D., Driesen, N.R., Morgan, P.T., et al. (2015). N-methyl-D-aspartate receptor antagonist effects on prefrontal cortical connectivity better model early than chronic schizophrenia. Biological Psychiatry *77*, 569–580.

APA (1994). Diagnostic and statistical manual of mental disorders : DSM-IV (Washington, DC: American Psychiatric Association).

Arcos-Burgos, M., Castellanos, F.X., Konecki, D., Lopera, F., Pineda, D., Palacio, J.D., Rapoport, J.L., Berg, K., Bailey-Wilson, J., and Muenke, M. (2004). Pedigree disequilibrium test (PDT) replicates association and linkage between DRD4 and ADHD in multigenerational and extended pedigrees from a genetic isolate. Molecular Psychiatry *9*, 252–259.

Ariano, M.A., Wang, J., Noblett, K.L., Larson, E.R., and Sibley, D.R. (1997). Cellular distribution of the rat D4 dopamine receptor protein in the CNS using anti-receptor antisera. Brain Research *752*, 26–34.

Arnsten, A.F.T., Murphy, B., and Merchant, K. (2000). The selective dopamine D4 receptor antagonist, PNU-101387G, prevents stress-induced cognitive deficits in monkeys. Neuropsychopharmacology *23*, 405–410.

Asaumi, Y., Hasuo, H., and Akasu, T. (2006). Dopamine Presynaptically Depresses Fast Inhibitory Synaptic Transmission via D4 Receptor-Protein Kinase A Pathway in the Rat Dorsolateral Septal Nucleus. Journal of Neurophysiology *96*, 591–601.

Asghari, V., Sanyal, S., Buchwaldt, S., Paterson, A., Jovanovic, V., and Van Tol, H.H.M. (1995). Modulation of intracellular cyclic AMP levels by different human dopamine D4 receptor variants. Journal of Neurochemistry *65*, 1157–1165.

Autry, A.E., Adachi, M., Nosyreva, E., Na, E.S., Los, M.F., Cheng, P., Kavalali, E.T., and Monteggia, L.M. (2011). NMDA receptor blockade at rest triggers rapid behavioural antidepressant responses. Nature *475*, 91–95.

Avale, M.E., Falzone, T.L., Gelman, D.M., Low, M.J., Grandy, D.K., and Rubinstein, M. (2004). The dopamine D4 receptor is essential for hyperactivity and impaired behavioral inhibition in a mouse model of attention deficit/hyperactivity disorder. Molecular Psychiatry *9*, 718–726.

Avila, I., Parr-Brownlie, L.C., Brazhnik, E., Castañeda, E., Bergstrom, D.A., and Walters, J.R. (2010). Beta frequency synchronization in basal ganglia output during rest and walk in a hemiparkinsonian rat. Experimental Neurology *221*, 307–319.

Axmacher, N., Mormann, F., Fernández, G., Elger, C.E., and Fell, J. (2006). Memory formation by neuronal synchronization. Brain Research Review *52*, 170–182.

Azdad, K., Piet, R., Poulain, D.A., and Oliet, S.H.R. (2003). Dopamine D4 receptor-mediated presynaptic inhibition of GABAergic transmission in the rat supraoptic nucleus. Journal of Neurophysiology *90*, 559–565.

Azouz, R., Gray, C.M., Nowak, L.G., and McCormick, D.A. (1997). Physiological properties of inhibitory interneurons in cat striate cortex. Cerebral Cortex *7*, 534–545.

Baimoukhametova, D.V., Hewitt, S.A., Sank, C.A., and Bains, J.S. (2004). Dopamine Modulates Use-Dependent Plasticity of Inhibitory Synapses. Journal of Neuroscience *24*, 5162–5171.

Baldessarini, R.J., and Frankenburg, F.R. (1991). Clozapine. A novel antipsychotic agent. New England Journal of Medicine *324*, 746–754.

Barr, C.L., Wigg, K.G., Bloom, S., Schachar, R., Tannock, R., Roberts, W., Malone, M., and Kennedy, J.L. (2000). Further evidence from haplotype analysis for linkage of the dopamine D4 receptor gene and attention-deficit hyperactivity disorder. American Journal of Medical Genetics *96*, 262–267.

Barr, M.S., Farzan, F., Tran, L.C., Chen, R., Fitzgerald, P.B., and Daskalakis, Z.J. (2010). Evidence for excessive frontal evoked gamma oscillatory activity in schizophrenia during working memory. Schizophrenia Research *121*, 146–152.

Barros, C.S., Calabrese, B., Chamero, P., Roberts, A.J., Korzus, E., Lloyd, K., Stowers, L., Mayford, M., Halpain, S., and Müller, U. (2009). Impaired maturation of dendritic spines without disorganization of cortical cell layers in mice lacking NRG1/ErbB signaling in the central nervous system. Proceedings of the National Academy of Science U. S. A. *106*, 4507–4512.

Bartos, M., Vida, I., and Jonas, P. (2007). Synaptic mechanisms of synchronized gamma oscillations in inhibitory interneuron networks. Nature Reviews Neuroscience *8*, 45–56.

Basar-Eroglu, C., Brand, A., Hildebrandt, H., Karolina Kedzior, K., Mathes, B., and Schmiedt, C. (2007). Working memory related gamma oscillations in schizophrenia patients. International Journal of Psychophysiology *64*, 39–45.

Bean, B.P. (2007). The action potential in mammalian central neurons. Nature Reviews Neuroscience *8*, 451–465.

Beaulieu, J.-M., and Gainetdinov, R.R. (2011). The Physiology, Signaling, and Pharmacology of Dopamine Receptors. Pharmacology Review *63*, 182–217.

Beazely, M.A., Tong, A., Wei, W.-L., Van Tol, H., Sidhu, B., and MacDonald, J.F. (2006). D2-class dopamine receptor inhibition of NMDA currents in prefrontal cortical neurons is platelet-derived growth factor receptor-dependent. Journal of Neurochemistry *98*, 1657–1663.

Behrens, M.M., Ali, S.S., Dao, D.N., Lucero, J., Shekhtman, G., Quick, K.L., and Dugan, L.L. (2007). Ketamine-induced loss of phenotype of fast-spiking interneurons is mediated by NADPH-oxidase. Science *318*, 1645–1647.

Belforte, J.E., Zsiros, V., Sklar, E.R., Jiang, Z., Yu, G., Li, Y., Quinlan, E.M., and Nakazawa, K. (2010). Postnatal NMDA receptor ablation in corticolimbic interneurons confers schizophrenia-like phenotypes. Nature Neuroscience *13*, 76–83.

Belujon, P., and Grace, A.A. (2014). Restoring mood balance in depression: ketamine reverses deficit in dopamine-dependent synaptic plasticity. Biological Psychiatry *76*, 927–936.

Benchenane, K., Tiesinga, P.H., and Battaglia, F.P. (2011). Oscillations in the prefrontal cortex: a gateway to memory and attention. Current Opinions in Neurobiology *21*, 475–485.

Bender, K.J., Ford, C.P., and Trussell, L.O. (2010). Dopaminergic Modulation of Axon Initial Segment Calcium Channels Regulates Action Potential Initiation. Neuron *68*, 500–511.

Benes, F.M., and Berretta, S. (2001). GABAergic interneurons: implications for understanding schizophrenia and bipolar disorder. Neuropsychopharmacology *25*, 1–27.

Benes, F.M., Taylor, J.B., and Cunningham, M.C. (2000). Convergence and plasticity of monoaminergic systems in the medial prefrontal cortex during the postnatal period: implications for the development of psychopathology. Cerebral Cortex *10*, 1014–1027.

Beneyto, M., and Lewis, D.A. (2011). Insights into the neurodevelopmental origin of schizophrenia from postmortem studies of prefrontal cortical circuitry. International Journal of Developmental Neuroscience *29*, 295–304.

Bentivoglio, M., and Morelli, M. (2005). The organization and circuits of mesencephalic dopaminergic neurons and the distribution of dopamine receptors in the brain. Handbook of Chemical Neuroanatomy *21*, 1–107.

Berger, B., Verney, C., Febvret, A., Vigny, A., and Helle, K.B. (1985). Postnatal ontogenesis of the dopaminergic innervation in the rat anterior cingulate cortex (area 24). Immunocytochemical and catecholamine fluorescence histochemical analysis. Developmental Brain Research *21*, 31–47.

Berger, B., Gaspar, P., and Verney, C. (1991). Dopaminergic innervation of the cerebral cortex: unexpected differences between rodents and primates. Trends in Neuroscience *14*, 21–27.

Berman, R.M., Cappiello, A., Anand, A., Oren, D.A., Heninger, G.R., Charney, D.S., and Krystal, J.H. (2000). Antidepressant effects of ketamine in depressed patients. Biological Psychiatry *47*, 351–354.

Bernaerts, P., and Tirelli, E. (2003). Facilitatory effect of the dopamine D4 receptor agonist PD168,077 on memory consolidation of an inhibitory avoidance learned response in C57BL/6J mice. Behavioral Brain Research *142*, 41–52.

Björklund, A., and Dunnett, S.B. (2007). Dopamine neuron systems in the brain: an update. Trends in Neuroscience *30*, 194–202.

Blot, K., Kimura, S.-I., Bai, J., Kemp, A., Manahan-Vaughan, D., Giros, B., Tzavara, E., and Otani, S. (2015). Modulation of hippocampus-prefrontal cortex synaptic transmission and disruption of executive cognitive functions by MK-801. Cerebral Cortex N. Y. N 1991 *25*, 1348–1361.

Bokil, H., Purpura, K., Schoffelen, J.-M., Thomson, D., and Mitra, P. (2007). Comparing spectra and coherences for groups of unequal size. Journal of Neuroscience Methods *159*, 337–345.

Börgers, C., Epstein, S., and Kopell, N.J. (2005). Background gamma rhythmicity and attention in cortical local circuits: A computational

study. Proceedings of the National Academy of Science U. S. A. *102*, 7002–7007.

Borisovska, M., Bensen, A.L., Chong, G., and Westbrook, G.L. (2013). Distinct Modes of Dopamine and GABA Release in a Dual Transmitter Neuron. Journal of Neuroscience *33*, 1790–1796.

Borroto-Escuela, D.O., Craenenbroeck, K.V., Romero-Fernandez, W., Guidolin, D., Woods, A.S., Rivera, A., Haegeman, G., Agnati, L.F., Tarakanov, A.O., and Fuxe, K. (2011). Dopamine D2 and D4 receptor heteromerization and its allosteric receptor–receptor interactions. Biochemical and Biophysical Research Communications *404*, 928–934.

Brazhnik, E., Cruz, A.V., Avila, I., Wahba, M.I., Novikov, N., Ilieva, N.M., McCoy, A.J., Gerber, C., and Walters, J.R. (2012). State-Dependent Spike and Local Field Synchronization between Motor Cortex and Substantia Nigra in Hemiparkinsonian Rats. Journal of Neuroscience *32*, 7869–7880.

Brazhnik, E., McCoy, A.J., Novikov, N., Hatch, C.E., and Walters, J.R. (2016). Ventral Medial Thalamic Nucleus Promotes Synchronization of Increased High Beta Oscillatory Activity in the Basal Ganglia-Thalamocortical Network of the Hemiparkinsonian Rat. Journal of Neuroscience *36*, 4196–4208.

Brenhouse, H.C., Sonntag, K.C., and Andersen, S.L. (2008). Transient D1 Dopamine Receptor Expression on Prefrontal Cortex Projection Neurons: Relationship to Enhanced Motivational Salience of Drug Cues in Adolescence. Journal of Neuroscience *28*, 2375–2382.

Brinkmann, B.G., Agarwal, A., Sereda, M.W., Garratt, A.N., Müller, T., Wende, H., Stassart, R.M., Nawaz, S., Humml, C., Velanac, V., et al. (2008). Neuregulin-1/ErbB signaling serves distinct functions in myelination of the peripheral and central nervous system. Neuron *59*, 581–595.

Bristow, L.J., Kramer, M.S., Kulagowski, J., Patel, S., Ragan, C.I., and Seabrook, G.R. (1997). Schizophrenia and L-745, 870, a novel dopamine D4 receptor antagonist. Trends in Pharmacology Science *18*, 186–188.

Broderick, P.A., and Piercey, M.F. (1998). Clozapine, haloperidol, and the D4 antagonist PNU-101387G: in vivo effects on mesocortical, mesolimbic, and nigrostriatal dopamine and serotonin release. Journal of Neural Transmission *105*, 749–767.

Bromberg-Martin, E.S., Matsumoto, M., and Hikosaka, O. (2010). Dopamine in motivational control: rewarding, aversive, and alerting. Neuron *68*, 815.

Browman, K.E., Curzon, P., Pan, J.B., Molesky, A.L., Komater, V.A., Decker, M.W., Brioni, J.D., Moreland, R.B., and Fox, G.B. (2005). A-412997, a selective dopamine D4 agonist, improves cognitive performance in rats. Pharmacological and Biochemical Behavior *82*, 148–155.

Brozoski, T.J., Brown, R.M., Rosvold, H.E., and Goldman, P.S. (1979). Cognitive deficit caused by regional depletion of dopamine in prefrontal cortex of rhesus monkey. Science *205*, 929–932.

Buonanno, A. (2010). The neuregulin signaling pathway and schizophrenia: from genes to synapses and neural circuits. Brain Research Bulletin *83*, 122–131.

Buonanno, A., and Fischbach, G.D. (2001). Neuregulin and ErbB receptor signaling pathways in the nervous system. Current Opinions in Neurobiology *11*, 287–296.

Buzsaki, G., and Wang, X.J. (2012). Mechanisms of gamma oscillations. Annual Review of Neuroscience *35*, 203–225.

Buzsáki, G., Anastassiou, C.A., and Koch, C. (2012). The origin of extracellular fields and currents — EEG, ECoG, LFP and spikes. Nature Reviews Neuroscience *13*, 407–420.

Cahill, M.E., Jones, K.A., Rafalovich, I., Xie, Z., Barros, C.S., Müller, U., and Penzes, P. (2012). Control of interneuron dendritic growth through NRG1/erbB4-mediated kalirin-7 disinhibition. Molecular Psychiatry *17*, 1, 99–107.

Campanac, E., and Hoffman, D.A. (2013). Repeated cocaine exposure increases fast-spiking interneuron excitability in the rat medial prefrontal cortex. Journal of Neurophysiology *109*, 2781–2792.

del Campo, N., Chamberlain, S.R., Sahakian, B.J., and Robbins, T.W. (2011). The roles of dopamine and noradrenaline in the pathophysiology and treatment of attention-deficit/hyperactivity disorder. Biological Psychiatry *69*, e145–e157.

Cannon, J., McCarthy, M.M., Lee, S., Lee, J., Börgers, C., Whittington, M.A., and Kopell, N. (2014). Neurosystems: brain rhythms and cognitive processing. European Journal of Neuroscience *39*, 705–719.

Cardin, J.A., Carlén, M., Meletis, K., Knoblich, U., Zhang, F., Deisseroth, K., Tsai, L.-H., and Moore, C.I. (2009). Driving fast-spiking cells induces gamma rhythm and controls sensory responses. Nature *459*, 663–667.

Carlén, M., Meletis, K., Siegle, J.H., Cardin, J.A., Futai, K., Vierling-Claassen, D., Rühlmann, C., Jones, S.R., Deisseroth, K., Sheng, M., et al. (2012). A critical role for NMDA receptors in parvalbumin interneurons for gamma rhythm induction and behavior. Molecular Psychiatry *17*, 537–548.

Carlson, G.C., Talbot, K., Halene, T.B., Gandal, M.J., Kazi, H.A., Schlosser, L., Phung, Q.H., Gur, R.E., Arnold, S.E., and Siegel, S.J. (2011). Dysbindin-1 mutant mice implicate reduced fast-phasic inhibition as a final common disease mechanism in schizophrenia. Proceedings of the National Academy of Science *108*, E962–E970.

Carreno, F.R., Donegan, J.J., Boley, A.M., Shah, A., DeGuzman, M., Frazer, A., and Lodge, D.J. (2015). Activation of a ventral hippocampus–medial prefrontal cortex pathway is both necessary and sufficient for an antidepressant response to ketamine. Molecular Psychiatry.

Ceci, A., Brambilla, A., Duranti, P., Grauert, M., Grippa, N., and Borsini, F. (1999). Effect of antipsychotic drugs and selective dopaminergic antagonists on dopamine-induced facilitatory activity in prelimbic cortical pyramidal neurons. An in vitro study. Neuroscience *93*, 107–115.

Celada, P., Lladó-Pelfort, L., Santana, N., Kargieman, L., Troyano-Rodriguez, E., Riga, M.S., and Artigas, F. (2013). Disruption of thalamocortical activity in schizophrenia models: relevance to antipsychotic drug action. International Journal of Neuropsychopharmacology CINP *16*, 2145–2163.

Cepeda, C., Radisavljevic, Z., Peacock, W., Levine, M.S., and Buchwald, N.A. (1992). Differential modulation by dopamine of responses evoked by excitatory amino acids in human cortex. Synapse *11*, 330–341.

Chang, F.-M., Kidd, J.R., Livak, K.J., Pakstis, A.J., and Kidd, K.K. (1996). The world-wide distribution of allele frequencies at the human dopamine D4 receptor locus. Human Genetics *98*, 91–101.

Chen, Y.-J., Zhang, M., Yin, D.-M., Wen, L., Ting, A., Wang, P., Lu, Y.-S., Zhu, X.-H., Li, S.-J., Wu, C.-Y., et al. (2010). ErbB4 in parvalbumin-positive interneurons is critical for neuregulin 1 regulation of long-term potentiation. Proceedings of the National Academy of Science *107*, 21818–21823.

Cho, A.K., Masayuki Hiramatsu, Schmitz, D.A., Toshitaka Nabeshima, and Tsutomu Kameyama (1991). Pharmacokinetic and pharmacodynamic properties of some phencyclidine analogs in rats. Pharmacological and Biochemical Behavior *39*, 947–953.

Cho, K.K.A., Hoch, R., Lee, A.T., Patel, T., Rubenstein, J.L.R., and Sohal, V.S. (2015). Gamma rhythms link prefrontal interneuron dysfunction with cognitive inflexibility in Dlx5/6(+/-) mice. Neuron *85*, 1332–1343.

Cho, R.Y., Konecky, R.O., and Carter, C.S. (2006). Impairments in frontal cortical gamma synchrony and cognitive control in schizophrenia. Proceedings of the National Academy of Science U. S. A. *103*, 19878–19883.

Chowdhury, G.M.I., Behar, K.L., Cho, W., Thomas, M.A., Rothman, D.L., and Sanacora, G. (2012). ^{1}H-[^{13}C]-nuclear magnetic resonance spectroscopy measures of ketamine's effect on amino acid neurotransmitter metabolism. Biological Psychiatry *71*, 1022–1025.

Chung, H.J., Ge, W.-P., Qian, X., Wiser, O., Jan, Y.N., and Jan, L.Y. (2009a). G protein-activated inwardly rectifying potassium channels mediate depotentiation of long-term potentiation. Proceedings of the National Academy of Science U. S. A. *106*, 635–640.

Chung, H.J., Qian, X., Ehlers, M., Jan, Y.N., and Jan, L.Y. (2009b). Neuronal activity regulates phosphorylation-dependent surface delivery of G protein-activated inwardly rectifying potassium channels. Proceedings of the National Academy of Science U. S. A. *106*, 629–634.

Cohen, J.Y., Haesler, S., Vong, L., Lowell, B.B., and Uchida, N. (2012). Neuron-type-specific signals for reward and punishment in the ventral tegmental area. Nature *482*, 85–88.

Corlett, P.R., Cambridge, V., Gardner, J.M., Piggot, J.S., Turner, D.C., Everitt, J.C., Arana, F.S., Morgan, H.L., Milton, A.L., Lee, J.L., et al. (2013). Ketamine Effects on Memory Reconsolidation Favor a Learning Model of Delusions. PLoS ONE *8*.

Corrigan, M.H., Gallen, C.C., Bonura, M.L., and Merchant, K.M. (2004). Effectiveness of the selective D4 antagonist sonepiprazole in schizophrenia: a placebo-controlled trial. Biological Psychiatry *55*, 445–451.

Coyle, J.T., Tsai, G., and Goff, D. (2006). Converging evidence of NMDA receptor hypofunction in the pathophysiology of schizophrenia. Annual N. Y. Academy of Science *1003*, 318–327.

Crandall, S.R., Cruikshank, S.J., and Connors, B.W. (2015). A Corticothalamic Switch: Controlling the Thalamus with Dynamic Synapses. Neuron *86*, 768–782.

Cui, X., Lefevre, E., Turner, K.M., Coelho, C.M., Alexander, S., Burne, T.H.J., and Eyles, D.W. (2014). MK-801-induced behavioural sensitisation alters dopamine release and turnover in rat prefrontal cortex. Psychopharmacology (Berlin) 1–9.

Cunningham, M.O., Hunt, J., Middleton, S., LeBeau, F.E.N., Gillies, M.G., Davies, C.H., Maycox, P.R., Whittington, M.A., and Racca, C. (2006). Region-Specific Reduction in Entorhinal Gamma Oscillations and Parvalbumin-Immunoreactive Neurons in Animal Models of Psychiatric Illness. Journal of Neuroscience *26*, 2767–2776.

Daub, H., Weiss, F.U., Wallasch, C., and Ullrich, A. (1996). Role of transactivation of the EGF receptor in signalling by G-protein-coupled receptors. Nature *379*, 557–560.

Davis, K.L., Kahn, R.S., Ko, G., and Davidson, M. (1991). Dopamine in schizophrenia: a review and reconceptualization. American Journal of Psychiatry *148*, 1474–1486.

Dawson, N., Morris, B.J., and Pratt,J. (2013). Subanaesthetic ketamine treatment alters prefrontal cortex connectivity with thalamus and ascending subcortical systems. Schizophrenia Bulletin *39*, 366–377.

Dawson, N., McDonald, M., Higham, D.J., Morris, B.J., and Pratt, J. (2014). Subanesthetic Ketamine Treatment Promotes Abnormal Interactions between Neural Subsystems and Alters the Properties of Functional Brain Networks. Neuropsychopharmacology *39*, 1786–1798.

Deakin, I.H., Nissen, W., Law, A.J., Lane, T., Kanso, R., Schwab, M.H., Nave, K.-A., Lamsa, K.P., Paulsen, O., Bannerman, D.M., et al. (2012). Transgenic overexpression of the type I isoform of neuregulin 1 affects working

memory and hippocampal oscillations but not long-term potentiation. Cerebral Cortex 1991 *22*, 1520–1529.

Delaville, C., McCoy, A.J., Gerber, C.M., Cruz, A.V., and Walters, J.R. (2015). Subthalamic nucleus activity in the awake hemiparkinsonian rat: relationships with motor and cognitive networks. Journal of Neuroscience *35*, 6918–6930.

Deleuze, C., and Huguenard, J.R. (2016). Two classes of excitatory synaptic responses in rat thalamic reticular neurons. Journal of Neurophysiology.

del Pino, I., García-Frigola, C., Dehorter, N., Brotons-Mas, J.R., Alvarez-Salvado, E., Martínez de Lagrán, M., Ciceri, G., Gabaldón, M.V., Moratal, D., Dierssen, M., et al. (2013). Erbb4 Deletion from Fast-Spiking Interneurons Causes Schizophrenia-like Phenotypes. Neuron *79*, 1152–1168.

Demiralp, T., Herrmann, C.S., Erdal, M.E., Ergenoglu, T., Keskin, Y.H., Ergen, M., and Beydagi, H. (2007). DRD4 and DAT1 Polymorphisms Modulate Human Gamma Band Responses. Cerebral Cortex *17*, 1007–1019.

Descarries, L., and Mechawar, N. (2000). Ultrastructural evidence for diffuse transmission by monoamine and acetylcholine neurons of the central nervous system. Progress in Brain Research *125*, 27–47.

Driesen, N.R., McCarthy, G., Bhagwagar, Z., Bloch, M., Calhoun, V., D'Souza, D.C., Gueorguieva, R., He, G., Ramachandran, R., Suckow, R.F., et al. (2013a). Relationship of resting brain hyperconnectivity and schizophrenia-like symptoms produced by the NMDA receptor antagonist ketamine in humans. Molecular Psychiatry *18*, 1199–1204.

Driesen, N.R., McCarthy, G., Bhagwagar, Z., Bloch, M.H., Calhoun, V.D., D'Souza, D.C., Gueorguieva, R., He, G., Leung, H.-C., Ramani, R., et al. (2013b). The impact of NMDA receptor blockade on human working memory-related prefrontal function and connectivity. Neuropsychopharmacology *38*, 2613–2622.

Dulawa, S.C., Grandy, D.K., Low, M.J., Paulus, M.P., and Geyer, M.A. (1999). Dopamine D4 receptor-knock-out mice exhibit reduced exploration of novel stimuli. Journal of Neuroscience *19*, 9550–9556.

Dupre, K.B., Cruz, A.V., McCoy, A.J., Delaville, C., Gerber, C.M., Eyring, K.W., and Walters, J.R. (2016). Effects of L-dopa priming on cortical high beta

and high gamma oscillatory activity in a rodent model of Parkinson's disease. Neurobiological Disorders *86*, 1–15.

Durstewitz, D., and Seamans, J.K. (2008). The Dual-State Theory of Prefrontal Cortex Dopamine Function with Relevance to Catechol-O-Methyltransferase Genotypes and Schizophrenia. Biological Psychiatry *64*, 739–749.

Ehrlichman, R.S., Gandal, M.J., Maxwell, C.R., Lazarewicz, M.T., Finkel, L.H., Contreras, D., Turetsky, B.I., and Siegel, S.J. (2009). N-methyl-d-aspartic acid receptor antagonist-induced frequency oscillations in mice recreate pattern of electrophysiological deficits in schizophrenia. Neuroscience *158*, 705–712.

Einevoll, G.T., Kayser, C., Logothetis, N.K., and Panzeri, S. (2013). Modelling and analysis of local field potentials for studying the function of cortical circuits. Nature Reviews Neuroscience *14*, 770–785.

Emanuel, S.L., Hughes, T.V., Adams, M., Rugg, C.A., Fuentes-Pesquera, A., Connolly, P.J., Pandey, N., Moreno-Mazza, S., Butler, J., Borowski, V., et al. (2008). Cellular and in vivo activity of JNJ-28871063, a nonquinazoline pan-ErbB kinase inhibitor that crosses the blood-brain barrier and displays efficacy against intracranial tumors. Molecular Pharmacology *73*, 338–348.

Engel, A.K., Moll, C.K.E., Fried, I., and Ojemann, G.A. (2005). Invasive recordings from the human brain: clinical insights and beyond. Nature Reviews Neuroscience *6*, 35–47.

Engel, M., Snikeris, P., Jenner, A., Karl, T., Huang, X.-F., and Frank, E. (2015). Neuregulin 1 Prevents Phencyclidine-Induced Behavioral Impairments and Disruptions to GABAergic Signaling in Mice. International Journal of Neuropsychopharmacology *18*, pyu114.

Falzone, T.L., Gelman, D.M., Young, J.I., Grandy, D.K., Low, M.J., and Rubinstein, M. (2002). Absence of dopamine D4 receptors results in enhanced reactivity to unconditioned, but not conditioned, fear. European Journal of Neuroscience *15*, 158–164.

Fanselow, M.S., and Dong, H.-W. (2010). Are the Dorsal and Ventral Hippocampus functionally distinct structures? Neuron *65*, 7.

Faraone, S.V., Doyle, A.E., Mick, E., and Biederman, J. (2001). Meta-analysis of the association between the 7-repeat allele of the dopamine D4

receptor gene and attention deficit hyperactivity disorder. American Journal of Psychiatry *158*, 1052–1057.

Fazzari, P., Paternain, A.V., Valiente, M., Pla, R., Luján, R., Lloyd, K., Lerma, J., Marín, O., and Rico, B. (2010). Control of cortical GABA circuitry development by Nrg1 and ErbB4 signalling. Nature *464*, 1376–1380.

Ferguson, S.S. (2003). Receptor tyrosine kinase transactivation: fine-tuning synaptic transmission. Trends in Neuroscience *26*, 119–122.

Ferrarelli, F., and Tononi, G. (2011). The Thalamic Reticular Nucleus and Schizophrenia. Schizophrenia Bulletin *37*, 306–315.

Ferre, S., Ciruela, F., Woods, A.S., Lluis, C., and Franco, R. (2007). Functional relevance of neurotransmitter receptor heteromers in the central nervous system. Trends in Neuroscience *30*, 440–446.

Ferre, S., Baler, R., Bouvier, M., Caron, M.G., Devi, L.A., Durroux, T., Fuxe, K., George, S.R., Javitch, J.A., Lohse, M.J., et al. (2009). Building a new conceptual framework for receptor heteromers. Nature Chemical Biology *5*, 131–134.

Fisahn, A., Neddens, J., Yan, L., and Buonanno, A. (2009). Neuregulin-1 Modulates Hippocampal Gamma Oscillations: Implications for Schizophrenia. Cerebral Cortex *19*, 612–618.

Fischer, C.E., Golas, A.C., Schweizer, T.A., Munoz, D.G., Ismail, Z., Qian, W., Tang-Wai, D.F., Rotstein, D.L., and Day, G.S. (2016). Anti N-methyl-D-aspartate receptor encephalitis: a game-changer? Expert Review of Neurotherapeutics *0*.

Flames, N., Long, J.E., Garratt, A.N., Fischer, T.M., Gassmann, M., Birchmeier, C., Lai, C., Rubenstein, J.L.R., and Marín, O. (2004). Short- and long-range attraction of cortical GABAergic interneurons by neuregulin-1. Neuron *44*, 251–261.

Florán, B., Florán, L., Erlij, D., and Aceves, J. (2004a). Activation of dopamine D4 receptors modulates [3H]GABA release in slices of the rat thalamic reticular nucleus. Neuropharmacology *46*, 497–503.

Florán, B., Florán, L., Erlij, D., and Aceves, J. (2004b). Dopamine D4 receptors inhibit depolarization-induced [3H]GABA release in the rat subthalamic nucleus. European Journal of Pharmacology *498*, 97–102.

Floresco, S.B., Magyar, O., Ghods-Sharifi, S., Vexelman, C., and Tse, M.T.L. (2006). Multiple Dopamine Receptor Subtypes in the Medial Prefrontal Cortex of the Rat Regulate Set-Shifting. Neuropsychopharmacology *31*, 297–309.

Frohlich, J., and Van Horn, J.D. (2014). Reviewing the ketamine model for schizophrenia. Journal of Psychopharmacology Oxford England *28*, 287–302.

Fuchs, E.C., Zivkovic, A.R., Cunningham, M.O., Middleton, S., LeBeau, F.E.N., Bannerman, D.M., Rozov, A., Whittington, M.A., Traub, R.D., Rawlins, J.N.P., et al. (2007). Recruitment of Parvalbumin-Positive Interneurons Determines Hippocampal Function and Associated Behavior. Neuron *53*, 591–604.

Furth, K.E., Wang, K.H., Buonanno, A., and Vullhorst, D. (2013). Dopamine, cognitive function, and gamma oscillations: role of D4 receptors. Frontiers in Cellular Neuroscience *7*, 102.

Fuster, J.M. (2001). The prefrontal cortex--an update: time is of the essence. Neuron *30*, 319–333.

Gainetdinov, R.R., Premont, R.T., Bohn, L.M., Lefkowitz, R.J., and Caron, M.G. (2004). Desensitization of G protein-coupled receptors and neuronal functions. Annual Review of Neuroscience *27*, 107–144.

Gajendran, N., Kapfhammer, J.P., Lain, E., Canepari, M., Vogt, K., Wisden, W., and Brenner, H.R. (2009). Neuregulin signaling is dispensable for NMDA- and GABA(A)-receptor expression in the cerebellum in vivo. Journal of Neuroscience *29*, 2404–2413.

Galderisi, S., Mucci, A., Volpe, U., and Boutros, N. (2009). Evidence-based medicine and electrophysiology in schizophrenia. Clinical EEG Neuroscience *40*, 62–77.

Gan, L., Falzone, T.L., Zhang, K., Rubinstein, M., Baldessarini, R.J., and Tarazi, F.I. (2004). Enhanced expression of dopamine D(1) and glutamate NMDA receptors in dopamine D(4) receptor knockout mice. Journal of Molecular Neuroscience MN *22*, 167–178.

Gao, W.-J. (2007). Acute Clozapine Suppresses Synchronized Pyramidal Synaptic Network Activity by Increasing Inhibition in the Ferret Prefrontal Cortex. Journal of Neurophysiology *97*, 1196–1208.

Gao, W.-J., and Goldman-Rakic, P.S. (2003). Selective modulation of excitatory and inhibitory microcircuits by dopamine. Proceedings of the National Academy of Science *100*, 2836–2841.

Gasca-Martinez, D., Hernandez, A., Sierra, A., Valdiosera, R., Anaya-Martinez, V., Floran, B., Erlij, D., and Aceves, J. (2010). Dopamine inhibits GABA transmission from the globus pallidus to the thalamic reticular nucleus via presynaptic D4 receptors. Neuroscience *169*, 1672–1681.

Gilmour, G., Dix, S., Fellini, L., Gastambide, F., Plath, N., Steckler, T., Talpos, J., and Tricklebank, M. (2012). NMDA receptors, cognition and schizophrenia – Testing the validity of the NMDA receptor hypofunction hypothesis. Neuropharmacology *62*, 1401–1412.

Gizer, I.R., Ficks, C., and Waldman, I.D. (2009). Candidate gene studies of ADHD: a meta-analytic review. Human Genetics *126*, 51–90.

Gloveli, T., Dugladze, T., Saha, S., Monyer, H., Heinemann, U., Traub, R.D., Whittington, M.A., and Buhl, the late E.H. (2005). Differential involvement of oriens/pyramidale interneurones in hippocampal network oscillations in vitro. Journal of Physiology *562*, 131–147.

Goldberg, E.M., Jeong, H.Y., Kruglikov, I., Tremblay, R., Lazarenko, R.M., and Rudy, B. (2011). Rapid developmental maturation of neocortical FS cell intrinsic excitability. Cerebral Cortex *21*, 666–682.

Goldberg, T.E., Egan, M.F., Gscheidle, T., Coppola, R., Weickert, T., Kolachana, B.S., Goldman, D., and Weinberger, D.R. (2003). Executive subprocesses in working memory: relationship to catechol-O-methyltransferase Val158Met genotype and schizophrenia. Archives in Genetic Psychiatry *60*, 889.

Goldman-Rakic, P.S. (1995). Cellular basis of working memory. Neuron *14*, 477.

Goldman-Rakic, P.S., Leranth, C., Williams, S.M., Mons, N., and Geffard, M. (1989). Dopamine synaptic complex with pyramidal neurons in primate cerebral cortex. Proceedings of the National Academy of Science U. S. A. *86*, 9015–9019.

Goldstein, R.Z., and Volkow, N.D. (2011). Dysfunction of the prefrontal cortex in addiction: neuroimaging findings and clinical implications. Nature Reviews Neuroscience *12*, 652–669.

González, S., Rangel-Barajas, C., Peper, M., Lorenzo, R., Moreno, E., Ciruela, F., Borycz, J., Ortiz, J., Lluís, C., Franco, R., et al. (2012a). Dopamine D4 receptor, but not the ADHD-associated D4.7 variant, forms functional heteromers with the dopamine D2S receptor in the brain. Molecular Psychiatry *17*, 650–662.

González, S., Moreno-Delgado, D., Moreno, E., Perez-Capote, K., Franco, R., Mallol, J., Cortes, A., Casado, V., Lluis, C., Ortiz, J., et al. (2012b). Circadian-related heteromerization of adrenergic and dopamine D4 receptors modulates melatonin synthesis and release in the pineal gland. PLoS Biology *10*, e1001347.

Gonzalez-Islas, C., and Hablitz, J.J. (2003). Dopamine Enhances EPSCs in Layer II–III Pyramidal Neurons in Rat Prefrontal Cortex. Journal of Neuroscience *23*, 867–875.

Gorelova, N., Seamans, J.K., and Yang, C.R. (2002). Mechanisms of Dopamine Activation of Fast-Spiking Interneurons That Exert Inhibition in Rat Prefrontal Cortex. Journal of Neurophysiology *88*, 3150–3166.

Goto, Y., and Grace, A.A. (2006). Alterations in Medial Prefrontal Cortical Activity and Plasticity in Rats with Disruption of Cortical Development. Biological Psychiatry *60*, 1259–1267.

Gottesman, I.I., and Gould, T.D. (2003). The Endophenotype Concept in Psychiatry: Etymology and Strategic Intentions. American Journal of Psychiatry *160*, 636–645.

Govindaiah, G., Wang, T., Gillette, M.U., Crandall, S.R., and Cox, C.L. (2010). Regulation of Inhibitory Synapses by Presynaptic D4 Dopamine Receptors in Thalamus. Journal of Neurophysiology *104*, 2757–2765.

Grace, A.A., Floresco, S.B., Goto, Y., and Lodge, D.J. (2007). Regulation of firing of dopaminergic neurons and control of goal-directed behaviors. Trends in Neuroscience.

Graziane, N.M., Yuen, E.Y., and Yan, Z. (2009). Dopamine D4 Receptors Regulate GABAA Receptor Trafficking via an Actin/Cofilin/Myosin-dependent Mechanism. Journal of Biological Chemistry *284*, 8329–8336.

Green, M.F. (1996). What are the functional consequences of neurocognitive deficits in schizophrenia? American Journal of Psychiatry *153*, 321–330.

Green, M.F. (2006). Cognitive impairment and functional outcome in schizophrenia and bipolar disorder. Journal of Clinical Psychiatry *67 Supplement 9*, 3-8-42.

Greengard, P., Allen, P.B., and Nairn, A.C. (1999). Beyond the dopamine receptor: the DARPP-32/protein phosphatase-1 cascade. Neuron *23*, 435–447.

Gregoriou, G.G., Paneri, S., and Sapountzis, P. (2015). Oscillatory synchrony as a mechanism of attentional processing. Brain Research *1626*, 165–182.

Grunze, H.C., Rainnie, D.G., Hasselmo, M.E., Barkai, E., Hearn, E.F., McCarley, R.W., and Greene, R.W. (1996). NMDA-dependent modulation of CA1 local circuit inhibition. Journal of Neuroscience *16*, 2034–2043.

Gu, Z., Jiang, Q., Fu, A.K.Y., Ip, N.Y., and Yan, Z. (2005). Regulation of NMDA receptors by neuregulin signaling in prefrontal cortex. Journal of Neuroscience *25*, 4974–4984.

Gu, Z., Jiang, Q., Yuen, E.Y., and Yan, Z. (2006). Activation of Dopamine D4 Receptors Induces Synaptic Translocation of Ca2+/Calmodulin-Dependent Protein Kinase II in Cultured Prefrontal Cortical Neurons. Molecular Pharmacology *69*, 813–822.

Guidi, M., Rani, A., Karic, S., Severance, B., Kumar, A., and Foster, T.C. (2015). Contribution of N-methyl-D-aspartate receptors to attention and episodic spatial memory during senescence. Neurobiology of Learning and Memory *125*, 36–46.

Guillery, R.W., and Sherman, S.M. (2002). Thalamic Relay Functions and Their Role in Corticocortical Communication. Neuron *33*, 163–175.

Gulledge, A.T., and Jaffe, D.B. (2001). Multiple Effects of Dopamine on Layer V Pyramidal Cell Excitability in Rat Prefrontal Cortex. Journal of Neurophysiology *86*, 586–595.

Gulyás, A.I., Megías, M., Emri, Z., and Freund, T.F. (1999). Total number and ratio of excitatory and inhibitory synapses converging onto single interneurons of different types in the CA1 area of the rat hippocampus. Journal of Neuroscience *19*, 10082–10097.

Haenschel, C., Bittner, R.A., Waltz, J., Haertling, F., Wibral, M., Singer, W., Linden, D.E.J., and Rodriguez, E. (2009). Cortical Oscillatory Activity Is

Critical for Working Memory as Revealed by Deficits in Early-Onset Schizophrenia. Journal of Neuroscience *29*, 9481–9489.

Hahn, C.-G., Wang, H.-Y., Cho, D.-S., Talbot, K., Gur, R.E., Berrettini, W.H., Bakshi, K., Kamins, J., Borgmann-Winter, K.E., Siegel, S.J., et al. (2006). Altered neuregulin 1–ErbB4 signaling contributes to NMDA receptor hypofunction in schizophrenia. Nature Medicine *12*, 824–828.

Hájos, N., Pálhalmi, J., Mann, E.O., Németh, B., Paulsen, O., and Freund, T.F. (2004). Spike Timing of Distinct Types of GABAergic Interneuron during Hippocampal Gamma Oscillations in vitro. Journal of Neuroscience *24*, 9127–9137.

Hakami, T., Jones, N.C., Tolmacheva, E.A., Gaudias, J., Chaumont, J., Salzberg, M., O'Brien, T.J., and Pinault, D. (2009). NMDA receptor hypofunction leads to generalized and persistent aberrant gamma oscillations independent of hyperlocomotion and the state of consciousness. PloS One *4*, e6755.

Hall, J., Whalley, H.C., Job, D.E., Baig, B.J., McIntosh, A.M., Evans, K.L., Thomson, P.A., Porteous, D.J., Cunningham-Owens, D.G., Johnstone, E.C., et al. (2006). A neuregulin 1 variant associated with abnormal cortical function and psychotic symptoms. Nature Neuroscience *9*, 1477–1478.

Hampson, E.C., Vaney, D.I., and Weiler, R. (1992). Dopaminergic modulation of gap junction permeability between amacrine cells in mammalian retina. Journal of Neuroscience *12*, 4911–4922.

Hanson, J.E., Weber, M., Meilandt, W.J., Wu, T., Luu, T., Deng, L., Shamloo, M., Sheng, M., Scearce-Levie, K., and Zhou, Q. (2013). GluN2B antagonism affects interneurons and leads to immediate and persistent changes in synaptic plasticity, oscillations, and behavior. Neuropsychopharmacology *38*, 1221–1233.

Harnett, M.T., Xu, N.-L., Magee, J.C., and Williams, S.R. (2013). Potassium Channels Control the Interaction between Active Dendritic Integration Compartments in Layer 5 Cortical Pyramidal Neurons. Neuron *79*, 516–529.

Hartigan, J.A., and Hartigan, P.M. (1985). The Dip Test of Unimodality. Annual Statistics *13*, 70–84.

Hashimoto, R., Straub, R.E., Weickert, C.S., Hyde, T.M., Kleinman, J.E., and Weinberger, D.R. (2004). Expression analysis of neuregulin-1 in the dorsolateral prefrontal cortex in schizophrenia. Molecular Psychiatry *9*, 299–307.

Hefft, S., and Jonas, P. (2005). Asynchronous GABA release generates long-lasting inhibition at a hippocampal interneuron–principal neuron synapse. Nature Neuroscience *8*, 1319–1328.

Heise, C.E., and Mitrofanis, J. (2005). Reduction in parvalbumin expression in the zona incerta after 6OHDA lesion in rats. Journal of Neurocytology *34*, 421–434.

Helms, C.M., Gubner, N.R., Wilhelm, C.J., Mitchell, S.H., and Grandy, D.K. (2008). D4 receptor deficiency in mice has limited effects on impulsivity and novelty seeking. Pharmacological and Biochemical Behavior *90*, 387–393.

Herrmann, C.S., and Demiralp, T. (2005). Human EEG gamma oscillations in neuropsychiatric disorders. Clinical Neurophysiology *116*, 2719–2733.

Herwerth, M., Jensen, V., Novak, M., Konopka, W., Hvalby, O., and Köhr, G. (2012). D4 Dopamine Receptors Modulate NR2B NMDA Receptors and LTP in Stratum Oriens of Hippocampal CA1. Cerebral Cortex *22*, 1786–1798.

Hioki, H., Okamoto, S., Konno, M., Kameda, H., Sohn, J., Kuramoto, E., Fujiyama, F., and Kaneko, T. (2013). Cell Type-Specific Inhibitory Inputs to Dendritic and Somatic Compartments of Parvalbumin-Expressing Neocortical Interneuron. Journal of Neuroscience *33*, 544–555.

Hippenmeyer, S., Vrieseling, E., Sigrist, M., Portmann, T., Laengle, C., Ladle, D.R., and Arber, S. (2005). A developmental switch in the response of DRG neurons to ETS transcription factor signaling. PLoS Biology *3*, e159.

Höflich, A., Hahn, A., Küblböck, M., Kranz, G.S., Vanicek, T., Windischberger, C., Saria, A., Kasper, S., Winkler, D., and Lanzenberger, R. (2015). Ketamine-Induced Modulation of the Thalamo-Cortical Network in Healthy Volunteers As a Model for Schizophrenia. International Journal of Neuropsychopharmacology *18*, 040.

Homayoun, H., and Moghaddam, B. (2007a). NMDA Receptor Hypofunction Produces Opposite Effects on Prefrontal Cortex Interneurons and Pyramidal Neurons. Journal of Neuroscience *27*, 11496–11500.

Homayoun, H., and Moghaddam, B. (2007b). Fine-Tuning of Awake Prefrontal Cortex Neurons by Clozapine: Comparison With Haloperidol and N-Desmethylclozapine. Biological Psychiatry *61*, 679–687.

Hong, L.E., Wonodi, I., Stine, O.C., Mitchell, B.D., and Thaker, G.K. (2008). Evidence of missense mutations on the neuregulin 1 gene affecting function of prepulse inhibition. Biological Psychiatry *63*, 17–23.

Hong, L.E., Summerfelt, A., Buchanan, R.W., O'Donnell, P., Thaker, G.K., Weiler, M.A., and Lahti, A.C. (2010). Gamma and delta neural oscillations and association with clinical symptoms under subanesthetic ketamine. Neuropsychopharmacology *35*, 632–640.

Hou, X.-J., Ni, K.-M., Yang, J.-M., and Li, X.-M. (2014). Neuregulin 1/ErbB4 enhances synchronized oscillations of prefrontal cortex neurons via inhibitory synapses. Neuroscience *261*, 107–117.

Huang, Y.Y., and Kandel, E.R. (1995). D1/D5 receptor agonists induce a protein synthesis-dependent late potentiation in the CA1 region of the hippocampus. Proceedings of the National Academy of Science *92*, 2446–2450.

Huang, Y.Z., Won, S., Ali, D.W., Wang, Q., Tanowitz, M., Du, Q.S., Pelkey, K.A., Yang, D.J., Xiong, W.C., Salter, M.W., et al. (2000). Regulation of neuregulin signaling by PSD-95 interacting with ErbB4 at CNS synapses. Neuron *26*, 443–455.

Hudson, M.R., Rind, G., O'Brien, T.J., and Jones, N.C. (2016). Reversal of evoked gamma oscillation deficits is predictive of antipsychotic activity with a unique profile for clozapine. Translational Psychiatry *6*, e784.

Hull, C., Adesnik, H., and Scanziani, M. (2009). Neocortical disynaptic inhibition requires somatodendritic integration in interneurons. Journal of Neuroscience *29*, 8991–8995.

Hyland, B.., Reynolds, J.N.., Hay, J., Perk, C.., and Miller, R. (2002). Firing modes of midbrain dopamine cells in the freely moving rat. Neuroscience *114*, 475–492.

Itil, T.M., Saletu, B., and Davis, S. (1972). EEG findings in chronic schizophrenics based on digital computer period analysis and analog power spectra. Biological Psychiatry *5*, 1–13.

Iyengar, S.S., and Mott, D.D. (2008). Neuregulin blocks synaptic strengthening after epileptiform activity in the rat hippocampus. Brain Research *1208*, 67–73.

Jackson, M.E., Homayoun, H., and Moghaddam, B. (2004). NMDA receptor hypofunction produces concomitant firing rate potentiation and burst activity reduction in the prefrontal cortex. Proceedings of the National Academy of Science U. S. A. *101*, 8467–8472.

Jadi, M.P., Behrens, M.M., and Sejnowski, T.J. (2015). Abnormal Gamma Oscillations in N-Methyl-D-Aspartate Receptor Hypofunction Models of Schizophrenia. Biological Psychiatry.

Janssen, M.J., Leiva-Salcedo, E., and Buonanno, A. (2012). Neuregulin Directly Decreases Voltage-Gated Sodium Current in Hippocampal ErbB4-Expressing Interneurons. Journal of Neuroscience *32*, 13889–13895.

Jay, T.M. (2003). Dopamine: a potential substrate for synaptic plasticity and memory mechanisms. Progress in Neurobiology *69*, 375–390.

Jentsch, J.D., Taylor, J.R., Jr, D.E.R., Elsworth, J.D., Youngren, K.D., and Roth, R.H. (1999). Dopamine D4 receptor antagonist reversal of subchronic phencyclidine-induced object retrieval/detour deficits in monkeys. Psychopharmacology (Berlin) *142*, 78–84.

Jia, X., and Kohn, A. (2011). Gamma Rhythms in the Brain. PLOS Biology *9*, 1001045.

Jiménez-Sánchez, L., Campa, L., Auberson, Y.P., and Adell, A. (2014). The role of GluN2A and GluN2B subunits on the effects of NMDA receptor antagonists in modeling schizophrenia and treating refractory depression. Neuropsychopharmacology *39*, 2673–2680.

Jones, N.C., Reddy, M., Anderson, P., Salzberg, M.R., O'Brien, T.J., and Pinault, D. (2012). Acute administration of typical and atypical antipsychotics reduces EEG gamma power, but only the preclinical compound LY379268 reduces the ketamine-induced rise in gamma power. International Journal of Neuropsychopharmacology *15*, 657–668.

Jones, N.C., Anderson, P., Rind, G., Sullivan, C., Buuse, M. van den, and O'Brien, T.J. (2014). Effects of aberrant gamma frequency oscillations on prepulse inhibition. International Journal of Neuropsychopharmacology *17*, 1671–1681.

Jonsson, E.G., Sedvall, G.C., Nothen, M.M., and Cichon, S. (2003). Dopamine D4 receptor gene (DRD4) variants and schizophrenia: meta-analyses. Schizophrenia Research *61*, 111–119.

Joshi, D., Fullerton, J.M., and Weickert, C.S. (2014). Elevated ErbB4 mRNA is related to interneuron deficit in prefrontal cortex in schizophrenia. Journal of Psychiatry Research *53*, 125–132.

Kalsbeek, A., Voorn, P., Buijs, R.M., Pool, C.W., and Uylings, H.B.M. (1988). Development of the dopaminergic innervation in the prefrontal cortex of the rat. Journal of Computational Neurology *269*, 58–72.

Kang, J., Jiang, L., Goldman, S.A., and Nedergaard, M. (1998). Astrocyte-mediated potentiation of inhibitory synaptic transmission. Nature Neuroscience *1*, 683–692.

Kapur, S., and Seeman, P. (2002). NMDA receptor antagonists ketamine and PCP have direct effects on the dopamine D2 and serotonin 5-HT2 receptors-implications for models of schizophrenia. Molecular Psychiatry *7*, 837–844.

Kellendonk, C., Simpson, E.H., Polan, H.J., Malleret, G., Vronskaya, S., Winiger, V., Moore, H., and Kandel, E.R. (2006). Transient and selective overexpression of dopamine D2 receptors in the striatum causes persistent abnormalities in prefrontal cortex functioning. Neuron *49*, 603–615.

Kezunovic, N., Hyde, J., Simon, C., Urbano, F.J., Williams, D.K., and Garcia-Rill, E. (2012). Gamma band activity in the developing parafascicular nucleus. Journal of Neurophysiology *107*, 772–784.

Kim, M.J., Dunah, A.W., Wang, Y.T., and Sheng, M. (2005). Differential roles of NR2A- and NR2B-containing NMDA receptors in Ras-ERK signaling and AMPA receptor trafficking. Neuron *46*, 745–760.

Kinney, J.W., Davis, C.N., Tabarean, I., Conti, B., Bartfai, T., and Behrens, M.M. (2006). A Specific Role for NR2A-Containing NMDA Receptors in the Maintenance of Parvalbumin and GAD67 Immunoreactivity in Cultured Interneurons. Journal of Neuroscience *26*, 1604–1615.

Kiss, T., Hoffmann, W.E., Scott, L., Kawabe, T.T., Milici, A.J., Nilsen, E.A., and Hajos, M. (2011a). Role of Thalamic Projection in NMDA Receptor-Induced Disruption of Cortical Slow Oscillation and Short-Term Plasticity. Frontiers in Psychiatry *2*, 14.

Kiss, T., Hoffmann, W.E., and Hajós, M. (2011b). Delta oscillation and short-term plasticity in the rat medial prefrontal cortex: modelling NMDA hypofunction of schizophrenia. International Journal of Neuropsychopharmacology CINP *14*, 29–42.

Kissler, J., Müller, M.M., Fehr, T., Rockstroh, B., and Elbert, T. (2000). MEG gamma band activity in schizophrenia patients and healthy subjects in a mental arithmetic task and at rest. Clinical Neurophysiology *111*, 2079–2087.

Kittelberger, K., Hur, E.E., Sazegar, S., Keshavan, V., and Kocsis, B. (2012). Comparison of the effects of acute and chronic administration of ketamine on hippocampal oscillations. Relevance for the NMDA receptor hypofunction model of schizophrenia. Brain Structure and Function *217*, 395–409.

Kocsis, B. (2012). Differential Role of NR2A and NR2B Subunits in N-Methyl-D-Aspartate Receptor Antagonist-Induced Aberrant Cortical Gamma Oscillations. Biological Psychiatry *71*, 987–995.

Kocsis, B., Brown, R.E., McCarley, R.W., and Hajos, M. (2013). Impact of Ketamine on Neuronal Network Dynamics: Translational Modeling of Schizophrenia-Relevant Deficits. Central Nervous System Neuroscience Therapeutics *19*, 437–447.

Kocsis, B., Lee, P., and Deth, R. (2014). Enhancement of gamma activity after selective activation of dopamine D4 receptors in freely moving rats and in a neurodevelopmental model of schizophrenia. Brain Structure and Function 1–8.

Kole, M.H.P., Letzkus, J.J., and Stuart, G.J. (2007). Axon Initial Segment Kv1 Channels Control Axonal Action Potential Waveform and Synaptic Efficacy. Neuron *55*, 633–647.

Kopell, N., Ermentrout, G.B., Whittington, M.A., and Traub, R.D. (2000). Gamma rhythms and beta rhythms have different synchronization properties. Proceedings of the National Academy of Science *97*, 1867–1872.

Korotkova, T., Fuchs, E.C., Ponomarenko, A., von Engelhardt, J., and Monyer, H. (2010). NMDA receptor ablation on parvalbumin-positive interneurons impairs hippocampal synchrony, spatial representations, and working memory. Neuron *68*, 557–569.

Kotecha, S.A., Oak, J.N., Jackson, M.F., Perez, Y., Orser, B.A., Van Tol, H.H.., and MacDonald, J.F. (2002). A D2 Class Dopamine Receptor Transactivates a Receptor Tyrosine Kinase to Inhibit NMDA Receptor Transmission. Neuron *35*, 1111–1122.

Kramer, M.S., Last, B., Getson, A., and Reines, S.A. (1997). The effects of a selective D4 dopamine receptor antagonist (L-745,870) in acutely psychotic inpatients with schizophrenia. D4 Dopamine Antagonist Group. Archives of Genetic Psychiatry *54*, 567–572.

Krivosheya, D., Tapia, L., Levinson, J.N., Huang, K., Kang, Y., Hines, R., Ting, A.K., Craig, A.M., Mei, L., Bamji, S.X., et al. (2008). ErbB4-neuregulin signaling modulates synapse development and dendritic arborization through distinct mechanisms. Journal of Biological Chemistry *283*, 32944–32956.

Kroener, S., Chandler, L.J., Phillips, P.E.M., and Seamans, J.K. (2009). Dopamine Modulates Persistent Synaptic Activity and Enhances the Signal-to-Noise Ratio in the Prefrontal Cortex. PLoS ONE *4*, e6507.

Kröner, S., Krimer, L.S., Lewis, D.A., and Barrionuevo, G. (2007). Dopamine Increases Inhibition in the Monkey Dorsolateral Prefrontal Cortex through Cell Type–Specific Modulation of Interneurons. Cerebral Cortex *17*, 1020–1032.

Krug, A., Markov, V., Eggermann, T., Krach, S., Zerres, K., Stöcker, T., Shah, N.J., Schneider, F., Nöthen, M.M., Treutlein, J., et al. (2008). Genetic variation in the schizophrenia-risk gene neuregulin1 correlates with differences in frontal brain activation in a working memory task in healthy individuals. NeuroImage *42*, 1569–1576.

Kruzich, P.J., Suchland, K.L., and Grandy, D.K. (2004). Dopamine D4 receptor-deficient mice, congenic on the C57BL/6J background, are hypersensitive to amphetamine. Synapse *53*, 131–139.

Krystal, J.H., Karper, L.P., Seibyl, J.P., Freeman, G.K., Delaney, R., Bremner, J.D., Heninger, G.R., Bowers, M.B., and Charney, D.S. (1994). Subanesthetic effects of the noncompetitive NMDA antagonist, ketamine, in humans.

Psychotomimetic, perceptual, cognitive, and neuroendocrine responses. Archives of Genetic Psychiatry *51*, 199–214.

Krystal, J.H., D'Souza, D.C., Karper, L.P., Bennett, A., Abi-Dargham, A., Abi-Saab, D., Cassello, K., Bowers, M.B., Vegso, S., Heninger, G.R., et al. (1999). Interactive effects of subanesthetic ketamine and haloperidol in healthy humans. Psychopharmacology (Berlin) *145*, 193–204.

Kulikova, S.P., Tolmacheva, E.A., Anderson, P., Gaudias, J., Adams, B.E., Zheng, T., and Pinault, D. (2012). Opposite effects of ketamine and deep brain stimulation on rat thalamocortical information processing. European Journal of Neuroscience *36*, 3407–3419.

Kunitachi, S., Fujita, Y., Ishima, T., Kohno, M., Horio, M., Tanibuchi, Y., Shirayama, Y., Iyo, M., and Hashimoto, K. (2009). Phencyclidine-induced cognitive deficits in mice are ameliorated by subsequent subchronic administration of donepezil: role of sigma-1 receptors. Brain Research *1279*, 189–196.

Kuznetsova, A., and Deth, R. (2008). A model for modulation of neuronal synchronization by D4 dopamine receptor-mediated phospholipid methylation. Journal of Computational Neuroscience *24*, 314–329.

Kwon, O.B., Longart, M., Vullhorst, D., Hoffman, D.A., and Buonanno, A. (2005). Neuregulin-1 reverses long-term potentiation at CA1 hippocampal synapses. Journal of Neuroscience *25*, 9378–9383.

Kwon, O.B., Paredes, D., Gonzalez, C.M., Neddens, J., Hernandez, L., Vullhorst, D., and Buonanno, A. (2008). Neuregulin-1 regulates LTP at CA1 hippocampal synapses through activation of dopamine D4 receptors. Proceedings of the National Academy of Science *105*, 15587.

LaHoste, G.J., Swanson, J.M., Wigal, S.B., Glabe, C., Wigal, T., King, N., and Kennedy, J.L. (1996). Dopamine D4 receptor gene polymorphism is associated with attention deficit hyperactivity disorder. Molecular Psychiatry *1*, 121–124.

Lahti, A.C., Koffel, B., LaPorte, D., and Tamminga, C.A. (1995). Subanesthetic doses of ketamine stimulate psychosis in schizophrenia. Neuropsychopharmacology *13*, 9–19.

Lambe, E.K., Krimer, L.S., and Goldman-Rakic, P.S. (2000). Differential postnatal development of catecholamine and serotonin inputs to

identified neurons in prefrontal cortex of rhesus monkey. Journal of Neuroscience *20*, 8780–8787.

Lammel, S., Hetzel, A., Häckel, O., Jones, I., Liss, B., and Roeper, J. (2008). Unique properties of mesoprefrontal neurons within a dual mesocorticolimbic dopamine system. Neuron *57*, 760–773.

Lauzon, N.M., Bishop, S.F., and Laviolette, S.R. (2009). Dopamine D1 versus D4 Receptors Differentially Modulate the Encoding of Salient versus Nonsalient Emotional Information in the Medial Prefrontal Cortex. Journal of Neuroscience *29*, 4836–4845.

Lavin, A., Nogueira, L., Lapish, C.C., Wightman, R.M., Phillips, P.E.M., and Seamans, J.K. (2005). Mesocortical Dopamine Neurons Operate in Distinct Temporal Domains Using Multimodal Signaling. Journal of Neuroscience *25*, 5013–5023.

Laviolette, S.R., Lipski, W.J., and Grace, A.A. (2005). A Subpopulation of Neurons in the Medial Prefrontal Cortex Encodes Emotional Learning with Burst and Frequency Codes through a Dopamine D4 Receptor-Dependent Basolateral Amygdala Input. Journal of Neuroscience *25*, 6066–6075.

Lazarewicz, M.T., Ehrlichman, R.S., Maxwell, C.R., Gandal, M.J., Finkel, L.H., and Siegel, S.J. (2009). Ketamine Modulates Theta and Gamma Oscillations. Journal of Cognitive Neuroscience *22*, 1452–1464.

Lee, S., and Jones, S.R. (2013). Distinguishing mechanisms of gamma frequency oscillations in human current source signals using a computational model of a laminar neocortical network. Frontiers in Human Neuroscience *7*, 869.

Lee, A.M., Hoy, J.L., Bonci, A., Wilbrecht, L., Stryker, M.P., and Niell, C.M. (2014). Identification of a brainstem circuit regulating visual cortical state in parallel with locomotion. Neuron *83*, 455–466.

Lenz, D., Krauel, K., Schadow, J., Baving, L., Duzel, E., and Herrmann, C.S. (2008). Enhanced gamma-band activity in ADHD patients lacks correlation with memory performance found in healthy children. Brain Research *1235*, 117–132.

Lewis, D.A., Hashimoto, T., and Volk, D.W. (2005). Cortical inhibitory neurons and schizophrenia. Nature Reviews Neuroscience *6*, 312–324.

Lewis, D.A., Fish, K.N., Arion, D., and Gonzalez-Burgos, G. (2011). Perisomatic inhibition and cortical circuit dysfunction in schizophrenia. Current Opinions in Neurobiology *21*, 866–872.

Li, H., Zhang, Z., Blackburn, M.R., Wang, S.W., Ribelayga, C.P., and O'Brien, J. (2013). Adenosine and Dopamine Receptors Coregulate Photoreceptor Coupling via Gap Junction Phosphorylation in Mouse Retina. Journal of Neuroscience *33*, 3135–3150.

Li, K.-X., Lu, Y.-M., Xu, Z.-H., Zhang, J., Zhu, J.-M., Zhang, J.-M., Cao, S.-X., Chen, X.-J., Chen, Z., Luo, J.-H., et al. (2012). Neuregulin 1 regulates excitability of fast-spiking neurons through Kv1.1 and acts in epilepsy. Nature Neuroscience *15*, 267–273.

Li, N., Lee, B., Liu, R.-J., Banasr, M., Dwyer, J.M., Iwata, M., Li, X.-Y., Aghajanian, G., and Duman, R.S. (2010). mTOR-dependent synapse formation underlies the rapid antidepressant effects of NMDA antagonists. Science *329*, 959–964.

Li, Y.-C., Xi, D., Roman, J., Huang, Y.-Q., and Gao, W.-J. (2009). Activation of Glycogen Synthase Kinase-3β Is Required for Hyperdopamine and D2 Receptor-Mediated Inhibition of Synaptic NMDA Receptor Function in the Rat Prefrontal Cortex. Journal of Neuroscience *29*, 15551–15563.

Lidow, M.S., Wang, F., Cao, Y., and Goldman-Rakic, P.S. (1998). Layer V neurons bear the majority of mRNAs encoding the five distinct dopamine receptor subtypes in the primate prefrontal cortex. Synapse *28*, 10–20.

Lipschitz, D.S., DSouza, D.C., White, J.A., Charney, D.S., and Krystal, I.H. (1997). Clozapine blockade of ketamine effects in healthy subjects. In Biological Psychiatry, pp. 76–76.

Lisman, J.E., Coyle, J.T., Green, R.W., Javitt, D.C., Benes, F.M., Heckers, S., and Grace, A.A. (2008). Circuit-based framework for understanding neurotransmitter and risk gene interactions in schizophrenia. Trends in Neuroscience *31*, 234–242.

Lladó-Pelfort, L., Troyano-Rodriguez, E., van den Munkhof, H.E., Cervera-Ferri, A., Jurado, N., Núñez-Calvet, M., Artigas, F., and Celada, P. (2016). Phencyclidine-induced disruption of oscillatory activity in prefrontal cortex: Effects of antipsychotic drugs and receptor ligands. European Neuropsychopharmacology *26*, 614–625.

Lodge, D., and Mercier, M.S. (2015). Ketamine and phencyclidine: the good, the bad and the unexpected. British Journal of Pharmacology *172*, 4254–4276.

Löscher, W., Annies, R., and Hönack, D. (1991). The N-methyl-D-aspartate receptor antagonist MK-801 induces increases in dopamine and serotonin metabolism in several brain regions of rats. Neuroscience Letters *128*, 191–194.

Luo, X., He, W., Hu, X., and Yan, R. (2014). Reversible overexpression of bace1-cleaved neuregulin-1 N-terminal fragment induces schizophrenia-like phenotypes in mice. Biological Psychiatry *76*, 120–127.

Lynall, M.-E., Bassett, D.S., Kerwin, R., McKenna, P.J., Kitzbichler, M., Muller, U., and Bullmore, E. (2010). Functional connectivity and brain networks in schizophrenia. Journal of Neuroscience *30*, 9477–9487.

Ma, J., and Leung, L.S. (2014). Deep brain stimulation of the medial septum or nucleus accumbens alleviates psychosis-relevant behavior in ketamine-treated rats. Behavioral Brain Research *266*, 174–182.

Maeng, S., Zarate, C.A., Du, J., Schloesser, R.J., McCammon, J., Chen, G., and Manji, H.K. (2008). Cellular Mechanisms Underlying the Antidepressant Effects of Ketamine: Role of α-Amino-3-Hydroxy-5-Methylisoxazole-4-Propionic Acid Receptors. Biological Psychiatry *63*, 349–352.

Maher, B.S., Marazita, M.L., Ferrell, R.E., and Vanyukov, M.M. (2002). Dopamine system genes and attention deficit hyperactivity disorder: a meta-analysis. Psychiatric Genetics *12*, 207–215.

Makara, J.K., and Magee, J.C. (2013). Variable dendritic integration in hippocampal CA3 pyramidal neurons. Neuron *80*, 1438–1450.

Malhotra, A.K., Adler, C.M., Kennison, S.D., Elman, I., Pickar, D., and Breier, A. (1997). Clozapine Blunts N-Methyl-d-Aspartate Antagonist-Induced Psychosis: A Study with Ketamine. Biological Psychiatry *42*, 664–668.

Manahan-Vaughan, D., von Haebler, D., Winter, C., Juckel, G., and Heinemann, U. (2008). A single application of MK801 causes symptoms of acute psychosis, deficits in spatial memory, and impairment of synaptic plasticity in rats. Hippocampus *18*, 125–134.

Mann, E.O., and Mody, I. (2010). Control of hippocampal gamma oscillation frequency by tonic inhibition and excitation of interneurons. Nature Neuroscience *13*, 205–212.

Markram, H., Toledo-Rodriguez, M., Wang, Y., Gupta, A., Silberberg, G., and Wu, C. (2004). Interneurons of the neocortical inhibitory system. Nature Reviews Neuroscience *5*, 793–807.

Martina, M., and Bergeron, R. (2008). D1 and D4 dopaminergic receptor interplay mediates coincident G protein-independent and dependent regulation of glutamate NMDA receptors in the lateral amygdala. Journal of Neurochemistry *106*, 2421–2435.

Mattay, V.S., Goldberg, T.E., Fera, F., Hariri, A.R., Tessitore, A., Egan, M.F., Kolachana, B., Callicott, J.H., and Weinberger, D.R. (2003). Catechol O-methyltransferase val158-met genotype and individual variation in the brain response to amphetamine. Proceedings of the National Academy of Science *100*, 6186–6191.

Maurice, N., Tkatch, T., Meisler, M., Sprunger, L.K., and Surmeier, D.J. (2001). D1/D5 Dopamine Receptor Activation Differentially Modulates Rapidly Inactivating and Persistent Sodium Currents in Prefrontal Cortex Pyramidal Neurons. Journal of Neuroscience *21*, 2268–2277.

McGinley, M.J., Vinck, M., Reimer, J., Batista-Brito, R., Zagha, E., Cadwell, C.R., Tolias, A.S., Cardin, J.A., and McCormick, D.A. (2015a). Waking State: Rapid Variations Modulate Neural and Behavioral Responses. Neuron *87*, 1143–1161.

McGinley, M.J., David, S.V., and McCormick, D.A. (2015b). Cortical Membrane Potential Signature of Optimal States for Sensory Signal Detection. Neuron *87*, 179–192.

Mei, L., and Nave, K.-A. (2014). Neuregulin-ERBB Signaling in the Nervous System and Neuropsychiatric Diseases. Neuron *83*, 27–49.

Mei, L., and Xiong, W.C. (2008). Neuregulin 1 in neural development, synaptic plasticity and schizophrenia. Nature Reviews Neuroscience *9*, 437–452.

Mei, Y.A., Griffon, N., Buquet, C., Martres, M.P., Vaudry, H., Schwartz, J.-C., Sokoloff, P., and Cazin, L. (1995). Activation of dopamine D4 receptor inhibits an L-type calcium current in cerebellar granule cells. Neuroscience *68*, 107–116.

Meltzer, H.Y., and Huang, M. (2008). In vivo actions of atypical antipsychotic drug on serotonergic and dopaminergic systems. Progress in Brain Research *172*, 177–197.

Meltzer, H.Y., Rajagopal, L., Huang, M., Oyamada, Y., Kwon, S., and Horiguchi, M. (2013). Translating the N-methyl-D-aspartate receptor antagonist model of schizophrenia to treatments for cognitive impairment in schizophrenia. International Journal of Neuropsychopharmacology CINP *16*, 2181–2194.

Meyer-Lindenberg, A., Miletich, R.S., Kohn, P.D., Esposito, G., Carson, R.E., Quarantelli, M., Weinberger, D.R., and Berman, K.F. (2002). Reduced prefrontal activity predicts exaggerated striatal dopaminergic function in schizophrenia. Nature Neuroscience *5*, 267–271.

Michaelides, M., Pascau, J., Gispert, J.D., Delis, F., Grandy, D.K., Wang, G.J., Desco, M., Rubinstein, M., Volkow, N.D., and Thanos, P.K. (2010). Dopamine D4 receptors modulate brain metabolic activity in the prefrontal cortex and cerebellum at rest and in response to methylphenidate. European Journal of Neuroscience *32*, 668–676.

Miller, E.K., and Cohen, J.D. (2001). An integrative theory of prefrontal cortex function. Annual Review of Neuroscience *24*, 167–202.

Miller, O.H., Yang, L., Wang, C.-C., Hargroder, E.A., Zhang, Y., Delpire, E., and Hall, B.J. (2014). GluN2B-containing NMDA receptors regulate depression-like behavior and are critical for the rapid antidepressant actions of ketamine. eLife *3*, e03581.

Miller, O.H., Moran, J.T., and Hall, B.J. (2016). Two cellular hypotheses explaining the initiation of ketamine's antidepressant actions: Direct inhibition and disinhibition. Neuropharmacology *100*, 17–26.

Miner, L.H., Schroeter, S., Blakely, R.D., and Sesack, S.R. (2003). Ultrastructural localization of the norepinephrine transporter in superficial and deep layers of the rat prelimbic prefrontal cortex and its spatial relationship to probable dopamine terminals. Journal of Computational Neurology *466*, 478–494.

Minzenberg, M.J., and Carter, C.S. (2012). Developing treatments for impaired cognition in schizophrenia. Trends in Cognitive Science *16*, 35–42.

Minzenberg, M.J., Firl, A.J., Yoon, J.H., Gomes, G.C., Reinking, C., and Carter, C.S. (2010). Gamma Oscillatory Power is Impaired During Cognitive

Control Independent of Medication Status in First-Episode Schizophrenia. Neuropsychopharmacology *35*, 2590–2599.

Missale, C., Nash, S.R., Robinson, S.W., Jaber, M., and Caron, M.G. (1998). Dopamine Receptors: From Structure to Function. Physiology Review *78*, 189–225.

Mitchell, A.S., and Chakraborty, S. (2013). What does the mediodorsal thalamus do? Frontiers in Systems Neuroscience *7*, 37.

Mitchell, R.M., Janssen, M.J., Karavanova, I., Vullhorst, D., Furth, K., Makusky, A., Markey, S.P., and Buonanno, A. (2013). ErbB4 reduces synaptic GABAA currents independent of its receptor tyrosine kinase activity. Proceedings of the National Academy of Science *110*, 19603–19608.

Miura, Y., Ito, T., and Kadokawa, T. (1987). Effects of intraseptally injected dopamine and noradrenaline on hippocampal synchronized theta wave activity in rats. Japanese Journal of Pharmacology *44*, 471–479.

Moca, V.V., Nikolić, D., Singer, W., and Mureşan, R.C. (2014). Membrane Resonance Enables Stable and Robust Gamma Oscillations. Cerebral Cortex N. Y. NY *24*, 119–142.

Moghaddam, B., Adams, B., Verma, A., and Daly, D. (1997). Activation of Glutamatergic Neurotransmission by Ketamine: A Novel Step in the Pathway from NMDA Receptor Blockade to Dopaminergic and Cognitive Disruptions Associated with the Prefrontal Cortex. Journal of Neuroscience *17*, 2921–2927.

Molina, L.A., Skelin, I., and Gruber, A.J. (2014). Acute NMDA Receptor Antagonism Disrupts Synchronization of Action Potential Firing in Rat Prefrontal Cortex. PLoS ONE *9*, e85842.

Moore, A.R., Zhou, W.-L., Potapenko, E.S., Kim, E.-J., and Antic, S.D. (2011). Brief dopaminergic stimulations produce transient physiological changes in prefrontal pyramidal neurons. Brain Research *1370*, 1–15.

Moreland, R.B., Patel, M., Hsieh, G.C., Wetter, J.M., Marsh, K., and Brioni, J.D. (2005). A-412997 is a selective dopamine D4 receptor agonist in rats. Pharmacology Biochemical Behavioral *82*, 140–147.

Motulsky, H.J., and Brown, R.E. (2006). Detecting outliers when fitting data with nonlinear regression – a new method based on robust nonlinear regression and the false discovery rate. BMC Bioinformatics *7*, 123.

Mrzljak, L., Bergson, C., Pappy, M., Huff, R., Levenson, R., and Goldman-Rakic, P.S. (1996). Localization of dopamine D4 receptors in GABAergic neurons of the primate brain. Nature *381*, 245–248.

Munk, M.H., Roelfsema, P.R., König, P., Engel, A.K., and Singer, W. (1996). Role of reticular activation in the modulation of intracortical synchronization. Science *272*, 271–274.

Murai, T., Nakako, T., Ikeda, K., Ikejiri, M., Ishiyama, T., and Taiji, M. (2014). Lack of dopamine D4 receptor affinity contributes to the procognitive effect of lurasidone. Behavioral Brain Research *261*, 26–30.

Muthukumaraswamy, S.D., Shaw, A.D., Jackson, L.E., Hall, J., Moran, R., and Saxena, N. (2015). Evidence that Subanesthetic Doses of Ketamine Cause Sustained Disruptions of NMDA and AMPA-Mediated Frontoparietal Connectivity in Humans. Journal of Neuroscience *35*, 11694–11706.

Nakagawa, T., Ukai, K., Ohyama, T., Gomita, Y., and Okamura, H. (2000). Effect of dopaminergic drugs on the reserpine-induced lowering of hippocampal theta wave frequency in rats. Nihon Shinkei Seishin Yakurigaku Zasshi (Japan) *20*, 71.

Nakao, K., and Nakazawa, K. (2014). Brain state-dependent abnormal LFP activity in the auditory cortex of a schizophrenia mouse model. Frontiers in Neuroscience *8*, 168.

Nakazawa, K., Zsiros, V., Jiang, Z., Nakao, K., Kolata, S., Zhang, S., and Belforte, J.E. (2012). GABAergic interneuron origin of schizophrenia pathophysiology. Neuropharmacology *62*, 1574–1583.

Nakazawa, S., Murai, T., Miyauchi, M., Kotani, M., and Ikeda, K. (2015). Behavioral and neurophysiological effects of Ro 10-5824, a dopamine D4 receptor partial agonist, in common marmosets. Psychopharmacology (Berlin) *232*, 3287–3295.

Naneix, F., Marchand, A.R., Di Scala, G., Pape, J.-R., and Coutureau, E. (2012). Parallel maturation of goal-directed behavior and dopaminergic systems during adolescence. Journal of Neuroscience *32*, 16223–16232.

Nayak, S., and Cassaday, H.J. (2003). The novel dopamine D4 receptor agonist (PD 168,077 maleate): Doses with different effects on locomotor

activity are without effect in classical conditioning. Progress in Neuropsychopharmacological and Biological Psychiatry *27*, 441–449.

Neddens, J., and Buonanno, A. (2010). Selective populations of hippocampal interneurons express ErbB4 and their number and distribution is altered in ErbB4 knockout mice. Hippocampus *20*, 724–744.

Neymotin, S.A., Lazarewicz, M.T., Sherif, M., Contreras, D., Finkel, L.H., and Lytton, W.W. (2011). Ketamine disrupts θ modulation of γ in a computer model of hippocampus. Journal of Neuroscience *31*, 11733–11743.

Nicodemus, K.K., Luna, A., Vakkalanka, R., Goldberg, T., Egan, M., Straub, R.E., and Weinberger, D.R. (2006). Further evidence for association between ErbB4 and schizophrenia and influence on cognitive intermediate phenotypes in healthy controls. Molecular Psychiatry *11*, 1062–1065.

Nicodemus, K.K., Law, A.J., Radulescu, E., Luna, A., Kolachana, B., Vakkalanka, R., Rujescu, D., Giegling, I., Straub, R.E., McGee, K., et al. (2010). Biological validation of increased schizophrenia risk with NRG1, ERBB4, and AKT1 epistasis via functional neuroimaging in healthy controls. Archives in Genetic Psychiatry *67*, 991–1001.

Nicolás, M.J., López-Azcárate, J., Valencia, M., Alegre, M., Pérez-Alcázar, M., Iriarte, J., and Artieda, J. (2011). Ketamine-Induced Oscillations in the Motor Circuit of the Rat Basal Ganglia. PLOS ONE *6*, e21814.

Niell, C.M., and Stryker, M.P. (2010). Modulation of visual responses by behavioral state in mouse visual cortex. Neuron *65*, 472–479.

Nikiforuk, A., Hołuj, M., Kos, T., and Popik, P. (2016). The effects of a 5-HT5A receptor antagonist in a ketamine-based rat model of cognitive dysfunction and the negative symptoms of schizophrenia. Neuropharmacology *105*, 351–360.

Nir, Y., Fisch, L., Mukamel, R., Gelbard-Sagiv, H., Arieli, A., Fried, I., and Malach, R. (2007). Coupling between Neuronal Firing Rate, Gamma LFP, and BOLD fMRI Is Related to Interneuronal Correlations. Current Biology *17*, 1275–1285.

Noain, D., Avale, M.E., Wedemeyer, C., Calvo, D., Peper, M., and Rubinstein, M. (2006). Identification of brain neurons expressing the dopamine D4

receptor gene using BAC transgenic mice. European Journal of Neuroscience *24*, 2429–2438.

Nosyreva, E., Szabla, K., Autry, A.E., Ryazanov, A.G., Monteggia, L.M., and Kavalali, E.T. (2013). Acute suppression of spontaneous neurotransmission drives synaptic potentiation. Journal of Neuroscience *33*, 6990–7002.

Nyíri, G., Stephenson, F.A., Freund, T.F., and Somogyi, P. (2003). Large variability in synaptic N-methyl-D-aspartate receptor density on interneurons and a comparison with pyramidal-cell spines in the rat hippocampus. Neuroscience *119*, 347–363.

O'Donnell, P. (2011). Adolescent Onset of Cortical Disinhibition in Schizophrenia: Insights from Animal Models. Schizophrenia Bulletin *37*, 484–492.

Okada, M., Onodera, K., Renterghem, C.V., Sieghart, W., and Takahashi, T. (2000). Functional Correlation of GABAA Receptor α Subunits Expression with the Properties of IPSCs in the Developing Thalamus. Journal of Neuroscience *20*, 2202–2208.

Okaty, B.W., Miller, M.N., Sugino, K., Hempel, C.M., and Nelson, S.B. (2009). Transcriptional and Electrophysiological Maturation of Neocortical Fast-Spiking GABAergic Interneurons. Journal of Neuroscience *29*, 7040–7052.

Olney, J.W., Newcomer, J.W., and Farber, N.B. (1999). NMDA receptor hypofunction model of schizophrenia. Journal of Psychiatric Research *33*, 523–533.

Onn, S.P., and Grace, A.A. (1994). Dye coupling between rat striatal neurons recorded in vivo: compartmental organization and modulation by dopamine. Journal of Neurophysiology *71*, 1917–1934.

Onn, S.-P., Wang, X.-B., Lin, M., and Grace, A.A. (2006). Dopamine D1 and D4 Receptor Subtypes Differentially Modulate Recurrent Excitatory Synapses in Prefrontal Cortical Pyramidal Neurons. Neuropsychopharmacology *31*, 318–338.

Otmakhova, N.A., and Lisman, J.E. (1996). D1/D5 Dopamine Receptor Activation Increases the Magnitude of Early Long-Term Potentiation at CA1 Hippocampal Synapses. Journal of Neuroscience *16*, 7478–7486.

Owen, S.F., Tuncdemir, S.N., Bader, P.L., Tirko, N.N., Fishell, G., and Tsien, R.W. (2013). Oxytocin enhances hippocampal spike transmission by modulating fast-spiking interneurons. Nature *500*, 458–462.

Oye, I., Paulsen, O., and Maurset, A. (1992). Effects of ketamine on sensory perception: evidence for a role of N-methyl-D-aspartate receptors. Journal of Pharmacology and Experimental Therapeutics *260*, 1209–1213.

Ozaki, M., Sasner, M., Yano, R., Lu, H.S., and Buonanno, A. (1997). Neuregulin-beta induces expression of an NMDA-receptor subunit. Nature *390*, 691–694.

Parlapani, E., Schmitt, A., Wirths, O., Bauer, M., Sommer, C., Rueb, U., Skowronek, M.H., Treutlein, J., Petroianu, G.A., Rietschel, M., et al. (2010). Gene expression of neuregulin-1 isoforms in different brain regions of elderly schizophrenia patients. World Journal of Biological Psychiatry *11*, 243–250.

Parnaudeau, S., O'Neill, P.-K., Bolkan, S.S., Ward, R.D., Abbas, A.I., Roth, B.L., Balsam, P.D., Gordon, J.A., and Kellendonk, C. (2013). Inhibition of Mediodorsal Thalamus Disrupts Thalamofrontal Connectivity and Cognition. Neuron *77*, 1151–1162.

Penit-Soria, J., Audinat, E., and Crepel, F. (1987). Excitation of rat prefrontal cortical neurons by dopamine: An in vitro electrophysiological study. Brain Research *425*, 263–274.

Pillai, G., Brown, N.A., McAllister, G., Milligan, G., and Seabrook, G.R. (1998). Human D2 and D4 dopamine receptors couple through βγ G-protein subunits to inwardly rectifying K+ channels (GIRK1) in a Xenopus oocyte expression system: selective antagonism by L-741,626 and L-745,870 respectively. Neuropharmacology *37*, 983–987.

Pinault, D. (2008). N-Methyl d-Aspartate Receptor Antagonists Ketamine and MK-801 Induce Wake-Related Aberrant γ Oscillations in the Rat Neocortex. Biological Psychiatry *63*, 730–735.

Pitcher, G.M., Beggs, S., Woo, R.-S., Mei, L., and Salter, M.W. (2008). ErbB4 is a suppressor of long-term potentiation in the adult hippocampus. Neuroreport *19*, 139–143.

Pitcher, G.M., Kalia, L.V., Ng, D., Goodfellow, N.M., Yee, K.T., Lambe, E.K., and Salter, M.W. (2011). Schizophrenia susceptibility pathway neuregulin

1-ErbB4 suppresses Src upregulation of NMDA receptors. Nature Medicine *17*, 470–478.

Pittman-Polletta, B.R., Kocsis, B., Vijayan, S., Whittington, M.A., and Kopell, N.J. (2015). Brain rhythms connect impaired inhibition to altered cognition in schizophrenia. Biological Psychiatry *77*, 1020–1030.

Porter, L.L., Rizzo, E., and Hornung, J.-P. (1999). Dopamine Affects Parvalbumin Expression during Cortical Development in vitro. Journal of Neuroscience *19*, 8990–9003.

Povysheva, N.V., and Johnson, J.W. (2012). Tonic NMDA receptor-mediated current in prefrontal cortical pyramidal cells and fast-spiking interneurons. Journal of Neurophysiology *107*, 2232–2243.

Quirk, M.C., Sosulski, D.L., Feierstein, C.E., Uchida, N., and Mainen, Z.F. (2009). A defined network of fast-spiking interneurons in orbitofrontal cortex: responses to behavioral contingencies and ketamine administration. Frontiers in Systems Neuroscience *3*, 13.

Ray, S. (2015). Challenges in the quantification and interpretation of spike-LFP relationships. Current Opinions in Neurobiology *31*, 111–118.

Ray, S., and Maunsell, J.H.R. (2011). Different Origins of Gamma Rhythm and High-Gamma Activity in Macaque Visual Cortex. PLoS Biology *9*, e1000610.

Reichenberg, A., Weiser, M., Rabinowitz, J., Caspi, A., Schmeidler, J., Mark, M., Kaplan, Z., and Davidson, M. (2002). A population-based cohort study of premorbid intellectual, language, and behavioral functioning in patients with schizophrenia, schizoaffective disorder, and nonpsychotic bipolar disorder. American Journal of Psychiatry *159*, 2027–2035.

Reimann, M.W., Anastassiou, C.A., Perin, R., Hill, S.L., Markram, H., and Koch, C. (2013). A Biophysically Detailed Model of Neocortical Local Field Potentials Predicts the Critical Role of Active Membrane Currents. Neuron *79*, 375–390.

Reimer, J., Froudarakis, E., Cadwell, C.R., Yatsenko, D., Denfield, G.H., and Tolias, A.S. (2014). Pupil Fluctuations Track Fast Switching of Cortical States during Quiet Wakefulness. Neuron *84*, 355–362.

Rivolta, D., Heidegger, T., Scheller, B., Sauer, A., Schaum, M., Birkner, K., Singer, W., Wibral, M., and Uhlhaas, P.J. (2015). Ketamine Dysregulates the Amplitude and Connectivity of High-Frequency Oscillations in Cortical-Subcortical Networks in Humans: Evidence from Resting-State Magnetoencephalography-Recordings. Schizophrenia Bulletin *41*, 1105–1114.

Robbins, T.W., and Arnsten, A.F.T. (2009). The neuropsychopharmacology of fronto-executive function: monoaminergic modulation. Annual Review of Neuroscience *32*, 267.

Robinson, S., Smith, D.M., Mizumori, S.J.Y., and Palmiter, R.D. (2004). Firing properties of dopamine neurons in freely moving dopamine-deficient mice: effects of dopamine receptor activation and anesthesia. Proceedings of the National Academy of Science U. S. A. *101*, 13329–13334.

Romo-Parra, H., Aceves, J., and Gutiérrez, R. (2005). Tonic modulation of inhibition by dopamine D4 receptors in the rat hippocampus. Hippocampus *15*, 254–259.

Rondou, P., Haegeman, G., and Van Craenenbroeck, K. (2010). The dopamine D4 receptor: biochemical and signalling properties. Cellular and Molecular Life Science *67*, 1971–1986.

Roopun, A.K., Cunningham, M.O., Racca, C., Alter, K., Traub, R.D., and Whittington, M.A. (2008). Region-specific changes in gamma and beta2 rhythms in NMDA receptor dysfunction models of schizophrenia. Schizophrenia Bulletin *34*, 962–973.

Rosen, A.M., Spellman, T., and Gordon, J.A. (2015a). Electrophysiological Endophenotypes in Rodent Models of Schizophrenia and Psychosis. Biological Psychiatry *77*, 1041–1049.

Rosen, Z.B., Cheung, S., and Siegelbaum, S.A. (2015b). Midbrain dopamine neurons bidirectionally regulate CA3-CA1 synaptic drive. Nature Neuroscience *18*, 1763–1771.

Rosenberg, D.R., and Lewis, D.A. (1995). Postnatal maturation of the dopaminergic innervation of monkey prefrontal and motor cortices: a tyrosine hydroxylase immunohistochemical analysis. Journal of Computational Neurology *358*, 383–400.

Rosenberg, J.R., Amjad, A.M., Breeze, P., Brillinger, D.R., and Halliday, D.M. (1989). The Fourier approach to the identification of functional coupling between neuronal spike trains. Progress in Biophysical Molecular Biology *53*, 1–31.

Ross, N.R., and Porter, L.L. (2002). Effects of dopamine and estrogen upon cortical neurons that express parvalbumin in vitro. Developmental Brain Research *137*, 23–34.

Rotaru, D.C., Yoshino, H., Lewis, D.A., Ermentrout, G.B., and Gonzalez-Burgos, G. (2011). Glutamate Receptor Subtypes Mediating Synaptic Activation of Prefrontal Cortex Neurons: Relevance for Schizophrenia. Journal of Neuroscience *31*, 142–156.

Rotaru, D.C., Lewis, D.A., and Gonzalez-Burgos, G. (2012). The role of glutamatergic inputs onto parvalbumin-positive interneurons: relevance for schizophrenia. Review of Neuroscience *23*, 97–109.

Rowe, D.C., Stever, C., Giedinghagen, L.N., Gard, J.M., Cleveland, H.H., Terris, S.T., Mohr, J.H., Sherman, S., Abramowitz, A., and Waldman, I.D. (1998). Dopamine DRD4 receptor polymorphism and attention deficit hyperactivity disorder. Molecular Psychiatry *3*, 419–426.

Rowland, L.M. (2005). Subanesthetic ketamine: how it alters physiology and behavior in humans. Aviation, Space, and Environmental Medicine *76*, C52-58.

Rubinstein, M., Phillips, T.J., Bunzow, J.R., Falzone, T.L., Dziewczapolski, G., Zhang, G., Fang, Y., Larson, J.L., McDougall, J.A., Chester, J.A., et al. (1997). Mice Lacking Dopamine D4 Receptors Are Supersensitive to Ethanol, Cocaine, and Methamphetamine. Cell *90*, 991–1001.

Rubinstein, M., Cepeda, C., Hurst, R.S., Flores-Hernandez, J., Ariano, M.A., Falzone, T.L., Kozell, L.B., Meshul, C.K., Bunzow, J.R., Low, M.J., et al. (2001). Dopamine D4 Receptor-Deficient Mice Display Cortical Hyperexcitability. Journal of Neuroscience *21*, 3756–3763.

Sakurai, T., Gamo, N.J., Hikida, T., Kim, S.-H., Murai, T., Tomoda, T., and Sawa, A. (2015). Converging models of schizophrenia - Network alterations of prefrontal cortex underlying cognitive impairments. Progress in Neurobiology *134*, 178–201.

Salt, T.E., and Eaton, S.A. (1996). Functions of ionotropic and metabotropic glutamate receptors in sensory transmission in the mammalian thalamus. Progress in Neurobiology *48*, 55–72.

Santana, N., Mengod, G., and Artigas, F. (2009). Quantitative Analysis of the Expression of Dopamine D1 and D2 Receptors in Pyramidal and GABAergic Neurons of the Rat Prefrontal Cortex. Cerebral Cortex *19*, 849–860.

Santana, N., Troyano-Rodriguez, E., Mengod, G., Celada, P., and Artigas, F. (2011). Activation of thalamocortical networks by the N-methyl-D-aspartate receptor antagonist phencyclidine: reversal by clozapine. Biological Psychiatry *69*, 918–927.

Saunders, J.A., Gandal, M.J., and Siegel, S.J. (2012). NMDA antagonists recreate signal-to-noise ratio and timing perturbations present in schizophrenia. Neurobiological Disorders *46*, 93–100.

Sawaguchi, T., and Goldman-Rakic, P.S. (1994). The role of D1-dopamine receptor in working memory: local injections of dopamine antagonists into the prefrontal cortex of rhesus monkeys performing an oculomotor delayed-response task. Journal of Neurophysiology *71*, 515–528.

Scanziani, M., Gähwiler, B.H., and Charpak, S. (1998). Target cell-specific modulation of transmitter release at terminals from a single axon. Proceedings of the National Academy of Science *95*, 12004–12009.

Scheidegger, M., Walter, M., Lehmann, M., Metzger, C., Grimm, S., Boeker, H., Boesiger, P., Henning, A., and Seifritz, E. (2012). Ketamine decreases resting state functional network connectivity in healthy subjects: implications for antidepressant drug action. PloS One *7*, e44799.

Schreiber, S., Fellous, J.-M., Tiesinga, P., and Sejnowski, T.J. (2004). Influence of Ionic Conductances on Spike Timing Reliability of Cortical Neurons for Suprathreshold Rhythmic Inputs. Journal of Neurophysiology *91*, 194–205.

Schultz, W. (2007). Multiple dopamine functions at different time courses. Annual Review of Neuroscience *30*, 259–288.

Schulz, S.B., Heidmann, K.E., Mike, A., Klaft, Z.J., Heinemann, U., and Gerevich, Z. (2012). First and second generation antipsychotics influence

hippocampal gamma oscillations by interactions with 5-HT(3) and D(3) receptors. British Journal of Pharmacology *167*, 1480–1491.

Seamans, J.K., and Yang, C.R. (2004). The principal features and mechanisms of dopamine modulation in the prefrontal cortex. Progress in Neurobiology *74*, 1–58.

Seamans, J.K., Durstewitz, D., Christie, B.R., Stevens, C.F., and Sejnowski, T.J. (2001). Dopamine D1/D5 receptor modulation of excitatory synaptic inputs to layer V prefrontal cortex neurons. Proceedings of the National Academy of Science *98*, 301–306.

Séguéla, P., Watkins, K.C., and Descarries, L. (1988). Ultrastructural features of dopamine axon terminals in the anteromedial and the suprarhinal cortex of adult rat. Brain Research *442*, 11–22.

Shaffer, C.L., Osgood, S.M., Smith, D.L., Liu, J., and Trapa, P.E. (2014). Enhancing ketamine translational pharmacology via receptor occupancy normalization. Neuropharmacology *86*, 174–180.

Shah, A.A., Sjovold, T., and Treit, D. (2004). Selective antagonism of medial prefrontal cortex D4 receptors decreases fear-related behaviour in rats. European Journal of Neuroscience *19*, 3393–3397.

Shamir, A., Kwon, O.-B., Karavanova, I., Vullhorst, D., Leiva-Salcedo, E., Janssen, M.J., and Buonanno, A. (2012). The importance of the NRG-1/ErbB4 pathway for synaptic plasticity and behaviors associated with psychiatric disorders. Journal of Neuroscience *32*, 2988–2997.

Shaw, A.D., Saxena, N., E Jackson, L., Hall, J.E., Singh, K.D., and Muthukumaraswamy, S.D. (2015). Ketamine amplifies induced gamma frequency oscillations in the human cerebral cortex. European Neuropsychopharmacology *25*, 1136–1146.

Sherman, S.M. (2013). The Function of Metabotropic Glutamate Receptors in Thalamus and Cortex. The Neuroscientist 1073858413478490.

Shigetomi, E., Tong, X., Kwan, K.Y., Corey, D.P., and Khakh, B.S. (2012). TRPA1 channels regulate astrocyte resting calcium and inhibitory synapse efficacy through GAT-3. Nature Neuroscience *15*, 70–80.

Shin, R.-M., Masuda, M., Miura, M., Sano, H., Shirasawa, T., Song, W.-J., Kobayashi, K., and Aosaki, T. (2003). Dopamine D4 Receptor-Induced

Postsynaptic Inhibition of GABAergic Currents in Mouse Globus Pallidus Neurons. Journal of Neuroscience *23*, 11662–11672.

Sigurdsson, T., Stark, K.L., Karayiorgou, M., Gogos, J.A., and Gordon, J.A. (2010). Impaired hippocampal–prefrontal synchrony in a genetic mouse model of schizophrenia. Nature *464*, 763–767.

Sik, A., Penttonen, M., Ylinen, A., and Buzsaki, G. (1995). Hippocampal CA1 interneurons: an in vivo intracellular labeling study. Journal of Neuroscience *15*, 6651–6665.

Silberberg, G., Darvasi, A., Pinkas-Kramarski, R., and Navon, R. (2006). The involvement of ErbB4 with schizophrenia: association and expression studies. American Journal of Medical Genetics *141B*, 142–148.

Simpson, E.H., Kellendonk, C., and Kandel, E. (2010). A possible role for the striatum in the pathogenesis of the cognitive symptoms of schizophrenia. Neuron *65*, 585–596.

Singer, W. (1993). Synchronization of Cortical Activity and its Putative Role in Information Processing and Learning. Annual Review of Physiology *55*, 349–374.

Sirota, A., Montgomery, S., Fujisawa, S., Isomura, Y., Zugaro, M., and Buzsáki, G. (2008). Entrainment of Neocortical Neurons and Gamma Oscillations by the Hippocampal Theta Rhythm. Neuron *60*, 683–697.

Smalley, S.L., Bailey, J.N., Palmer, C.G., Cantwell, D.P., McGough, J.J., Del'Homme, M.A., Asarnow, J.R., Woodward, J.A., Ramsey, C., and Nelson, S.F. (1998). Evidence that the dopamine D4 receptor is a susceptibility gene in attention deficit hyperactivity disorder. Molecular Psychiatry *3*, 427–430.

Smiley, J.F., and Goldman-Rakic, P.S. (1993). Heterogeneous targets of dopamine synapses in monkey prefrontal cortex demonstrated by serial section electron microscopy: a laminar analysis using the silver-enhanced diaminobenzidine sulfide (SEDS) immunolabeling technique. Cerebral Cortex *3*, 223–238.

Smith, J.W., Gastambide, F., Gilmour, G., Dix, S., Foss, J., Lloyd, K., Malik, N., and Tricklebank, M. (2011). A comparison of the effects of ketamine and phencyclidine with other antagonists of the NMDA receptor in rodent assays of attention and working memory. Psychopharmacology (Berlin) *217*, 255–269.

Sohal, V.S., Zhang, F., Yizhar, O., and Deisseroth, K. (2009). Parvalbumin neurons and gamma rhythms enhance cortical circuit performance. Nature *459*, 698–702.

Spellman, T.J., and Gordon, J.A. (2015). Synchrony in schizophrenia: a window into circuit-level pathophysiology. Current Opinions in Neurobiology *30*, 17–23.

Spencer, K.M., Salisbury, D.F., Shenton, M.E., and McCarley, R.W. (2008). Gamma-band auditory steady-state responses are impaired in first episode psychosis. Biological Psychiatry *64*, 369–375.

Stefansson, H., Petursson, H., Sigurdsson, E., Steinthorsdottir, V., Bjornsdottir, S., Sigmundsson, T., Ghosh, S., Brynjolfsson, J., Gunnarsdottir, S., Ivarsson, O., et al. (2002). Neuregulin 1 and Susceptibility to Schizophrenia. American Journal of Human Genetics *71*, 877–892.

Stone, J.M., Erlandsson, K., Arstad, E., Squassante, L., Teneggi, V., Bressan, R.A., Krystal, J.H., Ell, P.J., and Pilowsky, L.S. (2008). Relationship between ketamine-induced psychotic symptoms and NMDA receptor occupancy: a [(123)I]CNS-1261 SPET study. Psychopharmacology (Berlin) *197*, 401–408.

Stone, J.M., Dietrich, C., Edden, R., Mehta, M.A., De Simoni, S., Reed, L.J., Krystal, J.H., Nutt, D., and Barker, G.J. (2012). Ketamine effects on brain GABA and glutamate levels with 1H-MRS: relationship to ketamine-induced psychopathology. Molecular Psychiatry *17*, 664–665.

Sullivan, E.M., and O'Donnell, P. (2012). Inhibitory interneurons, oxidative stress, and schizophrenia. Schizophrenia Bulletin *38*, 373–376.

Swanson, J.M., Sunohara, G.A., Kennedy, J.L., Regino, R., Fineberg, E., Wigal, T., Lerner, M., Williams, L., LaHoste, G.J., and Wigal, S. (1998). Association of the dopamine receptor D4 (DRD4) gene with a refined phenotype of attention deficit hyperactivity disorder (ADHD): a family-based approach. Molecular Psychiatry *3*, 38–41.

Tamás, G., Buhl, E.H., Lörincz, A., and Somogyi, P. (2000). Proximally targeted GABAergic synapses and gap junctions synchronize cortical interneurons. Nature Neuroscience *3*, 366–371.

Tamura, H., Kawata, M., Hamaguchi, S., Ishikawa, Y., and Shiosaka, S. (2012). Processing of Neuregulin-1 by Neuropsin Regulates GABAergic

Neuron to Control Neural Plasticity of the Mouse Hippocampus. Journal of Neuroscience *32*, 12657–12672.

Tan, G.-H., Liu, Y.-Y., Hu, X.-L., Yin, D.-M., Mei, L., and Xiong, Z.-Q. (2012). Neuregulin 1 represses limbic epileptogenesis through ErbB4 in parvalbumin-expressing interneurons. Nature Neuroscience *15*, 258–266.

Tarazi, F.I., and Baldessarini, R.J. (2000). Comparative postnatal development of dopamine D1, D2 and D4 receptors in rat forebrain. International Journal of Developmental Neuroscience *18*, 29–37.

Tatard-Leitman, V.M., Jutzeler, C.R., Suh, J., Saunders, J.A., Billingslea, E.N., Morita, S., White, R., Featherstone, R.E., Ray, R., Ortinski, P.I., et al. (2015). Pyramidal Cell Selective Ablation of N-Methyl-D-Aspartate Receptor 1 Causes Increase in Cellular and Network Excitability. Biological Psychiatry *77*, 556–568.

Thomas, T.C., Kruzich, P.J., Joyce, B.M., Gash, C.R., Suchland, K., Surgener, S.P., Rutherford, E.C., Grandy, D.K., Gerhardt, G.A., and Glaser, P.E. (2007). Dopamine D4 receptor knockout mice exhibit neurochemical changes consistent with decreased dopamine release. Journal of Neuroscience Methods *166*, 306–314.

Thomas, T.C., Grandy, D.K., Gerhardt, G.A., and Glaser, P.E. (2009). Decreased Dopamine D4 Receptor Expression Increases Extracellular Glutamate and Alters Its Regulation in Mouse Striatum. Neuropsychopharmacology *34*, 436–445.

Tierney, P.L., Thierry, A.M., Glowinski, J., Deniau, J.M., and Gioanni, Y. (2008). Dopamine Modulates Temporal Dynamics of Feedforward Inhibition in Rat Prefrontal Cortex In Vivo. Cerebral Cortex *18*, 2251–2262.

Tiesinga, P., and Sejnowski, T.J. (2009). Cortical Enlightenment: Are Attentional Gamma Oscillations Driven by ING or PING? Neuron *63*, 727–732.

Ting, A.K., Chen, Y., Wen, L., Yin, D.-M., Shen, C., Tao, Y., Liu, X., Xiong, W.-C., and Mei, L. (2011). Neuregulin 1 promotes excitatory synapse development and function in GABAergic interneurons. Journal of Neuroscience *31*, 15–25.

Tost, H., Ende, G., Ruf, M., Henn, F.A., and Meyer-Lindenberg, A. (2005). Functional imaging research in schizophrenia. International Review of Neurobiology *67*, 95–118.

Towers, S.K., and Hestrin, S. (2008). D1-Like Dopamine Receptor Activation Modulates GABAergic Inhibition But Not Electrical Coupling between Neocortical Fast-Spiking Interneurons. Journal of Neuroscience *28*, 2633–2641.

Trantham-Davidson, H., Kröner, S., and Seamans, J.K. (2008). Dopamine Modulation of Prefrontal Cortex Interneurons Occurs Independently of DARPP-32. Cerebral Cortex *18*, 951–958.

Trantham-Davidson, H., Burnett, E.J., Gass, J.T., Lopez, M.F., Mulholland, P.J., Centanni, S.W., Floresco, S.B., and Chandler, L.J. (2014). Chronic Alcohol Disrupts Dopamine Receptor Activity and the Cognitive Function of the Medial Prefrontal Cortex. Journal of Neuroscience *34*, 3706–3718.

Traub, R.D., Whittington, M.A., Colling, S.B., Buzsáki, G., and Jefferys, J.G. (1996). Analysis of gamma rhythms in the rat hippocampus in vitro and in vivo. Journal of Physiology *493*, 471–484.

Troyano-Rodriguez, E., Lladó-Pelfort, L., Santana, N., Teruel-Martí, V., Celada, P., and Artigas, F. (2014). Phencyclidine Inhibits the Activity of Thalamic Reticular Gamma-Aminobutyric Acidergic Neurons in Rat Brain. Biological Psychiatry *76*, 937–945.

Tseng, K.Y., and O'Donnell, P. (2004). Dopamine–Glutamate Interactions Controlling Prefrontal Cortical Pyramidal Cell Excitability Involve Multiple Signaling Mechanisms. Journal of Neuroscience *24*, 5131–5139.

Tseng, K.Y., and O'Donnell, P. (2005). Post-pubertal Emergence of Prefrontal Cortical Up States Induced by D1–NMDA Co-activation. Cerebral Cortex *15*, 49–57.

Tseng, K.Y., and O'Donnell, P. (2007a). D2 Dopamine Receptors Recruit a GABA Component for Their Attenuation of Excitatory Synaptic Transmission in the Adult Rat Prefrontal Cortex. Synapse *61*, 843–850.

Tseng, K.-Y., and O'Donnell, P. (2007b). Dopamine Modulation of Prefrontal Cortical Interneurons Changes during Adolescence. Cerebral Cortex 1991 *17*, 1235–1240.

Tseng, K.Y., Mallet, N., Toreson, K.L., Le Moine, C., Gonon, F., and O'Donnell, P. (2006). Excitatory response of prefrontal cortical fast-spiking interneurons to ventral tegmental area stimulation in vivo. Synapse *59*, 412–417.

Tukker, J.J., Fuentealba, P., Hartwich, K., Somogyi, P., and Klausberger, T. (2007). Cell Type-Specific Tuning of Hippocampal Interneuron Firing during Gamma Oscillations in vivo. Journal of Neuroscience *27*, 8184–8189.

Tye, S.J., Covey, D.P., and Griessenauer, C.J. (2009). A Balancing Act: D4 Receptor Activation and the Neurobiological Basis of Emotional Learning. Journal of Neuroscience *29*, 10785–10787.

Uhlhaas, P.J., and Singer, W. (2010). Abnormal neural oscillations and synchrony in schizophrenia. Nature Reviews Neuroscience *11*, 100–113.

Uhlhaas, P.J., Roux, F., Singer, W., Haenschel, C., Sireteanu, R., and Rodriguez, E. (2009). The development of neural synchrony reflects late maturation and restructuring of functional networks in humans. Proceedings of the National Academy of Science *106*, 9866–9871.

Van Tol, H.H., Bunzow, J.R., Guan, H.C., Sunahara, R.K., Seeman, P., Niznik, H.B., and Civelli, O. (1991). Cloning of the gene for a human dopamine D4 receptor with high affinity for the antipsychotic clozapine. Nature *350*, 610–614.

Van Tol, H.H., Wu, C.M., Guan, H.C., Ohara, K., Bunzow, J.R., Civelli, O., Kennedy, J., Seeman, P., Niznik, H.B., and Jovanovic, V. (1992). Multiple dopamine D4 receptor variants in the human population. Nature *358*, 149–152.

Verney, C., Berger, B., Adrien, J., Vigny, A., and Gay, M. (1982). Development of the dopaminergic innervation of the rat cerebral cortex. A light microscopic immunocytochemical study using anti-tyrosine hydroxylase antibodies. Developmental Brain Research *5*, 41–52.

Vijayraghavan, S., Wang, M., Birnbaum, S.G., Williams, G.V., and Arnsten, A.F.T. (2007). Inverted-U dopamine D1 receptor actions on prefrontal

neurons engaged in working memory. Nature Neuroscience *10*, 376–384.

Vinck, M., Batista-Brito, R., Knoblich, U., and Cardin, J.A. (2015). Arousal and Locomotion Make Distinct Contributions to Cortical Activity Patterns and Visual Encoding. Neuron *86*, 740–754.

Vullhorst, D., Neddens, J., Karavanova, I., Tricoire, L., Petralia, R.S., McBain, C.J., and Buonanno, A. (2009). Selective expression of ErbB4 in interneurons, but not pyramidal cells, of the rodent hippocampus. Journal of Neuroscience *29*, 12255–12264.

Vullhorst, D., Mitchell, R.M., Keating, C., Roychowdhury, S., Karavanova, I., Tao-Cheng, J.-H., and Buonanno, A. (2015). A negative feedback loop controls NMDA receptor function in cortical interneurons via neuregulin 2/ErbB4 signalling. Nature Communications *6*, 7222.

Vysokanov, A., Flores-Hernandez, J., and Surmeier, D.J. (1998). mRNAs for clozapine-sensitive receptors co-localize in rat prefrontal cortex neurons. Neuroscience Letters *258*, 179–182.

Wang, H.-X., and Gao, W.-J. (2009). Cell Type-Specific Development of NMDA Receptors in the Interneurons of Rat Prefrontal Cortex. Neuropsychopharmacology *34*, 2028–2040.

Wang, H.-X., and Gao, W.-J. (2010). Development of calcium-permeable AMPA receptors and their correlation with NMDA receptors in fast-spiking interneurons of rat prefrontal cortex. Journal of Physiology *588*, 2823–2838.

Wang, X., Zhong, P., and Yan, Z. (2002). Dopamine D4 Receptors Modulate GABAergic Signaling in Pyramidal Neurons of Prefrontal Cortex. Journal of Neuroscience *22*, 9185–9193.

Wang, X., Zhong, P., Gu, Z., and Yan, Z. (2003). Regulation of NMDA Receptors by Dopamine D4 Signaling in Prefrontal Cortex. Journal of Neuroscience *23*, 9852–9861.

Wang, X., Gu, Z., Zhong, P., Chen, G., Feng, J., and Yan, Z. (2006). Aberrant regulation of NMDA receptors by dopamine D4 signaling in rats after phencyclidine exposure. Molecular and Cellular Neuroscience *31*, 15–25.

Wang, X.-H., Levitt, P., Grayson, D.R., and Murphy, E.H. (1995). Intrauterine cocaine exposure of rabbits: persistent elevation of GABA-immunoreactive neurons in anterior cingulate cortex but not visual cortex. Brain Research *689*, 32–46.

Wedemeyer, C., Goutman, J.D., Avale, M.E., Franchini, L.F., Rubinstein, M., and Calvo, D.J. (2007). Functional activation by central monoamines of human dopamine D4 receptor polymorphic variants coupled to GIRK channels in Xenopus oocytes. European Journal of Pharmacology *562*, 165–173.

Weiss, T., Veh, R.W., and Heinemann, U. (2003). Dopamine depresses cholinergic oscillatory network activity in rat hippocampus. European Journal of Neuroscience *18*, 2573–2580.

Weissman, A.D., Casanova, M.F., Kleinman, J.E., London, E.D., and De Souza, E.B. (1991). Selective loss of cerebral cortical sigma, but not PCP binding sites in schizophrenia. Biological Psychiatry *29*, 41–54.

Wen, L., Lu, Y.-S., Zhu, X.-H., Li, X.-M., Woo, R.-S., Chen, Y.-J., Yin, D.-M., Lai, C., Terry, A.V., Vazdarjanova, A., et al. (2010). Neuregulin 1 regulates pyramidal neuron activity via ErbB4 in parvalbumin-positive interneurons. Proceedings of the National Academy of Science *107*, 1211–1216.

Werner, P., Hussy, N., Buell, G., Jones, K.A., and North, R.A. (1996). D2, D3, and D4 dopamine receptors couple to G protein-regulated potassium channels in Xenopus oocytes. Molecular Pharmacology *49*, 656–661.

Whittington, M.A., Traub, R.D., and Jefferys, J.G.R. (1995). Synchronized oscillations in interneuron networks driven by metabotropic glutamate receptor activation. Nature *373*, 612–615.

Whittington, M.A., Cunningham, M.O., LeBeau, F.E.N., Racca, C., and Traub, R.D. (2011). Multiple origins of the cortical gamma rhythm. Developmental Neurobiology *71*, 92–106.

Wightman, R.M., and Robinson, D.L. (2002). Transient changes in mesolimbic dopamine and their association with “reward.” Journal of Neurochemistry *82*, 721–735.

Williams, G.V., and Goldman-Rakic, P.S. (1995). Modulation of memory fields by dopamine Dl receptors in prefrontal cortex.

Williams, L.M., Whitford, T.J., Nagy, M., Flynn, G., Harris, A.W.F., Silverstein, S.M., and Gordon, E. (2009). Emotion-elicited gamma synchrony in patients with first-episode schizophrenia: a neural correlate of social cognition outcomes. Journal of Psychiatry Neuroscience *34*, 303–313.

Wilson, F.A., O'Scalaidhe, S.P., and Goldman-Rakic, P.S. (1994). Functional synergism between putative gamma-aminobutyrate-containing neurons and pyramidal neurons in prefrontal cortex. Proceedings of the National Academy of Science *91*, 4009–4013.

Winterer, G., and Weinberger, D.R. (2004). Genes, dopamine and cortical signal-to-noise ratio in schizophrenia. Trends in Neuroscience *27*, 683–690.

Wójtowicz, A.M., van den Boom, L., Chakrabarty, A., Maggio, N., Haq, R. ul, Behrens, C.J., and Heinemann, U. (2009). Monoamines block kainate- and carbachol-induced γ-oscillations but augment stimulus-induced γ-oscillations in rat hippocampus in vitro. Hippocampus *19*, 273–288.

Womelsdorf, T., and Fries, P. (2007). The role of neuronal synchronization in selective attention. Current Opinions in Neurobiology *17*, 154–160.

Womelsdorf, T., Valiante, T.A., Sahin, N.T., Miller, K.J., and Tiesinga, P. (2014). Dynamic circuit motifs underlying rhythmic gain control, gating and integration. Nature Neuroscience *17*, 1031–1039.

Woo, R.-S., Li, X.-M., Tao, Y., Carpenter-Hyland, E., Huang, Y.Z., Weber, J., Neiswender, H., Dong, X.-P., Wu, J., Gassmann, M., et al. (2007). Neuregulin-1 Enhances Depolarization-Induced GABA Release. Neuron *54*, 599–610.

Woo, T.-U.W., Kim, A.M., and Viscidi, E. (2008a). Disease-specific alterations in glutamatergic neurotransmission on inhibitory interneurons in the prefrontal cortex in schizophrenia. Brain Research *1218*, 267–277.

Woo, T.-U.W., Shrestha, K., Lamb, D., Minns, M.M., and Benes, F.M. (2008b). N-methyl-D-aspartate receptor and calbindin-containing neurons in the anterior cingulate cortex in schizophrenia and bipolar disorder. Biological Psychiatry *64*, 803–809.

Wood, J., Kim, Y., and Moghaddam, B. (2012). Disruption of prefrontal cortex large scale neuronal activity by different classes of psychotomimetic drugs. Journal of Neuroscience *32*, 3022–3031.

Woolley, M.L., Waters, K.A., Reavill, C., Bull, S., Lacroix, L.P., Martyn, A.J., Hutcheson, D.M., Valerio, E., Bate, S., and Jones, D.N.C. (2008). Selective dopamine D4 receptor agonist (A-412997) improves cognitive performance and stimulates motor activity without influencing reward-related behaviour in rat. Behavioral Pharmacology *19*, 765–776.

Wu, J., and Hablitz, J.J. (2005). Cooperative Activation of D1 and D2 Dopamine Receptors Enhances a Hyperpolarization-Activated Inward Current in Layer I Interneurons. Journal of Neuroscience *25*, 6322–6328.

Xu, T.-X., and Yao, W.-D. (2010). D1 and D2 dopamine receptors in separate circuits cooperate to drive associative long-term potentiation in the prefrontal cortex. Proceedings of the National Academy of Science *107*, 16366–16371.

Xue, J.-G., Masuoka, T., Gong, X.-D., Chen, K.-S., Yanagawa, Y., Law, S.K.A., and Konishi, S. (2011). NMDA receptor activation enhances inhibitory GABAergic transmission onto hippocampal pyramidal neurons via presynaptic and postsynaptic mechanisms. Journal of Neurophysiology *105*, 2897–2906.

Yang, C.R., and Seamans, J.K. (1996). Dopamine D1 receptor actions in layers V-VI rat prefrontal cortex neurons in vitro: modulation of dendritic-somatic signal integration. Journal of Neuroscience *16*, 1922–1935.

Yang, J., Ye, M., Tian, C., Yang, M., Wang, Y., and Shu, Y. (2013a). Dopaminergic modulation of axonal potassium channels and action potential waveform in pyramidal neurons of prefrontal cortex. Journal of Physiology *591*, 3233–3251.

Yang, J.-M., Zhang, J., Chen, X.-J., Geng, H.-Y., Ye, M., Spitzer, N.C., Luo, J.-H., Duan, S.-M., and Li, X.-M. (2013b). Development of GABA circuitry of fast-spiking basket interneurons in the medial prefrontal cortex of erbb4-mutant mice. Journal of Neuroscience *33*, 19724–19733.

Yao, J.-J., Sun, J., Zhao, Q.-R., Wang, C.-Y., and Mei, Y.-A. (2013). Neuregulin-1/ErbB4 signaling regulates Kv4.2-mediated transient outward K+ current through the Akt/mTOR pathway. American Journal of Physiology - Cell Physiol. *305*, C197–C206.

Yau, H.-J., Wang, H.-F., Lai, C., and Liu, F.-C. (2003). Neural Development of the Neuregulin Receptor ErbB4 in the Cerebral Cortex and the Hippocampus: Preferential Expression by Interneurons Tangentially

Migrating from the Ganglionic Eminences. Cerebral Cortex *13*, 252–264.

Yin, D.-M., Sun, X.-D., Bean, J.C., Lin, T.W., Sathyamurthy, A., Xiong, W.-C., Gao, T.-M., Chen, Y.-J., and Mei, L. (2013a). Regulation of spine formation by ErbB4 in PV-positive interneurons. Journal of Neuroscience *33*, 19295–19303.

Yin, D.-M., Chen, Y.-J., Lu, Y.-S., Bean, J.C., Sathyamurthy, A., Shen, C., Liu, X., Lin, T.W., Smith, C.A., Xiong, W.-C., et al. (2013b). Reversal of Behavioral Deficits and Synaptic Dysfunction in Mice Overexpressing Neuregulin 1. Neuron *78*, 644–657.

Yonezawa, Y., Kuroki, T., Kawahara, T., Tashiro, N., and Uchimura, H. (1998). Involvement of gamma-aminobutyric acid neurotransmission in phencyclidine-induced dopamine release in the medial prefrontal cortex. European Journal of Pharmacology *341*, 45–56.

Young, J.W., Powell, S.B., Scott, C.N., Zhou, X., and Geyer, M.A. (2011). The effect of reduced dopamine D4 receptor expression in the 5-choice continuous performance task: Separating response inhibition from premature responding. Behavioral Brain Research *222*, 183–192.

Yuen, E.Y., and Yan, Z. (2009). Dopamine D4 Receptors Regulate AMPA Receptor Trafficking and Glutamatergic Transmission in GABAergic Interneurons of Prefrontal Cortex. Journal of Neuroscience *29*, 550–562.

Yuen, E.Y., and Yan, Z. (2011). Cellular Mechanisms for Dopamine D4 Receptor-induced Homeostatic Regulation of α-Amino-3-hydroxy-5-methyl-4-isoxazolepropionic Acid (AMPA) Receptors. Journal of Biological Chemistry *286*, 24957–24965.

Yuen, E.Y., Zhong, P., and Yan, Z. (2010). Homeostatic regulation of glutamatergic transmission by dopamine D4 receptors. Proceedings of the National Academy of Science *107*, 22308–22313.

Zanos, P., Moaddel, R., Morris, P.J., Georgiou, P., Fischell, J., Elmer, G.I., Alkondon, M., Yuan, P., Pribut, H.J., Singh, N.S., et al. (2016). NMDAR inhibition-independent antidepressant actions of ketamine metabolites. Nature *advance online publication*.

Zarate, C.A., Singh, J.B., Carlson, P.J., Brutsche, N.E., Ameli, R., Luckenbaugh, D.A., Charney, D.S., and Manji, H.K. (2006). A randomized trial of an N-

methyl-D-aspartate antagonist in treatment-resistant major depression. Archives in Genetic Psychiatry *63*, 856–864.

Zhang, K., Tarazi, F.I., and Baldessarini, R.J. (2001). Role of dopamine D4 receptors in motor hyperactivity induced by neonatal 6-hydroxydopamine lesions in rats. NeuropsychoPharmacology Off. Publ. Am. Coll. Neuropsychopharmacology *25*, 624–632.

Zhang, K., Grady, C.J., Tsapakis, E.M., Andersen, S.L., Tarazi, F.I., and Baldessarini, R.J. (2004). Regulation of working memory by dopamine D4 receptor in rats. Neuropsychopharmacology *29*, 1648–1655.

Zheng, P., Zhang, X.-X., Bunney, B.S., and Shi, W.-X. (1999). Opposite modulation of cortical N-methyl-d-aspartate receptor-mediated responses by low and high concentrations of dopamine. Neuroscience *91*, 527–535.

Zhou, F.-M., and Hablitz, J.J. (1999). Dopamine Modulation of Membrane and Synaptic Properties of Interneurons in Rat Cerebral Cortex. Journal of Neurophysiology *81*, 967–976.

CURRICULUM VITAE

Katrina Furth
208 Massachusetts Ave NE Apt 405 ~ Washington, DC 20002 ~ (585) 406-4203 ~ kfurth@bu.edu
Jan 16, 1988

Education

PhD candidate in the Graduate Program for Neuroscience — September 2011 – present
Boston University
Qualifying exam passed 10/24/13
Cumulative GPA of 4.0 (out of 4.0)

B.S. in Brain and Cognitive Science, with Highest Research Honors
May, 2010
University of Rochester
Concentration in Neurobiology
Cumulative GPA of 3.89 (out of 4.0)

Presentations and Publications

Peer-Reviewed Papers

- **Furth, K.**, McCoy, A.J., Dodge, C., Walters, J.R., Buonanno, A., Delaville, C. (2016). Neuronal correlates of ketamine and walking induced gamma oscillations in the medial prefrontal cortex and mediodorsal thalamus. *Psychopharmacology*, (in prep).
- **Furth, K**., Mastwal, S., Wang, K.H., Buonanno, A., Vullhorst, D. (2013). Dopamine, Cognitive Function, and Gamma Oscillations: Role of D4 Receptors. *Frontiers in Cellular Neuroscience,* 7(102).
- Mitchell, R.M., Janssen, M.J., Karavanova, I., Vullhorst, D., **Furth, K**., Makusky, A., Markey, S.P., Buonanno, A.. (2013). ErbB4 reduces synaptic GABAA currents independent of its receptor tyrosine kinase activity. Proceedings in the National Academy of Sciences, 110 (48).
- Jaeger T.F., **Furth K.**, and Hilliard C. (2012) Incremental phonological encoding during unscripted sentence production. *Frontiers in Psychology*, 3(481).
- Jaeger, T.F., **Furth, K.**, Hilliard, C. (2012). Phonological overlap affects lexical selection during sentence production. *Journal of Experimental Psychology: Learning, Memory, and Cognition,* 38(5).
- Butler, L., Jaeger, T.F., Bohnemeyer, J., **Furth, K.** (2011). Learning to express visual contrasts in the production of referring expressions in Yucatec Maya. *Proceedings from the Workshop on the Production of Referring Expressions.* Boston, MA. July, 2011.
- Hilliard, C., **Furth, K.**, Jaeger, T.F. (2011) Phonological encoding in sentence production. *The 33rd Annual meeting of the Cognitive Science Society (CogSci11).* Boston, MA. July, 2011.
- Gómez Gallo, C., Jaeger, T.F. & Furth, K. (2010). A Database for the Exploration of Spanish Planning. *Language Resources and Evaluation Conference (LREC).* Malta. May, 2010.

Talks and Posters

- **Furth, K.**, Walters, J.R., McCoy, A.J., Dodge, C., Buonanno, A., Delaville, C. (2016). Exploring a rodent model of schizophrenia: neuronal correlates of gamma oscillations induced by ketamine, locomotion, or dopamine D4 receptor activation in the medial prefrontal cortex and mediodorsal thalamus. *Russek Student Achievement Day.* (May 2016).
- **Furth, K.**, McCoy, A.J., Walters, J.R., Buonanno, A., Delaville, C. (2016). Association of ketamine, dopamine D4 receptor activation, and locomotion with gamma range activity in the

prefrontal cortex and mediodorsal thalamus. *Society for Neuroscience.* (expected November 2016).

- **Furth, K**., Hilliard, C., & Jaeger, T.F. (2010). Phonological Interference in Spontaneous Speech Production. (talk) *Architectures and Mechanisms of Language Processing.* York, United Kingdom. September, 2010.
- **Furth, K**., Hilliard, C. & Jaeger, T.F. (2010). Phonological Interference in Unscripted and Scripted Sentence Production. (poster) *The 6th International Workshop on Language Production.* Edinburgh, UK. September, 2010.
- Butler, L.K., Jaeger, T.F., **Furth, K**., Gómez Gallo, C., Lemieux, A. & Bohnemeyer, J. (2010). Psycholinguistics in the field: Accessibility-driven Production in Yukatek Maya. (poster) *The 23rd CUNY Sentence Processing Conference.* New York, NY. March, 2010.

Theses

- Furth, K. (2010). Phonological Inhibition in Spontaneous Speech Production. *University of Rochester Senior Honors Thesis Program.* (Bachelor's with honors) Rochester, NY. April, 2010.
- Furth, K (2016). The role of the dopamine D4 receptor in modulating state-dependent gamma oscillations. *Boston University, Graduate Program for Neuroscience*. Boston, MA. expected July 2016.

Teaching Experience

Marymount University **Arlington, VA**
Adjunct professor of biology Fall 2014- Spring 2015

- Taught a freshman biology lab, including quiz, exam, and paper preparation. The students performed 11 labs over the course of the semester and wrote 8 lab reports in the style of an academic research paper. Also led discussions on bioethics and taught students how to present research at academic conferences.

University of Rochester **Rochester, NY**
Study Group Leader for Neural Foundations of Behavior and General Chemistry Fall 2007- Fall 2009

- Developed lesson plans and organized materials to guide students through challenging problems in a small group.

Kaplan Review
Rochester, NY
Instructor at Kaplan Review Summer 2008-Fall 2010

- Used practice exams, question and answer techniques, and group games to conduct SAT prep for high school students.

10 week course in Scientists Teaching Science - Spring 2013

Awards and Honors

- Russek Student Achievement Award: Second Place
- Bishop Fellowship for Research in Brain and Cognitive Sciences
- Phi Beta Kappa Honor Society
- IES Study Abroad Excellence in the Sciences Scholarship

Research Experience

National Institutes of Health **Washington, DC**

- Graduate Student – Walters lab October 2013-present

Studied the effects of ketamine, locomotion, and dopamine D4 receptor activation on ongoing neural oscillations in the medial prefrontal cortex and mediodorsal thalamus. Learned how to implant chronic electrodes in rats, train rats to walk in circular treadmills, administer drugs, analyze data, sort single neurons and write scripts in MATLAB and Spike 2.

National Institutes of Health **Washington, DC**

- Graduate Student – Buonanno lab July 2012-Feb 2014

Studied the effects of dopamine on circuit activity in the hippocampus using patch-clamp electrophysiology. Learned how to make brain slices from living tissue, record physiological currents, fix and stain tissue and perform microscopy.

Boston University **Boston, MA**

- Rotation Student – Haydar lab January 2012-April 2012

Studied neuroanatomical differences between down syndrome model and wildtype mice in the amygdala, specifically examining interneurons. Learned confocal microscopy and observed multiple in utero electroporation experiments. Also learned transgenic mouse colony management.

- Rotation Student – Farb lab October 2011-December 2011

Studied the effects of pregnenolone sulfate on the localization and specifity of hippocampal place fields in familiar and novel environments. Learned to isolate cells using Offline Sorter and analyze the spiketrains using MATLAB and Neuroexplorer. Modeled the spiking activity in R. Set up a novel object recognition paradigm to test neurosteroids for cognitive enhancement. Learned behavioral and in vivo electrophysiology techniques.

- Rotation Student – Datta lab September 2011-October 2011

Studied the effects of sleep medications and antidepressants on the sleep architecture of rats. Focused on prenatal development. Learned rodent surgery and electrode creation.

- Rotation Student –Eden lab April 2012- June 2012

Visualized and modeled spiking data from human subthalamic nucleus during deep brain stimulator implantation surgery. Learned point process modeling and practiced statistical techniques.

University of Rochester **Rochester, NY**

- Laboratory Technician – Nordeen lab July 2010 – June 2011

Under supervision of Kathy and Ernie Nordeen, PhD., analyzed mechanisms of neural plasticity and learning in zebra finches.

- Laboratory Technician - Goldman lab January 2010-June 2010

Under supervision of Steve Goldman, PhD., worked on therapies for multiple sclerosis by studying thegrowth of human oligodendrocyte progenitor cells in mice.

- Research Assistant and Undergraduate Researcher Summer 2007-February 2011

Under supervision of Florian Jaeger, PhD., developed a multi-experiment study probing theory of availability-based production using phonological overlap between words in a sentence. Designed and ran multiple experiments studying Yukatek, Mayan. Lived in Valladolid, Mexico to gather data from indigenous people and run studies in Spanish. Supervised other undergraduate research assistants and ran undergraduate lab meetings.

- Senior Honors Thesis Researcher Fall 2009-Spring 2010

Designed and implemented an independent investigation of the difference between identity and similarity in phonological onset on disfluency.

Ad-Hoc Journal Review

- International Journal of Neuropharmacology (2012)

Ad-Hoc Testbank Question Writing

- LeVay, S., Baldwin, J., Baldwin, J., Discovering Human Sexuality, Third Edition, Sinauer Associates. (2015).

References

Dr. Judith Walters
Neurophysiological Pharmacology Section
National Institute of Neurological Disorders and Stroke
waltersj@ninds.nih.gov

Dr. Andres Buonanno, Senior Investigator
Laboratory of Developmental Neurobiology
National Institute of Child Health & Development
buonanno@mail.nih.gov

Dr. Shelley Russek, Professor
Pharmacology & Experimental Therapeutics
Boston University
srussek@bu.edu